A-to-I RNA Editing of Voltage-Gated Potassium Channels:

Regulation and Functional Consequences in *Drosophila melanogaster*.

By Rachel A. Maloney

B.S., Central Connecticut State University, 2004

A Dissertation Submitted in Partial Fulfillment of the Requirements for the Degree of Doctor of Philosophy in the Department of Molecular Biology, Cell Biology, and Biochemistry at Brown University

Providence, Rhode Island

May 2011

This dissertation by Rachel A. Maloney is accepted in its present form by the Department of Molecular Biology, Cell Biology, and Biochemistry as satisfying the dissertation requirement for the degree of Doctor of Philosophy.

Date_____ _____
Robert A. Reenan, Ph.D., Advisor

Recommended to the Graduate Council

Date_____ _____
Michael McKeown, Ph.D., Reader

Date_____ _____
Diane Lipscombe, Ph.D., Reader

Date_____ _____
Will Fairbrother, Ph.D., Reader

Date_____ _____
Blanka Rogina, Ph.D., Reader

Approved by the Graduate Council

Date_____ _____
Peter Weber, Dean of the Graduate School

Rachel A. Maloney

Brown University
Department Molecular Biology, Cell Biology, Biochemistry
Box G
Providence, RI 02912
(401) 863-6482
Rachel_Maloney@brown.edu

32 Roberts Street
Newington, CT 06111
(860) 690-2068

Birthplace: Hartford, Connecticut

Education

Ph.D. Brown University, Providence, RI 2006-Present
Molecular Biology, Cell Biology, and Biochemistry
Expected Graduation Date: July 2010
Title: "A-to-I RNA Editing of Voltage-Gated Potassium Channels: Regulation And Functional Consequences in *Drosophila melanogaster*."
Advisor: Professor Robert Reenan

University of Connecticut Health Center, Farmington, CT 2004-2006
Ph.D. Program in Biomedical Science
Concentration in Genetics and Developmental Biology
Advisor: Professor Robert Reenan

B.S. Central Connecticut State University, New Britain, CT 2000-2004
Magna Cum Laude, Departmental Honors
Major: Cellular and Molecular Biology
Minor: Chemistry

Research Experience

Doctoral Dissertation
Brown University, 2006-Present

- Conducted experiments in *Drosophila melanogaster* to investigate the regulation and functional consequences of A-to-I pre-mRNA editing of voltage-gated potassium channels.
- Used comparative genomics and nucleic acid folding application software to identify potential *cis*-regulatory elements and predict the secondary RNA structures formed to direct A-to-I editing of K_v channel genes.
- Assessed spatial and temporal distribution of Shaker channel editing through sequencing of RT-PCR products in *Drosophila* and generated developmental profiles of A-to-I editing in other K_v channel transcripts (*eag, Shab*).

- Generated expression constructs to mimic various isoforms of Shaker editing for electrophysiology studies.
- Disrupted K_v channel editing at endogenous loci by homologous recombination in *D. melanogaster*.
- Evaluated behavioral phenotypes in editing mutant flies including gross locomotor activity, sleep, mating behavior, and aggression.

Undergraduate Research
Central Connecticut State University, Department of Biology; 2002-2004
Laboratory of Dr. Tom King

- Performed recombination-mapping studies to localize the recessive hypotrichosis mutation in Charles River "hairless" rats.
- Used PCR of DNA microsatellite repeat markers in a panel of backcross rats and mapped this mutant allele to a different locus from the known "hairless" gene.
- Performed complementation analysis with other hairless mutant rats to identify additional alleles of the Charles River hairless mutation.
- Participated in mapping and complementation testing between a spontaneously recessive male-sterility mutation in mice (*mshi*) and genetically engineered estrogen receptor alpha null allele.
- Developed backcross panels of rats to identify and map the pseudo-autosomal region shared between X and Y-chromosomes.
- Performed skin graft exchanges between inbred mice strains to isolate minor X-linked histocompatibility genes.

Animal Care Technician
Central Connecticut State University, Department of Biology; 2004
- Maintained mouse and rat colonies used in faculty research.
- Provided animal husbandry care for both mice and rat stocks and various backcross panels.
- Communicated with various faculty regarding care and health of their experimental animals.

Teaching Experience

Biology Department, Brown University, Spring 2007
Teaching Assistant, Advanced Molecular Genetics
- Seminar course for both upper level undergraduate and first-year graduate students which covers genetic and molecular approaches to investigate complex biological phenomena through lectures and discussion of primary literature.
- Attended lectures, held office hours for student questions and tutoring.
- Collected and graded homework assignments, quizzes, and exams.
- Maintained grading spreadsheets and student information for faculty lecturers.

Biology Department, Central Connecticut State University, Summer 2004
Tutor, Chemistry for undergraduate pre-med majors.

- Held a six-week chemistry course for pre-med students requiring additional instruction in general and organic chemistry.
- Designed practice questions and topic-specific lecture and supplementary materials.
- Conducted review lectures based on student-initiated topics of interest.

Biology Department, Central Connecticut State University, Spring 2003
Teaching Assistant, Laboratory Tutorial for area middle-school students.

- Assisted faculty and students in a laboratory practicum designed to expose middle school students to forensic science and DNA technology.
- Helped students with fingerprint analysis, blood-typing, and genotype analysis through PCR and electrophoresis of DNA products.
- 4-5 sessions held over the course of the spring semester.

Publications

K. Ahern, G. Akkouris, P. Berry, R. Crissluis, I. Crooks, A. Dull, S. Grable, J. Jeruzal, J. Lanza, C. Lavoie, R. Maloney, M. Pitruzello, R. Sharma, T. Stoklasek, J. Tweeddale, and T.R. King. (2002) The Charles River "Hairless" Rat Mutation Maps to Chromosome 1: Allelic with *Fuzzy* and a Likely Orthologue of Mouse *Frizzy*. *The Journal of Heredity* 93 (3): 210-213.

Ryan MY, Maloney R, Reenan R, Horn R. (2008). Characterization of five RNA editing sites in Shab potassium channels. *Channels* (Austin) 2(3): 202-209.

Ingleby L, Maloney R, Jepson J, Horn R, Reenan R. (2009). Regulated RNA editing and functional epistasis in Shaker potassium channels. *Journal of General Physiology* Jan;133(1):17-27.

Conference Abstracts

Ryan, M, Maloney, R., Fineberg, J., Reenan, R.. and Horn, R. (2010) Lysine versus Arginine: RNA Editing in the *eag* Potassium Channel. *Biophysical Society* Annual Meeting. Vol 98, issue 3, supplement 1: pp116a.

K. Ahern, G. Akkouris, P. Berry, R. Crissluis, I. Crooks, A. Dull, S. Grable, J. Jeruzal, J. Lanza, C. Lavoie, R. Maloney, M. Pitruzello, R. Sharma, T. Stoklasek, J. Tweeddale, and T.R. King. (2002) The Charles River "Hairless" Rat Mutation Maps to Chromosome 1: Allelic with *Fuzzy* and a Likely Orthologue of Mouse *Frizzy*. Poster Presentation Eastern Colleges Science Conference. April 26, 2002. Niagra University, Niagra, NY.

Dedication

I dedicate this thesis to my mother, Mary Beth. You have always been, and will continue to be, a great source of love, strength and inspiration to me. You have taught me many values and principles that I apply to my life everyday, of which, hard work and determination is evidenced here within these pages. I could not have achieved all that I have without you. Thank you Mom, and I love you.

Acknowledgements

I would like to thank my advisor, Dr. Robert Reenan, for the amazing opportunity to pursue my thesis research in your lab. You have been an incredible mentor and I have learned so much working with you and I had a lot of fun too. Although you are a tough act to follow, I enjoyed trying to keep up with you. I believe that having a role model like you was the best example I could have followed for learning to be a successful and independent researcher. Thank you.

I would also like to thank Cindi Staber, my "surrogate Mom". I have learned so much working with you from fly biology to molecular techniques. I would not have achieved as much success with my project had it not been for you. Thank you for providing me with a shoulder to cry on when things were going wrong and smiles and laughs when things went right, and for chocolate too. I will not soon forget you.

I would like to thank the members of my thesis committee: Dr. Michael McKeown, Dr. Diane Lipscombe, Dr. Will Fairbrother, and Dr. Blanka Rogina. I appreciate all the time you took to participate in committee meetings as well as my defense. My project certainly grew as a result of the stimulating conversations we had and feedback I received from all of you. Thanks again.

I would also like to extend my gratitude towards Elaine Butler and Rosemarie Antoni for all their hard work and all that they do for everyone in the MCB department. I truly appreciate all the time and effort you expended in helping to make me feel welcome here at Brown University and for making my transition here as smooth as possible.

Last, but certainly not least, I would like to thank my dear friend and colleague Yiannis Savva. You have been a great friend and a tremendous source of strength and encouragement to me. You are a brave soul for sharing a seat next to me on this rollercoaster ride. Thanks.

Table of Contents

Table of Figures

List of Tables

Chapter 1: Introduction

Post-transcriptional gene regulation increases the diversity of protein products encoded within genomes.

The central dogma of molecular biology describes the manner in which cells utilize information encoded within their DNA to produce the many proteins that both maintain the cell itself and regulate interactions with its environment. In this model, the DNA is transcribed into a single-strand nucleic acid chain intermediate, messenger RNA (mRNA), which then serves as a template for translation machinery to build proteins in accordance with the code contained within the gene it was derived from. Some of these proteins are destined to then act directly on DNA to further control gene expression, replicate the genome during cell division, and maintain genome integrity. However, higher levels of regulation exist outside of this canonical flow of genetic information. For example, RNA-RNA and RNA-DNA interactions are used by the RNA-interference (RNAi) machinery for transcriptional and post-transcriptional gene silencing. Additionally, proteins interact with the messenger RNA for a variety of functions including pre-mRNA maturation, stability, and transport. Even further, proteins can modify mRNA to increase the diversity of protein products that can be encoded by a given genomic locus through both alternative splicing and RNA editing. Alternative splicing can alter the coding potential in the mature mRNA by the inclusion or exclusion of exons originally contained within the genomic locus. The resulting mature RNA can vary greatly from the genomic locus it was transcribed from through the cut-and-paste process of removing whole sections of continuous sequence of varying lengths (reviewed

by Black 2003). RNA editing, in contrast, results in more modest changes in the mRNA transcript that can include insertions, deletions, or conversion of bases that are not present in the genomic locus (Keegan, Gallo et al. 2001; Bass 2002). In essence, RNA editing is regulated and evolved point mutations made within transcripts rather than the gene itself. As a consequence, editing of a transcript can result in frame-shift mutations or alter codon meaning, leading to the production of differing protein products derived from the same gene.

One form of RNA editing, A-to-I editing, involves the conversion of adenosine bases in mRNA transcripts into inosine. Since inosine base pairs with cytosine, the cellular machinery recognizes inosine as guanosine (Basilio, Wahba et al. 1962). This can be observed as a mixed A/G peak in sequence chromatograms obtained from RT-PCR products while the corresponding genomic sequence yields a single peak for adenosine (Figure 1.2). Since A-to-I conversion in coding sequence can result in amino acid substitutions, this form of post-transcriptional gene modification can expand the protein coding capacity of the genome. In contrast to this more specific type of A-to-I editing, promiscuous editing activity can also be observed typically within untranslated regions (UTRs) and intronic regions containing retrotransposons as well as non-coding RNAs, involving the conversion of many adenosine residues (Lehmann and Bass 2000; Nishikura 2010). This type of abundant editing is thought to be involved in the regulation of various processes including; protein translation, acting in opposition to RNAi, and in viral defense by altering the secondary structures of the substrate.

Adenosine Deaminases Acting on RNA (ADAR) Catalyzes A-to-I RNA Editing

The conversion of adenosine to inosine involves a hydrolytic deamination reaction catalyzed by a class of enzymes named ADARs, or Adenosine Deaminases Acting on RNA (Figure 1.1A). This class of enzymes is conserved from worms to humans and is related to adenosine deaminases acting on tRNAs (ADATs), both of which were thought to evolve from more ancestral cytosine deaminase enzymes (Kim, Wang et al. 1994; Maydanovych and Beal 2006). The basic functional domains of ADARs are also conserved, consisting of differing numbers (1-3) of double-stranded RNA binding domains (dsRBDs), and a catalytic domain in the C-terminal region of the protein (Figure 1.1B). The number of ADAR genes varies between organisms. For example, humans express three different ADARS (ADAR1, ADAR2, and ADAR 3) and worms (*C. elegans*) have two, while the fruit fly *D. melanogaster*, contains only a single *adar* gene, *dAdar*.

ADARs recognize and bind to duplex RNA through their dsRNA binding domains (Maydanovych and Beal 2006; Xu, Wells et al. 2006). These domains are highly conserved not only within ADARs but also with other RNA binding proteins. These domains bind to the phosphate backbone of the duplex RNA and do not interact especially with the bases themselves. This interaction agrees with observations that ADAR target recognition is partly regulated by the structure of the duplex RNA rather than the primary sequence (Stephens, Haudenschild et al. 2004; Reenan 2005; Stefl, Xu et al. 2006). The catalytic domain of ADARs contains four highly conserved residues that are shared with cytidine deaminases (CDAs). Although deaminase activity of ADARs does not require the presence of a co-factor, three of the four conserved residues,

one histidine and two cystine residues, along with water, coordinate a zinc ion within the active site and are necessary for enzymatic activity (Kim, Wang et al. 1994; Lai, Drakas et al. 1995; Melcher, Maas et al. 1996). The fourth conserved residue, glutamic acid, is required for proton transfer during deamination (Figure 1.1C). Furthermore, an inositol-hexakisphosphate (IP_6) moiety was identified deep within the protein fold of the catalytic domain and is required for proper protein folding and activity (Macbeth, Schubert et al. 2005). The mammalian ADAR2 active site differs from CDAs in two residues, T375 which prevents cytidine from binding the active site and A455 whose function is not well understood (Betts, Xiang et al. 1994). These differences may explain why ADARs, related to CDAs with high conservation, do not deaminate cytidine residues and are specific to adenosine.

Transcriptional and post-transcriptional regulation of ADARs generates enzyme diversity.

Diversity of ADAR function can be achieved by increasing the number of protein isoforms generated from these loci by transcriptional and post-transcriptional regulation of *ADAR* transcripts. An excellent example of this can be observed in *D. melanogaster*, where a single *adar* locus (*dAdar*) can generate multiple protein isoforms by alternative splicing and A-to-I editing. Additionally, the use of alternative promoters along with splicing and editing are regulated developmentally to generate spatial and temporal patterns of protein expression (Palladino, Keegan et al. 2000). Transcriptional regulation generates differing 5' untranslated regions (UTRs) in the *dAdar* transcript. Alternative splicing alters both the region of the transcript coding the N-terminal portion of dADAR,

a region known to be involved in dimerization (Gallo, Keegan et al. 2003), and inclusion of the alternative exon (3a) increases the spacing between the two dsRBMs of the enzyme and has been postulated to affect binding specificity and affinity. The A-to-I auto-editing event changes a conserved serine (S) residue in the catalytic domain to glycine (G) and was shown to decrease editing activity in *in vitro* assays as well as within transgenic flies (Keegan, Brindle et al. 2005).

ADARs of both vertebrates and invertebrates have been shown to function as dimers. While vertebrate ADARs form homodimers with respect to different ADAR genes expressed, dAdar can form heterodimers between differentially spliced ADAR isoforms (Cho, Yang et al. 2003; Gallo, Keegan et al. 2003; Chilibeck, Wu et al. 2006). The end result of this coordination of regulatory events is the production of a diverse array of ADAR proteins with varying activity.

Vertebrate ADARs also undergo transcriptional regulation that leads to the generation of different enzyme isoforms with different activities. Alternative promoter use can generate two differing length ADAR1 enzymes in humans (Patterson and Samuel 1995). Production of the longer form of ADAR1 is under the control of an interferon-inducible promoter that activates during an immune response (Figure 1.1B). This form of ADAR can translocate from the nucleus to the cytoplasm to act against viral infection (Cattaneo, Schmid et al. 1988; Polson, Bass et al. 1996; Nishikura 2010). This longer form of ADAR1 contains two zDNA binding domains in addition to three dsRBDs. These domains have been proposed to function in localizing ADAR to areas where active transcription of editing substrates occurs. The shorter form of ADAR1 is constitutively expressed, located in the nucleus, and lacks part of the N-terminal region containing the

zDNA binding domains resulting from differential translation initiation site usage. Alternative splicing and auto-editing also occur in mammalian ADAR2 where these processes are coupled (Rueter, Dawson et al. 1999). Auto editing of the *ADAR2* transcript generates a new splice acceptor site, which results in the insertion of an additional 47 nucleotides, introducing a premature stop codon. Translation of these transcripts results in a truncated form of ADAR2 that lacks both dsRBDs and catalytic domain and is thought to be the product of inhibitory feedback mechanism that regulates the levels of ADAR2 within the cell.

ADARs bind and deaminate adenosines within double-stranded RNAs.

ADARs recognize and bind to double-stranded RNAs through their dsRBDs. These duplex RNA substrates can be either perfectly base-paired or contain internal mismatches and bulges. Imperfect duplexes that direct the editing of specific adenosines form between two complementary regions within the RNA transcript, with one region containing the target adenosine(s) and the other located typically within non-coding regions of the transcript. These highly conserved regions of homology, named editing site complementary sequence (ECS), are the cis-regulatory elements directing editing. These ECS elements can be in close proximity to the region of editing, forming a hairpin-like structure, or can be many kilobases away, forming complex structures such as pseudoknots, where large amounts of intervening sequence is looped out and excluded from the structure (Figure 1.3) (Higuchi, Single et al. 1993; Maas, Melcher et al. 1996; Hanrahan, Palladino et al. 2000; Bhalla, Rosenthal et al. 2004; Dawson, Sansam et al. 2004; Reenan 2005). Manipulation of these RNA secondary structure, through mutations

within ECS elements, demonstrate that imperfect dsRNA structures aid to restrict ADAR activity to specific adenosines and disruption of the local secondary structure surrounding an editing target is sufficient to abolish editing. Compensatory mutations, which restore the local secondary structure around the target also restore editing, demonstrating that it is the structure surrounding the target rather than primary sequence that directs site specificity. These disruptions/imperfections within the duplex are thought to control specificity by limiting where ADAR can bind on the duplex and help to position the active site over the correct adenosine.

However, ADARs do exhibit a preference for adenosines within certain sequence contexts, or neighboring preferences where the identity of the base 5' or 3' to a certain adenosine will affect editing efficiency of that site (Lehmann and Bass 2000; Wong, Sato et al. 2001; Bass 2002; Kallman, Sahlin et al. 2003). This was delineated during *in vitro* editing assays with perfect duplex RNA serving as a substrate. When dsRNA contains long stretches of perfect duplex, editing occurs promiscuously and many adenosines can be deaminated within this region in a nearly random fashion. The nearest neighbor preferences were observed where certain adenosines within the duplex were edited at very low frequency. Adenosines with another adenosine or uridine residue as a 5' neighbor are preferred by ADARs over a cytosine or a guanosine (A=T > C > G). This bias can also be observed in known endogenous targets of A-to-I editing where typically the neighboring base to a known target is another adenosine or uridine, and sometimes a cytidine.

If A-to-I editing within a transcript is conserved between two species it is thought that the ECS elements directing editing could be conserved as well (Aruscavage and Bass

2000; Hanrahan, Palladino et al. 2000; Reenan 2005). The sequenced and annotated genomes of many species, especially within *Drosophila* where twelve genomes from different species are available, allow for comparative genomic approaches to aid in the identification of ECS elements. Highly conserved regions between two species, contained within an otherwise highly variable intron, are the first indication of a potential regulatory role for that region. Certainly, other regulatory regions not involved in editing will have the same signature of conservation such as splicing signals and enhancers. Further computational modeling is needed to determine if the conserved region contains complementarity to the edited region in question. This can be accomplished using software applications that predict the secondary structure for a given nucleic acid sequence. Some software applications, such as mFold (Zuker 2003), predict secondary structures of single stranded nucleic acids based on free energy minimization where predicted structures are formed based on the assumption that nucleic acids will fold into the lowest energy state (optimization). More recently, programs such as Sfold (http://sfold.wadsworth.org) use a Boltzmann-weighted ensemble of many possible structures that can be adopted by a given sequence, and statistcal algorithms cluster thousands of predicted structures into a few distinct groups based on structure similarity (Ding, Chan et al. 2005). These clusters are represented by centroids that illustrate the consensus structure for a given cluster and also give a probability for that structure to be represented in the sampling population (probability mass). These programs aid in demonstrating that complementarity between the potential ECS element and the editing target sequence can, in principle, base pair. Further experimental validation is required before any function can be assigned to the conserved element. This is typically

accomplished through expression of minimal editing reporters containing the edited exon, the region containing the ECS and the downstream exon (for splicing purposes), which is then expressed in cell culture systems where editing of the substrate can be easily assessed and mutations within the ECS can be introduced to determine their affect on substrate editing (Higuchi, Single et al. 1993; Reenan 2005). *In vivo* ectopic expression systems, such as UAS-Gal4 in *Drosophila* or transgenic mouse models can be used for this purpose as well (Feldmeyer, Kask et al. 1999; Feng, Sansam et al. 2006; Kawahara, Grimberg et al. 2008; Jepson and Reenan 2009). Identification of ECS elements through comparative genomics allows for a starting point to introduce mutations that will disrupt editing *in vivo* without affecting the protein-coding region of the gene under investigation.

A-to-I RNA Editing is Necessary for Proper Nervous System Function

Evidence that A-to-I RNA editing functions in the nervous system includes the observation of high levels of inosine-containing mRNAs in rodent brains (Paul and Bass 1998), and from the phenotypes resulting from mutations in the ADAR enzyme itself. Abolishing all editing activity by the generation of ADAR null alleles in both flies and worms leads to morphologically normal, viable animals. However, these mutants exhibit severe neurological defects and behavioral abnormalities. In the worm *C. elegans*, loss of editing activity was shown to generate chemotaxis defects (Tonkin, Saccomanno et al. 2002). In *Drosophila*, loss of editing leads to severely uncoordinated movement, behavioral defects such as courtship display, temperature-sensitive paralysis, and age-dependent tremors. Furthermore, age-dependent neurodegeneration in photoreceptor

cells of the retina and lesions dispersed throughout the brain are observed (Palladino, Keegan et al. 2000). Despite the increase in severity of phenotypes and neurodegeneration in an age-dependent manner, *adar*-null flies have normal life spans under ideal conditions of care. Life spans are dramatically reduced, however, when mutant animals are housed under competitive conditions with wild-type animals demonstrating that the proper nervous system function and behavior achieved through RNA editing is necessary to compete for resources and survive in nature.

In contrast to invertebrate mutants lacking editing activity, loss of ADAR activity in mammals is lethal. Loss of ADAR1 was shown to be lethal, with death occurring during embryonic stage (~E14) and defects observed in hematopoiesis and increased apoptosis (Wang, Khillan et al. 2000; Hartner, Schmittwolf et al. 2004; Wang, Miyakoda et al. 2004; Hartner, Walkley et al. 2009). ADAR2 knockout heterozygotes are viable, but homozygotes exhibit post-natal lethality due to increased seizure susceptibility (Brusa, Zimmermann et al. 1995). In the case of *ADAR2* knockout mice, lethality can be rescued by expression of the AMPA receptor (GluR-B) that bears a mutation mimicking a constitutively edited subunit (Higuchi, Maas et al. 2000). Editing of this transcript, which normally occurs at very high levels, was shown to be dramatically decreased in *ADAR2* null mice, indicating that although overlapping specificities between ADAR1 and ADAR2 exist, editing by ADAR1 is insufficient to edit this transcript to levels required for normal nervous system function and thus ADAR2 bears the responsibility the editing of this transcript in mice (Melcher, Maas et al. 1996; Wong, Sato et al. 2001).

Gene Targets Recoded by A-to-I Editing Are Enriched in the Nervous System.

Many targets of A-to-I editing in vertebrates and invertebrates were discovered by chance when it was observed that mixed A/G peaks in sequences chromatograms from cDNAs mapped back to genomic regions containing only a single A peak. These few known targets were contained within transcripts encoding ligand-gated and voltage-gated ion channels.

In mammals, editing targets that lead to coding changes are limited. However, some of these targets have been well characterized. Glutamate receptor channel subunit transcripts (GluR) are one example. It is thought that four GluR subunits assemble to form a cation channel sensitive to the excitatory neurotransmitter glutamate. AMPA and kainate GluR receptor transcripts share an A-to-I editing site known as the Q/R site, where a conserved glutamine residue in the pore loop region of the channel is changed to an arginine residue by RNA editing (Seeburg and Hartner 2003). Editing at this site affects voltage dependent gating and more importantly the channel's permeability to Ca^{2+}. Editing occurs at nearly 100% efficiency in AMPA (GluRB) subunits and results in decreased permeability to calcium at excitatory synapses. Specific to AMPA (GluRB) subunits, the Q/R editing site was shown to be essential in mice where disruption of editing through mutations in the ECS element resulted in seizures and post-natal lethality (Brusa, Zimmermann et al. 1995; Feldmeyer, Kask et al. 1999). Editing of the Q/R site in kainate receptor subunits (GluR5 and GluR6) is conserved but is not edited at such high levels. GluR5/R6 editing is not essential, however disruption of editing results in increased susceptibility to seizures and defects in synaptic plasticity (Vissel, Royle et al.

2001). These sites are developmentally regulated and increase as the mice approach adult stage. The lower levels of editing at these sites indicate that glutamate receptors achieve diversity through alternative splicing and RNA editing by the presence of mixed populations of subunits available to form channels with both differentially spliced, edited, and unedited subunits coexisting simultaneously. Other vertebrate targets include the serotonin receptor $5HT_{2C}R$ that contains five editing sites clustered within a single exon. Editing of these sites changes 3 amino acids that affect the receptor's coupling to G proteins (Burns, Chu et al. 1997; Wang, O'Brien et al. 2000). Additionally, the voltage-gated potassium channel in humans ($hK_v1.1$) and mammals has a conserved editing site that substitutes a valine (V) for an isoleucine (I) residue in the pore domain of the channel and has been shown to exhibit conservation in its spatial and temporal regulation (Bhalla, Rosenthal et al. 2004). Mutational analysis of this editing site has been shown to alter channel inactivation properties, specifically recovery from fast inactivation, presumably by perturbing interactions between the inactivation particle and its docking site within the pore. While the known targets of editing that produce coding changes in vertebrates seem limited in number, the functional consequences for editing of these targets are important for proper nervous system function and in some cases are essential. As sequencing and bioinformatics technologies advance, more gene products recoded by A-to-I editing may still be discovered.

Unlike vertebrate systems, many RNA editing sites in coding regions have been discovered for *Drosophila* and other closely related *Drosophila* species. So far, the number of genes that contain validated site-specific editing sites is up to 24 and are largely nervous system specific (Jepson and Reenan 2007). In a single large-scale

comparative genomic screen, 16 new genes containing 53 editing sites were identified (Hoopengardner, Bhalla et al. 2003). This approach was made possible by the availability sequenced genomes for many closely related *Drosophila* species, the observed conservation of editing between different species of *Drosophila* such as sites within transcripts of the *paralytic* locus (Hanrahan, Palladino et al. 2000), and the viability of *Drosophila adar* null flies which facilitates the validation of potential editing candidates. Like vertebrates, the genes that are found to contain A-to-I editing sites encode for proteins involved in fast neurotransmission, both chemical and electrical. The recoding events introduced by RNA editing are found in highly conserved or invariant residues of the protein and are predicted, or have been demonstrated, to be functionally important (Figure 1.4). The classes of genes that undergo recoding by RNA editing include both voltage-gated and ligand-gated ion channels, and synaptic release machinery. Conservation of editing between both closely and sometimes distantly related species argues for the functional significance that RNA editing confers to complex nervous system function. The coding regions containing editing sites were found to exhibit a high degree of sequence conservation around the target adenosine between multiple *Drosophila* species and this conservation decreased with distance from the editing target. Furthermore, high sequence conservation was also seen in regions of neighboring introns and likely represents the ECS elements involved in editing of these sites.

A more detailed investigation into the conservation of editing between invertebrate species looked specifically at editing of a single gene, *synaptotagmin I* (*sytI*), which functions as a calcium sensor for neurotransmitter vesicle fusion with the

membrane at neuronal synapses (Reenan 2005). It was demonstrated that *sytI* transcripts contain editing sites that are conserved between many species of invertebrates, but these transcripts can also contain species-specific sites as well. Examination of both the coding regions surrounding these editing sites and the ECS elements between different species revealed both conserved and differing regions of the secondary RNA structures predicted to form within these species. Mutational perturbations to the secondary structures revealed that the highly conserved regions of secondary structure were necessary for species-shared editing sites of sytI and that slight differences in the secondary structure allows for species-specific sites to develop. Indeed even species-specificity could be transferred experimentally through subtle alterations in secondary structure.

Although *Drosophila* has numerous known editing targets and candidate ECS elements to accompany them, the significance of A-to-I editing of these transcripts both at the level of protein function and whole organism physiology is not well understood. Since *dAdar* null flies are viable, it is not likely that any known target of A-to-I editing in *Drosophila* would produce a severe phenotype upon mutation, such as the mammalian Q/R site of *GluR-B*, where editing is essential. The severe neurological and behavioral defects observed in *adar* null flies does suggest that the A-to-I editing at the level of single genes or specific targets within a gene transcript will yield more subtle phenotypes relating to behavioral outputs. *Drosophila* provides a wealth of RNA editing targets to investigate in genes that in some cases have been previously shown to affect animal behavior. One class of "behavioral" genes that was found in the comparative genomic screen to undergo A-to-I recoding in their mRNAs includes certain voltage-gated potassium channels. To date, there have been numerous studies investigating all aspects

of voltage-gated potassium channel (K_V channel) biology that includes, but is not limited to, K_V channel structure, channel physiology including biophysics and pharmacology, its involvement in neurophysiology, disease alleles, and animal behavior and function. Given the wealth of information already available for these targets of A-to-I RNA editing, these genes provide an attractive starting point to investigate the consequences of RNA editing at the individual gene level and the contributions of individual editing sites to overall normal physiology and behavior in the fly. *Shaker*, *ether-a-go-go*, and *Shab*, all K_V channel genes that contain target adenosines for ADAR activity, will be discussed in further detail below, as they are the focus for this current work.

Voltage-Gated Potassium Channels Are Conserved From Bacteria to Humans.

Genes encoding voltage-gated potassium channels are members of a large gene family resulting from gene duplication and subsequent selective mutations through evolution and have a high level of homology to other voltage-gated channels including sodium and calcium voltage-gated channels (Hille 2001). The resulting gene products are similar in that they code for voltage-sensitive, potassium selective channels; however, the members exhibit functional diversity in their gating properties, pharmacology, inactivation properties, and signaling capabilities (Hille 2001; MacKinnon 2003). For example, Shaker channels exhibit a fast, transient current that can activate quickly in response to changes in membrane potential and inactivate very quickly at voltage ranges similar to those that allow for channel opening (Iverson, Tanouye et al. 1988). Conversely, channels such as EAG and Shab open more slowly and do not inactive or inactivate incompletely, thus producing longer, more sustained currents (Robertson,

Warmke et al. 1996; Peng and Wu 2007). Voltage-gated potassium channels are conserved from single-cell organisms such as bacteria and yeast to invertebrates and vertebrates. However, different organisms possess different numbers of K_v channel genes. Amino acid sequence alignment reveals a high level of homology for related K_v channels from many different species and all contain a K+ channel signature motif (TxxTxGYGD) that constitutes the selectivity filter (Hille 2001). In the bacterial KvAP channel, which is thought to be the ancestral K_v channel, the first voltage-gated K^+ channel crystal structure was resolved. Since then, the crystal structure for a mammalian Shaker-type channel has become available as well (Figure 1.5B) (Jiang, Lee et al. 2003; Long, Campbell et al. 2005). This crystal structure exhibited a central conducting pore surrounded by four-fold voltage sensing "paddles" which are largely hydrophobic alpha-helical structures that contain positively charged arginine residues in the S4 voltage sensor.

Voltage-gated Potassium Channels Are Fundamental to the Excitability Properties of Cells by Regulating the Flow of Ions Across the Membrane.

Mutant screens for conditional behavioral phenotypes in *Drosophila* have been wildly successful. One paradigm, ether-induced leg shaking, has resulted in the generation of many mutations affecting K^+-conductances(Kaplan and Trout 1969). Subsequent mapping, cloning, and characterization of the genomic regions containing some of these mutations identified loci that encode different alpha subunits of voltage-gated potassium channels including *Shaker* (*Sh*) and *ether-a-go-go* (*eag*) (Kamb, Iverson et al. 1987; Pongs, Kecskemethy et al. 1988). Related K_V channel gene family members

all encode for similar, yet distinct alpha subunit proteins. The alpha subunits from a given gene function as tetramers to form selective pores in the membranes of excitable cells (MacKinnon 2003; Bezanilla 2005). Each subunit consists of 6 transmembrane domains where the first four domains comprise the voltage sensing domains (S1-S4), and the remaining two (S5 and S6) constitute the pore and contain the selectivity filter of the channel (Figure 1.5A). Additionally, the N-terminal and C-terminal regions of the protein are located on the intracellular side of the membrane. The N-terminal regions contain domains important for tetramerization, such as the T1 domain (Strang, Cushman et al. 2001), as well as associations with accessory subunits (Gulbis, Zhou et al. 2000). The C-termini contain domains that can interact with different signaling molecules (Guy, Durell et al. 1991; Magidovich, Orr et al. 2007). The fourth transmembrane segment, S4, is referred to as the main voltage sensor due to positively charged residues, usually arginine, which respond to changes in the membrane electric field.

Upon membrane depolarization, the charges located in S4 are thought to physically traverse some of the distance through the lipid bilayer in response to changes in membrane potential, and this movement leads to conformational changes that open the pore (Jiang, Ruta et al. 2003). Additional residues have recently been identified in the S2 and S3 domains that assist this motion by stabilizing intermediate conformational states as the S4 region traverses the bilayer via interactions between the arginine/lysine residues and the conserved positions in S2 and S3 (Tao, Lee et al. 2010). When these channels open, K^+ ions are conducted across the membrane at incredible rates ($>10^6$ ions / second) and with high specificity (Hille 2001). Potassium ions, typically found at higher concentrations within the cell compared to the extracellular environment, move down

their electrochemical gradient upon channel opening. Upon activation, the effect of potassium ion flow out of the cell through K^+ channels is the deflection of the membrane potential back toward the negatively polarized resting state. Consequently, voltage-gated potassium channels can regulate the overall excitability of a cell by regulating the resting membrane potential, duration of an action potential, and modulation of successive firing events. The decrease in membrane potential from potassium efflux results in the voltage sensors changing back to their resting conformation thus closing the pore of the channel in a process called deactivation.

Many channels are not limited to these two conformational states (open or closed). Channels such as Shaker in *Drosophila* can also exist in an inactivated form (Figure 1.6). In this case, once the channel opens in response to a change in membrane potential, ion flow can be interrupted by an occlusion of the pore from the intracellular side of the channel (Demo and Yellen 1991). The inactivation particle that occludes the pore can be encoded within the intracellular, N-terminal region of the protein; a process called N-type inactivation (Figure 1.6A), and can interact with residues within the pore of the channel (Zagotta, Hoshi et al. 1990; Zhou, Morais-Cabral et al. 2001). Before the channel can return to a closed conformation, this interaction needs to be disrupted (known as "foot-in-the-door"). Recovery from inactivation allows the channel to return to the fully closed non-conducting state—a prerequisite for further service in the activation process . Additional forms of inactivation can exist with C-type inactivation where the pore is occluded by regions of the C-terminal portion of the protein during prolonged depolarization events (Cordero-Morales, Jogini et al. 2007), and inactivation can be conferred upon a channel through inactivation particles provided by beta

accessory subunits that associate with the channel in a process known as trans-inactivation (Figure 1.6B) (Rettig, Heinemann et al. 1994). Both gating and inactivation kinetics can vary greatly depending on the channel type as well as the form of inactivation in question.

Shaker, Shab, and EAG encode related K_V channels with differing functions.

The *Shaker* locus encodes for the primary alpha subunit responsible for generating a fast-transient (I_A) K^+ current (Hille 2001). These channels possess fast gating kinetics and can also rapidly terminate conductance through N-type inactivation facilitated by an inactivation particle located within the N-terminus of the channel (Iverson, Tanouye et al. 1988; Timpe, Jan et al. 1988; Timpe, Schwarz et al. 1988; Zagotta, Hoshi et al. 1990; Demo and Yellen 1991). These channels can modulate successive firing events through their inactivation properties (Hille 2001) and can regulate the level of initial synaptic release of neurotransmitters at larval neuromuscular junctions and in cell culture (Peng and Wu 2007).

Drosophila Shab locus encodes a protein similar to Shaker channels, but the channels encoded by this locus generate slow, non-inactivating (I_K) currents (Butler, Wei et al. 1989; Covarrubias, Wei et al. 1991). Little is known about the *in vivo* role of these channels; however, studies of excitability at the larval neuromuscular junction and in neuronal cultures indicate that it is involved in regulating the rhythmic, repetitive firing events, likely through repolarization of the membrane following action potentials (Ueda and Wu 2006; Peng and Wu 2007).

Drosophila EAG channels are more unusual than Shaker and Shab. Although they have amino acid sequence similarity to both Shaker and Shab channels, especially within the pore region, these channels appear to be evolutionary "hybrids" in that they also share similarities to cyclic-nucleotide gated channels due to a high degree of similarity in the S2 transmembrane segment and the presence of a cyclic nucleotide binding domain in the C-terminal region of the protein (Drysdale, Warmke et al. 1991; Warmke, Drysdale et al. 1991). Although mutations in *eag* can have affects on multiple K^+ current types (see K_V channel diversity section), the main K^+ current affected in these mutants appear to be delayed rectifier currents (I_K) which responds slowly to depolarization events, but generates a sustained current (Wu, Ganetzky et al. 1983). Expression of *Drosophila* EAG channels in Xenopus oocytes revealed a voltage-dependent, K^+ selective channel that exhibits partial inactivation (Robertson, Warmke et al. 1996). Through the binding of intracellular messengers to these channels, membrane excitability can be altered by changes in neuronal activity. Both cGMP and cAMP were found to increase EAG activity, resulting in increased outward currents (Bruggemann, Pardo et al. 1993). Additionally, phosphorylation by CaMKII (Wang, Wilson et al. 2002), and interactions with the β-accessory subunit, Hyperkinetic, were also shown to enhance K^+ currents generated by EAG (Wilson, Wang et al. 1998). EAG has also been found to interact with second messengers, namely p38 MAP kinase, independent of ion conduction and affects cell proliferation (Hegle, Marble et al. 2006). Supporting this idea, an *eag* isoform generated by alternative splicing was recently identified that lacks the channel forming transmembrane domains while maintaining intracellular binding domains (see Alternative splicing of K_V channels, (Sun, Bostrom et al. 2009).

Hyperexcitability phenotypes arise in K_V gene mutant animals.

Given the role that K_V channels serve in regulating excitability, loss of function in these channels can increase resting membrane potentials as well as overall excitability in cell types such as neurons and muscles. Therefore, mutant animals for these genes exhibit hyperexcitable phenotypes. In the case of both mutations in *Shaker* and *eag,* this can be readily observed by leg shaking when flies are placed under ether anesthesia (Kaplan and Trout 1969). Additionally, studies at the larval muscular junction demonstrate that both *eag* and *Shaker* mutants display increased spontaneous excitatory junction potentials in the motor axon and subsequent increased release of neurotransmitter at the nerve terminal (Budnik, Zhong et al. 1990). The quality of these potentials, both frequency and duration, can differ between *Shaker* and *eag* mutants. *Sh* and *eag* double mutants exhibit a synergistic phenotype relative to either mutant alone, illustrating a genetic interaction between these loci. These hyperexcitable phenotypes can be genetically suppressed by introduction of mutations in voltage-gated sodium channels, such as mle^{napts} that decreases sodium channel expression. Furthermore, these effects appear to be important to the development of synapses at the neuromuscular junction as histology of this region in *Shaker* and *eag* mutants show marked increases in axon branching and the surface area of muscle occupied by these synapses.

In addition to commonly shared hyperexcitable leg-shaking phenotype, *Shaker* mutants also display wing scissoring behavior and aged adult flies show uncoordinated movements and quivering or shaking of their bodies when at rest (Kaplan and Trout 1969). Furthermore, it has been demonstrated that the quality of action potentials is

abnormal in *Shaker* mutants, which exhibit prolonged depolarization events that can be mimicked in wild-type animals through the administration of K^+ channel blocker, 4-aminopyridine (Tanouye, Ferrus et al. 1981). Since both processing and integration of sensory inputs depend on neuronal firing properties for the generation of correct behavioral outputs, it is not surprising that mutations in K_V channels can result in behavioral defects. These behavioral defects include locomotion, flight behavior, sensory perception such as olfaction, sleep, and learning and memory (Lichtinghagen, Stocker et al. 1990; Balakrishnan and Rodrigues 1991; Gasque, Labarca et al. 2006). These last two behaviors are particularly interesting in that the process of sleep and memory formation/retention appear to be linked.

Sleep is a highly conserved process across the animal kingdom, and *Drosophilidae* are no exception. Indeed, many features of sleep are exhibited in flies where circadian and metabolic components govern sleep (e.g. increased arousal thresholds follow sleep and sleep recovery follows deprivation (Cirelli and Bushey 2008)). Sleep is absolutely necessary as long-term sleep deprivation is lethal. However, the function of sleep is not well understood. Some competing ideas for the purpose of sleep include energy conservation, immune system function and repair, learning and memory consolidation, and homeostatic maintenance of brain function. A point mutation in *Shaker* (Sh^{mns}) was found in a mutant screen to dramatically reduce daily amounts of sleep in these flies compared to wild-type controls (Cirelli, Bushey et al. 2005). This point mutation changes a highly conserved threonine (T) residue in extracellular loop at the end of S1 to an isoleucine (I). This decrease in sleep was found to result from reductions in the duration of sleep rather than the number of sleep bouts. Sh^{mns} flies

maintain circadian rhythmicity for activity and also attempt to recover lost sleep following deprivation. These flies also performed normally in various tasks, but unlike wild-type flies, their performance was not affected following sleep deprivation. Furthermore, these flies exhibited reduced life spans compared to wild-type flies.

Discovery of the *minisleep* mutation was the first example of a K^+ channel gene being implicated in sleep. Since then other gene targets that interact with Shaker channels have also been found to affect sleep as well as memory deficits by affecting the I_A current elicited by Shaker channels. Loss of function mutants in *Hyperkinetic* (*Hk*), which encodes for the β-accessory subunit that associates with and modifies activity in Shaker and EAG channels, also exhibit reduced sleep (Bushey, Huber et al. 2007). This effect is mediated through *Hk* interaction with *Shaker*, as *Hk* / *Sh* double mutants do not exhibit synergistic effects with respect to the short sleeping phenotype. Rescue of this phenotype was achieved by expression of a wild-type copy of *Hk*. These short-sleeping flies were tested for learning and memory defects using a heat-box paradigm (Diegelmann, Zars et al. 2006) where flies are placed in a bisected piezoelectric chamber where temperature is independently controlled in each half. Flies are "trained" in this scenario when one side of the box is heated to ~39°C, while the other side is held at a more comfortable temperature of 22°C. During these training sessions, flies "learn" to have a preference for the cooler side of the box. Flies are tested by returning them to the chamber where both sides are now held at 22°C. Flies are measured to see if they maintain a preference for the lower temperature side during the training periods. Short-sleeping flies mutant for *Hk*, developed a preference for the cool side of the chamber, similar to wild-type flies. However, this preference was not maintained like wild-type

flies following training, suggesting defects in short-term memory. These memory deficits were also rescued by transgene expression of wild-type Hk in the nervous system. This study helped not only reinforce the idea that neuronal excitability, especially through I_A currents, is involved in generating normal sleep but further demonstrated a link between the requirement of sleep for memory formation.

More recently, a forward genetic screen for abnormal sleep phenotypes identified a protein that affects *Shaker* expression, termed *sleepless* (*sss*). Mutations in *sss* resulted in a dramatic (~80%) reduction in total sleep in mutant flies, again attributed to decreased sleep bout duration and decreased amounts of sleep bouts (Koh, Joiner et al. 2008). These flies also had reduced sleep recovery following sleep deprivation. This study also characterized a known mutant *quiver* (shown to affect *Shaker*-mediated currents) as an allele of *sss* in complementation tests. Indeed, expression levels of Shaker protein were significantly reduced in *sss* mutants, demonstrating the link that this mutant affects sleep through its regulation of Shaker expression. This *sss* locus is thought to encode for a glycosylphosphatidylinositol (GPI)-anchored protein and further studies classified this protein as a Ly-6/neurotoxin family member that could potentially complex with K_V channels like Shaker either at the plasma membrane or within the endoplasmic reticulum (Wu, Joiner et al. 2009). This study found overlapping expression of *Sh* and *sss* in both the central and peripheral nervous systems of wild-type flies. In *sss* mutants, Sh expression is both dramatically reduced and mislocalized to cell bodies rather than fiber tracts. Transgene expression of *sleepless* in wake-promoting, cholinergic neurons rescued the short-sleeping phenotype, suggesting that decreased excitability in these neurons in required for normal sleep maintenance. Furthermore, Shaker and sss appear to affect

each other's expression levels. Sleepless is thought to either bind directly to Shaker channels to help form stabilized complexes and promote Shaker channel trafficking to, or retention at the membrane. These studies clearly implicate Shaker–dependent currents in regulating excitability within neural circuits involved in sleep maintenance. How excitability changes during sleep and wake cycles to promote normal balance between activity and sleep remain to be understood.

The role of Shaker channel biology in learning and memory processes is conserved in mice and rats as well. RNAi knockdown experiments directed at $K_V1.1$ in rats demonstrated that decreased expression of this channel leads to memory impairment in multiple learning paradigms, and this effect is reversible when antisense inhibition is removed (Meiri, Ghelardini et al. 1997). Furthermore, mutations that knockout $K_V\beta1.1$ in mice, the accessory subunit that interacts with $K_V1.1$ channels to confer inactivation, increased neuronal excitability. This resulted in mutant aged mice performing better than wild-type animals in a water maze to measure spatial learning, suggesting that decreases in excitability could be a mechanism for age-related mental decline (Murphy, Fedorov et al. 2004).

Mutations in the vertebrate homologs of *Shaker* (*KCNA*/$K_V1.1$) result in hyperexcitability and seizure susceptibility (Rho, Szot et al. 1999; Rajakulendran, Schorge et al. 2007). In humans, mutations in these channels can result in various forms of generalized epilepsy and more specifically, movement disorders such as episodic-ataxia (EA1) and neuromyotonia. Episodic ataxia is characterized by periods of uncoordinated movement (ataxia), and between episodes, chronic muscle contraction or rippling (myokymia) can be observed. Stress and sudden or vigorous voluntary

movements aggravate this condition. Several missense mutations, inherited in an autosomal dominant fashion, have mapped to *KCNA1* (Browne, Gancher et al. 1994; Imbrici, Gualandi et al. 2008; Demos, Macri et al. 2009). These mutations generate substitutions in highly conserved residues within the channel subunit. Expression of these mutant channels in Xenopus oocytes, reveal decreased currents as well as changes in gating properties, including shifts in voltage dependence to more positive potentials and slowed inactivation kinetics (Boland, Price et al. 1999). Disorders involving hyperexcitability at the neuromuscular junction, such neuromyotonia, also involve mutations in *KCNA1,* but can also be an acquired through an autoimmune-based mechanism where generation of endogenous antibodies directed against these channels at the NMJ is thought to disrupt channel activity (Maddison 2006; Poujois, Antoine et al. 2006). Both vertebrate (including humans) and invertebrate Shaker channels share a high level of amino acid identity (~75%), as well as many characteristics of human epilepsy. Therefore, seizure modeling in both rodents and *Drosophila* provide attractive models in which the pathology of human epilepsy disorders can be further investigated (Rho, Szot et al. 1999; Glasscock, Qian et al. 2007; Song and Tanouye 2008). These models hold great promise for investigation of genetic interactions leading to enhancement or suppression of seizures, as well as providing a system to test the efficacy of pharmacological agents used to treat this disorder.

Mutant phenotypes of *eag* can contribute to those produced by other K_V channel mutants, such as *Shaker*. Mutations in *eag* can affect potassium currents distinctly encoded for by other K_V channel genes (Zhong and Wu 1991). In addition, EAG channel's ability to interact with intracellular signaling molecules through its conserved

nucleotide binding domain and the presence of putative phosophorylation sites provide additional mechanisms by which these channels can influence neuronal plasticity and behavior (Bruggemann, Pardo et al. 1993; Wang, Wilson et al. 2002; Hegle, Marble et al. 2006).

One process affected in *eag* mutant flies is olfaction. *eag* animals were unable to detect a subset of odorants including short chain ketones, acetate esters and propionic acid (Dubin, Liles et al. 1998). Electroantennogram recordings showed decreased activity compared to wild-type controls in response to exposure with this specific set of odorants. The decreased sensitivity toward exogenous sources of cyclic-nucleotide analogs (cAMP and cGMP) in *eag* mutants support the idea that decreased sensitivity toward these odorants likely results from defects in signal transduction pathways through which the cyclic nucleotide binding domain of EAG channels is involved.

In addition to olfaction, there is a demonstrated link between EAG function, calcium/calmodulin protein kinase II (CaMKII) activity, and learning and memory. Inhibition of either CaMKII by peptide inhibitors expressed in transgenic flies or mutations that abolish EAG activity both result in learning defects in multiple behavioral paradigms as well as hyperexcitability at the larval neuromuscular junction (Griffith, Verselis et al. 1993; Griffith, Wang et al. 1994). This suggests that a similar pathway for learning, memory, and normal synaptic function requires the activity of both EAG channels and CaMKII activity. Indeed, it was later demonstrated that these two proteins not only directly interact, but they can regulate each other's activity. First, EAG was found to be a substrate of CaMKII, where a conserved threonine residue located in the c-terminus of the protein is phosphorylated by CaMKII. This phosphorylation event

increases channel activity as loss of this regulation results in decreased currents and enhanced inactivation of this channel (Wang, Wilson et al. 2002). Conversely, in the presence of increased intracellular calcium levels or calmodulin, both indicative of increased neuronal activity, CaMKII was found to bind and form a complex with the C-terminal intracellular domain of EAG channels. This interaction leads to activation of CaMKII by phosphorylation, similar to autophosphorylation, and this interaction as well as activation of CaMKII persists after intracellular calcium/calmodulin levels drop (Sun, Hodge et al. 2004). This established a link between excitability at the neuronal membrane with intracellular signaling cascades which likely feedback to further modulate neuronal excitability and plasticity.

These few examples of how both *Shaker* and *eag* can genetically interact and the resulting phenotypes that arise when these protein functions are disrupted provide insight into how overall excitability plays a central role in neuronal plasticity. Membrane excitability as well as the downstream intracellular signaling effects demonstrates the necessity for these processes in sensory perception, the generation of correct behavioral responses to various stimuli, complex phenomena such as memory and sleep, and the tuning of fine motor control. Undoubtedly, future studies looking at Shaker and EAG function will likely uncover additional involvement in the generation and regulation of complex behaviors.

Post-transcriptional Modifications Increase K_v Channel Diversity

Different types of neurons have distinct excitability properties, and this is achieved in part by differential expression of diverse arrays of voltage-gated potassium channels in a cell-specific manner. This diversity can arise from differential expression of various Kv channel genes, but post-transcriptional modifications to Kv channel transcripts and formation of heterotetrameric complexes enhance the level of diversity even further.

Alpha subunits of similar type form tetrameric complexes that constitute a functioning K^+ channel, mediated through the cytoplasmic, N-terminal T1 domains (Covarrubias, Wei et al. 1991; Shen and Pfaffinger 1995). This process is also facilitated through the association of beta accessory subunits that interact with each alpha subunit through this domain as well, and can be observed in a resolved crystal structure (Gulbis, Zhou et al. 2000). This differs from Na^+ and Ca^{2+} voltage-gated channels that have four repeated domains (homologous to the K^+ channel alpha subunit) contained within a single transcript and opens the possibility for increased diversity through the regulation of K^+ channel assembly. The first evidence of the potential for different alpha subunits to form channels came from the observation that *eag* mutants influenced different types of potassium currents in larval muscle that are known to be eliminated in other K_v channel gene mutants such as *Shaker* and *slopoke* (Zhong and Wu 1991). This observation has raised the possibility that the *EAG* subunit may coassemble with other alpha subunits, such as those encoded by the *Shaker* locus, to form novel channels with unique properties. Further studies have investigated this possibility both in heterologous expression systems as well as *in vivo*. In heterologous expression systems where both

Shaker and *eag* are expressed in *Xenopus* oocytes, it was demonstrated that functional channels can form and that the fast-transient current generated by *Shaker* channels is affected when expressed in the presence of *eag*. The observed effects involved changes in the inactivation kinetics of the fast-transient current, and were mediated through the C-terminal portion of the EAG subunit where intracellular second messengers can interact with this protein (Chen, Hoshi et al. 1996). Studies performed *in vivo* have also been utilized to investigate the genetic interactions between *Shaker* and *eag* mutant alleles. An array of effects in the fast-transient Shaker current (I_A) from electrophysiology studies in larval muscle preparations generated by allele-specific combinations, demonstrate the interaction of these genes (Zhong and Wu 1993). Furthermore, this study also perturbed EAG channel function pharmacologically with antagonists to Ca^{2+}/calmodulin and application of cGMP and found effects in I_A that were eliminated in an *eag* mutant background. These results, taken together, support a model where *eag* likely contributes a common subunit to different K^+ channels. However, there have been conflicting results with this expression system that appear to be the result of differences in experimental conditions, as others have failed to recapitulate effects in I_A when co-expressing these channel subunits and could not demonstrate direct association of these subunits in immunoprecipitation studies (Tang, Schulteis et al. 1998).

Further diversity of K_V channel subunits can be achieved through alternative splicing of pre-mRNA transcripts. Most alternative splicing that occurs for a given transcript generate variation at the 5' and 3' ends with a constitutively conserved core of approximately 8 exons that represent the transmembrane domains of the subunit (Kamb, Iverson et al. 1987; Pongs, Kecskemethy et al. 1988; Schwarz, Tempel et al. 1988).

Thus, most variation generated, but not all, exists in the N-terminal and C-terminal intracellular regions of the protein and leads to changes in the hydrophobic qualities of the region. Most characterization of alternative splicing in K_V channel transcripts has occurred in *Shaker*. Originally, four different cDNAs (ShA-D) from *Shaker* were identified and characterized (Iverson, Tanouye et al. 1988; Timpe, Jan et al. 1988; Timpe, Schwarz et al. 1988). Here, a central conserved core of exons was present within the all transcript types and variation was observed at the 5' and 3' ends of the transcript. Variation at the 3' end of the transcript exists in two forms generated by two distinct clusters of exons. Each of the two alternative exon groups are shared by two splice forms, where ShA and ShC are identical in their 3' ends as ShB and ShD are identical in theirs. There is more variation in the 5' ends of *Shaker* transcripts where 3 alternative exons are available to chose from. Functional studies of these different transcripts express in *Xenopus* oocytes demonstrate that the four isoforms all produce voltage-dependent potassium channels that produce the fast-inactivating current characteristic to I_A, but with slightly differing kinetics. Specifically, these splice variants all appear to have similar rates of activation and voltage dependence, so it is thought that regions conserved between all splice variants, the core transmembrane domains, are responsible for governing these properties. Variability exists in the N- and C-termini and here it is demonstrated that differentially spliced forms of the channel show differences in rates of inactivation and recovery from inactivation, showing these intracellular regions govern these processes.

Distribution of different *Shaker* isoforms is extensive and overlapping. Methods including immunostaining with antibodies that specifically bind to certain isoforms of

Shaker as well as antibody staining in mutant backgrounds deficient for certain splice forms have been employed to examine the spatial distribution of *Shaker* isoform expression at different stages of development (Schwarz, Papazian et al. 1990; Rogero and Tejedor 1995; Rogero, Hammerle et al. 1997). Shaker channel expression was detected throughout development but is higher in third-instar larvae and late pupae and peak levels are observed at adulthood. Staining shows that while *Sh* channels are expressed throughout the nervous system, the pattern is discrete and non-uniform. The staining patterns of specific splice variants of Sh exhibit overlapping staining patterns and these patterns change as development progresses. These studies demonstrate that many Shaker isoforms are utilized throughout development and in the functioning adult nervous system to generate diverse excitability properties in the nervous system in a highly specific manner. Beyond studies involving these four isoforms, there are currently 9 annotated transcripts contained in the *Drosophila* genome databases (http://flybase.org) although the function and expression of these additional splice variants have yet to be characterized. Hence, there is the possibility for identification of even more splice variants for this transcript in the future.

Less is known about alternative splicing of transcripts derived from other K_V channel genes such as *eag* and *Shab*. Even though alternative splice products are observed in channel transcripts such as *eag*, which currently has four annotated transcript isoforms, the specific properties of these channels and the effect they have in regulating excitability has yet to be determined. Recently, however, a new splice variant of *eag* was reported which lacks the sequences encoding for the transmembrane domains of the peptide and is predicted to not form a channel (Sun, Bostrom et al. 2009). The

occurrence of this spliced product is induced by the presence of PKA and PKC and is thought to serve as a scaffold protein capable of engaging in intracellular signaling cascades. Lastly, aberrant splicing of the *eag* human homolog (hERG) was shown to produce a channel that fails to target to the membrane (Gong, Zhang et al. 2008). The mutation leading to this abnormal splicing was determined to be one pathogenic mechanism in the development of type 2 long-QT cardiac syndrome that is characterized by prolonged action potentials in cardiac muscles.

Although the picture of alternative splicing in K_V channel transcripts is far from complete, it is clear that this form of post-transcriptional gene regulation is utilized by cells to greatly increase the diversity of channel proteins generated, even from a single gene. Ultimately this aids in allowing cells to finely tune their excitability properties with expression of unique arrays of channels with diverse functional properties.

More recently it has become apparent that K_V channels can undergo recoding events facilitated by A-to-I RNA editing as a means of diversifying and/or regulating the functional properties of these proteins and thus the excitability of cells. Some K_V channel editing was discovered during a large comparative genomic screen (Hoopengardner, Bhalla et al. 2003) and includes the genes *Shaker*, *eag*, and the human *Shaker* homolog *$hK_V1.1$*. This editing was found to be conserved across multiple species and recodes highly conserved residues within these transcripts. Other K_V channel targets were discovered accidentally when studies aimed at cloning K_V channels revealed sequence variation between clones, such as the case for the squid K_V2 channel (Patton, Silva et al. 1997). The regulation of the editing events for these targets and more importantly the

functional consequences at both the protein level and whole organism function are not well known.

A more in-depth study of A-to-I editing of K_V channels has been reported for the single editing site located in $hK_V1.1$ (Bhalla, Rosenthal et al. 2004). This editing site results in the substitution of a highly conserved isoleucine residue (I400) to valine in the S6 pore-lining region of the channel. This editing site was conserved in *Drosophila Shab* channels and their homolog in squid (sqK_V2), but not in *Drosophila Shaker* channels. Furthermore, it was found that editing of *$hK_V1.1$* transcripts showed a spatial regulation with highest levels of editing observed in the medulla, thalamus, and spinal cord. This spatial distribution was also conserved in mice and rats. Since the $hK_V1.1$ gene (*KCNA1*) is entirely exonic, there were no introns to look for ECS elements directing editing. In the case of this gene, deletions surrounding the editing site defined the minimal sequence region capable of directing editing, and this region was predicted and experimentally verified through mutational analysis to form a hairpin structure. Electrophysiology studies comparing edited and unedited channels showed that editing altered the kinetics of inactivation by β-accessory subunits. Specifically, editing at this site decreased the extent of inactivation and increased the rate of recovery from inactivation. When this mutation was introduced into fly Shaker channels, the effect was similar even though this specific site is not found in this gene. This study helped to provide insight into how RNA editing can be utilized to change the functional properties of a protein to suit the needs of a cell beyond the constraints of genomic information.

Recently, further studies investigating this I400V site in $hK_V1.1$ have shown that editing of this target can affect its response to the presence of intracellular lipids such as

arachadonic acid (Decher, Streit et al. 2010). Building on previously reported data demonstrating the ability of highly unsaturated fatty acids (HUFAs) to confer inactivation on non-inactivating channels (Oliver, Lien et al. 2004), this group sought to investigate the mechanism that supports these observations. HUFAs were found to interact with $hK_V1.1$ channels from the intracellular side of the membrane and competed for binding with both β-subunits and chemicals known to block the channel's open pore. Further, binding of arachadonic acid binding was found to interfere with deactivation kinetics for these channels at negative membrane potentials, suggesting that HUFAs can inactivate these channels through and "open channel block." When channels were expressed with the I400V edit, the channels were resistant to inactivation mediated by arachadonic acid. These results, taken together with studies looking at editing effects on β-subunit mediated inactivation, indicates that editing of this conserved residue is a means by which a cell can regulate potassium conductance by changing the inactivation properties of its voltage gated K^+ channels.

More interestingly, experiments expressing different stoichiometric ratios between edited and unedited alpha subunits of $hK_V1.1$ indicate that even a single edited subunit within the tetramer is sufficient to confer this resistance to inactivation on the whole channel. Until now, it was not known whether effects generated by editing were dominant, or additive in that some gradient of effects would be generated that depends on the number of subunits edited. It appears that at least for this target, editing of one subunit is sufficient, but this may or may not be the case for different editing sites in other genes. This evidence does change our perception of RNA editing, particularly when considering the levels of editing for a given target. It is now apparent that lower

levels of editing observed for a given target will not necessarily translate to reduced effects on protein activity. Especially with edited proteins that function as multimers, there is now the possibility that the effects conferred by even low levels of editing can be amplified in the correct context.

Earlier studies investigating K_V channel transcript editing came from squid such as *Loligo pealei*. Discovery of K_V channel editing in squid occurred when the channel K_V2, the homolog to *Drosophila Shab* and human *KCNB* channels, was cloned and found to have A/G sequence mismatches in cDNAs that did not agree with the genomic sequences (Patton, Silva et al. 1997). A total of 17 of these sites were identified between the regions of S4 and S6, and resulted in 12 possible amino acid substitutions. While many of these sites were edited at low levels (~10%), four sites were edited at higher levels. Three of these sites showed >90% editing and include two I/V changes, one in S4 and the other in S6, and a Y/C change in the pore loop region of the channel. The I/V edit site in S6 is the conserved site seen in $hK_V1.1$ and *Drosophila Shab* channel transcripts. A fourth site, edited at around 30%, changes a serine residue in S6 to glycine. Functional studies for channels containing the Y/C site in the pore, or I/V in S6 showed effects on channel deactivation kinetics and the rate of slow inactivation. Similar to other genes with editing sites in the conducting region, it appears that editing can play a substantial role in gating and conductance properties of K_V channels.

In addition to changes in channel kinetics, RNA editing appears to regulate channel assembly as well. Editing sites identified within the highly conserved T1-domain in squid $K_V1.1A$ channels show that these sites can affect both the expression level of functional channels as well as gating properties (Rosenthal and Bezanilla 2002).

While expression of fully edited channels (within the T1 domain) did not produce detectable currents, singly edited and combinations of editing sites together did with varying properties. Two sites within the T1 domain, N45S and K132E, both shifted the voltage dependence of activation to more positive potentials and increased rates of deactivation. Other single editing sites within this region had little to no effect on these parameters. The R87G editing event recodes a residue within a highly conserved motif within the T1 domain and was shown to dramatically decrease the amount of functional channels expressed to ~3% compared to genomic (fully unedited) channel levels. Other single editing sites within this region were also shown to decrease functional expression, but not as extensively (30% to 60% reduction compared to unedited expression levels). Transcripts from this gene were also found to contain editing sites within its transmembrane domains (S1, S3), and a single edit site in the pore. Channels fully edited in these regions exhibit decreased conductance with relation to voltage and also deactivate faster than the genomic version of the channel. Single edit sites within these regions were found to contribute to these observed differences in varying degrees. While the effects of transmembrane editing sites on gating are interesting, the sites within the T1 domain affect both channel formation as well as gating. How T1 edit sites help regulate subunit interaction is not clear. These effects could be the result of direct interactions between these residues from different subunits, or they could be more indirect by modifying the secondary structure of these regions. What is even less clear, is how editing of these residues in this N-terminal region regulates gating properties for the channel. However, mutations within the T1 domain have been shown to affect voltage dependence and deactivation kinetics, establishing a role for T1 domain interactions with

channel gating (Cushman, Nanao et al. 2000). Regardless, editing of this gene transcript in squid enables simultaneous regulation of channel expression and gating properties.

In the comparative genomic study that identified nervous system targets subject to A-to-I recoding events in *Drosophila* (Hoopengardner, Bhalla et al. 2003), both *Shaker* and *eag* were found to contain multiple editing sites predicted to generate amino acid substitutions (Figure 1.7). Editing within *Shaker* transcripts occurs within five sites distributed throughout the transcript. The first site actually contains two adenosine residues in the first and second position within the reading frame and is predicted to recode a lysine residue within the T1 tetramerization domain to glutamate, arginine, or glycine depending on the editing combination of these two residues. A single editing site within the extracellular loop adjacent to the S4 voltage sensor recodes an isoleucine residue to methionine. The last three sites reside within the S6 pore region (isoleucine/valine), and the intracellular C-terminus where editing recodes a threonine residue to alanine and glycine to arginine.

The editing sites contained within *eag* transcripts are restricted to the pore and intracellular C-terminal regions. The first site is located on the extracellular vestibule of the pore where a lysine residue is substituted to arginine. The remaining sites introduce substitutions either within, or adjacent to, the cyclic nucleotide binding domain in the C-terminus of the subunit (tyrosine/cystine, asparagine/aspartic acid and lysine/arginine). Beyond the predicted amino acid substitutions generated through A-to-I RNA editing of these transcripts, the biological significance of editing these site and how they affect channel function are unknown. However, the recoding events do occur in functionally

significant regions of the protein and likely alter channel function in unique ways that other post-transcriptional regulation cannot produce.

Hypothesis and Current Motivations for this Study

The preceding sections highlight both A-to-I RNA editing as a powerful form of post-transcriptional mRNA modification that can greatly enhance the coding potential of genes, and the biological significance of one class of genes targeted by this form of regulation, voltage-gated potassium channels. These targets provide an ideal starting point to further enhance our understanding of this post–transcriptional regulation as it relates to proper nervous system function. The available crystal structure enables us to better appreciate where substitutions induced by RNA editing exist within the three-dimensional context of the channel. This is accompanied by a vast foundation of information that detail channel physiology and phenotypic effects in mutant animals. This makes examining RNA editing in these genes particularly attractive. Furthermore, *Drosophila* provide an excellent model system to study RNA editing due to the straightforward genetic manipulations in this system, the viability of the *dAdar* null mutants, established behavioral and physiological assays developed to assess nervous system function, and the availability of annotated genomes for multiple different *Drosophila* species.

Given the severe neurological and behavioral defects observed in *dAdar* null flies, and the role of voltage-gated potassium channels in nervous system function and the generation of complex behaviors, the expectation is that K_V channel editing should modulate behavior and fine motor skills. I would also anticipate that the specific

behaviors such as gross motor skills, hyperexcitability, sensory perception, sleep, and learning and memory to be the physiological and behavioral processes most affected by perturbations in RNA editing of these targets due to their previous implications with different mutant alleles of these genes.

In this study, I examine the post-transcriptional gene regulation of the K_V channel transcripts *Shaker*, *Shab* and *eag* in *Drosophila*. These studies further our understanding of how these events are regulated within these channel transcripts. Specifically, I assess both the spatial and temporal control of RNA editing of these targets within the fly, as regulation of editing in this manner has been previously demonstrated for other gene targets. Furthermore, I identify the cis-regulatory elements (ECS) directing editing of these substrates to further our knowledge of how editing of these channels is achieved.

In collaborative efforts, I examine channel function as it relates to different editing states. Previously examined K_V channels that undergo editing were shown to have alterations in their kinetic parameters such as inactivation introduced through A-to-I editing. Understanding how editing affects the kinetic properties of other K_V channel targets, such as *Shaker* and *Shab*, provide a better understanding of the range of functional diversity that these channels are capable of and help us predict how editing of certain sites may affect overall excitability for the neurons that express these channels.

Lastly, I investigate the *in vivo* effects of K_V channel editing by introducing mutations into the *Shaker* and *eag* loci of the fly genome by homologous recombination. These changes generate flies deficient for editing by introducing mutations in ECS elements that disrupt the duplex environment surrounding the editing target or by simply changing the codon by removing the available target adenosine. Additionally, mutations

that hardwire guanosine into the genomic locus to mimic constitutively edited channel transcripts are introduced. In this system, the specific contribution of these editing events as they relate to fly physiology and behavior are investigated within an otherwise wild-type context where the expression and function of the dADAR enzyme as well as the editing events in other targets of RNA editing remains uninterrupted. It is in the context of this system, that the significance of Shaker and EAG editing in producing proper coordination and fine motor skills, as well as complex behaviors is revealed.

Literature Cited

Aruscavage, P. J. and B. L. Bass (2000). "A phylogenetic analysis reveals an unusual sequence conservation within introns involved in RNA editing." Rna **6**(2): 257-69.

Balakrishnan, R. and V. Rodrigues (1991). "The shaker and shaking-B genes specify elements in the processing of gustatory information in Drosophila melanogaster." J Exp Biol **157**: 161-81.

Basilio, C., A. J. Wahba, et al. (1962). "Synthetic polynucleotides and the amino acid code. V." Proc Natl Acad Sci U S A **48**: 613-6.

Bass, B. L. (2002). "RNA editing by adenosine deaminases that act on RNA." Annu Rev Biochem **71**: 817-46.

Betts, L., S. Xiang, et al. (1994). "Cytidine deaminase. The 2.3 A crystal structure of an enzyme: transition-state analog complex." J Mol Biol **235**(2): 635-56.

Bezanilla, F. (2004). "RNA editing of a human potassium channel modifies its inactivation." Nat Struct Mol Biol **11**(10): 915-16.

Bezanilla, F. (2005). "Voltage-gated ion channels." IEEE Trans Nanobioscience **4**(1): 34-48.

Bhalla, T., J. J. Rosenthal, et al. (2004). "Control of human potassium channel inactivation by editing of a small mRNA hairpin." Nat Struct Mol Biol **11**(10): 950-6.

Black, D. L. (2003). "Mechanisms of alternative pre-messenger RNA splicing." Annu Rev Biochem **72**: 291-336.

Boland, L. M., D. L. Price, et al. (1999). "Episodic ataxia/myokymia mutations functionally expressed in the Shaker potassium channel." Neuroscience **91**(4): 1557-64.

Browne, D. L., S. T. Gancher, et al. (1994). "Episodic ataxia/myokymia syndrome is associated with point mutations in the human potassium channel gene, KCNA1." Nat Genet **8**(2): 136-40.

Bruggemann, A., L. A. Pardo, et al. (1993). "Ether-a-go-go encodes a voltage-gated channel permeable to K+ and Ca2+ and modulated by cAMP." Nature **365**(6445): 445-8.

Brusa, R., F. Zimmermann, et al. (1995). "Early-onset epilepsy and postnatal lethality associated with an editing-deficient GluR-B allele in mice." Science **270**(5242): 1677-80.

Budnik, V., Y. Zhong, et al. (1990). "Morphological plasticity of motor axons in Drosophila mutants with altered excitability." J Neurosci **10**(11): 3754-68.

Burns, C. M., H. Chu, et al. (1997). "Regulation of serotonin-2C receptor G-protein coupling by RNA editing." Nature **387**(6630): 303-8.

Bushey, D., R. Huber, et al. (2007). "Drosophila Hyperkinetic mutants have reduced sleep and impaired memory." J Neurosci **27**(20): 5384-93.

Butler, A., A. G. Wei, et al. (1989). "A family of putative potassium channel genes in Drosophila." Science **243**(4893): 943-7.

Cattaneo, R., A. Schmid, et al. (1988). "Biased hypermutation and other genetic changes in defective measles viruses in human brain infections." Cell **55**(2): 255-65.

Chen, M. L., T. Hoshi, et al. (1996). "Heteromultimeric interactions among K+ channel subunits from Shaker and eag families in Xenopus oocytes." Neuron **17**(3): 535-42.

Chilibeck, K. A., T. Wu, et al. (2006). "FRET analysis of in vivo dimerization by RNA-editing enzymes." J Biol Chem **281**(24): 16530-5.

Cho, D. S., W. Yang, et al. (2003). "Requirement of dimerization for RNA editing activity of adenosine deaminases acting on RNA." J Biol Chem **278**(19): 17093-102.

Cirelli, C. and D. Bushey (2008). "Sleep and wakefulness in Drosophila melanogaster." Ann N Y Acad Sci **1129**: 323-9.

Cirelli, C., D. Bushey, et al. (2005). "Reduced sleep in Drosophila Shaker mutants." Nature **434**(7037): 1087-92.

Cordero-Morales, J. F., V. Jogini, et al. (2007). "Molecular driving forces determining potassium channel slow inactivation." Nat Struct Mol Biol **14**(11): 1062-9.

Covarrubias, M., A. A. Wei, et al. (1991). "Shaker, Shal, Shab, and Shaw express independent K+ current systems." Neuron **7**(5): 763-73.

Cushman, S. J., M. H. Nanao, et al. (2000). "Voltage dependent activation of potassium channels is coupled to T1 domain structure." Nat Struct Biol **7**(5): 403-7.

Dawson, T. R., C. L. Sansam, et al. (2004). "Structure and sequence determinants required for the RNA editing of ADAR2 substrates." J Biol Chem **279**(6): 4941-51.

Decher, N., A. K. Streit, et al. (2010). "RNA editing modulates the binding of drugs and highly unsaturated fatty acids to the open pore of Kv potassium channels." Embo J.

Demo, S. D. and G. Yellen (1991). "The inactivation gate of the Shaker K+ channel behaves like an open-channel blocker." Neuron **7**(5): 743-53.

Demos, M. K., V. Macri, et al. (2009). "A novel KCNA1 mutation associated with global delay and persistent cerebellar dysfunction." Mov Disord **24**(5): 778-82.

Diegelmann, S., M. Zars, et al. (2006). "Genetic dissociation of acquisition and memory strength in the heat-box spatial learning paradigm in Drosophila." Learn Mem **13**(1): 72-83.

Ding, Y., C. Y. Chan, et al. (2005). "RNA secondary structure prediction by centroids in a Boltzmann weighted ensemble." Rna **11**(8): 1157-66.

Drysdale, R., J. Warmke, et al. (1991). "Molecular characterization of eag: a gene affecting potassium channels in Drosophila melanogaster." Genetics **127**(3): 497-505.

Dubin, A. E., M. M. Liles, et al. (1998). "The K+ channel gene ether a go-go is required for the transduction of a subset of odorants in adult Drosophila melanogaster." J Neurosci **18**(15): 5603-13.

Feldmeyer, D., K. Kask, et al. (1999). "Neurological dysfunctions in mice expressing different levels of the Q/R site-unedited AMPAR subunit GluR-B." Nat Neurosci **2**(1): 57-64.

Feng, Y., C. L. Sansam, et al. (2006). "Altered RNA editing in mice lacking ADAR2 autoregulation." Mol Cell Biol **26**(2): 480-8.

Gallo, A., L. P. Keegan, et al. (2003). "An ADAR that edits transcripts encoding ion channel subunits functions as a dimer." Embo J **22**(13): 3421-30.

Gasque, G., P. Labarca, et al. (2006). "Bridging behavior and physiology: ion-channel perspective on mushroom body-dependent olfactory learning and memory in Drosophila." J Cell Physiol **209**(3): 1046-53.

Glasscock, E., J. Qian, et al. (2007). "Masking epilepsy by combining two epilepsy genes." Nat Neurosci **10**(12): 1554-8.

Gong, Q., L. Zhang, et al. (2008). "A splice site mutation in hERG leads to cryptic splicing in human long QT syndrome." J Mol Cell Cardiol **44**(3): 502-9.

Griffith, L. C., L. M. Verselis, et al. (1993). "Inhibition of calcium/calmodulin-dependent protein kinase in Drosophila disrupts behavioral plasticity." Neuron **10**(3): 501-9.

Griffith, L. C., J. Wang, et al. (1994). "Calcium/calmodulin-dependent protein kinase II and potassium channel subunit eag similarly affect plasticity in Drosophila." Proc Natl Acad Sci U S A **91**(21): 10044-8.

Gulbis, J. M., M. Zhou, et al. (2000). "Structure of the cytoplasmic beta subunit-T1 assembly of voltage-dependent K+ channels." Science **289**(5476): 123-7.

Guy, H. R., S. R. Durell, et al. (1991). "Similarities in amino acid sequences of Drosophila eag and cyclic nucleotide-gated channels." Science **254**(5032): 730.

Hanrahan, C. J., M. J. Palladino, et al. (2000). "RNA editing of the Drosophila para Na(+) channel transcript. Evolutionary conservation and developmental regulation." Genetics **155**(3): 1149-60.

Hartner, J. C., C. Schmittwolf, et al. (2004). "Liver disintegration in the mouse embryo caused by deficiency in the RNA-editing enzyme ADAR1." J Biol Chem **279**(6): 4894-902.

Hartner, J. C., C. R. Walkley, et al. (2009). "ADAR1 is essential for the maintenance of hematopoiesis and suppression of interferon signaling." Nat Immunol **10**(1): 109-15.

Hegle, A. P., D. D. Marble, et al. (2006). "A voltage-driven switch for ion-independent signaling by ether-a-go-go K+ channels." Proc Natl Acad Sci U S A **103**(8): 2886-91.

Higuchi, M., S. Maas, et al. (2000). "Point mutation in an AMPA receptor gene rescues lethality in mice deficient in the RNA-editing enzyme ADAR2." Nature **406**(6791): 78-81.

Higuchi, M., F. N. Single, et al. (1993). "RNA editing of AMPA receptor subunit GluR-B: a base-paired intron-exon structure determines position and efficiency." Cell **75**(7): 1361-70.

Hille, B. (2001). Ionic Channels of Excitable Membranes, 3rd Edition **Massachusetts: Sinauer Associates**: 7-21, 61-92, 134-158.

Hille, B. (2001). "Ionic Channels of Excitable Membranes."

Hoopengardner, B., T. Bhalla, et al. (2003). "Nervous system targets of RNA editing identified by comparative genomics." Science **301**(5634): 832-6.

Imbrici, P., F. Gualandi, et al. (2008). "A novel KCNA1 mutation identified in an Italian family affected by episodic ataxia type 1." Neuroscience **157**(3): 577-87.

Iverson, L. E., M. A. Tanouye, et al. (1988). "A-type potassium channels expressed from Shaker locus cDNA." Proc Natl Acad Sci U S A **85**(15): 5723-7.

Jepson, J. E. and R. A. Reenan (2007). "Genetic approaches to studying adenosine-to-inosine RNA editing." Methods Enzymol **424**: 265-87.

Jepson, J. E. and R. A. Reenan (2009). "Adenosine-to-inosine genetic recoding is required in the adult stage nervous system for coordinated behavior in Drosophila." J Biol Chem **284**(45): 31391-400.

Jiang, Y., A. Lee, et al. (2003). "X-ray structure of a voltage-dependent K+ channel." Nature **423**(6935): 33-41.

Jiang, Y., V. Ruta, et al. (2003). "The principle of gating charge movement in a voltage-dependent K+ channel." Nature **423**(6935): 42-8.

Kallman, A. M., M. Sahlin, et al. (2003). "ADAR2 A-->I editing: site selectivity and editing efficiency are separate events." Nucleic Acids Res **31**(16): 4874-81.

Kamb, A., L. E. Iverson, et al. (1987). "Molecular characterization of Shaker, a Drosophila gene that encodes a potassium channel." Cell **50**(3): 405-13.

Kaplan, W. D. and W. E. Trout, 3rd (1969). "The behavior of four neurological mutants of Drosophila." Genetics **61**(2): 399-409.

Kawahara, Y., A. Grimberg, et al. (2008). "Dysregulated editing of serotonin 2C receptor mRNAs results in energy dissipation and loss of fat mass." J Neurosci **28**(48): 12834-44.

Keegan, L. P., J. Brindle, et al. (2005). "Tuning of RNA editing by ADAR is required in Drosophila." Embo J **24**(12): 2183-93.

Keegan, L. P., A. Gallo, et al. (2001). "The many roles of an RNA editor." Nat Rev Genet **2**(11): 869-78.

Keegan, L.P., A. Leroy, et al. (2004), "Adenosine deaminases acting on RNA (ADARs): RNA-editing enzymes." Genome Biology **5**(2) 209.1-10.

Kim, U., Y. Wang, et al. (1994). "Molecular cloning of cDNA for double-stranded RNA adenosine deaminase, a candidate enzyme for nuclear RNA editing." Proc Natl Acad Sci U S A **91**(24): 11457-61.

Koh, K., W. J. Joiner, et al. (2008). "Identification of SLEEPLESS, a sleep-promoting factor." Science **321**(5887): 372-6.

Lai, F., R. Drakas, et al. (1995). "Mutagenic analysis of double-stranded RNA adenosine deaminase, a candidate enzyme for RNA editing of glutamate-gated ion channel transcripts." J Biol Chem **270**(29): 17098-105.

Lehmann, K. A. and B. L. Bass (2000). "Double-stranded RNA adenosine deaminases ADAR1 and ADAR2 have overlapping specificities." Biochemistry **39**(42): 12875-84.

Lichtinghagen, R., M. Stocker, et al. (1990). "Molecular basis of altered excitability in Shaker mutants of Drosophila melanogaster." Embo J **9**(13): 4399-407.

Long, S. B., E. B. Campbell, et al. (2005). "Crystal structure of a mammalian voltage-dependent Shaker family K+ channel." Science **309**(5736): 897-903.

Maas, S., T. Melcher, et al. (1996). "Structural requirements for RNA editing in glutamate receptor pre-mRNAs by recombinant double-stranded RNA adenosine deaminase." J Biol Chem **271**(21): 12221-6.

Macbeth, M. R., H. L. Schubert, et al. (2005). "Inositol hexakisphosphate is bound in the ADAR2 core and required for RNA editing." Science **309**(5740): 1534-9.

MacKinnon, R. (2003). "Potassium channels." FEBS Lett **555**(1): 62-5.

Maddison, P. (2006). "Neuromyotonia." Clin Neurophysiol **117**(10): 2118-27.

Magidovich, E., I. Orr, et al. (2007). "Intrinsic disorder in the C-terminal domain of the Shaker voltage-activated K+ channel modulates its interaction with scaffold proteins." Proc Natl Acad Sci U S A **104**(32): 13022-7.

Maydanovych, O. and P. A. Beal (2006). "Breaking the central dogma by RNA editing." Chem Rev **106**(8): 3397-411.

Meiri, N., C. Ghelardini, et al. (1997). "Reversible antisense inhibition of Shaker-like Kv1.1 potassium channel expression impairs associative memory in mouse and rat." Proc Natl Acad Sci U S A **94**(9): 4430-4.

Melcher, T., S. Maas, et al. (1996). "A mammalian RNA editing enzyme." Nature **379**(6564): 460-4.

Murphy, G. G., N. B. Fedorov, et al. (2004). "Increased neuronal excitability, synaptic plasticity, and learning in aged Kvbeta1.1 knockout mice." Curr Biol **14**(21): 1907-15.

Nishikura, K. (2010). "Functions and regulation of RNA editing by ADAR deaminases." Annu Rev Biochem **79**: 321-49.

Oliver, D., C. C. Lien, et al. (2004). "Functional conversion between A-type and delayed rectifier K+ channels by membrane lipids." Science **304**(5668): 265-70.

Palladino, M. J., L. P. Keegan, et al. (2000). "A-to-I pre-mRNA editing in Drosophila is primarily involved in adult nervous system function and integrity." Cell **102**(4): 437-49.

Palladino, M. J., L. P. Keegan, et al. (2000). "dADAR, a Drosophila double-stranded RNA-specific adenosine deaminase is highly developmentally regulated and is itself a target for RNA editing." Rna **6**(7): 1004-18.

Patterson, J. B. and C. E. Samuel (1995). "Expression and regulation by interferon of a double-stranded-RNA-specific adenosine deaminase from human cells: evidence for two forms of the deaminase." Mol Cell Biol **15**(10): 5376-88.

Patton, D. E., T. Silva, et al. (1997). "RNA editing generates a diverse array of transcripts encoding squid Kv2 K+ channels with altered functional properties." Neuron **19**(3): 711-22.

Paul, M. S. and B. L. Bass (1998). "Inosine exists in mRNA at tissue-specific levels and is most abundant in brain mRNA." Embo J **17**(4): 1120-7.

Peng, I. F. and C. F. Wu (2007). "Differential contributions of Shaker and Shab K+ currents to neuronal firing patterns in Drosophila." J Neurophysiol **97**(1): 780-94.

Polson, A. G., B. L. Bass, et al. (1996). "RNA editing of hepatitis delta virus antigenome by dsRNA-adenosine deaminase." Nature **380**(6573): 454-6.

Pongs, O., N. Kecskemethy, et al. (1988). "Shaker encodes a family of putative potassium channel proteins in the nervous system of Drosophila." Embo J **7**(4): 1087-96.

Poujois, A., J. C. Antoine, et al. (2006). "Chronic neuromyotonia as a phenotypic variation associated with a new mutation in the KCNA1 gene." J Neurol **253**(7): 957-9.

Rajakulendran, S., S. Schorge, et al. (2007). "Episodic ataxia type 1: a neuronal potassium channelopathy." Neurotherapeutics **4**(2): 258-66.

Reenan, R. A. (2005). "Molecular determinants and guided evolution of species-specific RNA editing." Nature **434**(7031): 409-13.

Rettig, J., S. H. Heinemann, et al. (1994). "Inactivation properties of voltage-gated K+ channels altered by presence of beta-subunit." Nature **369**(6478): 289-94.

Rho, J. M., P. Szot, et al. (1999). "Developmental seizure susceptibility of kv1.1 potassium channel knockout mice." Dev Neurosci **21**(3-5): 320-7.

Robertson, G. A., J. M. Warmke, et al. (1996). "Potassium currents expressed from Drosophila and mouse eag cDNAs in Xenopus oocytes." Neuropharmacology **35**(7): 841-50.

Rogero, O., B. Hammerle, et al. (1997). "Diverse expression and distribution of Shaker potassium channels during the development of the Drosophila nervous system." J Neurosci **17**(13): 5108-18.

Rogero, O. and F. J. Tejedor (1995). "Immunochemical characterization and developmental expression of Shaker potassium channels from the nervous system of Drosophila." J Biol Chem **270**(43): 25746-51.

Rosenthal, J. J. and F. Bezanilla (2002). "Extensive editing of mRNAs for the squid delayed rectifier K+ channel regulates subunit tetramerization." Neuron **34**(5): 743-57.

Rueter, S. M., T. R. Dawson, et al. (1999). "Regulation of alternative splicing by RNA editing." Nature **399**(6731): 75-80.

Schwarz, T. L., D. M. Papazian, et al. (1990). "Immunological characterization of K+ channel components from the Shaker locus and differential distribution of splicing variants in Drosophila." Neuron **4**(1): 119-27.

Schwarz, T. L., B. L. Tempel, et al. (1988). "Multiple potassium-channel components are produced by alternative splicing at the Shaker locus in Drosophila." Nature **331**(6152): 137-42.

Seeburg, P. H. and J. Hartner (2003). "Regulation of ion channel/neurotransmitter receptor function by RNA editing." Curr Opin Neurobiol **13**(3): 279-83.

Shen, N. V. and P. J. Pfaffinger (1995). "Molecular recognition and assembly sequences involved in the subfamily-specific assembly of voltage-gated K+ channel subunit proteins." Neuron **14**(3): 625-33.

Song, J. and M. A. Tanouye (2008). "From bench to drug: human seizure modeling using Drosophila." Prog Neurobiol **84**(2): 182-91.

Stefl, R., M. Xu, et al. (2006). "Structure and specific RNA binding of ADAR2 double-stranded RNA binding motifs." Structure **14**(2): 345-55.

Stephens, O. M., B. L. Haudenschild, et al. (2004). "The binding selectivity of ADAR2's dsRBMs contributes to RNA-editing selectivity." Chem Biol **11**(9): 1239-50.

Strang, C., S. J. Cushman, et al. (2001). "A central role for the T1 domain in voltage-gated potassium channel formation and function." J Biol Chem **276**(30): 28493-502.

Sun, X. X., S. L. Bostrom, et al. (2009). "Alternative splicing of the eag potassium channel gene in Drosophila generates a novel signal transduction scaffolding protein." Mol Cell Neurosci **40**(3): 338-43.

Sun, X. X., J. J. Hodge, et al. (2004). "The eag potassium channel binds and locally activates calcium/calmodulin-dependent protein kinase II." J Biol Chem **279**(11): 10206-14.

Tang, C. Y., C. T. Schulteis, et al. (1998). "Shaker and ether-a-go-go K+ channel subunits fail to coassemble in Xenopus oocytes." Biophys J **75**(3): 1263-70.

Tanouye, M. A., A. Ferrus, et al. (1981). "Abnormal action potentials associated with the Shaker complex locus of Drosophila." Proc Natl Acad Sci U S A **78**(10): 6548-6552.

Tao, X., A. Lee, et al. (2010). "A gating charge transfer center in voltage sensors." Science **328**(5974): 67-73.

Timpe, L. C., Y. N. Jan, et al. (1988). "Four cDNA clones from the Shaker locus of Drosophila induce kinetically distinct A-type potassium currents in Xenopus oocytes." Neuron **1**(8): 659-67.

Timpe, L. C., T. L. Schwarz, et al. (1988). "Expression of functional potassium channels from Shaker cDNA in Xenopus oocytes." Nature **331**(6152): 143-5.

Tonkin, L. A., L. Saccomanno, et al. (2002). "RNA editing by ADARs is important for normal behavior in Caenorhabditis elegans." Embo J **21**(22): 6025-35.

Ueda, A. and C. F. Wu (2006). "Distinct frequency-dependent regulation of nerve terminal excitability and synaptic transmission by IA and IK potassium channels revealed by Drosophila Shaker and Shab mutations." J Neurosci **26**(23): 6238-48.

Vissel, B., G. A. Royle, et al. (2001). "The role of RNA editing of kainate receptors in synaptic plasticity and seizures." Neuron **29**(1): 217-27.

Wang, Q., J. Khillan, et al. (2000). "Requirement of the RNA editing deaminase ADAR1 gene for embryonic erythropoiesis." Science **290**(5497): 1765-8.

Wang, Q., M. Miyakoda, et al. (2004). "Stress-induced apoptosis associated with null mutation of ADAR1 RNA editing deaminase gene." J Biol Chem **279**(6): 4952-61.

Wang, Q., P. J. O'Brien, et al. (2000). "Altered G protein-coupling functions of RNA editing isoform and splicing variant serotonin2C receptors." J Neurochem **74**(3): 1290-300.

Wang, Z., G. F. Wilson, et al. (2002). "Calcium/calmodulin-dependent protein kinase II phosphorylates and regulates the Drosophila eag potassium channel." J Biol Chem **277**(27): 24022-9.

Warmke, J., R. Drysdale, et al. (1991). "A distinct potassium channel polypeptide encoded by the Drosophila eag locus." Science **252**(5012): 1560-2.

Wilson, G. F., Z. Wang, et al. (1998). "Interaction of the K channel beta subunit, Hyperkinetic, with eag family members." J Biol Chem **273**(11): 6389-94.

Wong, S. K., S. Sato, et al. (2001). "Substrate recognition by ADAR1 and ADAR2." Rna **7**(6): 846-58.

Wu, C. F., B. Ganetzky, et al. (1983). "Potassium currents in Drosophila: different components affected by mutations of two genes." Science **220**(4601): 1076-8.

Wu, M. N., W. J. Joiner, et al. (2009). "SLEEPLESS, a Ly-6/neurotoxin family member, regulates the levels, localization and activity of Shaker." Nat Neurosci **13**(1): 69-75.

Xu, M., K. S. Wells, et al. (2006). "Substrate-dependent contribution of double-stranded RNA-binding motifs to ADAR2 function." Mol Biol Cell **17**(7): 3211-20.

Zagotta, W. N., T. Hoshi, et al. (1990). "Restoration of inactivation in mutants of Shaker potassium channels by a peptide derived from ShB." Science **250**(4980): 568-71.

Zhong, Y. and C. F. Wu (1991). "Alteration of four identified K+ currents in Drosophila muscle by mutations in eag." Science **252**(5012): 1562-4.

Zhong, Y. and C. F. Wu (1993). "Modulation of different K+ currents in Drosophila: a hypothetical role for the Eag subunit in multimeric K+ channels." J Neurosci **13**(11): 4669-79.

Zhou, M., J. H. Morais-Cabral, et al. (2001). "Potassium channel receptor site for the inactivation gate and quaternary amine inhibitors." Nature **411**(6838): 657-61.

Zuker, M. (2003). "Mfold web server for nucleic acid folding and hybridization prediction." Nucleic Acids Res **31**(13): 3406-15.

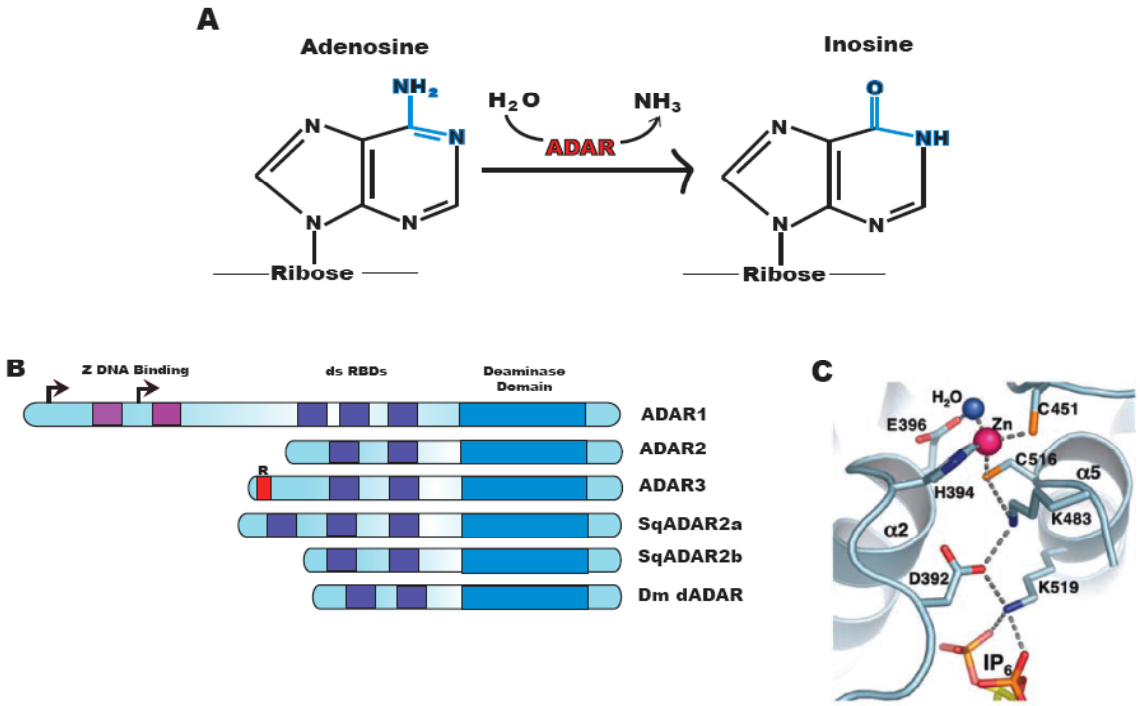

Figure 1.1: Overview of A-to-I RNA Editing and ADAR Conservation
(**A**) Schematic representing the hydrolytic conversion of adenosine to inosine catalyzed by ADAR enzymes. (**B**) Conservation of ADAR enzymes from vertebrates, squid, and *Drosophila melanogaster*, (redrawn from information contained in Nishikura, K. 2010 and Keegan, LP et al. 2004). While all ADARs have a conserved deaminase domain (blue), the number of double-stranded RNA binding domains (purple) can vary between different ADAR isoforms and between different species. Vertebrate ADAR1 has two isoforms generated from the use of alternative promoters, one of which is inducible by interferon (p150) and the other is constitutive (p110). Vertebrate ADAR3 also contains an arginine-rich domain (red), however this domain and the enzyme function are not known. (**C**) Ribbon diagram depicting the catalytic active site of ADAR2 with the conserved histidine (H394) and two cystine residues (C451 and C510) essential for catalytic function (from Macbeth, M. R., H. L. Schubert, et al. (2005). "Inositol hexakisphosphate is bound in the ADAR2 core and required for RNA editing." Science **309**(5740): 1534-9. Reprinted with permission from AAAS).

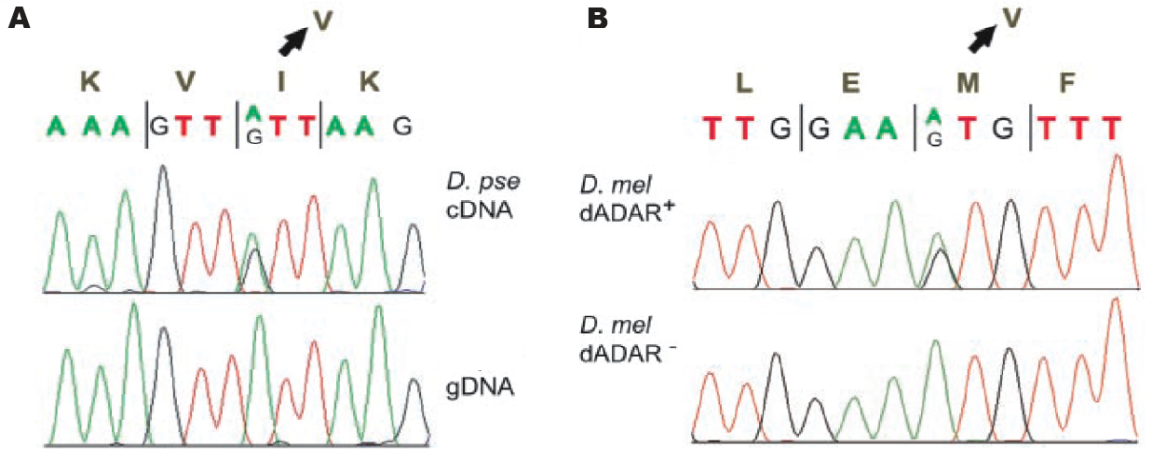

Figure 1.2: Sequence Signature of an A-to-I Editing Event
(**A**) Sequence chromatograms for the sodium channel transcript *DSCI*, (CG9071), in *Drosophila pseudoobscura*. A mixed A/G signal present in cDNA molecules that is absent from the corresponding genomic sequence is indicative of an A-to-I editing event. The predicted amino acid substitution resulting from editing this base is indicated above the chromatogram (isoleucine to valine). (**B**) Within the same *DSCI* transcript in *Drosophila melanogaster*, editing events observed in cDNAs are only present in wild-type flies (top), while *dAdar*-null flies have only genomic encoded version in cDNA sequences (bottom), (from Hoopengardner, B., T. Bhalla, et al. (2003). "Nervous system targets of RNA editing identified by comparative genomics." Science **301**(5634): 832-6. Reprinted with permission from AAAS).

A

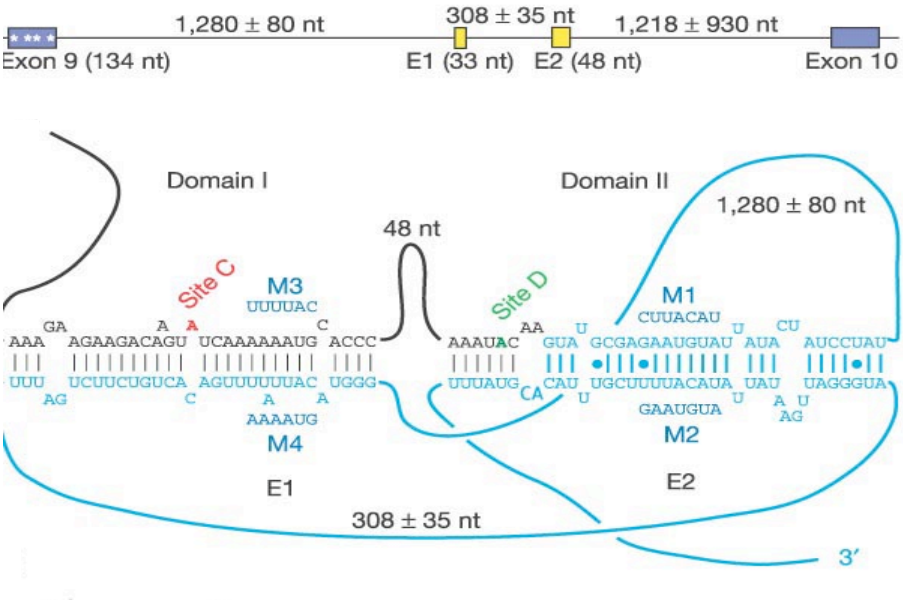

B

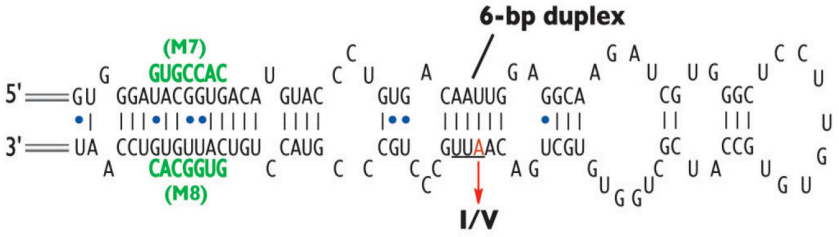

Figure 1.3: Diversity in RNA Duplex Substrates Recognized by ADARs
(**A**) RNA editing of *synaptotagminI* transcripts in *Drosophila melanogaster* results from the formation of a complex pseudoknot structure. The transcription unit is depicted above the structure and results from the intramolecular base pair interactions between the 5' edited exon 9 and two conserved *cis*-regulatory elements (ECS) located in the downstream intron (yellow boxes). Mutations used in analysis of this structure are depicted M1-M4 (Reenan, R. A. (2005). "Molecular determinants and guided evolution of species-specific RNA editing." Nature **434**(7031): 409-13. Reprinted by permission from Macmillan Publishers Ltd: Nature). (**B**) A hairpin structure forms between complementary sequences contained within the edited exon that directs editing of human $K_V1.1$ transcripts (Bhalla, T., J. J. Rosenthal, et al. (2004). "Control of human potassium channel inactivation by editing of a small mRNA hairpin." Nat Struct Mol Biol **11**(10): 950-6. Reprinted by permission from Macmillan Publishers Ltd: Nat Struct Mol Biol). A single editing site in this hairpin structure results in the substitution of a conserved isoleucine residue to valine. Mutations used to verify this structure are depicted M7 and M8.

Figure 1.4: A-to-I RNA Editing Recodes Highly Conserved Amino Acids
Amino acid alignment of the S6 domains from different K_V channels is conserved from humans to bacteria. Completely conserved residues are highlighted in red while residues highlighted in blue are shared with human (*hKCNA1*) K_V1.1 channels. Editing recodes the isoleucine residue (yellow) to valine in human K_V1.1 and *Drosophila* Shab channels (Bhalla, T., J. J. Rosenthal, et al. (2004). "Control of human potassium channel inactivation by editing of a small mRNA hairpin." Nat Struct Mol Biol **11**(10): 950-6. Reprinted by permission from Macmillan Publishers Ltd: Nat Struct Mol Biol).

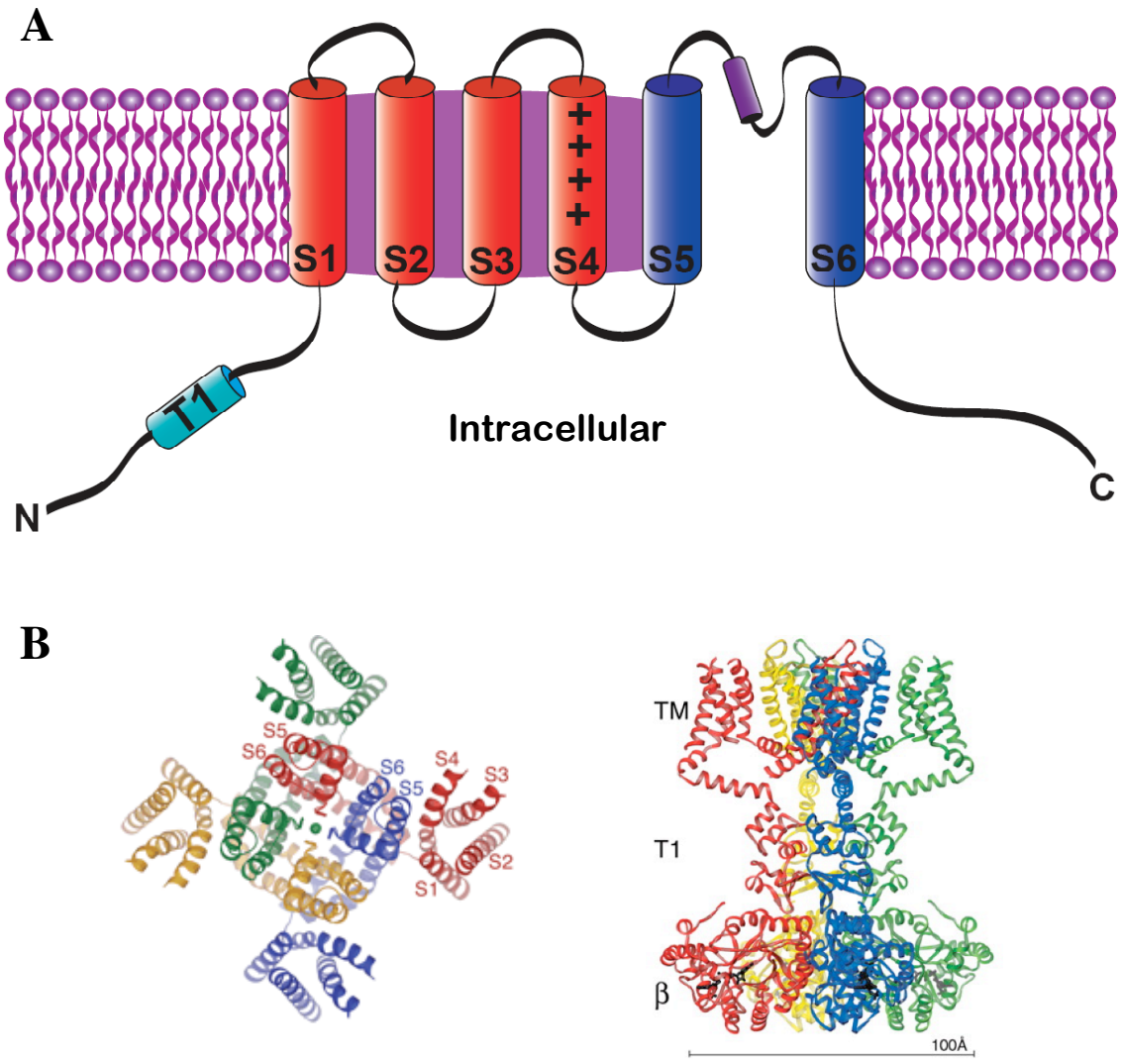

Figure 1.5: K_V Channel Alpha-Subunit Topography and Membrane Organization
(**A**) Diagram depicting the structure of a single K_V channel alpha subunit. There are six helical transmembrane-spanning domains, S1-S6. S1 through S4 (red) comprise the voltage-sensing domains, while S5 and S6 comprise the pore-forming region. The selectivity filter is depicted in purple. The N-terminal domain includes the T1 tetramerization domain and is located on the intracellular side of the membrane along with the C-terminal portion of the peptide. (**B**) K_V channel alpha-subunits co-assemble forming tetrameric complexes that constitute functional channels. Ribbon diagrams representing the crystal structure of mammalian $K_V1.2$ channels (From Long, S. B., E. B. Campbell, et al. (2005). "Crystal structure of a mammalian voltage-dependent Shaker family K+ channel." Science **309**(5736): 897-903. Reprinted with permission from AAAS). The left panel is a top view of the channel, with a potassium ion centered in the pore (green), and depicts the symmetrical arrangements of the subunits in the membrane. The right panel is a side view of $K_V1.2$ assembled with beta-accessory subunits.

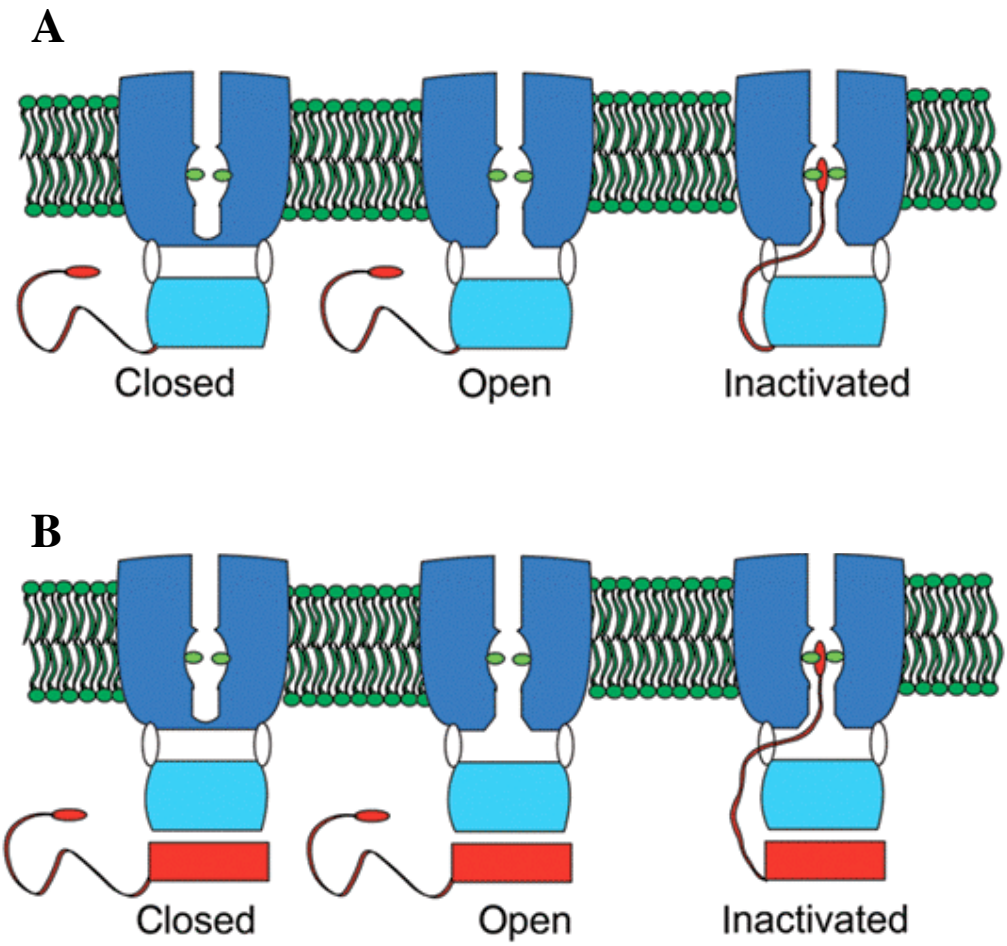

Figure 1.6: Different Conformational States of K_V Channels
(**A**) K_V channels can exist in conducting (open), and non-conducting (closed, inactivated) states (From Bezanilla, F. (2004). "RNA editing of a human potassium channel modifies its inactivation." Nat Struct Mol Biol **11**(10): 915-16. Reprinted by permission from Macmillan Publishers Ltd: Nat Struct Mol Biol). The T1 domain is depicted in light blue, and the inactivation particle is contained within the N-terminal region of the peptide (red), similar to Shaker channels. Upon channel opening, the inactivation particle can bind to residues within the pore (green), blocking ion conduction by occluding the pore. (**B**) Similar to the above model, this diagram represents inactivation conferred by beta-accessory subunits (red) to non-inactivating type channels. These beta-subunits can supply inactivation particles to a channel complex that lacks the N-terminal inactivation particle.

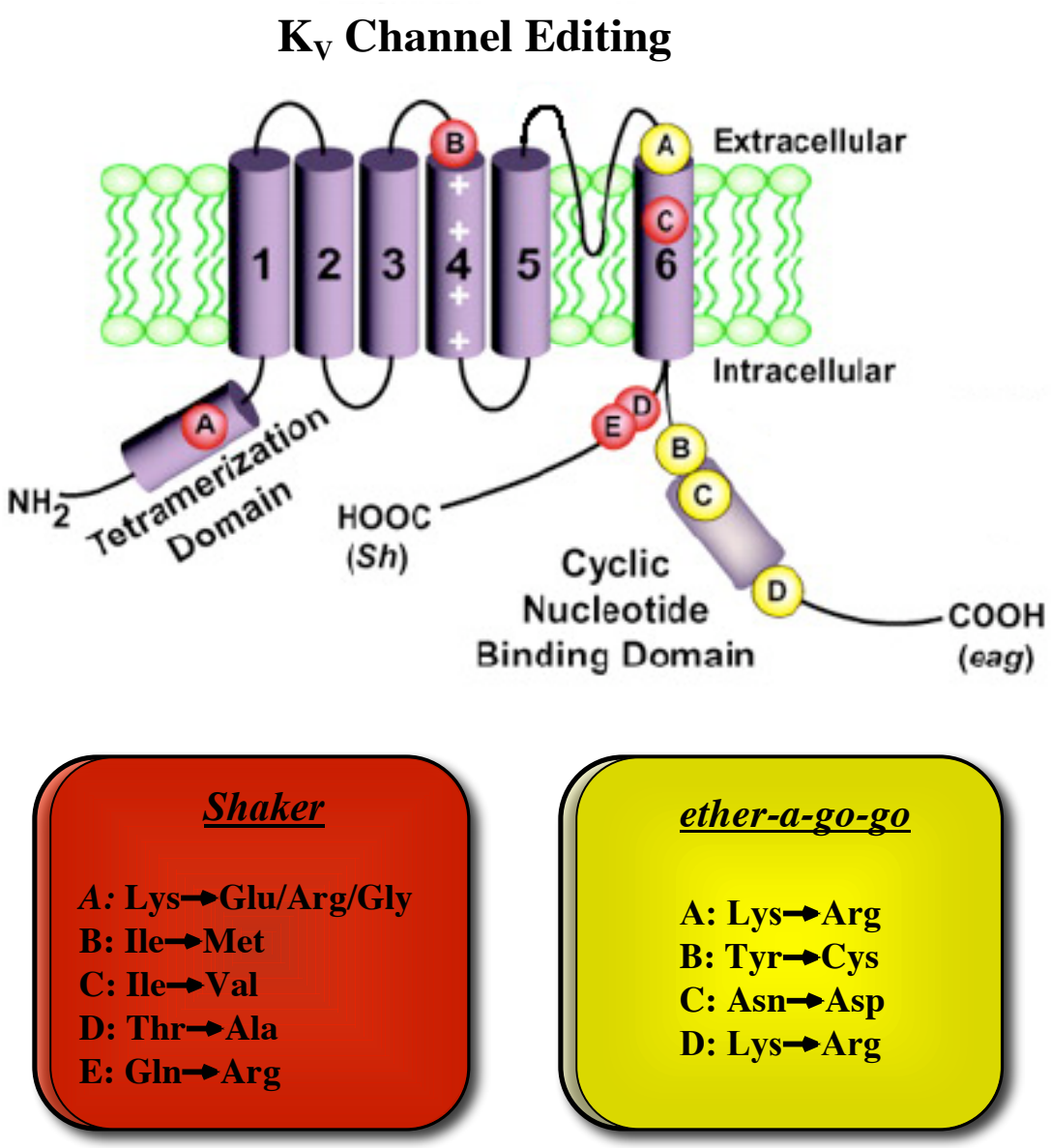

Figure 1.7: A-to-I RNA Editing Generates Amino Acid Substitutions in Shaker and EAG Channels. K_V channel subunit (top) depicts the positions where editing sites recode amino acids within Shaker and EAG (adapted from Hoopengardner, B., T. Bhalla, et al. (2003). "Nervous system targets of RNA editing identified by comparative genomics." Science **301**(5634): 832-6. Reprinted with permission from AAAS). Editing sites within Shaker are colored red, while EAG editing sites are shown in yellow. Color-coded boxes list the amino acid substitutions generated by each editing site.

Chapter 2:

Characterization of five RNA editing sites in *Shab* potassium channels.

This chapter consists of previously published data. "Characterization of five RNA editing sites in Shab potassium channels." by Mary Y. Ryan, Rachel Maloney, Robert Reenan, and Richard Horn. (2008). Channels **2**(3): 1-8. My specific contribution to this publication are included in figure 2.1 and consist of descriptive analysis of *Shab* RNA editing, including the developmental analysis of *Shab* editing in *Drosophila*. The electrophysiology analysis of *Shab* editing was performed by Mary Y. Ryan and Richard Horn (Thomas Jefferson University, Philadelphia, PA).

Abstract

RNA editing revises the genetic code at precise locations, creating single base changes in mRNA. These changes can result in altered coding potential and modifications to protein function. Sequence analysis of the *Shab* potassium channel of *Drosophila melanogaster* revealed five such RNA editing sites. Four are constitutively edited (I583V, T643A, Y660C and I681V) and one undergoes developmentally regulated editing (T671A). These sites are located in the S4, S5–S6 loop and the S6 segments of the channel. We examined the biophysical consequences of editing at these sites by creating point mutations, each containing the genomic (unedited) base at one of the five sites in the background of a channel in which all other sites are edited. We also created a completely unedited construct. The function of these constructs was characterized using two-microelectrode voltage clamp in *Xenopus* oocytes. Each individual 'unediting' mutation slowed the time course of deactivation and the rise time during channel activation. Two of the mutants exhibited significant hyperpolarized shifts in their midpoints of activation. Constructs that deactivated slowly also inactivated slowly, supporting a mechanism of closed-state inactivation. One of the editing sites, position 660, aligns with the *Shaker* 449 residue, which is known to be important in tetraethylammonium (TEA) block. The aromatic, genomically-encoded residue tyrosine at this position in *Shab* enhances TEA block 14 fold compared to the edited residue, cysteine. These results show that both the position of the RNA editing site and the identity of the substituted amino acid are important for channel function.

Introduction

Genetic information is systematically decoded according to the central dogma of genetics: DNA-to-RNA-to-protein. This orderly process is perturbed, however, by an enzyme called adenosine deaminase acting on RNA (ADAR). ADAR recognizes specific double-stranded structures in pre-mRNA after transcription, and deaminates specific adenosine (A) nucleotides to inosines(I).[1] Inosines are then read as guanosines by all of the molecular machinery of a cell. This A → I change can therefore effectuate a variety of downstream consequences, for example, creating an alternative splice site or, most importantly for this study, altering the codon for an amino acid, thus resulting in a point mutation in the resultant protein. This type of RNA editing primarily affects genes that encode for neuronal signaling proteins such as voltage-gated potassium (K_V) channels.[2] K_V channels are unique in that they are edited in diverse animal phyla: mollusks (sqK_V2), arthropods (*Shab* and *Shaker*) and mammals ($K_V1.1$). [3–5] In this study, we discovered five RNA editing sites in the Drosophila Shab channel, a member of the K_V2 super-family, using RT-PCR. The point mutation I583V occurs in the S4 voltage sensor; T643A in the pore helix; Y660C in the extracellular turret; T671A and I681V in the S6 segment. All five sites are highly edited in flies. We therefore characterized each site by systematically mutating each site back to the genomically encoded (i.e., 'unedited') amino acid on the background of a fully edited channel, and examined the biophysical consequences on voltage-clamped potassium currents. Our results showed myriad effects on the kinetics and voltage dependence of channel function, suggesting an important role of RNA editing in regulation of ion channel activity.

Results

We discovered that the *Shab* potassium channel of *Drosophila melanogaster* contains five RNA editing sites where particular amino acids can be recoded to alternate residues. All five sites are located on exon two of the *Shab* locus (Fig. 2.1A). Figure 2.2 shows these sites as colored symbols in a topological cartoon of the *Shab* channel. The five sites and editing mutations are (**unedited**/edited): **Ile**583Val in the S4 voltage sensor, RIMRILR(**I**/V)LKLARHST; **Thr**643Ala in the pore helix, VSIPE(**T**/A)FWWAG; **Tyr**660Cys in the extracellular turret, TVGYGDI(**Y**/C)PTTALGK; **Thr**671Ala ALGKVIG(**T**/A)VCCICGV and **Ile**681Val CCICGVLV(**I**/V)ALPIPIIV in the S6 segment.

Editing sites can be developmentally regulated in both vertebrate and invertebrate systems.[6–9] We determined the temporal pattern of regulation for these five sites in *Shab* (Fig. 2.1B). Four of the five sites are constitutively edited at high levels throughout development, and one site (residue 671) shows a moderate (<2-fold) decrease in editing in adult flies. These results contrast with a general increase in editing observed at several other sites in *Drosophila*.[10,11]

Because of the high level of editing in adult flies (>55% at four of the five sites), we denote the wild-type (WT) *Shab* channel as the fully edited variant. Consequently, each point mutant created for functional study contains the genetically encoded amino acid (the unedited form) at one of the five positions. We also created a completely unedited construct, identified as Genomic, containing the genomically encoded amino acid at each of the five sites.

To examine the functional consequences of these unediting mutations, we characterized the biophysical properties of each in channels expressed in *Xenopus* oocytes. Families of currents were obtained using voltage pulses from −70 mV to +70 mV in 5-mV increments from a holding potential of −100 mV (Fig. 2.2). None of these variants inactivates over the time and voltage range shown. Superficially the currents are comparable, although the V681I mutant and the Genomic construct deactivate more slowly than the others at the end of a depolarization (see below).

Figure 2.3 shows the voltage dependence of activation of each mutant compared to WT *Shab*. The normalized conductances were obtained from tail currents and fitted with a fourth-power Boltzmann function. Although residue 583 is housed in the critical S4 segment of the voltage sensor, V583I is the most similar to WT with indistinguishable midpoints and slopes underlying the voltage dependence of activation (Table 2.1 and Fig. 2.3A). A643T and C660Y have activation curves with shapes similar to that of the WT; however both are left shifted at their midpoints by 3.9 mV and 11.4 mV, respectively (Table 2.1 and Fig. 2.3B and C). A671T and the Genomic constructs have midpoint shifts in the same range as A643T, 4.2 mV and 5.6 mV respectively; however the activation curve is steeper at more depolarized voltages (Table 2.1 and Fig. 2.3D and F). The most prominent difference is exhibited by V681I, which has a 13.5-mV hyperpolarizing shift and a steeper voltage dependence of activation (Table 2.1 and Fig. 2.3E).

Further examination of the activation of these channels revealed differences in kinetics among the mutants. The inset of Figure 2.4 illustrates this comparison with

color-coded sample traces showing the response to a depolarization to +10 mV. At this voltage WT (black), V583I (red) and C660Y (blue) activate most rapidly, V681I (orange) and A643T (green) activate at an intermediate rate, and the slowest activation is exhibited by A671T (violet) and Genomic (teal) constructs. These trends are also apparent in the plot of 10–90% activation rise times (Fig. 2.4). At more depolarized voltages, differences in rise times became less distinct for all the channel types except A643T and A671T, which remained slower than the others (Fig. 2.4).

The kinetics of deactivation also differed significantly among the six variants we examined. The inset of Figure 2.5 shows normalized tail currents at −40 mV following a depolarization to +50 mV. As observed for activation kinetics, V683I and the Genomic construct deactivate most slowly. A671T and V583I deactivate most rapidly, and the remaining three constructs are intermediate. The time course of deactivation was fitted by a double exponential relaxation composed of a fast and slow component with time constants and weights shown in Figure 2.5. The slow overall kinetics of deactivation for V681I is due to both larger time constants and a preponderance of the slow component. The predominance of the slow component in the Genomic construct is especially evident at more depolarized voltages.

To measure inactivation kinetics we used 30-s depolarizations to six test voltages. Figure 2.6A shows the time constants of inactivation estimated from single exponential relaxations. The V681I and Genomic constructs inactivate most slowly. These two constructs also have the slowest kinetics of deactivation (Fig. 2.5A). In general, all *Shab* potassium currents tend to inactivate more completely at more hyperpolarized voltages

(Fig. 2.6B). V681I and Genomic constructs exhibit both the slowest and the least complete inactivation at +50 mV (Fig. 2.6 inset).

The third editing site (residue 660) aligns with residue 449 of *Shaker* (Fig. 2.7C inset). This residue at the extracellular mouth of the pore is known to contribute to the docking site for extracellular blockers like tetraethylammonium (TEA) and toxins in *Shaker*. Specifically, high-affinity TEA block requires either a tyrosine or phenylalanine at this position.[12–14] Although the genomic sequence for this residue encodes for tyrosine, the edited (WT) residue is cysteine. To test whether this residue plays a similar role in *Shab* as in *Shaker*, we examined TEA block of WT *Shab* and the C660Y mutant. In accordance with previous studies, Figure 2.7 shows that a tyrosine at this position enhances TEA block. Figures 2.7A and B show reversible block at two TEA concentrations, and Figure 2.7C plots the fraction of blocked channels against extracellular TEA concentration. These data show that the tyrosine variant (K_i = 1.14 mM ± 0.09 mM) is 14-fold more sensitive to TEA block than the cysteine variant (K_i = 16.36 mM ± 1.04 mM), thus confirming the importance for block of an aromatic residue at this position.

Discussion

RNA editing is a strategy that allows a cell to make point mutations enzymatically without altering the archival genomic information that encodes proteins. The action of ADAR enzymes depends on a variety of factors, perhaps most critically on the formation of recognizable double-stranded RNA (dsRNA) targets.[15] Further specific diversification of amino acid side-chains occurs through regulation of the levels—and activity—of different isoforms of ADAR, each with its own specificity for dsRNA structures.[1] Changes in the levels of editing observed in *Shab* during fly development (Fig. 2.1B) may reflect gross changes in nervous system structure; however, they may also indicate an additional level of regulation governing ADAR enzymatic efficiency or recognition of editing sites involving yet unknown factors (e.g., chaperone proteins). The editing of mRNA encoding ion channels typically causes rather subtle changes of biophysical properties due to point mutations. However, some coding changes can produce dramatic alterations in function. The canonical example is editing of the Gln/Arg site in neuronal glutamate receptor channels.[16] In this case, the unedited form of the protein is lethal, presumably because unedited channels are excessively permeant to calcium ions, which are toxic when overabundant inside neurons. By contrast, our data show that editing produces rather modest effects on the gating of *Shab* channels. These results are in accord with studies of the orthologous potassium channel (sqK_V2) in squid. We will discuss the differences between RNA editing of these two channels below.

The predominant functional consequences of RNA editing on *Shab* are alterations of the voltage dependence and kinetics of channel gating. We also observed an order-of-

magnitude alteration of the affinity of an extracellular blocker in response to a single point mutation. Effects on gating are not surprising in that the point mutations occur in highly conserved locations of the channel protein, either in the voltage-sensing S4 segment or in the pore domain that houses the activation, and perhaps the inactivation, gates. Nevertheless, the effects would have been difficult to predict, because except for one case (Y660C), the editing mutations are all relatively conservative, and all of them preserve the charge of the side-chain. The tyrosine-cysteine switch, although involving two uncharged residues, is accompanied by a change of aromaticity. Because *Shab* channels are edited at levels >50% in four of the five sites (Fig. 2.1B), we used the fully edited channel as our wild-type (WT) and examined the effects of single 'unediting' mutations at the five sites. We also created a completely unedited (Genomic) channel.

Two out of the six 'unediting' constructs produced significant hyperpolarizing shifts in the activation G-V curve, compared to the fully edited WT. The most prominent effect, a 13.5-mV shift, is found in V681I in the S6 segment, the construct with the steepest voltage dependence of activation. The main difference between valine and isoleucine is that the latter is ~18% larger in volume due to an extra methyl group. This residue apparently orients towards the aqueous cavity of the permeation pathway,[17–19] where it can interact with intracellular pore blockers like the inactivation gate of KV1 channels.[5,17] The effect of this point mutation on activation gating may be due to its proximity to a downstream Pro-Ile-Pro motif (Fig. 2.8) that is somehow involved in opening and closing of the activation gate.[20–24] Unexpectedly, mutation of the editing site in the voltage sensing domain, residue 583 in the middle of the S4 segment, had no effect

on the voltage dependence of activation, reflected in the G-V relationship. Summarizing, RNA editing of the three most downstream editing sites each caused small depolarizing shifts of activation. Therefore, editing of these three sites tends to make the *Shab* channel less prone to open, which would enhance the excitability of a neuron containing the edited channels.

Each mutagenic departure from the fully edited WT construct slows activation kinetics. The slowest activation is exhibited by A671T, located just above the middle of the pore helix.[18] The side-chain of this residue is oriented towards the S5 segment of its own subunit. It could therefore affect gating movements that involve relative displacements of these two helices. Perhaps the larger and more hydrophilic threonine side-chain interferes mildly with such a tertiary conformational change. Notably, this site is the least edited in adult flies (<50%; Fig. 2.1B). Therefore, the genomic residue, threonine, is most prevalent. The slower activation of *Shab* channels with Thr671 would tend to make neurons with this residue more excitable.

Deactivation, the closing of the activation gate, differs for each construct. It has complicated kinetics, in that the time course requires a double-exponential fit. Deactivation is slowest in the Genomic construct, indicating that, in general, editing speeds deactivation. V681I, near the bottom of the S6 segment, also has significantly slower deactivation than WT due both to larger time constants and to the largest proportion of the slow component among the mutants. Inactivation time constants for both Genomic and V681I are also significantly slower than in the other constructs. V583I in the S4 segment deactivates faster than completely edited *Shab*. The reason for this

effect is not obvious. In the recent crystal structure of an open K_V channel, [18] the homologous residue is an isoleucine and is oriented towards the space, perhaps an aqueous vestibule, between the voltage sensing and pore domains. This putative aqueous vestibule may have a dynamic, voltage-sensitive contour that contributes to voltage-dependent gating.[25] Residues lining aqueous vestibules are likely to play a role in shaping the electric field in the vicinity of the S4 segment.

The aromatic, genomic residue tyrosine at the 660 position in *Shab*, which aligns with the well known *Shaker* 449 position, enhances TEA block 14 fold compared to the edited residue, cysteine. This result verifies the importance of the aromatic residue at this position for TEA block of potassium channels. There are two reported orientations of tyrosines observed in crystal structures of KcsA potassium channels,[26,27] one of which may correspond to the *en face* orientation of an aromatic side-chain at this position in *Shaker* potassium channels.[28] A clue to the orientation of this tyrosine in *Shab*, and the peptide backbone in this region, could be provided by its inhibition constant for TEA, ~1 mM. This is however roughly midway between the affinities for TEA block of *Shaker* and wild-type KcsA,[14,29] leaving the aromatic's orientation undefined for the moment. Because this residue is situated at the outer mouth of the pore where it can interact with extracellular pore blockers, it raises the possibility that an editing mutation of this residue might affect the binding of some unidentified toxin or endogenous molecule that plugs the pore. Thus, mutation of this residue might play a role in the co-evolution of *Drosophila* with a poisonous predator or food source.

Our initial examination of *Shab* currents failed to reveal an inactivation process.

This was surprising because of a previous study demonstrating so-called U-type inactivation in mammalian $K_V2.1$ channels.[30] This type of inactivation is evident even for short-duration depolarizations, given repetitively. It is manifest as a form of cumulative inactivation, indicating that inactivation proceeds more rapidly from the holding potential than from a depolarized potential that activates channel opening.[30] We tested for cumulative inactivation, without success, using voltage protocols that clearly revealed inactivation in mammalian $K_V2.1$ channels (data not shown). However, K_V2 channels from squid have a very slow inactivation process that can be observed during activating depolarizations.[3] We observed a similar inactivation process in response to 30-s depolarizations (Fig. 2.6). One shared feature between these orthologs is that in both cases depolarization decreased the rate of inactivation, in contrast to the K_V1 phenotype observed in *Shaker* channels.[31] The voltage dependence of K_V2 channel inactivation, as well as the cumulative inactivation observed for mammalian $K_V2.1$ channels, suggests that all of these channels tend to inactivate from pre-open closed states along the activation pathway, a feature that appears to be shared with K_V3 and K_V4 channels.[32,33]

There is some overlap in the RNA editing sites and amino acid changes in *Drosophila* and squid potassium channels from the K_V2 superfamily. Two of the five sites we describe in *Drosophila* are not edited in the sqK_V2 gene (note the red sites in Fig. 2.8), and one of the three remaining editing sites, found in both *Drosophila* and squid, produces a different point mutation in sqK_V2. Whereas editing of Thr671 in *Shab* changes this residue to alanine, the aligned mutation in sqK_V2 converts a serine to a glycine. Moreover, the consequences of these changes differ in each channel type. For

example, the Y → C editing site in sqK_V2 (Fig. 2.8) does not significantly influence the conductance-voltage relationship, and it slows deactivation by a factor of two compared to the genomic construct.[3] The opposite change in *Shab* (C → Y) in a fully edited background produces a significant hyperpolarizing shift in the midpoint of activation and has very little impact on the deactivation time constant relative to the all-edited construct (Table 2.1 and Fig. 2.5A). Another difference between K_V2 channels in squid and *Drosophila* concerns inactivation. In squid, the most pronounced effect on the inactivation rate is a ~1.5-fold slowing of inactivation when cysteine is substituted for the genomic tyrosine at the residue that aligns with *Shab*'s 660. Our results reveal almost no effect on inactivation rate when mutating this residue in *Shab*. The largest effect we observed for a point mutation was at residue 681 in the S6 segment (Fig. 2.6). The inactivation rate is faster for the edited residue, valine, than for the genomic isoleucine. This agrees with the results for sqK_V2, although the magnitude of the effect is larger in *Shab*. The conservation of editing sites between these two orthologs suggests that their role is preserved by evolutionary selection. The challenge for us is to learn whether this conservation is due to the biophysical consequences of the editing mutations, or perhaps due to effects of the mutations on the biogenesis or trafficking of the channels in the nervous systems of these animals. A further question concerns the need for enzymatic regulation of these sites and the role of that regulation in development and adaptation to changes in the environment. In the sqK_V1.1 channel, for example, twenty-two of twenty-six RNA editing sites substitute a larger amino acid for a smaller one.[34] This same pattern is seen in intracellular proteins from organisms that have adapted to cold environments;

the smaller, edited amino acid may allow the proteins more flexibility at lower temperatures.[34]

Materials and Methods

RNA editing analysis

All RNA extractions were performed using TRIzol (Invitrogen) on whole flies. *Shab* transcripts were amplified by RT-PCR using gene-specific primers at all steps. Levels of editing for individual editing sites were obtained by direct sequencing of RT-PCR products from at least three independent reactions per sample. Areas under the curves were determined from electropherogram traces and editing level expressed as {% editing} = (area G/total area A +G) * 100.

Molecular biology for expression studies

All *Shab* constructs were inserted into the pBSTA vector for expression in oocytes. Editing mutations at the four sites were generated using the QuikChange Site-Directed Mutagenesis Kit (Stratagene) and verified by direct sequencing. Each of the five 'unediting' point mutations converted the edited amino acid to the genomically encoded one, in the background of the fully edited channel. We also created a completely unedited construct, identified as Genomic, containing the genomically encoded amino acid at each of the five sites. cRNA was prepared by in vitro transcription (mMessage mMachine Ultra, Ambion).

Electrophysiology

Stage V to VI *Xenopus* oocytes were injected with cRNA. The oocytes were kept at 18°C for 1–2 d until they were used for recording. Potassium current was recorded with the two-microelectrode voltage clamp technique using an OC-725C voltage clamp (Warner Instruments, Hamden, CT) in a standard Ringers solution (in mM): 116 NaCl, 2 KCl, 1.8 MgCl2, 2 CaCl2, 5 HEPES, pH 7.6. Recording electrodes were filled with 3 M KCl. Perfusion experiments were performed with an ALA VM8 (ALA Scientific) gravity-flow delivery system. Summarized data are presented as mean ± SEM.

Acknowledgments

The *Shab*11 channel was a gift from Dr. Lawrence Salkoff.

References

1. Bass BL. RNA editing by adenosine deaminases that act on RNA. Annu Rev Biochem 2002;71:817–46. [PubMed: 12045112]

2. Seeburg PH, Hartner J. Regulation of ion channel/neurotransmitter receptor function by RNA editing. Curr Opin Neurobiol 2003;13:279–83. [PubMed: 12850211]

3. Patton DE, Silva T, Bezanilla F. RNA editing generates a diverse array of transcripts encoding squid KV2 K + channels with altered functional properties. Neuron 1997;19:711–22. [PubMed: 9331360]

4. Hoopengardner B, Bhalla T, Staber C, Reenan R. Nervous system targets of RNA editing identified by comparative genomics. Science 2003;301:832–6. [PubMed: 12907802]

5. Bhalla T, Rosenthal JJC, Holmgren M, Reenan R. Control of human potassium channel inactivation by editing of a small mRNA hairpin. Nature Struct Biol 2004;11:950–6.

6. Lomeli H, Mosbacher J, Melcher T, Hoger T, Geiger JR, Kuner T, Monyer H, Higuchi M, Bach A, Seeburg PH. Control of kinetic properties of AMPA receptor channels by nuclear RNA editing. Science 1994;266:1709–13. [PubMed: 7992055]

7. Bernard A, Khrestchatisky M. Assessing the extent of RNA editing in the TMII regions of GluR5 and GluR6 kainate receptors during rat brain development. J Neurochem 1994;62:2057–60. [PubMed:7512622]

8. Keegan LP, Brindle J, Gallo A, Leroy A, Reenan RA, O'Connell MA. Tuning of RNA editing by ADAR is required in *Drosophila*. Embo J 2005;24:2183–93. [PubMed: 15920480]

9. Ohlson J, Pedersen JS, Haussler D, Ohman M. Editing modifies the GABA(A) receptor subunit alpha3. RNA 2007;13:698–703. [PubMed: 17369310]

10. Hanrahan CJ, Palladino MJ, Ganetzky B, Reenan RA. RNA editing of the *Drosophila* para Na+ channel transcript. Evolutionary conservation and developmental regulation. Genetics 2000;155:1149–60. [PubMed: 10880477]

11. Palladino MJ, Keegan LP, O'Connell MA, Reenan RA. dADAR, a *Drosophila* double-stranded RNAspecific adenosine deaminase is highly developmentally regulated and is itself a target for RNA editing. RNA 2000;6:1004–18. [PubMed: 10917596]

12. MacKinnon R, Yellen G. Mutations affecting TEA blockade and ion permeation in

voltage-activated K+ channels. Science 1990;250:276–9. [PubMed: 2218530]

13. Kavanaugh MP, Varnum MD, Osborne PB, Christie MJ, Busch AE, Adelman JP, North RA. Interaction between tetraethylammonium and amino acid residues in the pore of cloned voltage-dependent potassium channels. J Biol Chem 1991;266:7583–7. [PubMed: 2019588]

14. Heginbotham L, MacKinnon R. The aromatic binding site for tetraethylammonium ion on potassium channels. Neuron 1992;8:483–91. [PubMed: 1550673]

15. Higuchi M, Single FN, Kohler M, Sommer B, Sprengel R, Seeburg PH. RNA editing of AMPA receptor subunit GluR-B: a base-paired intron-exon structure determines position and efficiency. Cell 1993;75:1361–70. [PubMed: 8269514]

16. Seeburg PH. A-to-I editing: new and old sites, functions and speculations. Neuron 2002;35:17–20. [PubMed: 12123604]

17. Zhou M, Morais-Cabral JH, Mann S, MacKinnon R. Potassium channel receptor site for the inactivation gate and quaternary amine inhibitors. Nature 2001;411:657–61. [PubMed: 11395760]

18. Long SB, Tao X, Campbell EB, MacKinnon R. Atomic structure of a voltage-dependent K+ channel in a lipid membrane-like environment. Nature 2007;450:376–82. [PubMed: 18004376]

19. Panyi G, Deutsch C. Probing the cavity of the slow inactivated conformation of Shaker potassium channels. J Gen Physiol 2007;129:403–18. [PubMed: 17438120]

20. Holmgren M, Shin KS, Yellen G. The activation gate of a voltage-gated K+ channel can be trapped in the open state by an intersubunit metal bridge. Neuron 1998;21:617–21. [PubMed: 9768847]

21. Del Camino D, Holmgren M, Liu Y, Yellen G. Blocker protection in the pore of a voltage-gated K+ channel and its structural implications. Nature 2000;403:321–5. [PubMed: 10659852]

22. Del Camino D, Yellen G. Tight steric closure at the intracellular activation gate of a voltage-gated K+ channel. Neuron 2001;32:649–56. [PubMed: 11719205]

23. Labro AJ, Raes AL, Bellens I, Ottschytsch N, Snyders DJ. Gating of *Shaker*-type channels requires the flexibility of S6 caused by prolines. J Biol Chem 2003;278:50724–31. [PubMed: 13679372]

24. Webster SM, Del Camino D, Dekker JP, Yellen G. Intracellular gate opening in Shaker K+ channels defined by high-affinity metal bridges. Nature 2004;428:864–8. [PubMed: 15103379]

25. Nguyen TP, Horn R. Movement and crevices around a sodium channel S3 segment. J Gen Physiol 2002;120:419–36. [PubMed: 12198095]

26. Doyle DA, Cabral JM, Pfuetzner RA, Kuo AL, Gulbis JM, Cohen SL, Chait BT, MacKinnon R. The structure of the potassium channel: Molecular basis of K+ conduction and selectivity. Science 1998;280:69–77. [PubMed: 9525859]

27. Lenaeus MJ, Vamvouka M, Focia PJ, Gross A. Structural basis of TEA blockade in a model potassium channel. Nature Struct Biol 2005;12:454–9.

28. Ahern CA, Eastwood AL, Lester HA, Dougherty DA, Horn R. A cation-π interaction between extracellular TEA and an aromatic residue in potassium channels. J Gen Physiol 2006;128:649–57. [PubMed: 17130518]

29. Heginbotham L, LeMasurier M, Kolmakova-Partensky L, Miller C. Single *Streptomyces lividans* K+ channels: Functional asymmetries and sidedness of proton activation. J Gen Physiol 1999;114:551–9. [PubMed: 10498673]

30. Klemic KG, Shieh CC, Kirsch GE, Jones SW. Inactivation of KV2.1 potassium channels Biophys. J 1998;74:1779–89.

31. Hoshi T, Zagotta WN, Aldrich RW. Two types of inactivation in Shaker K+ channels: effects of alterations in the carboxy-terminal region. Neuron 1991;7:547–56. [PubMed: 1931050]

32. Klemic KG, Kirsch GE, Jones SW. U-type inactivation of KV3.1 and *Shaker* potassium channels. Biophys J 2001;81:814–26. [PubMed: 11463627]

33. Kaulin YA, Santiago-Castillo JA, Rocha CA, Covarrubias M. Mechanism of the modulation of KV4:KChIP-1 channels by external K+ Biophys J 2008;94:1241–51. [PubMed: 17951301]

34. Rosenthal JJC, Bezanilla F. Extensive editing of mRNAs for the squid delayed rectifier K+ channel regulates subunit tetramerization. Neuron 2002;34:743–57. [PubMed: 12062021]

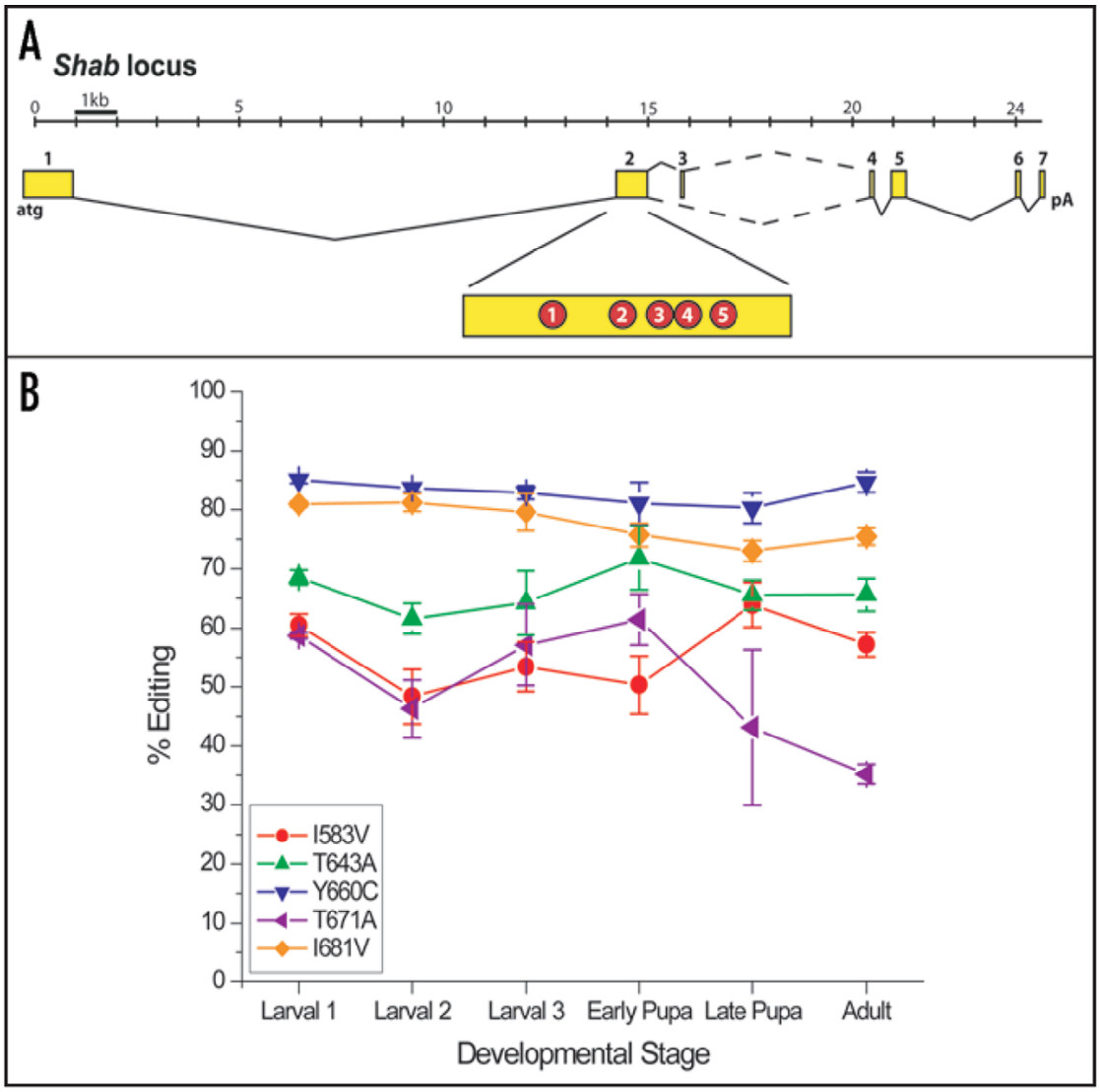

Figure 2.1.
Editing of the *Shab* locus. (A) The *Shab* locus transcription unit is shown with numbered exons (yellow), constitutive splice sites (solid lines) and alternative splice sites (dashed lines). The five RNA editing sites are indicated in red circles in exon 2. (B) The level of RNA editing for each site is shown as determined by whole-fly RNA preparation for three larval and two pupal stages and adult flies.

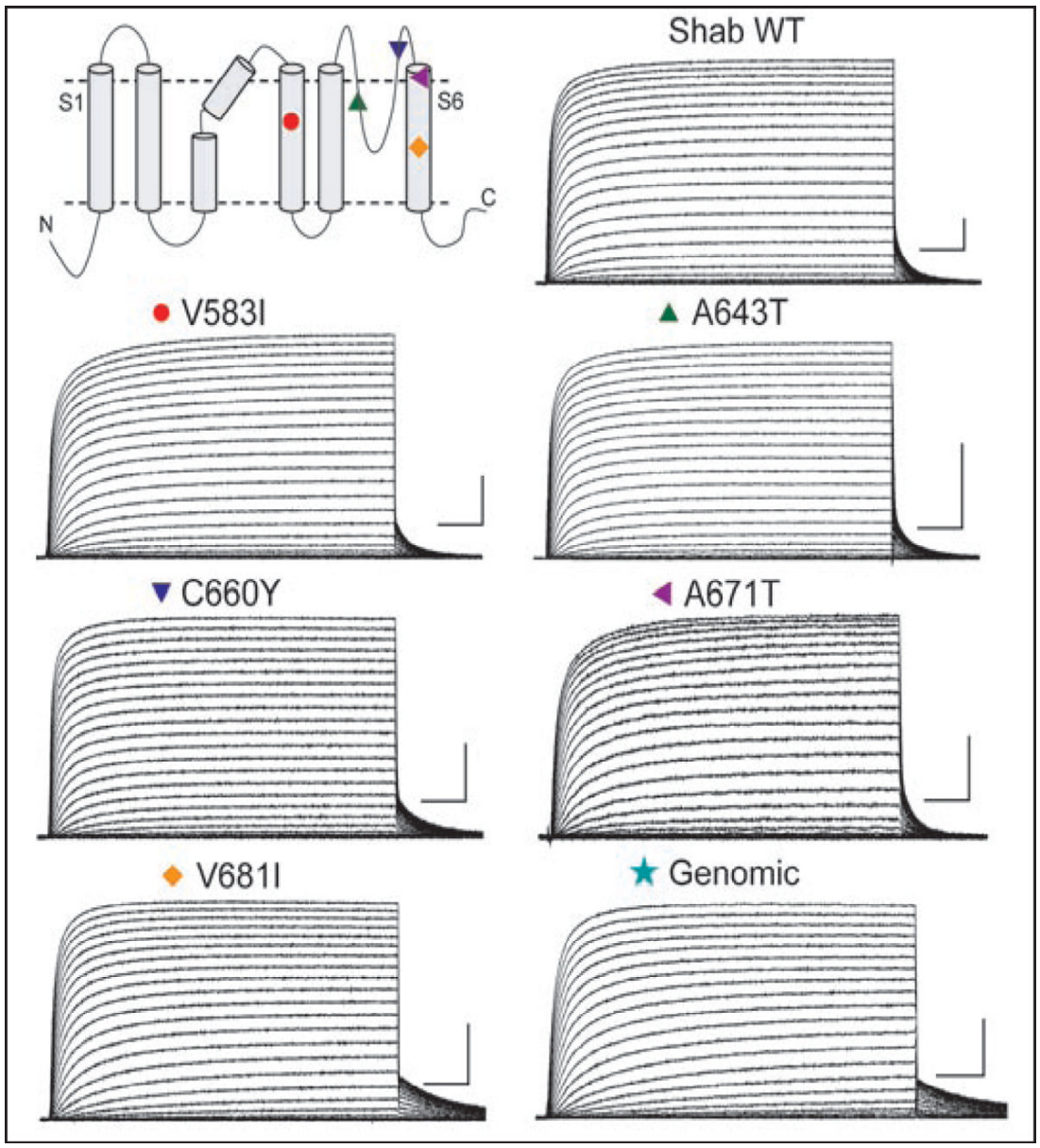

Figure 2.2.
Topology of the *Shab* channel indicating the approximate positions of the five edit sites. Also shown are representative currents for each channel. Symbols correspond to positions found on the topology model. Scale bar on each trace: 25 ms and 5 μA.

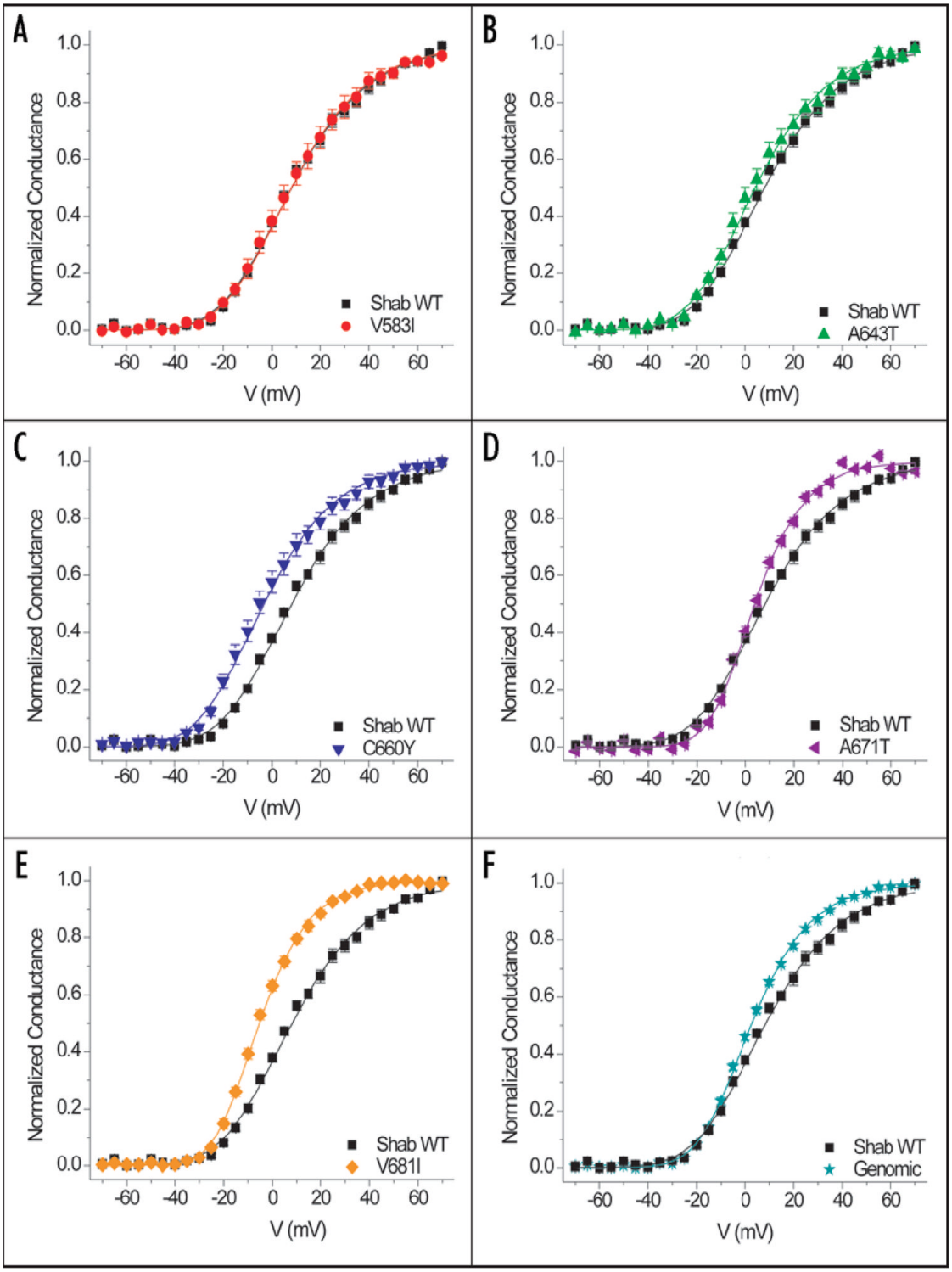

Figure 2.3.
Comparison of conductance-voltage relationships between WT *Shab* and each editing site mutant. Data fit by a Boltzmann function raised to the fourth power: Normalized conductance = $[1/(1 + \exp(q(V - V1/2)\ F/RT)]4$, where q is the slope, V1/2 is the midpoint, and RT/F = 25 mV. Parameters of fits in Table 1.

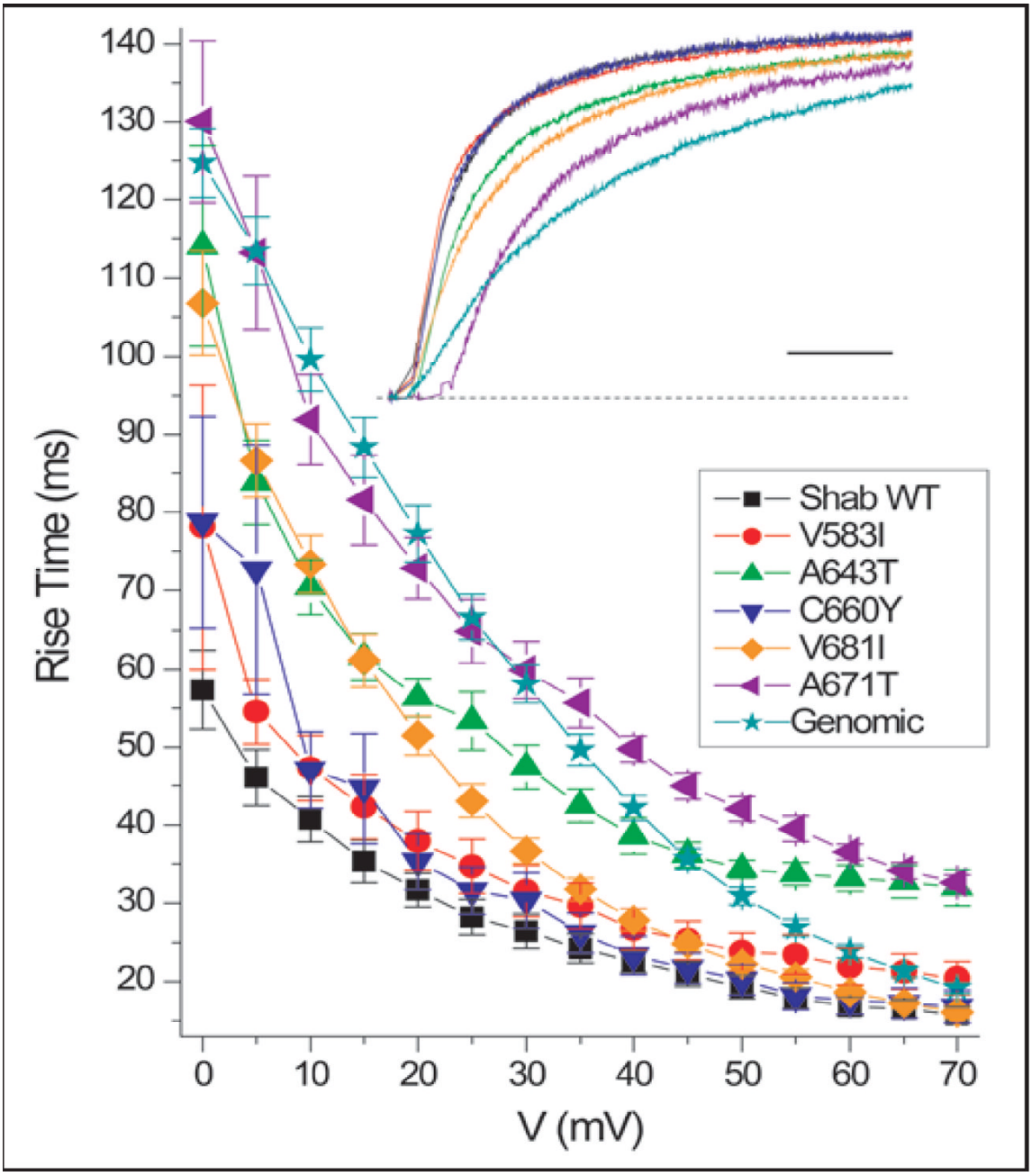

Figure 2.4.
Activation kinetics of *Shab* and editing site mutants. Rise time is a measurement of the time required for channel to pass from 10% to 90% of its maximum current during a depolarization. Differences are more pronounced at more hyperpolarized voltages where the A643T (n = 7), V681I (n = 8), A671T (n = 10) and Genomic (n = 10) constructs have slower rise times. A643T and A671T continue to have slower rise times through +70 mV. For WT, V583I and C660Y (n = 7). Inset: Representative traces of each editing mutant upon activation at +10 mV. Currents were normalized to the current at 200 ms after the depolarization. Scale bar 20 ms.

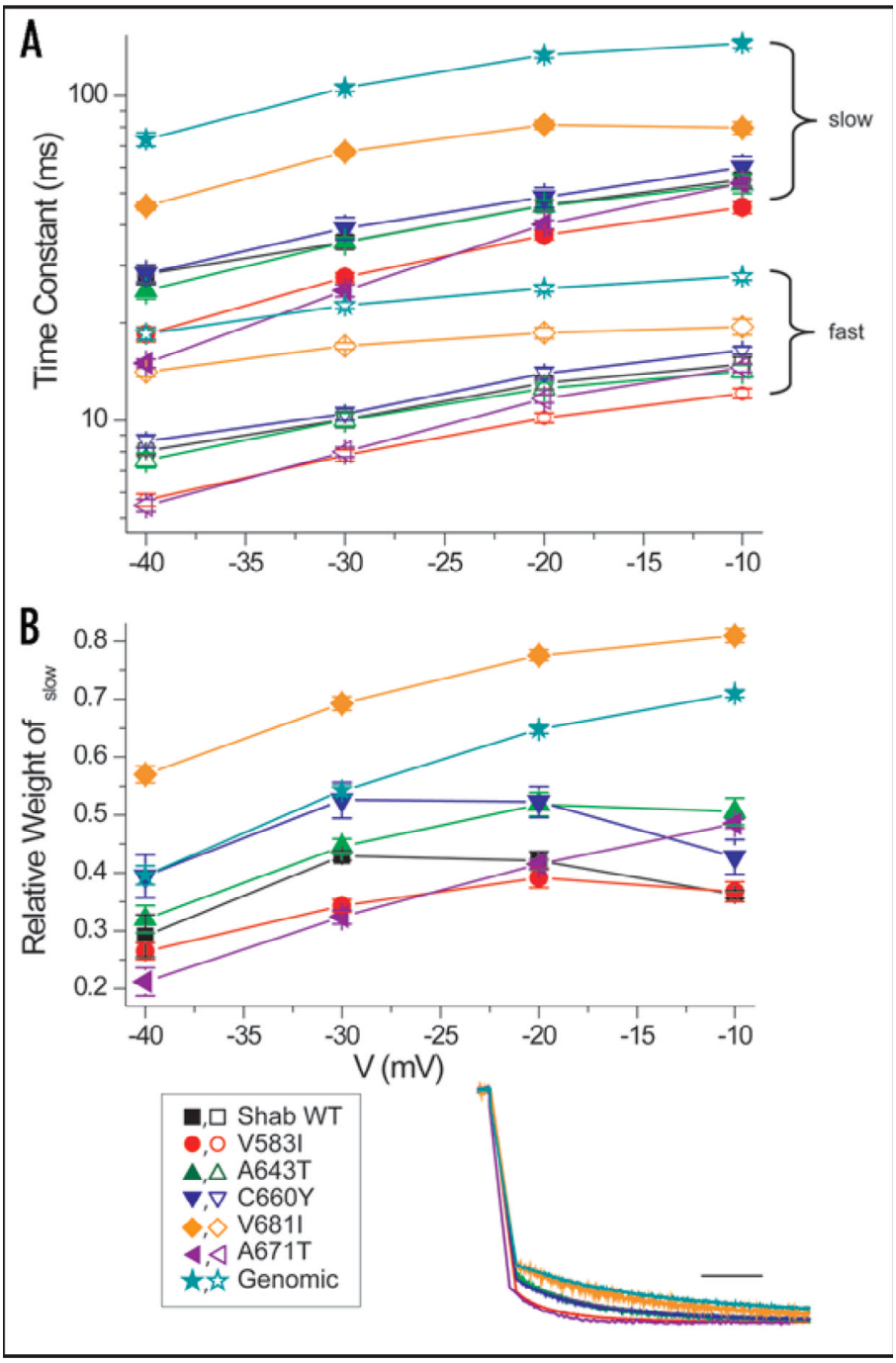

Figure 2.5.
Deactivation kinetics of WT (n = 6) and editing site mutants. (A) Deactivation kinetics of each channel have a fast (open symbol) and slow (closed symbol) component. Deactivation of V681I (n = 8) and Genomic (n = 8) are consistently slower, and V583I (n = 10) is faster, over the voltage range. The number of recorded cells was: A643T (n = 9), C660Y (n = 7) and A671T (n = 7). (B) Relative weight of the slow component of the deactivation time constant for each channel. V681I has the greatest relative weight for the slow component and V583I has the smallest. Inset: Representative traces of deactivation at −40 mV from a depolarization to +50 mV. Currents were normalized to the outward current 50 ms after the depolarization. Scale bar 10 ms.

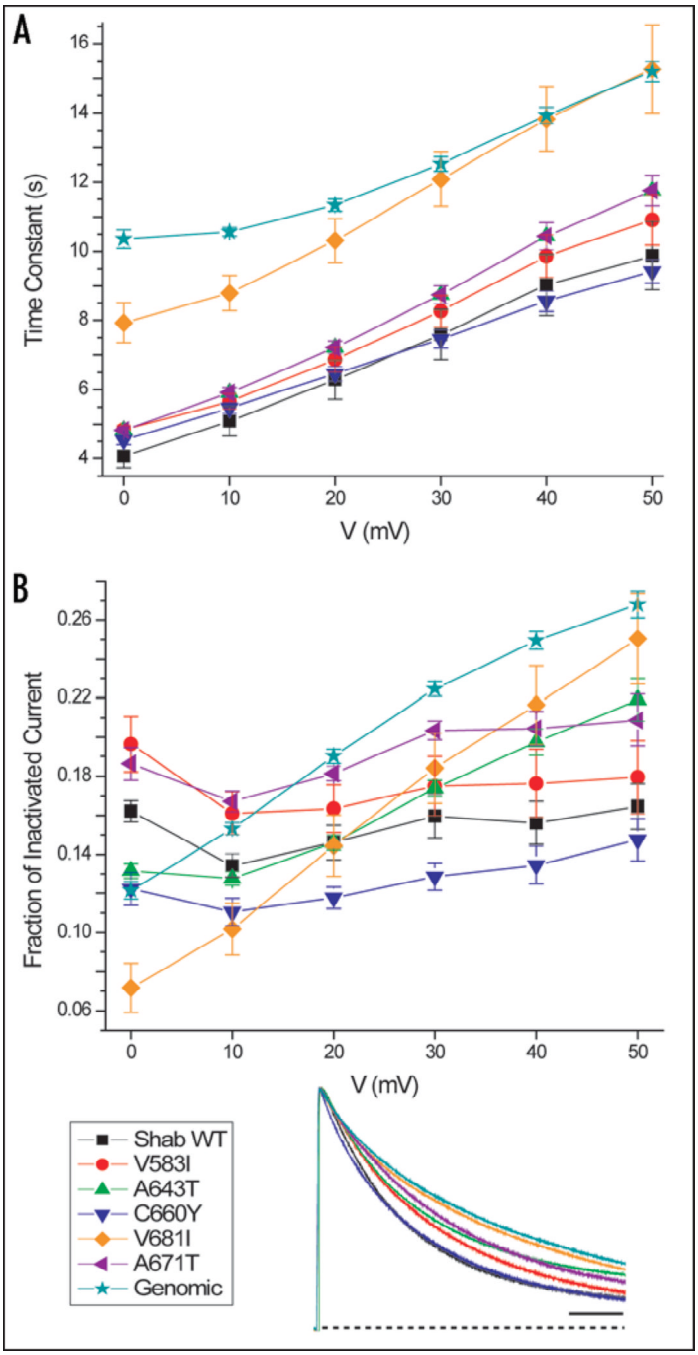

Figure 2.6.
Inactivation kinetics of *Shab* RNA edit sites. (A) Inactivation time constant of editing mutant sites. V681I (n = 8) and Genomic (n = 9) have uniformly slower inactivation time constants over the voltage range. Number of recorded cells: WT (n = 8) and all other constructs (n = 7). (B) The fraction of inactivated current compares the peak current with the current at the end of the 30-s depolarization. All constructs inactivate more completely at more hyperpolarized voltages. V681I and Genomic do not inactivate as completely as the other constructs. Inset: Representative traces of inactivation at +50 mV. Currents were normalized to the peak current of the trace. Scale bar 5 s.

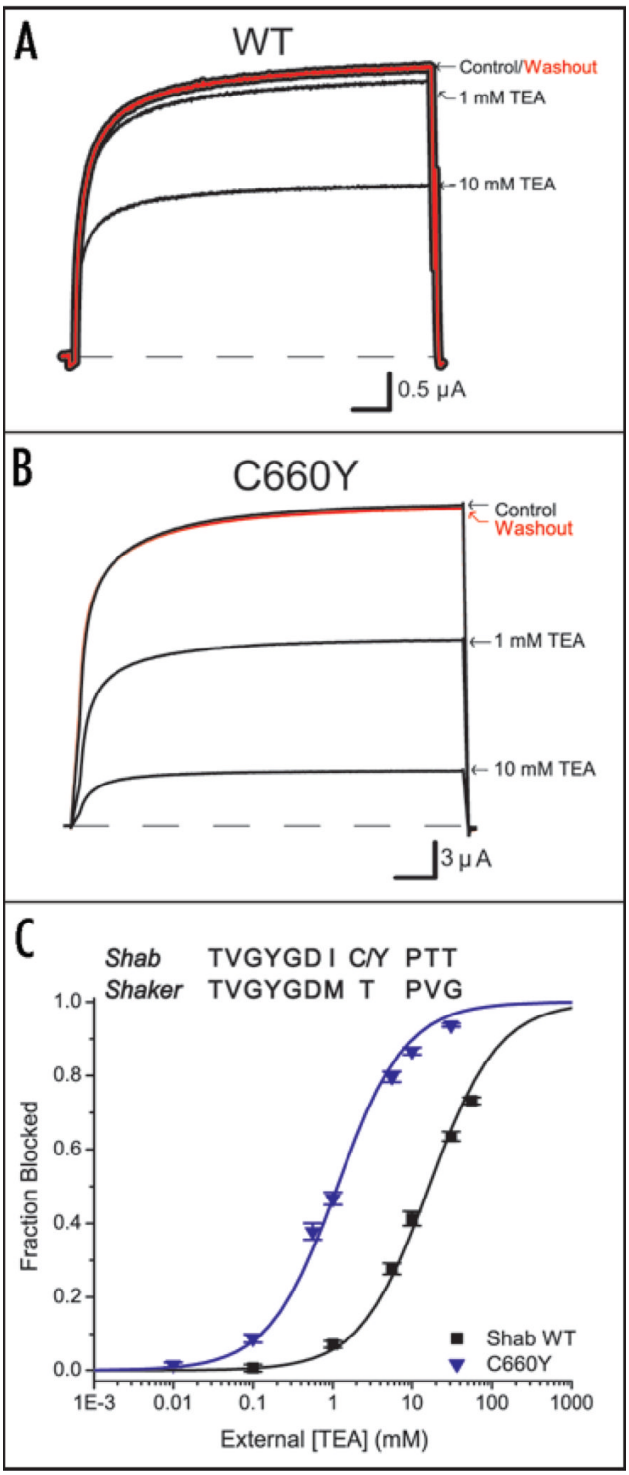

Figure 2.7.
Influence of extracellular pore residue on TEA block. (A) and (B) Both WT and C660Y exhibit reversible TEA block at +50 mV. C660Y is more sensitive as shown at 1 mM and 10 mM TEA. Scale bars are 10 ms. (C) TEA sensitivity was measured for WT (n = 5) and C660Y (n = 6) and fit using a standard binding equation. Inset above: Amino acid sequence alignment of the pore region comparing the TEA binding site in *Shab* (position 660) to the corresponding site in *Shaker* (position 449).

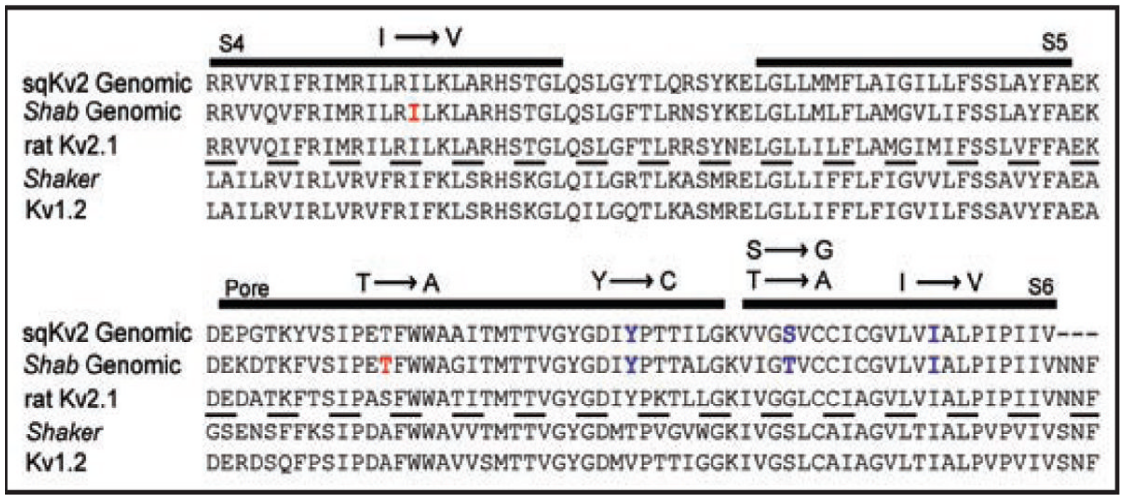

Figure 2.8.
Aligned sequences of squid, *Drosophila Shab* (fully genomic), rat $K_V2.1$, *Drosophila Shaker* and rat $K_V1.2$. In red are two RNA editing sites found only in *Shab*. Shown in blue are three RNA editing sites found in both *Shab* and sqK_V2. Note the second site has the same location but a different resultant amino acid change for squid (S → G) vs. *Drosophila* (T → A). Figure adapted from Patton et al.[3]

Table 1

Midpoints of activation and equivalent charge from conductance-voltage relationships

	***Shab* WT (n = 8)**	**V583I (n = 9)**	**A643T (n = 8)**	**C660Y (n = 6)**	**V681I (n = 8)**	**A671T (n = 14)**	***Shab* Genomic (n = 9)**
$V_{1/2}$ (mV)	8.2 ± 1.2	8.1 ± 2.4	4.3 ± 2.3	−3.2* ± 2.2	−5.3* ± 0.8	4.0 ± 0.8	2.6 ± 0.5
q (e_0)	1.3 ± 0.07	1.4 ± 0.1	1.4 ± 0.1	1.4 ± 0.1	2.0* ± 0.1	1.9* ± 0.06	1.6 ± 0.03

* Indicates data are statistically significant compared to WT ($p < 0.05$, 1-way ANOVA with Scheffé correction).

Chapter 3:

Regulated RNA Editing and Functional Epistasis in *Shaker* Potassium Channels.

This chapter consists of previously published data. "Regulated RNA Editing and Functional Epistasis in Shaker Potassium Channels." by Lindsey Ingleby*, Rachel Maloney*, James Jepson, Richard Horn, and Robert Reenan. (2009). Journal of General Physiology **133**(1): 17-27. (*) These authors contributed equally to this work. My specific contributions to this publication include the data presented in figures 3.1 and 3.2. This includes the developmental analysis of *Shaker* editing, as well as the spatial distribution of *Shaker* editing isoform analysis. Additionally, I generated the mutations within the *Shaker* expression constructs used in electrophysiology studies of channel function.

Abstract

Regulated point modification by an RNA editing enzyme occurs at four conserved sites in the *Drosophila Shaker* potassium channel. Single mRNA molecules can potentially represent any of $2^4 = 16$ permutations (isoforms) of these natural variants. We generated isoform expression profiles to assess sexually dimorphic, spatial, and temporal differences. Striking tissue-specific expression was seen for particular isoforms. Moreover, isoform distributions showed evidence for coupling (linkage) of editing sites. Genetic manipulations of editing enzyme activity demonstrated that a chief determinant of *Shaker* editing site choice resides not in the editing enzyme, but rather, in unknown factors intrinsic to cells. Characterizing the biophysical properties of currents in nine isoforms revealed an unprecedented feature, functional epistasis; biophysical phenotypes of isoforms cannot be explained simply by the consequences of individual editing effects at the four sites. Our results unmask allosteric communication across disparate regions of the channel protein and between evolved and regulated amino acid changes introduced by RNA editing.

Introduction

Genomic information unfolds according to a well-established paradigm; the amino acid sequence of a protein is encoded by a literal one-to-one mapping from each genotypic codon to one of 20 amino acids. This central paradigm assumes robust correspondence between DNA and its transcribed RNA copy. A notable interloper in this orderly enterprise is an enzyme that chemically alters individual nucleotides of RNA. Action of the adenosine deaminase acting on RNA (ADAR) enzymes results in the hydrolytic deamination of adenosine-to-inosine (A-to-I) in double-stranded (ds) RNA substrates (Bass, 2002). ADAR modification can affect numerous biological readouts, including alternative RNA splice choices, opposition to RNA interference pathways, and altered microRNA processing (Rueter et al., 1999; Bass, 2006 ; Nishikura, 2006). One outcome of A-to-I editing, however, has overt consequences for information encoding— inosine is recognized as guanosine (G) by the translation machinery (Basilio et al., 1962), rendering almost half of the codons of the genetic code re-assignable to edited versions encoding different amino acids. Inexplicably, animal genes that encode components of rapid electrical and chemical neurotransmission dominate gene targets of this recoding aspect of editing (Seeburg and Hartner, 2003) and usually require intronic cis elements to form a dsRNA structure that serves as an ADAR substrate (Herbert, 1996). Genetic deficiency for ADAR activity or altered ADAR function can cause behavioral dysfunction, both of which have been implicated in neurological disease (Higuchi et al., 2000; Palladino et al., 2000a, Tonkin et al., 2002; Maas et al., 2006; Mehler and Mattick, 2007). Nevertheless, the functional consequences of A-to-I RNA editing for sites in most ADAR gene targets

remain unknown.

Inosine can be detected in mature mRNA from many mammalian tissues, but it reaches peak levels in material isolated from the brain (Paul and Bass, 1998). This simple observation is complicated by certain facts; there are three known editing enzymes (ADAR1-3) in mammals, different isoforms of these ADARs can be produced by alternative processing mechanisms, and ADARs act as a dimer (for review see Keegan et al., 2004). Nevertheless, regulation has been shown to occur at the level of individual editing sites via strong enzyme preference. For instance, the GluR-B AMPA receptor (Q/R) site is edited efficiently only by ADAR2, whereas the paralogous GluR-6 kainate receptor (Q/R) site is edited by ADAR1 (Maas et al., 1996). Even editing sites within several nucleotides of one another can require different ADARs, such as in mammalian serotonin-2C receptor editing (Liu et al., 1999). Conversely, the GluR-B (R/G) site and mammalian GABA receptor transcripts are efficiently edited by either ADAR1 or ADAR2 (Melcher et al., 1996; Ohlson et al., 2007). Both spatial and temporal regulation of specific editing has also been shown to occur. In vertebrates and invertebrates alike, there are marked increases in A-to-I editing for many specific targets throughout development (Bernard and Khrestchatisky, 1994; Lomeli et al., 1994; Palladino et al., 2000b; Keegan et al., 2005; Ohlson et al., 2007). Layering onto this developmental control, spatial regulation of ADAR-mediated recoding produces differing degrees of specific target editing within different regions of the nervous system. In addition, target transcripts with multiple editing sites, like the serotonin-2C receptor, can produce numerous edited isoforms combinatorially (Burns et al., 1997). Neither the temporal nor

spatial patterns of specific editing of ADAR targets in mammals have been shown to correlate with known patterns of ADAR gene expression, tacitly implying other unknown factors (Lai et al., 1997; Liu et al., 1999; Paupard et al., 2000).

Voltage-gated potassium channels play crucial roles in determining the firing properties of neurons (Hille, 2001) and are the only common gene target of A-to-I editing among three major animal phyla: chordates, mollusks, and arthropods. In mollusks, extensive editing of the squid channel, sqKv1.1, was shown to regulate functional expression through effects on tetramerization, whereas a subset of the extensive editing sites of sqKv2 affect channel closure and slow inactivation (Patton et al., 1997; Rosenthal and Bezanilla, 2002). In neither case are the RNA structures that direct editing known, nor the reason for such extensive editing. In another invertebrate, *Drosophila*, RNA editing of Kv2 (*Shab*) channels has been shown to affect channel biophysics (Ryan et al., 2008). In chordates, the mammalian intronless Kv1.1 gene was shown to undergo spatially regulated editing through the formation of a small RNA hairpin contained within the coding sequence (Hoopengardner et al., 2003; Bhalla et al., 2004). RNA editing of one position within the Kv1.1 potassium channel was shown to dramatically affect the process of channel inactivation.

Here, we describe the in vivo production of editing isoforms for the *Shaker* potassium channel from the arthropod, *Drosophila melanogaster*. The *Shaker* gene possesses four developmentally regulated A-to-I editing sites in highly conserved regions of the channel protein. Expression profiling of the 16 possible isoforms reveals that 15 are expressed. Unexpectedly, we found dramatic tissue-specific differences in *Shaker*

isoform expression levels spanning almost two orders of magnitude. Linkage analyses reveal that the editing of certain sites affects the likelihood that other sites are also edited. ADAR expression studies in transgenic flies revealed that unknown factors, intrinsic to certain locations, predominate in this spatial regulation and that ADAR preference plays a minimal role. The regulatory complexities of *Shaker* editing extended beyond spatial and temporal scales. Characterization of the biophysical properties of the more abundant *Shaker* isoforms reveals a functional epistasis; the consequence of an editing mutation, particularly on inactivation rate, depends on whether distant sites are also edited.

Materials and Methods

Fly Stocks and Expression Studies

The *Drosophila melanogaster* wild-type stock used was Canton-S. For rescue experiments, the *dADAR 5G1* -null allele was used. In brief, *dADAR 5G1* /FM7;; *elav*-pSwitch females were crossed to males containing a rescuing transgene expressing the dADAR-3/4 isoform (TM3::UAS-dADARwt5/TM6). *dADAR 5G1* /Y;;TM3::UAS-dADARwt5/*elav* -pSwitch males were selected and aged for 7 d. Animals were then fed food containing 200 μ M RU-486 to induce ADAR expression for 7 d and then harvested for analyses.

RNA Editing Analysis

All RNA extractions were performed using TRIzol (Invitrogen) on whole flies/larvae or various dissected body parts as indicated in Results. *Shaker* transcripts were amplified by reverse transcription (RT)-PCR using gene-specifi c primers at all steps. For isoform profiles, cDNAs were cloned from at least three independent RT-PCR reactions for each sample and subjected to automated sequence analysis (see Table S1, available at http://www.jgp.org/cgi/content/full/jgp.200810133/DC1). Levels of editing for individual editing sites determined for developmental and rescue studies were obtained by direct sequencing of RT-PCR products from at least three independent reactions per sample. Areas under the curves were determined from electropherogram traces and editing level expressed as: { % editing } = (area G/total area A+G) * 100. Where editing levels for individual sites were obtained from isoform profiles (Fig. 3.3), the number of clones edited at a given site was divided by the total number of clones in the sample.

Expression Clones, Mutagenesis, and Transfection

For functional studies we used chimeras consisting of the N terminus of *Shaker* B and the C terminus common to *Shaker* A and C. These cDNA chimeras were generated by using a naturally occurring XbaI restriction enzyme cutting site found in *Shaker* exon 4. The C-terminal region clones were isolated from *Drosophila* by RT-PCR and sequence verified. In some experiments fast inactivation was abolished by the deletion of residues 6 – 46. The point mutations T449V and V463A were constructed to inhibit slow

inactivation. All *Shaker* constructs were inserted into the pGW1 vector for expression in mammalian cells. Editing mutations at the four sites were generated using the QuikChange Site-Directed Mutagenesis kit (Agilent Technologies) and verified by sequencing. Transfection of tsA201 cells was accomplished using standard calcium phosphate methodology. All isoforms were cotransfected with the auxiliary subunit *Hyperkinetic* (provided by G. Wilson, University of Michigan, Ann Arbor, MI). Recordings were taken 1 – 3 d after transfection.

Electrophysiology and Data Analysis

Standard whole cell patch clamp recording methods were used to record ionic currents (Ding and Horn, 2003). Electrode resistance ranged between 0.8 and 1.6 M Ω , and series resistance was compensated so that voltage errors were < 3 mV. Patch pipettes contained (in mM): 105 CsF, 35 NaCl, 10 EGTA, and 10 HEPES, pH 7.4. The bath solution contained (in mM): 150 NaCl, 2 KCl, 1.5 CaCl 2 , 1 MgCl 2 , and 10 HEPES, pH 7.4. All experiments were performed at room temperature. pCLAMP (MDS Analytical Technologies) software was used for data acquisition and analysis. Further analysis used Origin (Microcal), Microsoft Excel, and in-house FORTRAN programs. We analyzed the isoform distributions (Fig. 3.2) with the program Mendel 7.0 (http://www.genetics.ucla.edu/software/mendel).

Online Supplemental Material

The supplemental material includes four tables and three figures. Table S3.1 summarizes the DNA sequence profiling of 821 *Shaker* cDNA clones from various tissue samples and their distributions among the various 16 isoforms. Tables S3.2 – S3.4 summarize the inactivation parameters, conductance-voltage parameters, and deactivation time constants for nine *Shaker* editing isoforms. Fig. S3.1 shows the circle diagram depicting the ensemble average basepairing probabilities for the structure pairing the evolutionarily conserved e1 element with the coding sequence at *Shaker* editing site 1. Fig. S3.2 shows the circle diagram depicting base-pairing probabilities with the largest centroid of the structure pairing the evolutionarily conserved e2 and e3 elements with the coding sequences at *Shaker* editing sites 2 – 4. Fig. S3.4 shows the local predicted dsRNA secondary structures pairing conserved intronic editing site complementary sequences (ECSs) with the regions surrounding the edited adenosines. The online supplemental material is available at http://www.jgp.org/cgi/content/full/jgp.200810133/DC1.

Results

RNA Editing of *Drosophila Shaker*

RNA editing of *Drosophila Shaker* has been reported to occur at six positions (Hoopengardner et al., 2003). Two sites are edited at low levels (< 5%) in the T1 domain of the channel and were not considered here. The remaining four editing sites are distributed in two exons (Fig. 3.1 A). Site 1 is located in exon 7, separated by 19,323 nucleotides in genomic sequence from site 2 in downstream exon 12. Sites 3 and 4 are adjacent in exon 12, 74 nucleotides downstream of site 2, with a separation of only 6 nucleotides. ADAR-mediated recoding requires a dsRNA intermediate, frequently formed by base-pairing interactions with intronic ECSs. We have previously shown that phylogenetic conservation of editing sites is accompanied by a high degree of conservation for the ECS elements that direct dsRNA structure formation (Hanrahan et al., 2000; Reenan et al., 2000). We used comparative genomics of the 12 sequenced *Drosophila* genomes (http://flybase.org/) to search for conserved ECS elements in *Shaker*. In the intron downstream of exon 7, we found an invariant conserved element (Fig. 3.1 A, e1) located 1,289 nt from site 1. Computational folding of the pre-mRNA region encompassing site 1 and e1 was performed using SFOLD, a program that uses sampling of the Boltzmann-weighted ensemble of RNA secondary structures and statistical clustering methods to more effectively characterize structured RNA (Ding et al., 2005, 2006). An ensemble structure was obtained that paired site 1 with e1 generating a structure that, in appearance, is similar to many known ADAR substrates

(Figs. S3.1 and S3.3). This predicted structure is absolutely conserved in all 12 *Drosophila* species, whereas all remaining flanking sequences are quite divergent. A similar analysis for the region near editing sites 2 – 4 revealed two conserved elements (e2 and e3) in the upstream intron flanking exon 12 (Figs. S3.2 and S3.3). Thus, it appears that three distinct dsRNA domains control the editing of *Shaker* sites 1 – 4. We then compared *Shaker* editing for five species spanning the phylogenetic distances covered by the "12 genomes" and found editing at sites 1 – 4 conserved in all cases (unpublished data). Lastly, we assessed editing of the *Shaker* ortholog in six species of mosquito and honey bee, where we found neither evidence for RNA editing nor any evidence for conservation of intronic elements e1 – e3 in species that do not edit (unpublished data). Thus, editing of *Shaker* at sites 1 – 4 appears to be Diptera specific and possibly restricted to the family Drosophilidae.

Editing of *Shaker* sites 1 – 4 alters amino acids encoded at positions that are invariant or highly conserved in all vertebrate and invertebrate Kv1 family orthologs (Fig. 3.1 B). Site 1 is at the top of the voltage-sensing transmembrane segment S4 and results in an isoleucine-to-methionine (I360M) substitution, site 2 is in the S6 segment and is recoded from isoleucine-to-valine (I464V), and sites 3 and 4 are in the S6 T cytoplasmic tail separated by one amino acid, resulting in threonine-to-alanine (T489A) and glutamine-to-arginine (Q491R) recoding, respectively.

Because several editing sites have been reported to undergo developmentally regulated modification in vertebrate and invertebrate systems, we investigated the temporal regulation at each editing site in *Shaker* (Fig. 3.1 C). Site 1 is edited in both C-

terminal alternative splice forms, *ShakerA* and *ShakerB*. Determination of the level of editing throughout development revealed that site 1 is largely unregulated in terms of editing level and is edited efficiently (>60%). Despite occurring in the same ion channel transcript, sites 2 – 4 display highly regulated editing and variable extents of editing. Like numerous other *Drosophila* editing sites, sites 2 – 4 are predominantly adult specific (Hanrahan et al., 2000, Palladino et al., 2000b).

Isoform Distributions

Fig. 3.2 A shows the color-coded distribution of the $2^4 = 16$ possible isoforms in whole larvae and seven different tissues of adult *Drosophila*. For each tissue, 96 – 111 individual cDNA clones were sequenced for a total of 821 sequences (Table S3.1). The editing status at each site is represented by an A (unedited) or a G (edited) in linear order, rather than by amino acid change. We detected 15/16 possible isoforms, spanning a range from 0.1 (1/821 for AGAG and GGAG) to 22.7% (186/821 for GAAA), in our total dataset. Although the male and female populations were statistically indistinguishable ($P > 0.3$; Fisher's exact test of homogeneity) (Lange, 2003), the distributions were significantly different for all other pairwise comparisons between tissue populations ($P < 0.001$). The most dramatic difference among the tissues is seen for the isoform GAAA, which comprises, for example, 75 (68%) of the 111 cDNA clones in the male wing and is completely absent in 100 cDNA clones from female heads.

Examination of the distributions of isoforms shows evidence for coupling (linkage) between editing sites. For example, in the adult male wing there are 78 out of 111 clones

in which sites 3 and 4 are both unedited (xxAA) and none in which site 3 is unedited and site 4 is edited (xxAG). This is not due simply to the paucity of editing at site 4 because 11 out of 111 clones were of the form xxxG. A similar pattern is seen for all other tissues. For example, there are 14 out of 100 clones of xxAA from male heads, but none of xxAG. In contrast, there are 17 xxGA ' s and 69 xxGG ' s. Therefore, if site 3 is unedited, site 4 is almost never edited. Likewise, if site 3 is edited, site 4 is usually edited also. This can be considered a positive cooperativity of editing between sites 3 and 4. Fig. 3.2 B shows a statistical analysis of the coupling between editing sites in each population (Lange, 2003). The colormap represents Lewontin's D ' statistic that ranges between 1 and 1 for sites that show either negative or positive cooperativity, respectively (Lewontin, 1964). At completely independent sites D' = 0. Starred squares show significant coupling between the indicated sites ($P < 0.02$; Fisher's exact test). An intriguing pattern appears from these data. For all populations, sites 3 and 4 are highly coupled, always in the positive direction. Sites 1 and 3 are also coupled in all tissues, but the sign depends on the tissue: negative cooperativity for eye, antenna, and wing, and positive cooperativity for all other tissues. Moreover, significant coupling occurs among all sites for eye, antenna, and wing, although the sign of D' can be either positive or negative. One of the most surprising observations is the ubiquitous coupling between sites 1 and 3, despite being separated by many thousands of nucleotides in the immature mRNA.

Specificity of ADAR for Particular Editing Sites *In Vivo*

To seek an explanation for the striking spatial and temporal control of editing seen for *Shaker*, we examined *dADAR* 's contribution to regulation. The *dADAR* locus is capable of generating several different isoforms by alternative splicing (Palladino et al., 2000b). dADAR has also been demonstrated to act as a protein dimer on RNA substrates (Gallo et al., 2003). Thus, we reasoned that much of the temporal and spatial regulation of *Shaker* editing could be attributed to a program of regulated expression and combinatorial action of different dADAR isoforms. To test this hypothesis, we used the pSwitch-GAL4 binary expression system (Roman et al., 2001) to rescue nervous system expression of dADAR in flies genetically deficient for all detectable editing activity of the *dADAR* locus, including editing of all four *Shaker* sites studied here (Palladino et al., 2000a, Hoopengardner et al., 2003). We chose one of the most abundant *dADAR* isoforms produced in adults and constructed transgenic flies expressing its cDNA version, eliminating any possible interaction between alternative ADAR enzymes. Levels of editing were determined for each site individually in transgenic animals from two tissue samples, adult male head and adult male wing, and compared with the levels of editing seen in wildtype controls as well as the isoform expression profile data (Fig. 3.3). In the adult male head, it is clear that a single isoform of dADAR is capable of editing all four sites in similar ratios as those seen in wild-type controls, albeit at somewhat reduced levels at each site (Fig. 3.3 A). The site-specific editing levels seen by this method also correlate well with the editing levels determined for each site individually from the profiling data of Fig. 3.2 A. Contrasting with these data are the levels of editing seen in

the adult male wing (Fig. 3.3 B). Here, site 1 is much more highly edited in the wing than in the adult head, in keeping with control samples and profiling data. We do observe slight differences in the editing levels in rescued animals with respect to controls in both tissues, which we attribute to differences between the artificial expression system (GAL4:UAS) used in these experiments and endogenous *dADAR* regulation. Nevertheless, there is clear evidence that the efficacy of a single ADAR isoform on particular editing sites can be significantly affected by factors intrinsic to, and predominating in, the cells in which the ADAR is expressed.

Functional Diversity of *Shaker* Isoforms

We selected 9 of the 16 possible isoforms for detailed functional characterization. Each was expressed transiently in a mammalian cell line, and whole cell currents were characterized. The channel-forming α-subunits were coexpressed with the auxiliary subunit *Hyperkinetic* , a cytoplasmic protein that associates with *Shaker* in *Drosophila* (Chouinard et al., 1995). Because the expression levels were so high in all of these isoforms, we were able to examine whole cell currents carried by Cs +, which is two orders of magnitude less conductive than K + (Heginbotham and MacKinnon, 1993). Fig. 3.4 shows examples of families of currents elicited by depolarizations from a holding potential of -120 up to +70 mV. The top row shows unedited (AAAA) and fully edited (GGGG) isoforms. The bottom row shows the two isoforms with the most extreme functional phenotypes in terms of the kinetics of inactivation. GGGA has the fastest, and AAGA the slowest, rates of inactivation among the nine variants we examined. The

rate of inactivation during a depolarization is well fit by a single exponential relaxation. Fig. 3.5 A shows the time constants for these fits. Although most of these kinetic parameters are comparable among the nine isoforms, AAGA stands out as the slowest over a wide range of voltages, with inactivation time constants approximately threefold slower than those of GGGA. Steady-state inactivation also varied among the nine isoforms, with midpoints differing as much as 11.8 mV (Fig. 3.5 B and Table S3.2). The fractional extent of inactivation induced by a 100-ms depolarization to -20 mV (Fig. 3.5 B) also varied among the isoforms, from 0.92 ± 0.02 for GGGA to 0.78 ± 0.01 for AAGA. This steady-state behavior is consistent with the kinetics of inactivation in that the isoform that inactivates most rapidly also inactivates most completely, and the isoform that inactivates most slowly inactivates least completely. Like entry into the inactivated state, the rate of recovery from inactivation at -120 mV, after a 75-ms depolarization to +70 mV (Fig. 3.5 C, inset), also had an approximately threefold range, with GGGA the slowest and AAGG the fastest (Table S3.2). Thus, isoforms that inactivate rapidly tend to recover slowly, and vice versa.

Activation Gating

The kinetics and steady-state properties of fast inactivation are coupled to the conformation of the activation gate (Armstrong and Bezanilla, 1974; Bezanilla et al., 1991). Because of this coupling, activation is difficult to characterize in channels that, in response to a depolarization, inactivate on a comparable time scale as they open (e.g., Fig. 3.4). The differences in fast inactivation among the isoforms could, therefore,

be due to differences in activation gating. To test this possibility and analyze the properties of activation gating directly, we examined the same nine isoforms in constructs lacking the N-terminal inactivation ball (Δ6-36) (Hoshi et al., 1990). Fig. 3.6 shows examples of families of currents, mostly outward currents carried by Cs +, for the same isoforms depicted in Fig. 3.4. Note the inward current carried by extracellular K + ions at hyperpolarized voltages and the gating current visible as a shoulder on the rising phase of the activating Cs + currents. G-V curves were generated from tail currents and had one or two Boltzmann components (Table S3.3). Fig. 3.7 plots G-V curves from four isoforms, including the most (GAAA) and least (AAAG) depolarized variants. The midpoints of the major (hyperpolarized) components differed by at most 11 mV among the nine isoforms (Table S3.3), a similar range as we obtained for steady-state inactivation (Fig. 3.5 B). The coupling between steady-state activation and inactivation is shown clearly in Fig. 3.7 B, which plots the midpoints of inactivation against those of activation. The relationship has a slope of 0.86 ± 0.13 with a correlation coefficient of 0.93. A noticeable difference among the isoforms shown in Fig. 3.6 is that AAGA has faster kinetics of deactivation at -120 mV than those of the other three isoforms. The rate of deactivation varied widely among the isoforms (Table S3.4). Fig. 3.8 (A and B) demonstrates this point with tail currents from the fastest (AAGG) and slowest (AGAA) deactivating isoforms over a voltage range of -60 to -140 mV. Fig. 3.8 C shows a complete lack of correlation between the kinetics of deactivation and those of inactivation. This suggests that the rate of ball-and-chain inactivation in these isoforms is controlled by factors quite separate from those controlling movement of the activation gate. The kinetics of gate

opening were not examined in detail because of the kinetic overlap of gating and ionic current under the conditions of these experiments. Although the biophysical properties of these nine isoforms manifest the natural functional variability that can be achieved through RNA editing, they also reveal an unprecedented feature, namely a functional epistasis. The isoform AAGA inactivates distinctly slower than any of the others (Figs. 3.5 A and 3.8 C). Yet this biophysical phenotype cannot be accounted for by point mutations at any of the four sites. AAGA is edited only at the third site, but the slowing of inactivation occurs only if the other three sites are unedited. For example, the point mutation AAAG-to-AAGG has no effect on inactivation kinetics; nor does AGAA-to-AGGA. Only the point mutation AAAA-to-AAGA produces this slowing. This result unmasks an allosteric communication across disparate regions of the channel protein. Because other biophysical properties of AAGA are unremarkable, it is unlikely that the channel has undergone gross structural changes, leaving the underlying mechanism of this epistasis a matter of speculation. Nevertheless, it suggests that caution is required in interpreting the biophysical consequences of point mutations. A protein's response to mutation at one site may depend in unpredictable ways on seemingly benign or neutral changes at other sites quite removed in primary sequence.

Discussion

RNA modification by ADAR enzymes provides an excellent example of a system for diversifying protein expression from multiple loci, but acting peculiarly, at the behest of neurons. Despite knowledge of editing enzymes and their targets, little information has been gleaned about the regulation of RNA editing in vivo. In mammals, there is clear evidence for spatial and temporal regulation of RNA editing, as well as functional variation between edited and unedited protein isoforms. However, analysis of the regulation of editing in mammals is complicated by the presence of multiple ADAR genes and a paucity of genes targeted for protein recoding. For example, ADAR1 is known to have an RNA editing function in the nervous system, yet ADAR1-deficient mice die early in embryogenesis for reasons that appear to be unrelated to nervous system function (Wang et al., 2000). ADAR1's role in adult editing will need to be addressed in conditional mutants. Animals lacking ADAR2 display profound neuropathological phenotypes, but can be rescued by a copy of the GluR-B subunit preedited at the Q/R site, even though substantial residual levels of editing are seen for other known ADAR targets (Higuchi et al., 2000).

In striking contrast with the limitations inherent in mammalian studies, *Drosophila melanogaster* provides an ideal system for studies of regulation because fruit flies have only one ADAR gene and many (> 150) editing sites in nervous system genes. We chose to study RNA editing of the *Shaker* potassium channel, one of the most well-understood and thoroughly characterized ion channels in biology. Genetic perturbations to *Shaker* orthologs or their β-subunits have been linked to fly behavioral phenotypes as

well as human diseases, such as episodic ataxia, epilepsy, impaired learning, and sleep disorders (Giese et al., 1998; Cirelli et al., 2005; Gasque et al., 2006; Bushey et al., 2007; Douglas et al., 2007; Jen et al., 2007). In addition, *Drosophila Shaker* has been shown to be subject to posttranscriptional processing by temporally and spatially regulated alternative splicing to generate functionally distinct protein isoforms (Kamb et al., 1987; Hardie et al., 1991; Rogero et al., 1997).

Regulated RNA Editing of *Shaker*

We show here that *Shaker* is subject to tightly regulated RNA editing events at four highly conserved sites in two widely separated exons (exon 7 and exon 12) (Fig. 3.1 A) within the *Shaker* transcription unit. Comparative genomics reveals conserved RNA editing coupled with ultra-conserved intronic sequences that are the presumptive cis-acting elements proximal to all four editing sites. Computational predictions strongly support three dsRNA structures directed by these elements: e1 pairing with site 1, e3 pairing with site 2, and e2 pairing with sites 3 and 4 (Figs. S3.1 – S3.3). Corroborative evidence for the independent nature of these structures is seen when addressing the spatial and temporal control of *Shaker* editing. We observed dramatic developmental regulation for sites 2 – 4 that reside in exon 12, whereas site 1 in exon 7 is edited at comparable levels at all stages (Fig. 3.1 C). Spatial regulation suggests an even more fine-grained tuning of this independence (Fig. 3.2). Male wing tissue, which should contain mostly chemo- and mechanosensory neurons, expresses the GAAA isoform predominantly (68%), whereas this isoform is found at very low levels in the male head

(1%). Conversely, the most abundant isoform in heads, AAGG (27%), was not detected in wing tissue. Male antennal tissue also has GAAA as its most abundant isoform, potentially marking this as a *Shaker* isoform of peripheral sensory neurons. Eye tissue provides an even more stark display of mechanistic independence in editing; the most abundant isoforms here are GAAA (33%) and AGGG (23%). We also observed a near absolute dependence of editing at site 4 on editing at site 3. In 821 cDNAs from our total dataset, 300 were edited at site 4 and 295 of these (98.3%) were also edited at site 3. This dramatic polarized positive cooperativity of editing between two sites may be influenced by the proximity of these sites on the mRNA (Figs. S3.2 and S3.3), although the regulatory mechanisms are unknown.

The diverse expression of isoforms seen here could be explained by programmatic expression of different alternative splice forms of the dADAR protein (Palladino et al., 2000b). To test this notion, we genetically eliminated expression of endogenous dADAR and reexpressed, using the pSwitch-GAL4 binary expression system, a single dADAR isoform. All four *Shaker* editing sites can be edited by this single dADAR isoform in fly brain tissue in a ratio similar to wild-type flies expressing all endogenous dADAR isoforms (Fig. 3.3). Remarkably, wing tissue expressing a single dADAR isoform also preserves the very skewed pattern of editing seen in the wild-type wing; that is, predominant editing of site 1. We propose two potential models for how the staging of editing at different sites might be coordinated. In the first, all cells would generate the three predicted structures necessary for editing *Shaker* sites 1 – 4 (Figs. S3.1 – S3.3), but that additional positive or negative factors (we envision RNA-binding proteins) would

assist or frustrate ADAR recognition of each RNA structural domain on a site-by-site, cell-specific basis. A second model could invoke RNA chaperones (again, RNA-binding proteins) to act positively or negatively in the formation of the dsRNA structures within each domain. In this model, dADAR passively edits only the *Shaker* transcripts where appropriate dsRNA structures have formed.

Either of these models could be used to generate the isoform profiles we see. For example, in wing tissue where the GAAA isoform predominates, neurons would express factors that decrease ADAR binding to, or formation of, the structure directing the editing of sites 2 – 4. In eye tissue, where GAAA and AGGG predominate, two types of neurons could be imagined, a " wing-like " neuron (expressing GAAA) and an additional cell type where factors would eliminate editing at site 1, but promote editing at sites 2 – 4 (expressing AGGG). Such models do not readily explain the cooperativity of editing seen for the distant sites 1 and 3, positive in some tissues and negative in others. The mechanism of this linkage is speculative but may include a higher-order structure of the dsRNA along with cell-specific factors, bringing these two sites into proximity where ADAR can act cooperatively on them.

Our rescue data also suggest a simple mechanism for the linkage of editing at sites 3 and 4 because clearly one isoform can edit both sites 3 and 4 (Fig. 3.3 A). The dsRNA structure predicted to form by pairing between e2 and sites 3 and 4 places the editing sites in an imperfect duplex separated by 5 base-pairs (Fig. S3.3). Editing at site 3 would create an A-I mispair, altering the duplex character of this region and changing ADAR binding to the substrate in such as way as to allow site 4 to be modified. Thus, we

propose that the "factor" promoting editing at site 4, generating the structure necessary for editing, is the dADAR enzyme itself. Of course, more work at the single-cell level will be necessary to resolve these models. Recently, such single-cell analyses of RNA editing in mammalian cells concluded that, for editing of AMPA and serotonin 2C receptors, additional factors beyond ADAR expression were necessary to explain observed patterns of editing (Sergeeva et al., 2007).

Functional Epistasis

The four conserved editing sites in *Shaker* are all located in regions associated with channel gating, either on top of the S4 voltage sensor (site 1) or in the transmembrane segment housing the activation gate (sites 2 – 4). It is not surprising, therefore, that mutations of these residues produce an array of effects on either the voltage dependence or kinetics of gating. The most striking feature of our biophysical interrogation of isoforms is the dramatic slowing of inactivation, seen only in the relatively rare isoform AAGA (Figs. 3.4, 3.5 A, and 3.8 C). Although editing site 3 (residue 489) might be expected to affect ball-and-chain inactivation, because it lies below the cytoplasmic entrance of the open channel where it may encounter either the inactivation ball or its chain (Long et al., 2005), the T489A mutation only has this effect when the other three sites are unedited. We consider this phenotypic interdependence among the sites a type of functional epistasis (Cordell, 2002) that indicates the presence of an allosteric gating network among dispersed residues of the channel protein. Sites 2 – 4 are in either the helical S6 segment or its cytoplasmic extension, suggesting that mutations may

energetically propagate their gating perturbations along the pore-lining S6 segment (Yifrach and MacKinnon, 2002). However, none of these three residues appears to contribute directly to the binding site for the inactivation ball (Zhou et al., 2001). It remains to be seen whether "patterns" of RNA editing, rather than alterations of individual residues, are regulated in specific tissues to produce specific functional consequences. Our results do indicate, nevertheless, that the combinatorics of recoding at multiple sites begets a potpourri of functional phenotypes dependent on context. Moreover, for a multimeric protein like a potassium channel, a further source of diversity is available if heteromers contribute to the functional population of channels in a cell. This will depend on the relative numbers and identities of isoforms expressed in individual cells, a topic that can be addressed by single-cell PCR. Our studies make clear that a thorough appreciation of the organismal significance of editing for ADAR targets will undoubtedly require detailed knowledge of the varied regulatory landscape of editing, even for single gene targets.

References

Armstrong, C.M., and F. Bezanilla . 1974. Charge movement associated with the opening and closing of the activation gates of theNa channels. *J. Gen. Physiol.* 63: 533 – 552.

Basilio, C., A.J. Wahba , P. Lengyel , J.F. Speyer , and S. Ochoa . 1962. Synthetic polynucleotides and the amino acid code. V. *Proc. Natl. Acad.Sci. USA.* 48: 613 – 616.

Bass, B.L. RNA editing by adenosine deaminases that act on RNA. 2002. *Annu. Rev. Biochem.* 71: 817 – 846.

Bass, B.L. How does RNA editing affect dsRNA-mediated gene silencing? 2006. *Cold Spring Harb. Symp. Quant. Biol*. 71: 285 – 292.

Bernard, A., and M. Khrestchatisky. 1994. Assessing the extent of RNA editing in the TMII regions of GluR5 and GluR6 kainate receptors during rat brain development. *J. Neurochem.* 62: 2057 – 2060.

Bezanilla, F. , E. Perozo , D.M. Papazian , and E. Stefani . 1991. Molecular basis of gating charge immobilization in *Shaker* potassium channels. *Science.* 254: 679 – 683.

Bhalla, T., J.J. Rosenthal , M. Holmgren , and R. Reenan . 2004. Control of human potassium channel inactivation by editing of a small mRNA hairpin. *Nat. Struct. Mol. Biol.* 11: 950 – 956.

Burns, C.M., H. Chu, S.M. Rueter, L.K. Hutchinson , H. Canton , E. Sanders-Bush , and R.B. Emeson . 1997. Regulation of serotonin-2C receptor G-protein coupling by RNA editing. *Nature* . 387:303 – 308.

Bushey, D., R. Huber, G. Tononi, and C. Cirelli . 2007. *Drosophila Hyperkinetic* mutants have reduced sleep and impaired memory. *J. Neurosci.* 27: 5384 – 5393.

Chouinard, S.W., G.F. Wilson, A.K. Schlimgen, and B. Ganetzky. 1995. A potassium channel beta subunit related to the aldo-keto reductase superfamily is encoded by the *Drosophila Hyperkinetic* locus. *Proc. Natl. Acad. Sci. USA.* 92: 6763 – 6767.

Cirelli, C., D. Bushey, S. Hill, R. Huber, R. Kreber, B. Ganetzky, and G. Tononi. 2005. Reduced sleep in *Drosophila Shaker* mutants. *Nature.* 434: 1087 – 1092.

Cordell, H.J. 2002. Epistasis: what it means, what it doesn' t mean, and statistical methods to detect it in humans. *Hum. Mol. Genet.* 11:2463 – 2468.

Ding, S., and R. Horn. 2003. Effect of S6 tail mutations on charge movement in *Shaker*

potassium channels. *Biophys. J.* 84: 295 – 305.

Ding, Y., C.Y. Chan, and C.E. Lawrence. 2005. RNA secondary structure prediction by centroids in a Boltzmann weighted ensemble. *RNA.* 11: 1157 – 1166.

Ding, Y., C.Y. Chan, and C.E. Lawrence. 2006. Clustering of RNA secondary structures with application to messenger RNAs. *J. Mol. Biol.* 359: 554 – 571.

Douglas, C.L., V.V. Vyazovskiy, T.L. Southard, S.Y. Chiu, A. Messing, G. Tononi, and C. Cirelli. 2007. Sleep in Kcna2 knockout mice. *BMC Biol.* 5: 42.

Gallo, A., L.P. Keegan, G.M. Ring, and M.A. O ' Connell. 2003. An ADAR that edits transcripts encoding ion channel subunits functions as a dimer. *EMBO J.* 22: 3421 – 3430.

Gasque, G., P. Labarca, R. Delgado, and A. Darszon. 2006. Bridging behavior and physiology: ion-channel perspective on mushroom body-dependent olfactory learning and memory in *Drosophila. J. Cell. Physiol.* 209: 1046 – 1053.

Giese, K.P., J.F. Storm, D. Reuter, N.B. Fedorov, L.R. Shao, T. Leicher, O. Pongs, and A.J. Silva. 1998. Reduced K+ channel inactivation, spike broadening, and after-hyperpolarization in Kvbeta1.1-deficient mice with impaired learning. *Learn. Mem.* 5: 257-273.

Hanrahan, C.J., M.J. Palladino, B. Ganetzky, and R.A. Reenan. 2000. RNA editing of the *Drosophila para* Na(+) channel transcript. Evolutionary conservation and developmental regulation. *Genetics.* 155: 1149 – 1160.

Hardie, R.C., D. Voss, O. Pongs, and S.B. Laughlin. 1991. Novel potassium channels encoded by the *Shaker* locus in *Drosophila* photoreceptors. *Neuron.* 6: 477 – 486.

Heginbotham, L., and R. MacKinnon. 1993. Conduction properties of the cloned *Shaker* K + channel. *Biophys. J.* 65: 2089 – 2096.

Herbert, A. RNA editing, introns and evolution. 1996. *Trends Genet.* 12: 6 – 9.

Higuchi, M., S. Maas, F.N. Single, J. Hartner, A. Rozov, N. Burnashev, D. Feldmeyer, R. Sprengel, and P.H. Seeburg. 2000. Point mutation in an AMPA receptor gene rescues lethality in mice deficient in the RNA-editing enzyme ADAR2. *Nature.* 406: 78 – 81.

Hille, B. 2001 . Ion Channels of Excitable Membranes. Sinauer Associates, Sunderland, MA. 814 pp.

Hoopengardner, B., T. Bhalla, C. Staber, and R. Reenan. 2003. Nervous system targets of RNA editing identifi d by comparative genomics. *Science.* 301: 832 – 836.

Hoshi, T., W.N. Zagotta, and R.W. Aldrich. 1990. Biophysical and molecular mechanisms of *Shaker* potassium channel inactivation. *Science.* 250: 533 – 538.

Jen, J.C., T.D. Graves, E.J. Hess, M.G. Hanna, R.C. Griggs, and R.W. Baloh. 2007. Primary episodic ataxias: diagnosis, pathogenesis and treatment. *Brain.* 130: 2484 – 2493.

Kamb, A., L.E. Iverson, and M.A. Tanouye. 1987. Molecular characterization of *Shaker* , a *Drosophila* gene that encodes a potassium channel. *Cell.* 50: 405 – 413.

Keegan, L.P., A. Leroy, D. Sproul, and M.A. O ' Connell. 2004. Adenosine deaminases acting on RNA (ADARs): RNA-editing enzymes. *Genome Biol.* 5: 209.

Keegan, L.P., J. Brindle, A. Gallo, A. Leroy, R.A. Reenan, and M.A. O ' Connell. 2005. Tuning of RNA editing by ADAR is required in *Drosophila. EMBO J.* 24: 2183 – 2193.

Lai, F., C.X. Chen, K.C. Carter, and K. Nishikura. 1997. Editing of glutamate receptor B subunit ion channel RNAs by four alternatively spliced DRADA2 double-stranded RNA adenosine deaminases. *Mol. Cell. Biol.* 17: 2413 – 2424.

Lange, K. 2003. Mathematical and Statistical Methods for Genetic Analysis. Springer, NY. 361 pp.

Lewontin, R.C. 1964. The interaction of selection and linkage. I. General considerations; heterotic models. *Genetics.* 49: 49 – 67.

Liu, Y., R.B. Emeson, and C.E. Samuel. 1999. Serotonin-2C receptor pre-mRNA editing in rat brain and in vitro by splice site variants of the interferon-inducible double-stranded RNA-specific adenosine deaminase ADAR1. *J. Biol. Chem.* 274: 18351 – 18358.

Lomeli, H., J. Mosbacher, T. Melcher, T. H ö ger, J.R. Geiger, T. Kuner, H. Monyer, M. Higuchi, A. Bach, and P.H. Seeburg. 1994. Control of kinetic properties of AMPA receptor channels by nuclear RNA editing. *Science.* 266: 1709 – 1713.

Long, S.B., E.B. Campbell, and R. MacKinnon. 2005. Crystal structure of a mammalian voltage-dependent *Shaker* family K + channel. *Science.* 309: 897 – 903.

Maas, S., T. Melcher, A. Herb, P.H. Seeburg, W. Keller, S. Krause, M. Higuchi, and M.A. O ' Connell. 1996. Structural requirements for RNA editing in glutamate receptor pre-mRNAs by recombinant double-stranded RNA adenosine deaminase. *J. Biol. Chem.* 271: 12221 – 12226.

Maas, S., Y. Kawahara, K.M. Tamburro, and K. Nishikura. 2006. A-to-I RNA editing and human disease. *RNA Biol.* 3: 1 – 9.

Mehler, M.F., and J.S. Mattick. 2007. Noncoding RNAs and RNA editing in brain development, functional diversifi cation, and neurological disease. *Physiol. Rev.* 87: 799 – 823

Melcher, T. , S. Maas, A. Herb, R. Sprengel, P.H. Seeburg, and M. Higuchi. 1996. A mammalian RNA editing enzyme. *Nature.* 379: 460 – 464.

Nishikura, K. Editor meets silencer: crosstalk between RNA editing and RNA interference. 2006. *Nat. Rev. Mol. Cell Biol.* 7: 919 – 931.

Ohlson, J., J.S. Pedersen, D. Haussler, and M. Ohman. 2007. Editing modifies the GABA(A) receptor subunit alpha3. *RNA.* 13: 698 – 703.

Palladino, M.J., L.P. Keegan, M.A. O ' Connell, and R.A. Reenan. 2000a. A-to-I pre mRNA editing in *Drosophila* is primarily involved in adult nervous system function and integrity. *Cell.* 102: 437 – 449.

Palladino, M.J., L.P. Keegan, M.A. O ' Connell, and R.A. Reenan. 2000b. dADAR, a *Drosophila* double-stranded RNA-specific adenosine deaminase is highly developmentally regulated and is itself a target for RNA editing. *RNA.* 6: 1004 – 1018.

Patton, D.E., T. Silva, and F. Bezanilla. 1997. RNA editing generates a diverse array of transcripts encoding squid Kv2 K+ channels with altered functional properties. *Neuron.* 19: 711 – 722.

Paul, M.S., and B.L. Bass. 1998. Inosine exists in mRNA at tissuespecific levels and is most abundant in brain mRNA. *EMBO J.*17: 1120 – 1127.

Paupard, M.C., M.A. O ' Connell, A.P. Gerber, and R.S. Zukin. 2000. Patterns of developmental expression of the RNA editing enzyme rADAR2. *Neuroscience.* 95: 869 – 879.

Reenan, R.A., C.J. Hanrahan, and B. Ganetzky. 2000. The *mle(napts)* RNA helicase mutation in *Drosophila* results in a splicing catastrophe of the *para* Na+ channel transcript in a region of RNA editing. *Neuron.* 25: 139 – 149.

Rogero, O., B. H ä mmerle, and F.J. Tejedor. 1997. Diverse expression and distribution of *Shaker* potassium channels during the development of the *Drosophila* nervous system. *J. Neurosci.* 17: 5108 – 5118.

Roman, G., K. Endo, L. Zong, and R.L. Davis. 2001. P[Switch], a system for spatial and temporal control of gene expression in *Drosophilamelanogaster. Proc. Natl. Acad. Sci. USA.* 98: 12602 – 12607.

Rosenthal, J.J., and F. Bezanilla. 2002. Extensive editing of mRNAs for the squid delayed rectifi er K+ channel regulates subunit tetramerization. *Neuron.* 34: 743 – 757.

Rueter, S.M., T.R. Dawson, and R.B. Emeson. 1999. Regulation of alternative splicing by RNA editing. *Nature.* 399: 75 – 80.

Ryan, M.Y., R. Maloney, R. Reenan, and R. Horn. 2008. Characterization of five RNA editing sites in *Shab* potassium channels. *Channels.* 2-3: 202 – 209.

Seeburg, P.H., and J. Hartner. 2003. Regulation of ion channel/neurotransmitter receptor function by RNA editing. *Curr. Opin. Neurobiol.* 13: 279 – 283.

Sergeeva, O.A., B.T. Amberger, and H.L. Haas. 2007. Editing of AMPA and serotonin 2C receptors in individual central neurons, controlling wakefulness. *Cell. Mol. Neurobiol.* 27: 669 – 680.

Tonkin, L.A., L. Saccomanno, D.P. Morse, T. Brodigan, M. Krause, and B.L. Bass. 2002. RNA editing by ADARs is important for normal behavior in *Caenorhabditis elegans. EMBO J.* 21: 6025 – 6035.

Wang, Q., J. Khillan, P. Gadue, and K. Nishikura. 2000. Requirement of the RNA editing deaminase ADAR1 gene for embryonic erythropoiesis. *Science.* 290: 1765 – 1768.

Yifrach, O., and R. MacKinnon. 2002. Energetics of pore opening in a voltage-gated K + channel. *Cell.* 111: 231 – 239.

Zhou, M., J.H. Morais-Cabral, S. Mann, and R. MacKinnon. 2001 . Potassium channel receptor site for the inactivation gate and quaternary amine inhibitors. *Nature.* 411: 657 – 661.

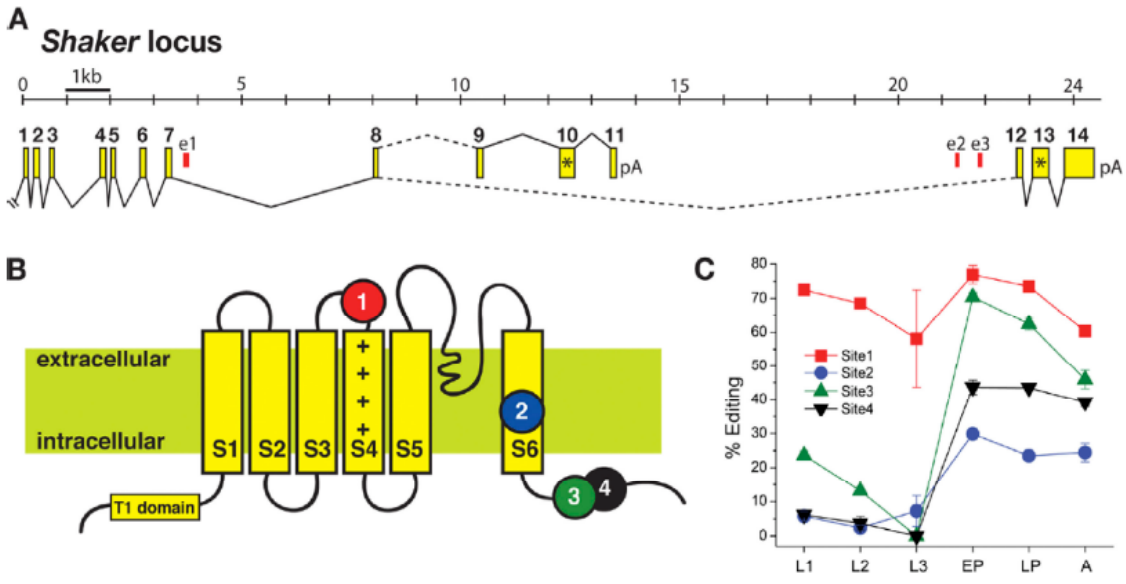

Figure 3.1. Editing of the *Shaker* locus.
(A) The *Shaker* locus transcription unit is shown with numbered exons (yellow), constitutive splice sites (solid lines), alternative splice sites (broken lines), and stop codons (asterisks). The position of conserved elements predicted to direct editing, e1 – e3, is shown in red. (B) The position of *Shaker* editing sites 1 – 4 is depicted on a generic cartoon of Kv channel topology. (C) Developmental profile of editing in whole animals for sites 1 – 4 is shown for larval, pupal, and adult stages. Color code as in B.

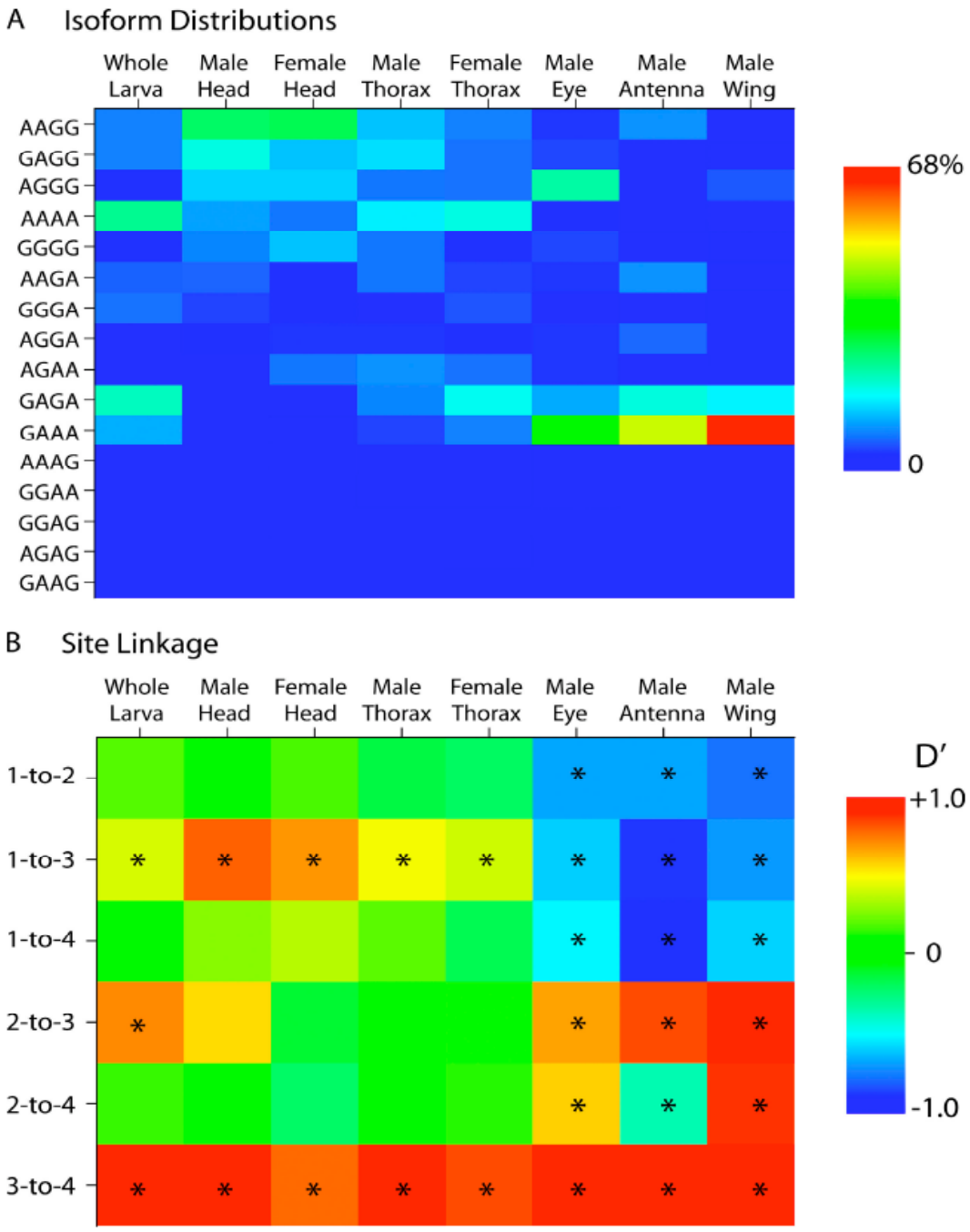

Figure 3.2. Isoform distributions. (A) Distributions of 16 possible isoforms in eight populations. Percentage of population accorded to each isoform is color-coded. (B) Pairwise linkage between editing at the four sites is color coded as Lewontin ' s D ' statistic, where +1 and -1 represent complete positive or negative coupling, and 0 represents independence. The starred squares indicate significant coupling ($P < 0.02$; Fisher's exact test).

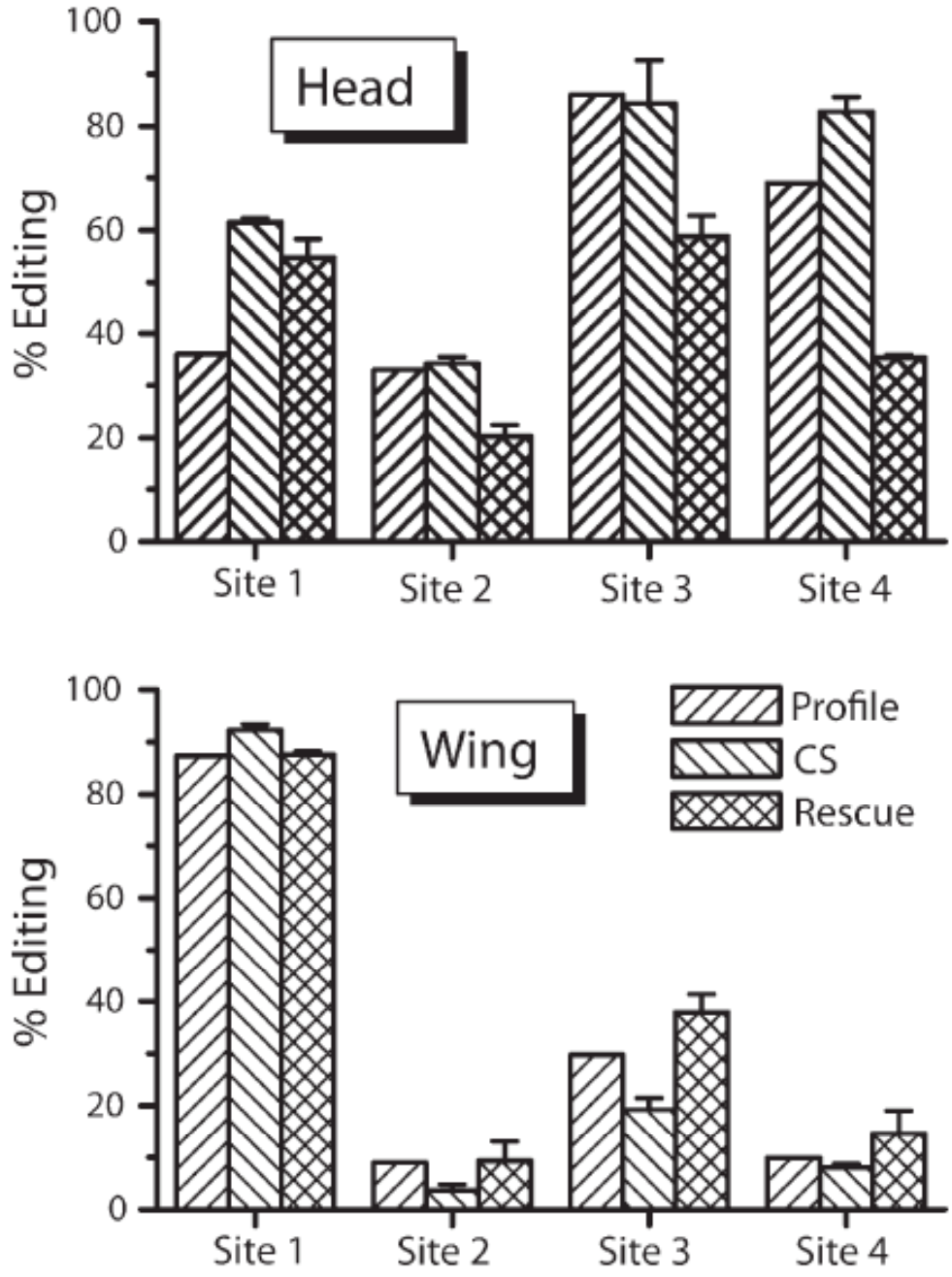

Figure 3.3. Contribution of ADAR to tissue-specific editing patterns. The top panel shows quantitation of RNA editing levels in head samples for sites 1 – 4 from isoform profiling (Profile), direct RT-PCR sequence analysis (see Materials and methods), wild-type (CS), and direct RT-PCR sequence analysis from dADAR-null animals rescued with a single dADAR isoform expressed pan-neuronally. The bottom panel shows quantitation of RNA editing levels in wing samples, as in the top panel.

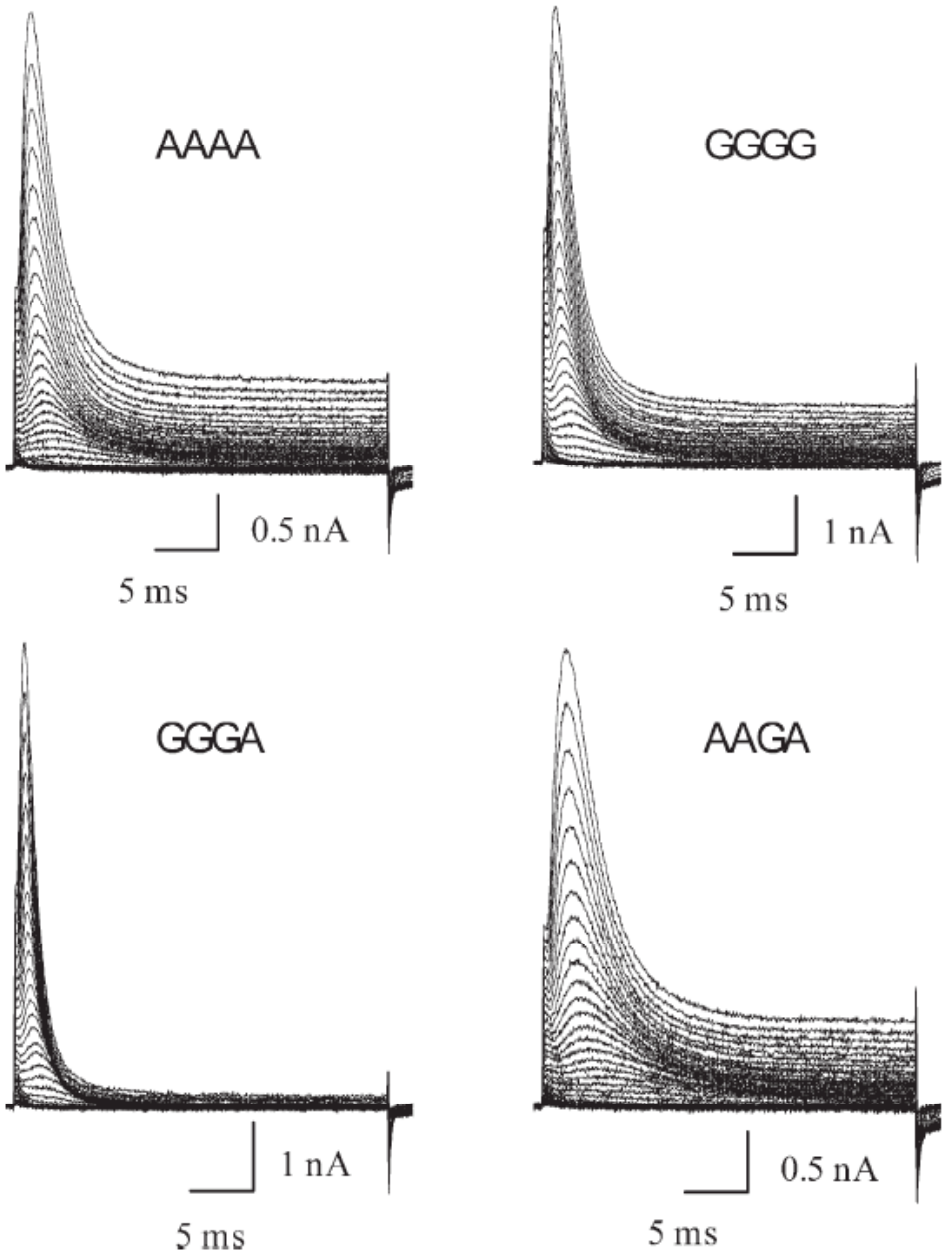

Figure 3.4. Whole cell cesium currents of four selected isoforms. Currents were generated from depolarizations between -120 and +70 mV in 5-mV increments. The two isoforms with the fastest and slowest inactivation kinetics are shown in the bottom panels.

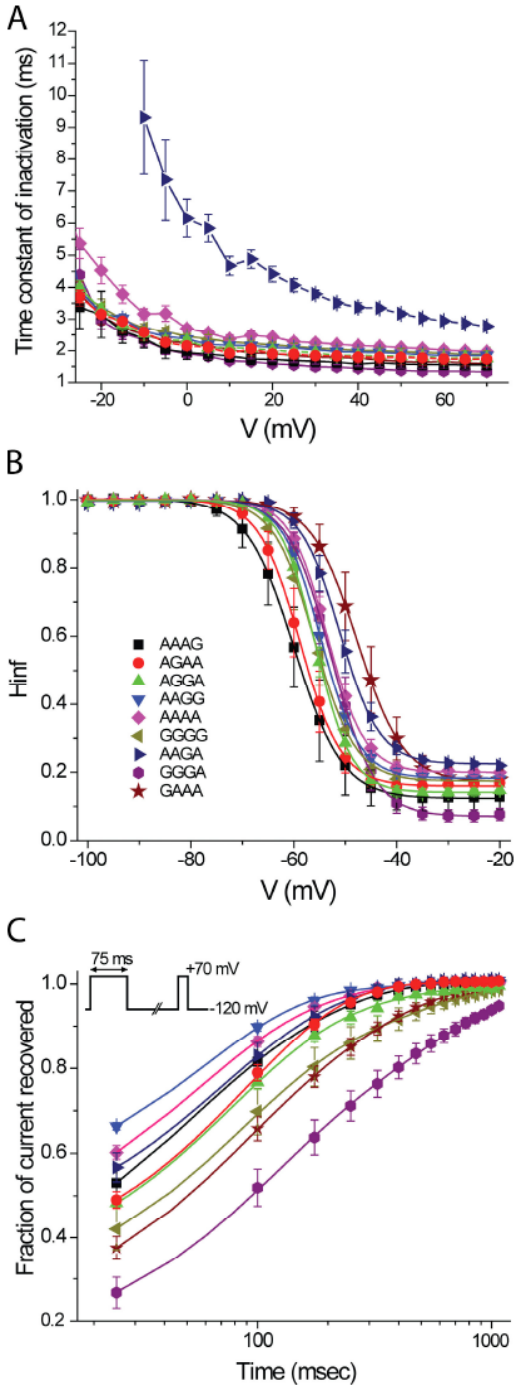

Figure 3.5. Kinetics and steady-state properties of inactivation. (A) Time constants of inactivation show that AAGA is distinctly slower than the other isoforms. (B) Diversity of steady-state inactivation curves obtained in response to 100-ms prepulses. (C) Kinetics of recovery from inactivation at -120 mV (see inset for voltage protocol). Theory curves are single exponential relaxations (Table S3.2).

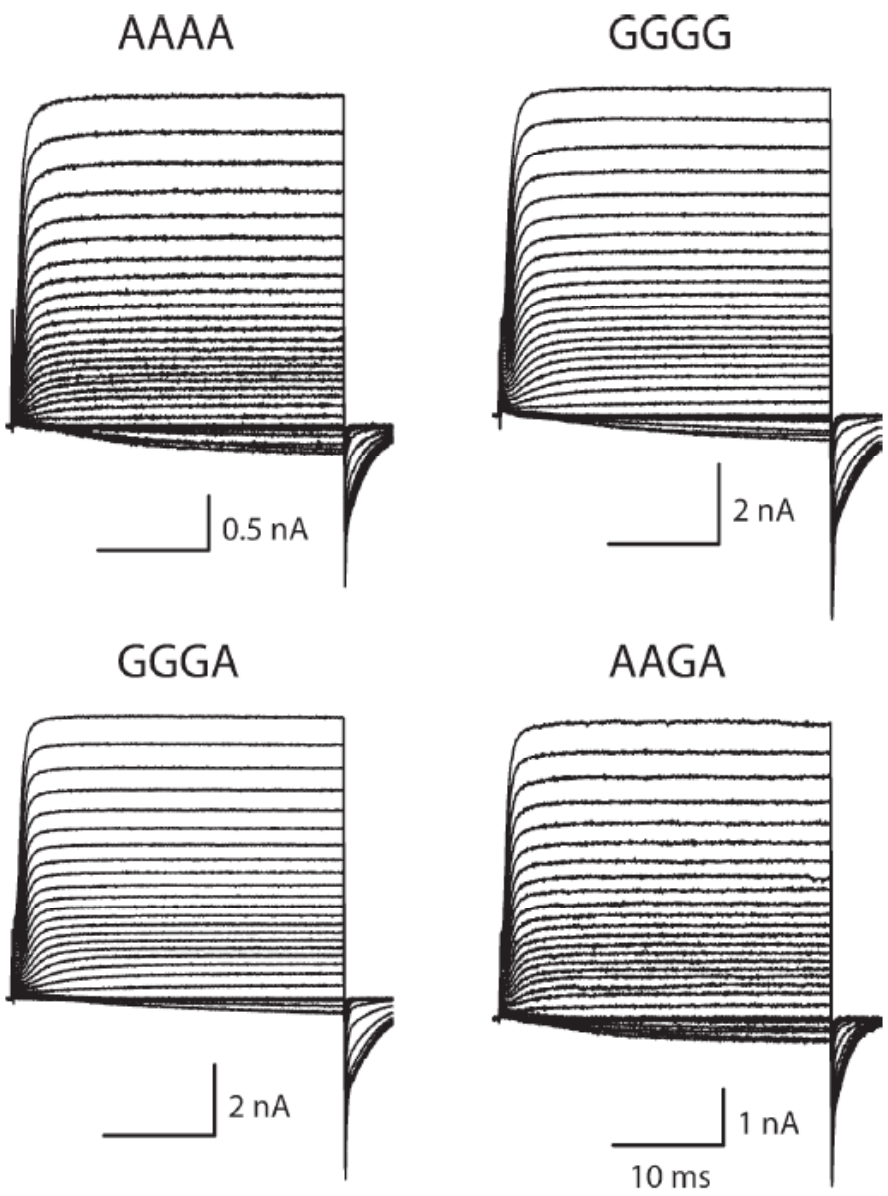

Figure 3.6. Cesium currents in selected ball-deleted isoforms. Voltages as in Fig. 3.4, using the same four isoforms.

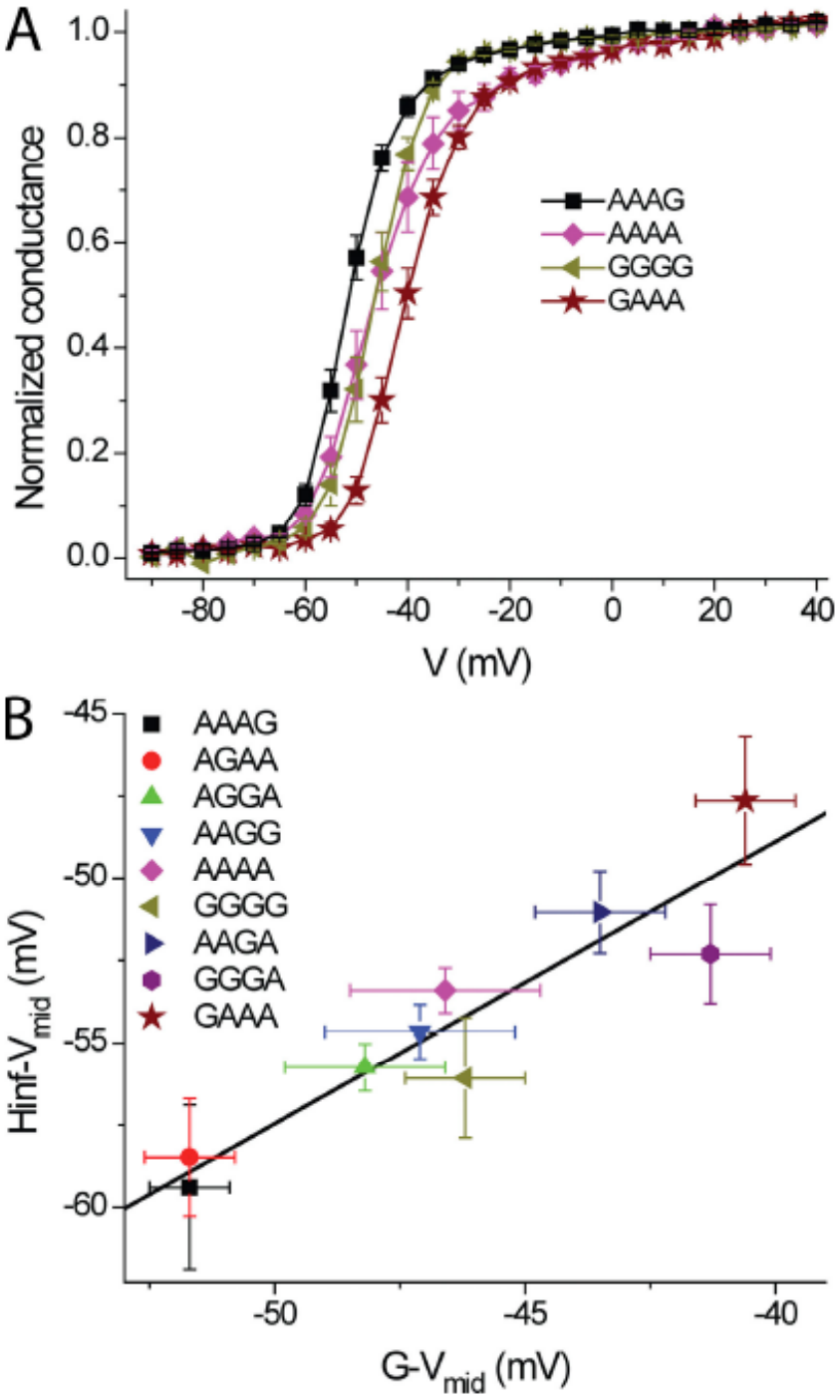

Figure 3.7. Steady-state activation and inactivation compared. (A) G-V curves for AAAA, GGGG, and the two most shifted isoforms (Table S3.3). (B) Strong correlation between midpoints of steady-state activation and inactivation.

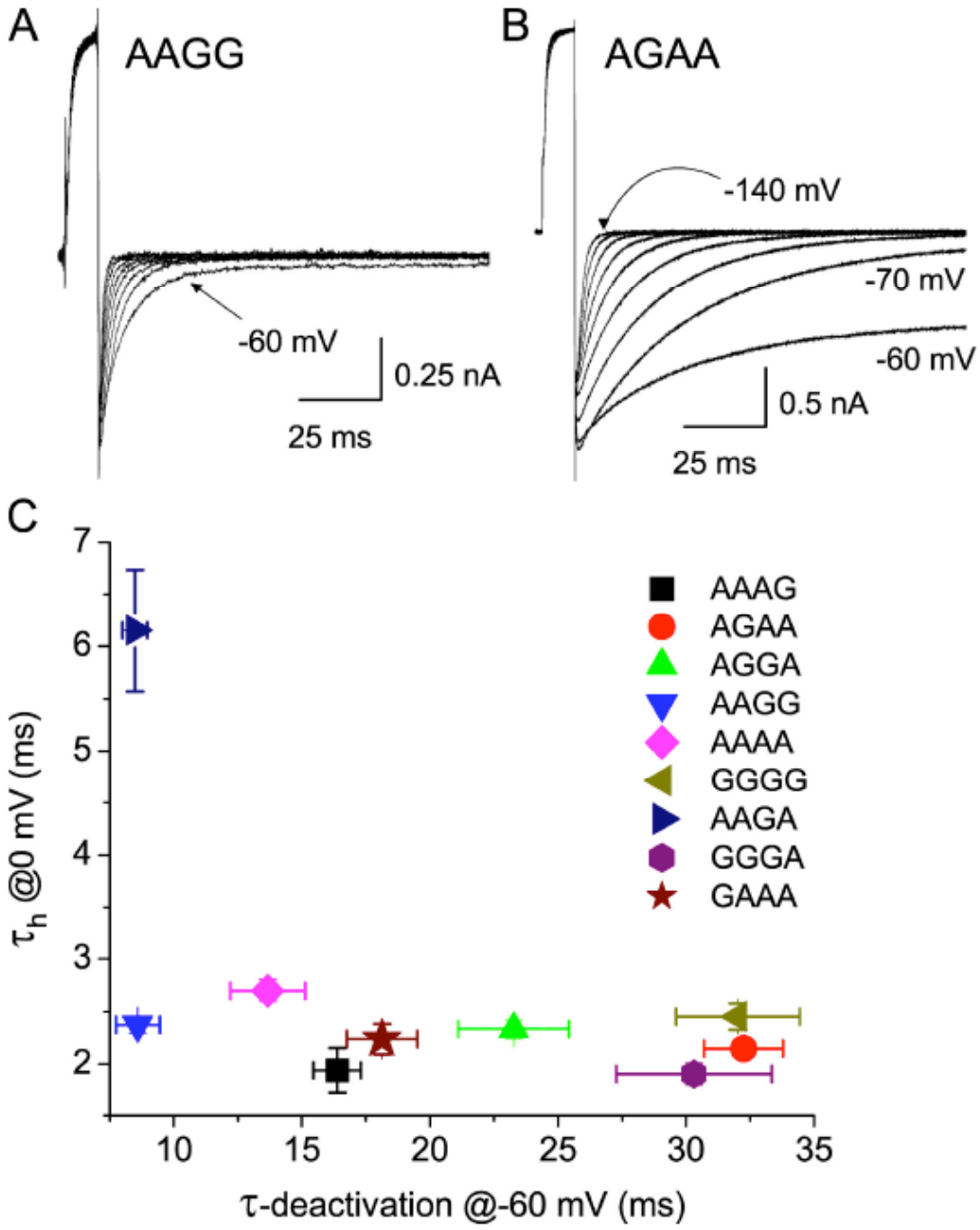

Figure 3.8. Kinetics of deactivation and inactivation. (A) Deactivation kinetics in the two most extreme isoforms of inactivation-removed mutants. Tail current kinetics measured over a range from -60 to -140 mV (Table S3.4). (B) Poor correlation between inactivation and deactivation time constants among the isoforms.

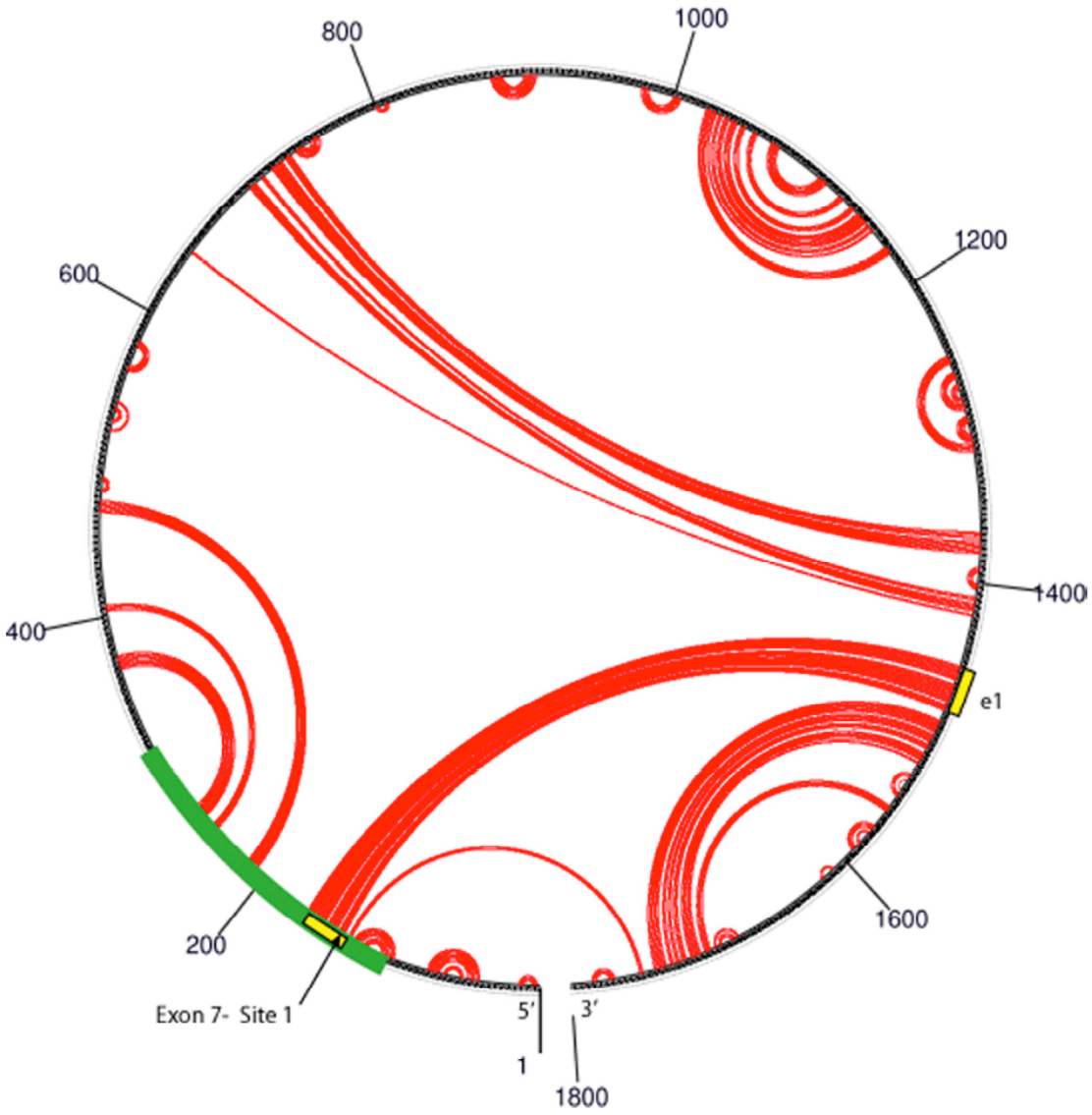

Figure S3.1. SFOLD analysis of *Shaker* editing site 1 (exon 7). Sequences were submitted to the SFOLD server (http://sfold.wadsworth.org/) spanning (1,800 nt) the exon 7 editing sites. Intron 6, 100 nt; exon 7, 172 nt; intron 7, 1,528 nt. Results are presented in the sir_graph format, depicting base-pairing interactions as connecting lines (red) (Ding, Y., C.Y. Chan, and C.E. Lawrence. 2005. *RNA*. 11:1157–1166). Sequence coordinates are indicated around the circle. Exonic regions are highlighted in green, and conserved pairing regions are indicated in yellow. For *Shaker* site 1, two centroids were predicted, both of which paired e1 with the editing site (see Fig. S3.3 A). Thus, 100% of the probability mass was contained in the ensemble-predicted pairing.

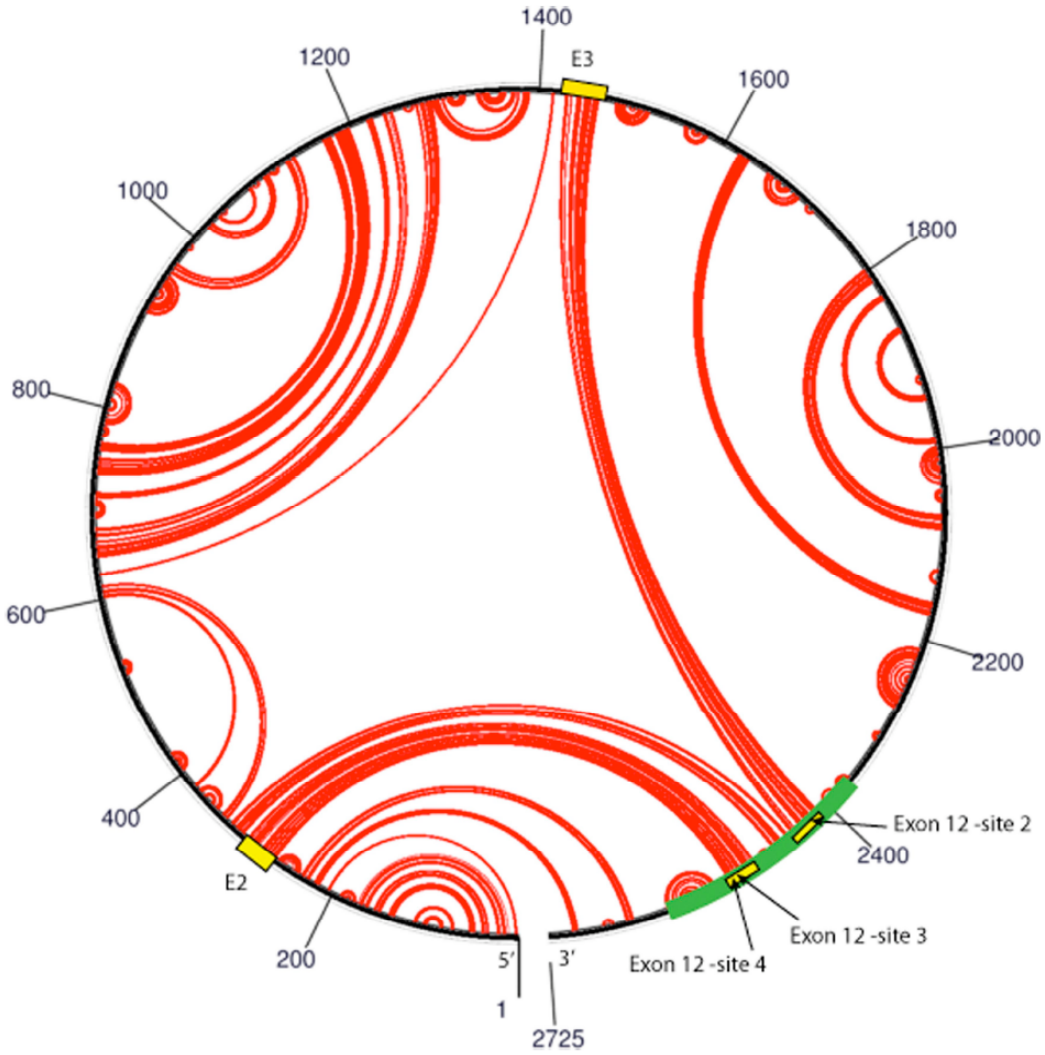

Figure S3.2. SFOLD analysis of *Shaker* editing sites 2–4 (exon 12). Sequences were submitted to the SFOLD server (http://sfold.wadsworth.org/) spanning (2,725 nt) the exon 12 editing sites. Intron 11, 2,386 nt; exon 12, 194 nt; intron 12, 145 nt. Results are presented in the sir_graph format, depicting base-pairing interactions as connecting lines (red) (Ding, Y., C.Y. Chan, and C.E. Lawrence. 2005. *RNA*. 11:1157–1166). Sequence coordinates are indicated around the circle. Exonic regions are highlighted in green, and conserved pairing regions are indicated in yellow. For Shaker sites 2–4, two centroids were predicted. Only centroid 1 is shown here. Centroid 1 (51.9%) and centroid 2 (48.1%) both pair e2 with sites 3–4 (see Fig. S3.3 C). Only centroid 1 pairs e3 with site 2 (see Fig. S3.3 B). Thus, the structure predicted for site 2 encompasses only 51.9% of the probability mass of the predicted structures.

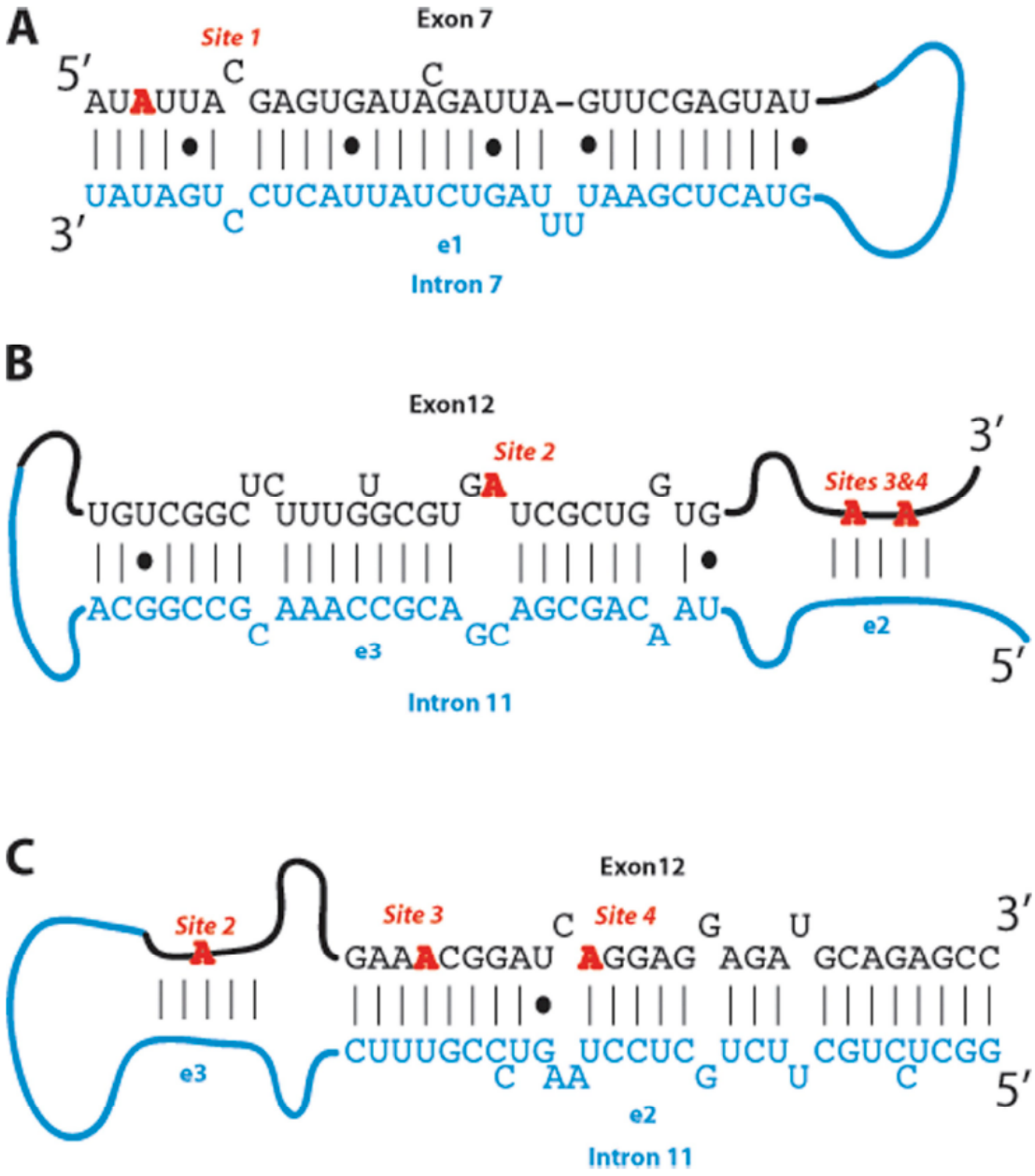

Figure S3.3. Predicted local RNA secondary structures of *Shaker* editing sites 1–4. All predicted structures show *Shaker* exonic sequences (black) containing the edited adenosines (red) pairing with absolutely conserved intronic pairing partners (e1–e3; blue). (A) *Shaker* editing site 1 structure. (B) *Shaker* editing site 2 structure with sites 3–4 shown in less detail. (C) *Shaker* editing sites 3–4 with site 2 shown in less detail.

TABLE S1
Detailed Editing Isoform Profiles

	AAAA	AAAG	AAGA	AGAA	GAAA	AAGG	AGGA	GGAA	AGAG	GAGA	GAAG	AGGG	GGGA	GGAG	GAGG	GGGG	Total
Male Head	11	0	7	2	1	27	3	0	0	2	0	14	5	0	19	9	100
Female Head	8	2	3	8	0	28	4	1	0	2	0	14	3	1	13	13	100
Male Thorax	16	0	8	10	5	13	4	2	0	9	0	8	2	0	15	8	100
Female Thorax	19	1	5	8	9	9	3	2	1	18	0	8	6	0	8	4	101
Male Antennae	1	0	11	1	52	11	8	0	0	21	0	1	3	0	1	0	110
Male eye	3	0	4	4	32	4	4	1	0	11	0	22	1	0	5	5	96
Male Wing	3	0	3	0	75	0	1	0	0	18	0	7	0	0	2	2	111
Larvae (L1)	25	0	7	2	12	9	2	0	0	22	0	3	8	0	9	4	103
Totals	86	3	48	35	186	101	29	6	1	103	0	77	28	1	72	45	821

Sequence analyses were performed on 821 cDNAs from the tissue samples as indicated. The cDNAs were characterized by the editing status of Shaker editing sites 1–4 into one of 16 possible isoforms. Only the GAAG isoform was not observed in these studies.

TABLE S2

Inactivation Parameters

	V_{mid} (mV)	q	τ_{rec} (ms)
AAAG	−59.4 ± 2.5	7.18 ± 0.26	85.6 ± 10.7
AGAA	−58.5 ± 1.8	7.90 ± 0.16	89.3 ± 5.4
AGGA	−55.7 ± 0.7	7.41 ± 0.30	101.5 ± 8.4
AAGG	−54.7 ± 0.8	7.19 ± 0.15	65.3 ± 4.4
AAAA	−53.4 ± 0.7	7.39 ± 0.17	75.2 ± 4.5
GGGG	−56.1 ± 1.8	8.02 ± 0.14	134.3 ± 22.2
AAGA	−51.0 ± 1.2	7.16 ± 0.22	87.0 ± 8.9
GGGA	−52.3 ± 1.5	6.64 ± 0.18	214.5 ± 23.8
GAAA	−47.6 ± 1.9	7.21 ± 0.22	144.1 ± 10.9

Steady-state inactivation and time constant of recovery from inactivation at −120 mV. Steady-state inactivation relationships (Fig. 5 B) were fit by a standard Boltzmann function with estimates of the midpoint (V_{mid}) and slope (q with units of elementary electric charge) shown here. Single exponential relaxations were fit to recovery from inactivation (Fig. 5 C) with estimates of the time constants (τ_{rec}) shown here.

TABLE S3

Parameters for G-V Fits Using Single or Double (When Necessary) Boltzmann Functions

	V_{mid1} (mV)	q_1	w_1	V_{mid2} (mV)	q_2
AAAG	−51.73 ± 0.80	6.11 ± 0.16	0.80 ± 0.02	−9.32 ± 20.34	0.59 ± 0.22
AGAA	−51.72 ± 0.92	5.77 ± 0.33	0.82 ± 0.03	1.66 ± 28.48	0.48 ± 0.14
AGGA	−48.24 ± 1.56	5.61 ± 0.20	0.83 ± 0.01	−13.49 ± 5.01	0.88 ± 0.10
AAGG	−47.06 ± 1.89	4.89 ± 0.14	0.76 ± 0.01	-3.26 ± 7.91	0.95 ± 0.14
AAAA	−46.64 ± 1.95	5.31 ± 0.27	0.75 ± 0.03	−8.81 ± 5.87	0.80 ± 0.18
GGGG	−46.22 ± 1.21	5.18 ± 0.08	1.00		
AAGA	−43.53 ± 1.29	5.44 ± 0.27	0.74 ± 0.03	−17.22 ± 5.98	0.87 ± 0.04
GGGA	−41.33 ± 1.16	5.04 ± 0.26	1.00		
GAAA	−40.61 ± 1.04	5.20 ± 0.16	0.82 ± 0.01	0.56 ± 3.45	0.86 ± 0.14

The normalized double Boltzmann function is

$$G(V) = \frac{W_1}{1+\exp\left\{q_1\left(V_{mid1}-V\right)\right\}} + \frac{1-W_1}{1+\exp\left\{q_2\left(V_{mid2}-V\right)\right\}},$$

where W_1 is the fractional weight of the first component, the midpoints are in units of mV, and the slopes are in units of elementary charge.

TABLE S4

Deactivation Time Constants (in ms) at Indicated Membrane Potentials

V (mV)	AAGG	AAAA	GAAA	GGGG	AGGA	GGGA	AGAA	AAGA	AAAG
−140	0.94 ± 0.06	1.07 ± 0.06	1.52 ± 0.10	1.60 ± 0.09	1.49 ± 0.15	1.51 ± 0.07	1.84 ± 0.15	0.83 ± 0.04	1.02 ± 0.03
−135	1.10 ± 0.07	1.38 ± 0.14	1.77 ± 0.11	1.88 ± 0.10	1.78 ± 0.18	1.79 ± 0.07	2.14 ± 0.10	0.97 ± 0.05	1.19 ± 0.03
−130	1.26 ± 0.07	1.49 ± 0.09	2.03 ± 0.11	2.25 ± 0.14	2.08 ± 0.21	2.11 ± 0.09	2.62 ± 0.12	1.08 ± 0.06	1.40 ± 0.04
−125	1.36 ± 0.09	1.78 ± 0.16	2.35 ± 0.16	2.71 ± 0.18	2.43 ± 0.21	2.55 ± 0.09	3.21 ± 0.16	1.24 ± 0.06	1.63 ± 0.06
−120	1.57 ± 0.13	2.07 ± 0.14	2.79 ± 0.18	3.24 ± 0.21	3.08 ± 0.29	3.09 ± 0.11	3.92 ± 0.21	1.42 ± 0.07	1.92 ± 0.07
−115	1.78 ± 0.14	2.54 ± 0.30	3.26 ± 0.18	3.89 ± 0.28	3.55 ± 0.43	3.78 ± 0.11	4.68 ± 0.38	1.67 ± 0.07	2.28 ± 0.09
−110	2.04 ± 0.17	2.81 ± 0.23	3.83 ± 0.24	4.84 ± 0.37	4.31 ± 0.48	4.73 ± 0.16	6.33 ± 0.30	1.93 ± 0.08	2.71 ± 0.11
−105	2.39 ± 0.16	3.23 ± 0.25	4.50 ± 0.22	5.90 ± 0.46	5.15 ± 0.57	5.56 ± 0.12	8.07 ± 0.46	2.23 ± 0.08	3.21 ± 0.15
−100	2.60 ± 0.26	3.66 ± 0.23	5.18 ± 0.26	7.18 ± 0.61	6.29 ± 0.68	6.85 ± 0.15	10.19 ± 0.77	2.51 ± 0.10	3.75 ± 0.17
−95	2.96 ± 0.29	4.27 ± 0.28	6.03 ± 0.28	8.68 ± 0.75	7.53 ± 0.81	8.11 ± 0.20	12.23 ± 0.59	2.86 ± 0.11	4.49 ± 0.24
−90	3.41 ± 0.29	5.15 ± 0.50	6.93 ± 0.33	10.58 ± 0.93	8.82 ± 1.04	9.76 ± 0.32	14.71 ± 0.71	3.29 ± 0.12	5.24 ± 0.28
−85	3.82 ± 0.36	5.83 ± 0.53	8.00 ± 0.39	12.69 ± 1.18	10.33 ± 1.17	11.60 ± 0.49	17.82 ± 0.91	3.67 ± 0.15	6.12 ± 0.32
−80	4.29 ± 0.44	6.91 ± 0.83	9.07 ± 0.50	15.22 ± 1.36	12.36 ± 1.47	13.60 ± 0.68	21.78 ± 1.19	4.25 ± 0.22	7.30 ± 0.43
−75	4.98 ± 0.55	7.79 ± 0.80	10.47 ± 0.59	18.27 ± 1.81	14.25 ± 1.78	16.15 ± 0.93	26.14 ± 1.50	4.89 ± 0.25	8.71 ± 0.51
−70	5.91 ± 0.67	9.18 ± 0.99	12.29 ± 0.79	22.10 ± 2.21	17.04 ± 2.25	19.21 ± 1.36	29.25 ± 2.60	5.63 ± 0.25	10.70 ± 0.66
−65	7.16 ± 0.86	11.10 ± 1.21	14.55 ± 1.12	26.80 ± 2.55	20.28 ± 2.48	23.65 ± 2.03	34.19 ± 2.31	6.81 ± 0.39	13.51 ± 0.84
−60	8.60 ± 0.86	13.67 ± 1.46	18.13 ± 1.38	32.02 ± 2.42	23.27 ± 2.16	30.31 ± 3.03	32.24 ± 1.54	8.48 ± 0.49	16.38 ± 0.93
−55	11.12 ± 1.21	15.37 ± 0.96	22.13 ± 1.68	34.74 ± 0.73	24.80 ± 1.09	37.89 ± 3.80	34.62 ± 5.93	10.72 ± 0.72	17.26 ± 0.82
−50	14.01 ± 1.91	17.77 ± 0.71	24.92 ± 1.77	32.57 ± 1.21	25.35 ± 1.23	39.52 ± 2.91	28.45 ± 1.56	12.29 ± 0.62	18.93 ± 1.41

From single exponential fits to deactivation (Fig. 8).

Chapter 4:

Conservation of *Shaker* mRNA Editing Across Multiple *Drosophila* Species

Introduction

To understand the biological significance of RNA editing events in K_V channels, an assessment of the conservation of editing within *Shaker* transcripts was determined for multiple *Drosophila* species and members of other insect species. Although these editing sites have been demonstrated for *Shaker* transcripts in *D. melanogaster*, it is not known whether these sites are conserved for other *Drosophila* and insect species as well, or if species-specific editing sites exist. Understanding the degree of conservation for these editing sites between different species may be indicative of a functional significance for editing of this gene. Additionally, conservation of Shaker editing between species provides a starting point to use comparative genomics to identify conserved regions, such as ECS elements, that participate in regulating editing in Shaker channels.

Previous studies have reported conservation of multiple editing sites between related genes in different species. The single isoleucine-to-valine editing site in human $K_V1.1$ channels is conserved in *Drosophila* Shab channels (Bhalla, Rosenthal et al. 2004) and in squid K_V2 channels (Patton, Silva et al. 1997). These results indicate that this editing site is conserved across different species in otherwise different K_V channel types, suggesting that editing of this site may be utilized in the context of different channel types to modify activity and that natural selection has convergently evolved certain editing sites (see Chapter 1).

Conservation of editing between species has also provided a starting point with which to identify the ECS elements directing editing. This is the case for RNA editing of the voltage-gated sodium channel gene *paralytic*, in which editing sites are conserved between *D. melanogaster* and *D. virilis* (Hanrahan, Palladino et al. 2000). This conservation of editing led to the identification of ECS elements in these transcripts by comparing intronic sequences between these two species, searching for regions of high conservation in an otherwise variable region of the gene.

Other examples of conservation in RNA editing between species can be observed for the *synaptotagmin I* (*syt*I) transcript. This transcript in different *Drosophila* and other insect species (e.g. honey bees, beetles, mosquitoes) contains both conserved as well as species-specific sites, while some insects such as beetles do not edit *sytI* (Reenan 2005). This work also utilized comparative genomics to identify the ECS elements directing editing and found that small changes within the duplex structures formed by the ECS elements pairing with the edited region were responsible for observed species-specific editing sites.

Another investigation of RNA editing conservation focused on multiple editing sites within the transcripts of the nicotinic acetylcholine receptor alpha6 subunit (*nAChR*) gene. Editing of these sites was compared between *Drosophila*, *Apis mellifera* (honey bees) and *Anopheles gambiae* (mosquitoes). Both conserved and species-specific sites were identified (Jin, Tian et al. 2007). Interestingly, it was also observed that some species have a genome-encoded G in positions of known editing sites in other species. This suggested that RNA editing might facilitate advances in genome evolution whereby some species integrated the base conversion introduced by editing into a permanent

genomic change, likely due to a selective advantage to protein function conferred by editing.

It is clear from these studies that conservation of editing events across different insect species argues in favor for the significance of RNA editing in expanding protein function in flies and other insects. The conservation of editing events also allows for the identification of ECS elements and the examination of the duplex structures they form with edited targets. These similarities and differences between both closely and distantly related species provide clues to the evolution of these regulatory elements and the editing sites they direct.

Methods

Shaker Editing Analysis

In order to assess *Shaker* transcript editing, cDNA from multiple *Drosophila* and insect species were sequenced to determine whether known editing sites were conserved and if new sites could be identified. RNA was prepared from the heads of *D. melanogaster*, *D. pseudoobscura*, *D. tropicalis*, *D. mercatorum*, and *D. virilis* flies. Additionally, analysis was also extended to other insect species including the honey bee, *Apis mellifera*, and multiple mosquito species including *Aedes aegypti*, and five different members of the *Anopheles* genus (Figure 4.1). For RNA extraction, approximately 15 heads were homogenized in 0.5mL of TriReagent (Molecular Research Center, Inc.) and RNA was extracted according to the manufactures suggested protocol via isopropanol precipitation. RNA pellets were eluted in 25μL of nuclease-free water. A 25μL RT-PCR reaction was performed for each sample using 5.0μL of RNA, 2.0μL random primer [10mM], 10mM

dNTP, 5X Reaction Buffer, and 1μL each of rRNasin ribonuclease inhibitor and M-MLV-Rtase (Promega Corp. cat#M170B). Samples were incubated at 37°C for one hour. *Shaker* transcript PCR amplification was carried out using species-specific primers (2μM) in a 50μL reaction using 2μL of cDNA for the template, 5X Buffer, 25mM $MgCl_2$, 2.5mM dNTP, and 0.25 μL GoTaq DNA Polymerase (Promega Corp. cat#M8295). PCR products were run on 0.8% agarose gel and the corresponding bands were excised and purified using the Wizard SV Gel and PCR Clean-Up System (Promega #A9282). Sequencing reactions were performed in a 20μL reaction consisting of 1μL of purified PCR product as a template, 10 μM primer, 10X buffer (supplied with enzyme), and 2μL of Big Dye Terminator v. 3.1 (Applied Biosystems). Sequence samples were cleaned using Agencourt Clean Seq magnetic beads (Agencourt Bioscience Co.) and washed 2X with freshly prepared 80% ethanol on a magnetic plate (Agencourt SPRIPlate 96R-magnetic plate). Samples were eluted in 40 μL of nuclease free water and shipped for processing (University of Wisconsin Biotech Center, Madison, WI).

Comparative Genomic Alignment for the Identification of ECS elements

The UCSC Genome Browser (http://genome.ucsc.edu/) was used to examine genomic regions of both *Shaker* (CG12348) and *ether-a-go-go* (CG10952). The genomes of multiple *Drosophila* species are available in this database to simultaneously compare conservation within these genes. Regions of high conservation in intronic regions flanking the exon containing the editing site were identified as putative ECS elements. Nucleic acid structural predictions were performed using the Sfold web server (http://sfold.wadsworth.org). Input sequences encompassed 100 bases upstream from the

first conserved element through the end of the target exon for *eag*. In *Shaker*, intervening intronic sequences were shortened to accommodate sequence size limitations of the Sfold program.

Results

Sequence analysis of *Shaker* cDNAs among *Drosophila* species showed near complete conservation of RNA editing at all six sites. Exceptions include the first two editing sites within the T1 domain of the N-terminus of the protein. Both of these sites were absent in *D. pseudoobscura* for two 3' alternative splice forms examined, while *D. virilis* and *D. mercatorum* were each lacking a single site in only one splice variant (Figure 4.2). Due to the low levels of editing at these sites (<15%), it is possible that in these species the levels were too low to detect in sequence reads. More often, the biggest differences observed between different *Drosophila* species were in the levels of editing at each site. The most extreme differences are shown in Figure 4.3. Differences in editing levels within the same species can be observed for differentially spliced *Shaker* transcripts, such as the I/M site near the S4 voltage sensor in *D. mercatorum*. Additionally, differences in editing levels for the Q/R site in the C-terminal region of the protein were observed between *D. mercatorum* and *D. tropicalis* when compared to *D. melanogaster* (Figure 4.3). Otherwise, editing levels between *Drosophila* species did not appreciably differ. Additionally, no new sites or species-specific sites were identified in this study. Editing of *Shaker* homologs in bees or mosquitoes was not detected,

indicating that *Shaker* editing is specific to *Drosophila*, and likely other Brachyceran members (Figure 4.1).

In order to better understand these differences in editing levels observed between *Drosophila* species, comparative genomics was employed to identify conserved regions directing editing of these sites. Genome databases such as UCSC genome browser (http://genome.ucsc.edu) and Flybase (http://flybase.org) were used to compare sequences between different *Drosophila* species. As shown in figure 4.4A, regions of high conservation are observed within the 5' intron adjacent to the exon containing the last three editing sites in *Shaker*. When these sequences are aligned, these regions exhibit nearly complete conservation across all *Drosophila* species (Figure 4.4B). With the exception of a few base changes, most of variation is present at the edges of the conserved regions. Furthermore, these regions were found to be complementary to the edited exon using the Sfold web server (see Chapter 1) to predict base-pair interactions between the conserved regions and the editing sites. Various duplex structures generated by base-pair interactions were examined in detail (Figure 4.5). Putative ECS elements that are completely conserved were predicted to generate identical structures, while some species containing few or single base changes in these conserved regions generate similar, yet slightly different structures in regions surrounding editing sites. Although these structural differences may not be drastic, they may explain the differences in editing efficiency of these sites between *Drosophila* species. Additionally, this analysis was used to identify a single conserved region in the downstream intron from the I/M editing site in exon 7, again with complementarity to the coding region surrounding the editing site (data not shown). The predicted complementarity of these highly conserved regions

to the edited exon support the idea that these regions are likely the ECS elements directing editing of these sites in *Shaker*.

A similar analysis was performed for the intronic regions flanking an edited exon in the *eag* locus. Similar to the organization of *Shaker*, two regions of high conservation were found in the intron upstream of exon 13, which contains two editing sites (site B: Y/C and site C: N/D) (Figure 4.6A). Here again, these regions were predicted to base pair with the coding region containing the editing sites using the Sfold web server. (Figure 4.6B) Two classes of structures are predicted using this program, both of which demonstrate base-pair interactions between the predicted ECS elements and the edited exon. The high level of conservation of these elements along with the strongly predicted base-pairing interactions suggest that these two conserved intronic regions are the likely ECS elements directing editing of sites B and C in *eag*.

Discussion

Examination of the conservation of *Shaker* RNA editing allows for a better appreciation of how significant this form of post-transcriptional modification is for proper nervous system function. Indeed, the conservation of this regulation is evidence for its biological significance. Although editing of this transcript was not conserved in all species of insects examined, the conservation within the *Drosophila* genus demonstrates that once this form of *Shaker* regulation developed, evolution has maintained editing of *Shaker* through subsequent species divergence. Again, this argues that RNA editing of *Shaker* is fundamental for proper nervous system function within *Drosophila* and possibly is necessary for fly-specific behavior.

Conservation of RNA editing for a given gene further allows for the identification of the cis-regulatory elements (ECSs) that direct editing. This is based on the idea that if editing of a gene such as *Shaker* or *eag* were conserved, then the ECS elements directing editing of these sites would be conserved as well. This certainly appears to be the case with respect to *Shaker* and *eag* where examination of the genomic regions surrounding known editing sites contain regions of high conservation that are predicted to contain complementarity to the editing site regions. Further examination of these regions using computer applications to predict nucleic acid structures provide additional evidence that these regions can form duplex structures required for RNA editing by ADARs. This conservation and structural predictions for these regions imply that these regions are likely the ECS elements directing editing of these sites in *Shaker* and *eag*.

The identification of these conserved ECS regions within *Shaker* and *eag* provide a starting point to investigate the regulation and functional consequences of editing in these transcripts. Figure 4.7 summarizes the results of this study, depicting both the organization of *Sh* and *eag* transcription units, including the location of the putative ECS elements, and a simplified diagram of RNA folding based on Sfold predictions. Further studies will be required to confirm the identity of the ECS elements regulating editing in these transcripts by mutational analysis. Furthermore, these regions provide targets for mutagenesis to perturb editing at these sites (see Chapter 5). Mutations introduced into the ECS elements will allow for disruption of editing in these transcripts without having to change the coding regions of these genes.

Literature Cited

Bhalla, T., J. J. Rosenthal, et al. (2004). "Control of human potassium channel inactivation by editing of a small mRNA hairpin." Nat Struct Mol Biol **11**(10): 950-6.

Hanrahan, C. J., M. J. Palladino, et al. (2000). "RNA editing of the Drosophila para Na(+) channel transcript. Evolutionary conservation and developmental regulation." Genetics **155**(3): 1149-60.

Jin, Y., N. Tian, et al. (2007). "RNA editing and alternative splicing of the insect nAChR subunit alpha6 transcript: evolutionary conservation, divergence and regulation." BMC Evol Biol **7**: 98.

Patton, D. E., T. Silva, et al. (1997). "RNA editing generates a diverse array of transcripts encoding squid Kv2 K+ channels with altered functional properties." Neuron **19**(3): 711-22.

Reenan, R. A. (2005). "Molecular determinants and guided evolution of species-specific RNA editing." Nature **434**(7031): 409-13.

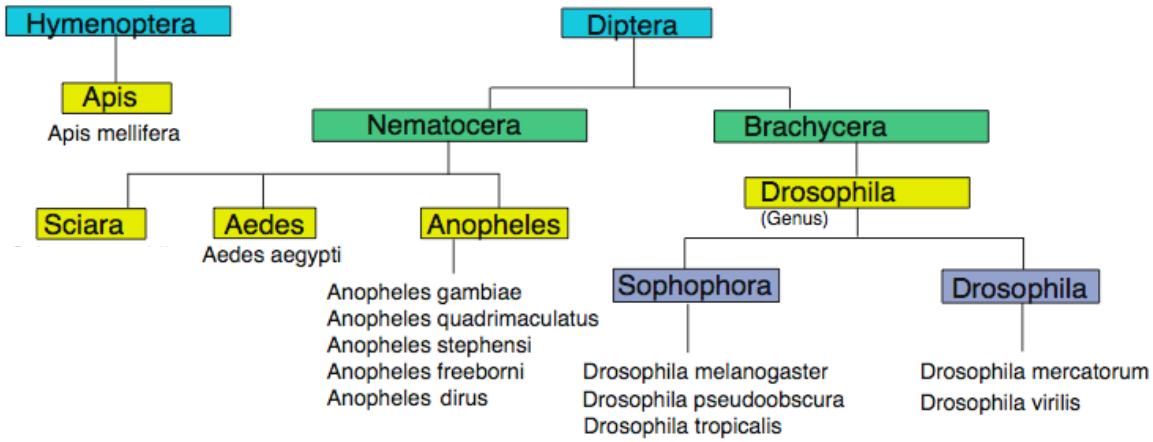

Figure 4.1: Different Insect Species Examined For Conservation Of *Shaker* RNA Editing. Tree diagram depicting the evolutionary relationships between different insects examined for conservation of *Shaker* RNA editing. Specific species examined are listed under their corresponding genus or subgenus classes. Only *Drosophila* species were found to edit their *Shaker* transcripts while no editing was detected for *Apis*, *Aedes*, and *Anopheles* species.

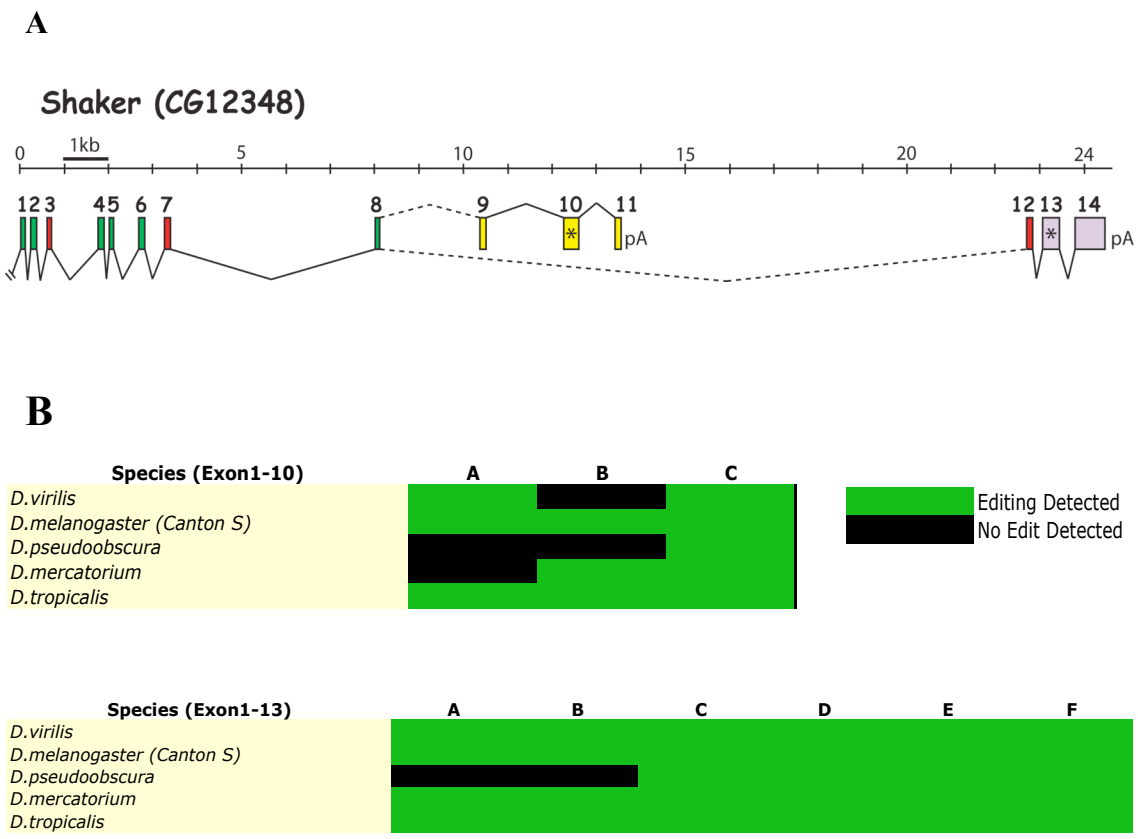

Figure 4.2: Summary of *Shaker* Editing Conservation in Multiple *Drosophila* Species. (A) Shaker transcription unit diagram depicting two alternative splice variants with differing 3' ends (yellow and lavender exon clusters). Exons containing editing sites are shown in red. Exon 3 contains the two editing sites located in the T1 domain, and Exon 7 contains the I/M site near the S4 voltage sensor. The alternative Exon 12 contains the three remaining editing sites located within the S6 and C-terminal regions of the protein. Alternative splicing at the 5' end of the transcript was not examined. (B) Editing between five different *Drosophila* species for both transcript isoforms are summarized. Sites are labeled A through F starting at the 5' end of the transcript.

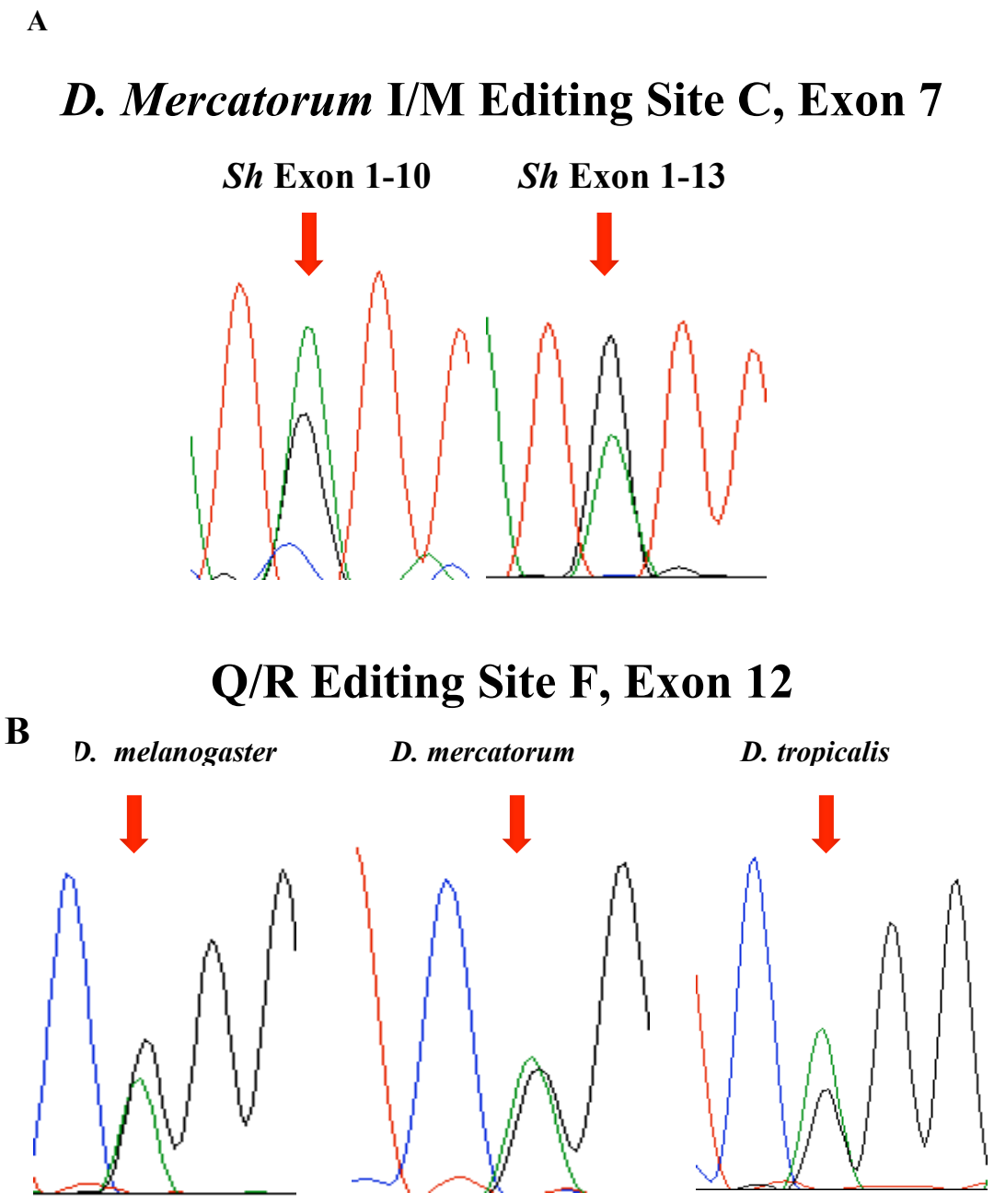

Figure 4.3: Variation Exists in the Conserved *Shaker* Editing Sites Between *Drosophila* Species. (A) Sequence chromatograms from *Shaker* cDNA in *D. mercatorum*. The I/M editing site (site C) located adjacent to the S4 voltage sensor is indicated by a red arrow. The ratio of A/G (green and black respectively) differs between two alternative splice variants of *Shaker* transcripts within the same species. (B) The Q/R editing site in the C-terminal of the protein is present in one *Shaker* isoform and indicated by a red arrow. Variation in the levels of editing for this conserved site exists between different *Drosophila* species.

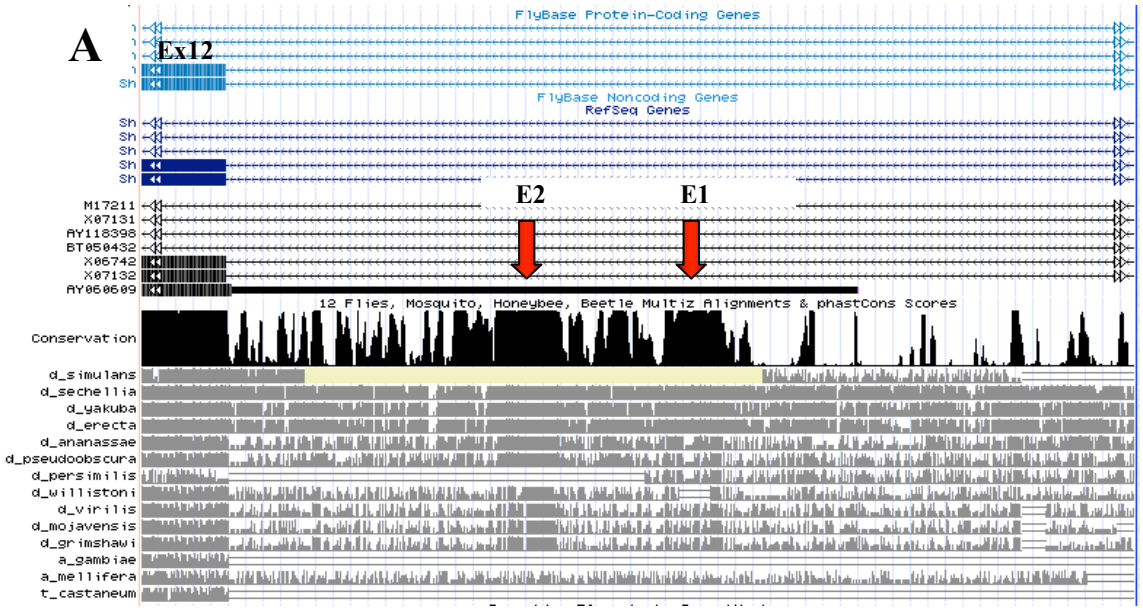

B

E1: ~60 nt

```
CGGCTCCTGCTTCTGCTCCTAAGTCCCGTTTCCCTGTGCTTCCCGATTCCGGTGCATGTG  virilis
CGGCTCCTGCTTCTGCTCCTAAGTCCCGTTTCCCTGTGCTTCCCGATTCCGGTGCATGTG  pseudoobscura
CGGCTCCTGCTTCTGCTCCTAAGTCCCGTTTCCCTGTGCTTCCCGATTCCGGTGCATGTG  ananassae
CGGCTCCTGCTTCTGCTCCTAAGTCCCGTTTCCCTGTGCTTCCCGATTCCGGTGCATGTG  erecta
CGGCTCCTGCTTCTGCTCCTAAGTCCCGTTTCCCTGTGCTTCCCGATTCCGGTGCATGTG  yakuba
CGGCTCCTGCTTCTGCTCCTAAGTCCCGTTTCCCTGTGCTTCCCGATTCCGGTGCATGTG  simulans
CGGCTCCTGCTTCTGCTCCTAAGTCCCGTTTCCCTGTGCTTCCCGATTCCGGTGCATGTG  melanogaster
CGGCTCCTGCTTCTGCTCCTAAGTCCCGTTTCCCTGTGCTTCCCGAATCCGGTGCATGTG  grimshawi
CGGCTCCTGCTTCTGCTCCTAAGTCCCGTTTCCCTGTGCTTCCGATTCCGGTGCATGTG  willistoni
CGGCTCCTGCTTCTGCTCCTAAGTCCCGTTTCCCTGTGCTTCCCGATTCCGGTGCA     sechellia
CGGCTCCTGCTTCTGCTCCTAAGTCCCGTTTCCCTGTGCTTCCCGA-TCCGGTGCATGTG  mojavensis
```

E2: ~50 nt

```
TTTTATGTCAAGTTTAACAGCGACGACGCCAAACGCCGGCACATTTTGTTTATT  ananassae
TTTTATGTCAAGTTTAACAGCGACGACGCCAAACGCCGGCACATTTTGTTTATT  erecta
TTTTATGTCAAGTTTAACAGCGACGACGCCAAACGCCGGCACATTTTGTTTATT  yakuba
TTTTATGTCAAGTTTAACAGCGACGACGCCAAACGCCGGCACATTTTGTTTATT  sechellia
TTTTATGTCAAGTTTAACAGCGACGACGCCAAACGCCGGCACATTTTGTTTATT  simulans
TTTTATGTCAAGTTTAACAGCGACGACGCCAAACGCCGGCACATTTTGTTTATT  melanogaster
   TATGTCAAGTTTAACAGCGACGACGCCAAACGCCGGCACATTTTGTTTAT    willistoni
TTTTGTGTCAAGTTTAACAGCGACGACGCCAAACGCCGGCACATTTTGTTTATT  pseudoobscura
   TATGTCAAGTTTAACAGCGACGACGCCAAACGCCGGCACATTTTGTTTA     grimshawi
     TGTCAAGTTTAACAGCGACGACGCCAAACGCCGGCACATTTTGTTTATT   mojavensis
TTTTGTGTCAAGTTTAACAGCGACGACGCCCAAGGCCGGCACATTTTGTTTATt  persimilis
```

Figure 4.4: Identification of Conserved Intronic Regions within *Shaker*.
(A) Comparative genomic alignment of the Shaker region containing Exon 12 (edited exon) and the adjacent 5' intron in UCSC genome browser (http://genome.ucsc.edu) across twelve insect genomes. Genomic orientation is presented in the 3' to 5' orientation. Arrows indicate two regions of high conservation within the upstream intron of the edited exon, named E1 and E2 (for ECS 1 and 2) from 5' to 3'. (B) Sequence alignments for both E1 and E2 in multiple *Drosophila* species. Length of putative ECS element is indicated above each alignment. Base differences within these regions are highlighted in red.

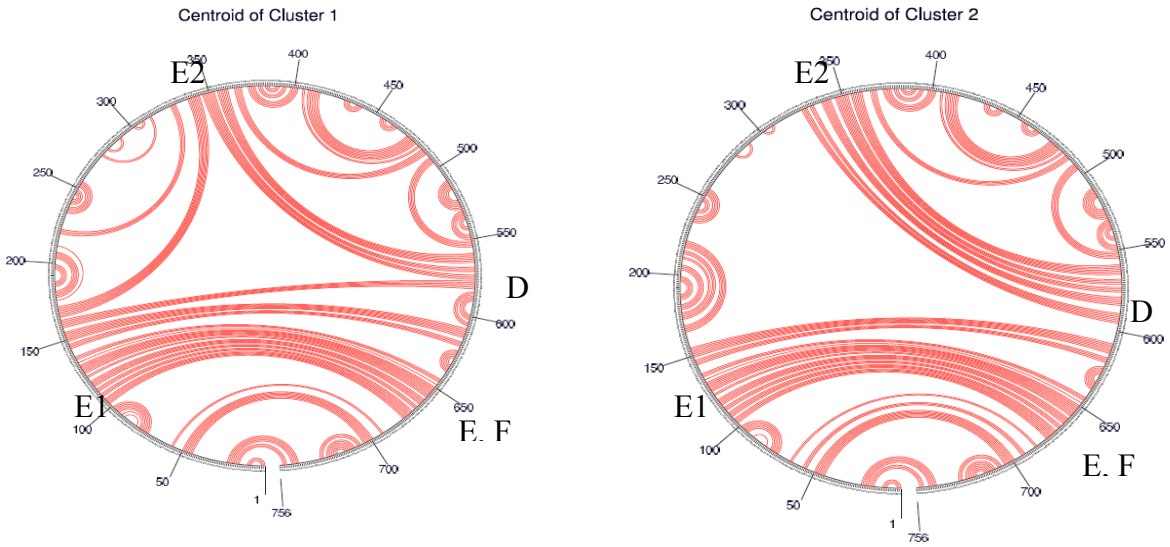

Figure 4.5: Structural Predictions for Base-Pair Interactions Between Conserved Intronic Regions and *Shaker* Sites D, E, and F. Conserved regions (E1 and E2) in 5' intron adjacent to sites D-F in *Shaker* are predicted to have complementarity to the editing sites. Base–pair interactions are displayed as red lines. Input sequence spans the perimeter of the circle. Predictions were performed using Sfold web server (http://sfold.wadsworth.org).

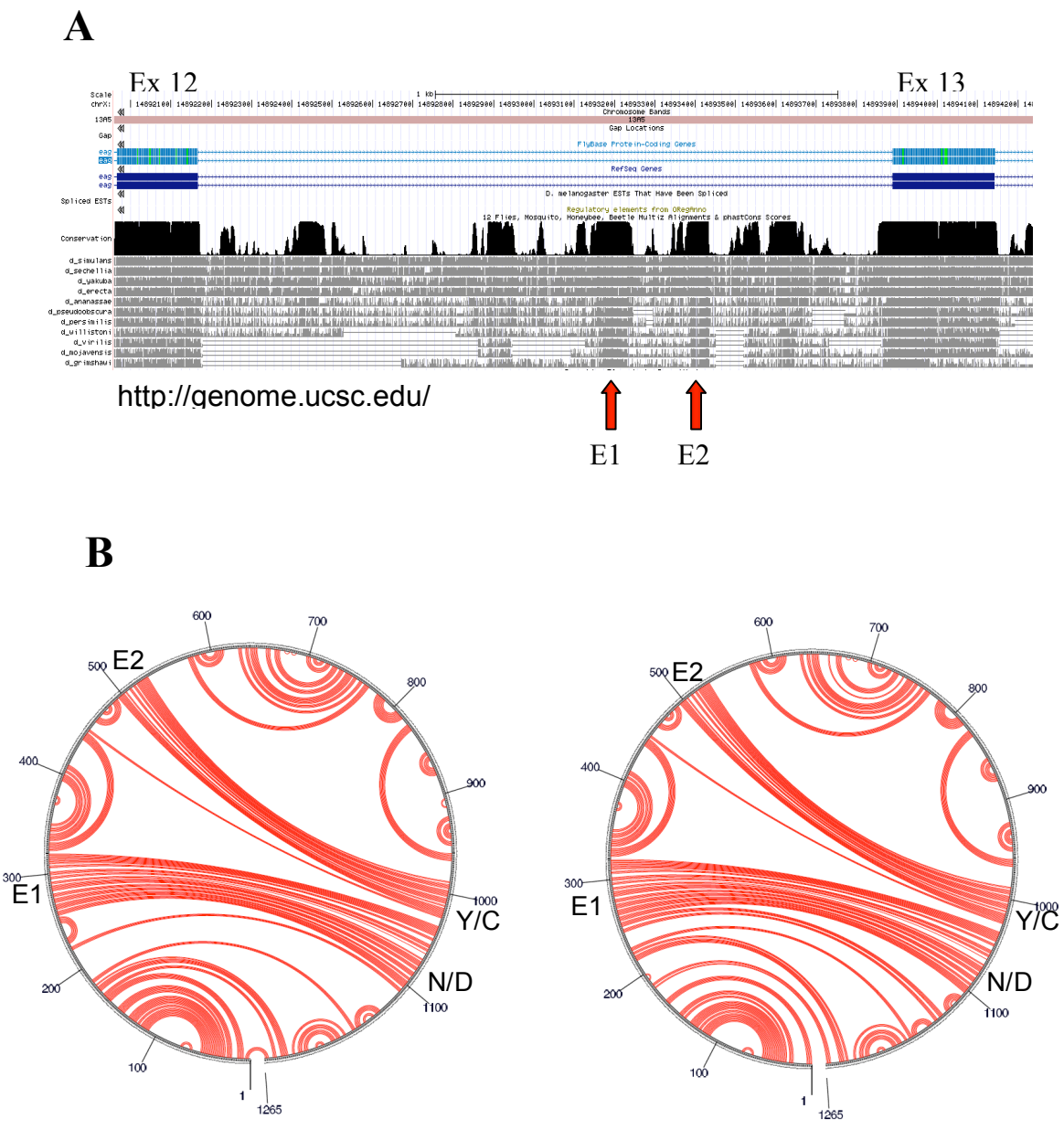

Figure 4.6: Conserved Intronic Regions Identified Within the *eag* Locus Are Predicted to Base-pair With Coding Regions Containing Editing Sites.
(A) UCSC Genome Browser alignment of the *eag* genomic region spanning exon 12 to exon 13 (edited exon) contains two highly conserved regions across multiple *Drosophila* species (red arrows). Conserved regions are named E1 and E2 from 5' to 3'. (B) Centroid diagrams depicting base-pair interactions (red lines) between E1/E2 and two editing sites contained in exon 13. Structures were generated using Sfold web server (http://sfold.wadsworth.org) which predicted two major classes of structures could be generated from this sequence, both of which are predicted to pair the putative ECS element with the editing sites within exon 13.

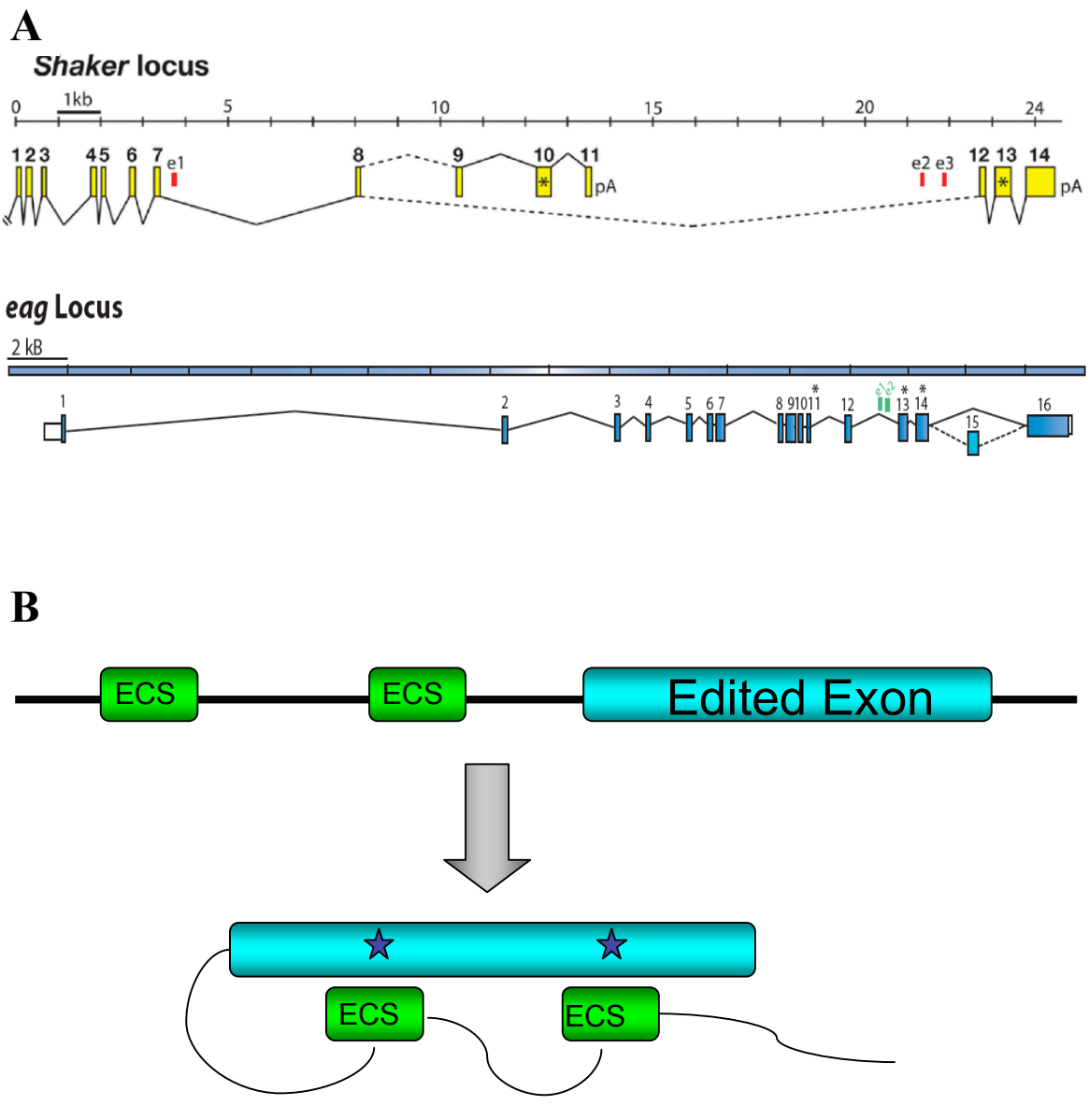

Figure 4.7: Organization of *Shaker* and *eag* Transcription Units and Predicted Base-Pair Interactions Between ECS Elements and Editing Sites.
(A) Transcription unit organization for the *Shaker* and *eag* loci. Exons 3, 7, and 12 in *Shaker* contain editing sites and ECS elements are displayed as red squares. Editing sites in *eag* are located in exons 11,13, and 14 and ECS elements are represented by green squares. (B) Model for the predicted folding of ECS elements in *Shaker* / *eag* to the exon containing editing sites (stars) as predicted by sFold web server.

Chapter 5:

Investigating the *In Vivo* Significance of *Shaker* and *ether-a-g-go* RNA Editing

Introduction

RNA editing of *Shaker* (*Sh*) and *ether-a-go-go* (*eag*) mRNA transcripts can provide a functionally significant form of gene regulation needed for proper nervous system function and generation of appropriate behaviors in the fly. The generation of mutant flies deficient for this regulation would be ideal to further examine the *in vivo* consequences of editing these genes. Loss of editing in these genes may provide clues as to why editing is important and may identify the physiological processes that depend on editing of *Sh* and *eag* for normal functioning. However, the *dAdar*-null phenotype is both complex and severe, owing to the loss of multiple editing events simultaneously, and an *Adar* -/- context is therefore inappropriate system in which to investigate the role of editing in specific gene targets.

Mutations in *Shaker* and *eag* have revealed an array of different behavioral phenotypes demonstrating the significance of these proteins in regulating membrane excitability, coordinated movement, courtship behavior, sleep, and learning and memory (see Chapter 1). It is likely, then, that the highly conserved regulation of *Shaker* and *eag* by RNA editing contributes to the correct generation of these behaviors by modulating the activity of channels encoded by these loci.

Previous studies examining the regulation of RNA editing in other *Drosophila* targets have demonstrated that mutations within the ECS element are sufficient to disrupt specific editing directed by the duplex structures formed between the ECS and the editing

site (see Chapter 1, Bhalla, Rosenthal et al. 2004; Reenan 2005). The putative ECS elements regulating editing within *Shaker* and *eag* have likely been identified in neighboring introns of edited exons (see Chapter 4). To perturb editing in *eag* transcripts, mutations were introduced into putative ECS elements to specifically abolish editing of sites within this transcript. Editing of *Shaker* site C (I/M) was altered by introducing point mutations in the target adenosine. These mutations were introduced into the endogenous loci of *Shaker* and *eag* by homologous recombination in the fly (see below).

Current methods to study gene function in *Drosophila* typically employ ectopic expression systems in which an engineered transgene, typically generated using cDNA, may be expressed under both spatial and temporal control using cell-type specific promoters and activators of transcription (reviewed in Jepson and Reenan 2007). With these expression systems, specific gene products may be over-expressed in various wild type and mutant genetic backgrounds to investigate the role of gene function or to examine the effects of specific mutations. Such systems have limitations, however, especially for the study of certain types of proteins such as ion channels. Due to the diverse and distinct expression patterns of ion channel isoforms for Shaker and EAG, ectopic gene expression systems cannot recapitulate the natural patterns generated by expression from the endogenous locus and post-transcriptional modifications such as alternative splicing (see Chapter 1). Indeed, transgene expression of *Shaker* and *eag*, regardless of the genetic background, will likely generate significant phenotypes that are independent of the mutation or process under investigation simply by affecting the normal expression of the channel. This system is therefore unsuitable to investigate RNA editing of *Shaker* and *eag*, especially since behavioral phenotypes are anticipated.

A method for introducing mutations into the *Drosophila* genome by homologous recombination has been described (Rong and Golic 2000; Rong, Titen et al. 2002; Staber 2010). This method of gene targeting successfully integrates engineered pieces of DNA into a genomic locus of interest and involves the generation of a p-element plasmid that contains large regions of homology (~5 kB) to the locus being targeted. P-elements can be readily introduced into the germline of *Drosophila* by injecting embryos with these plasmids and subsequent integration into random genomic locations by standard transformation (Spradling and Rubin 1982). Transgenic flies can then be crossed to fly lines containing recombinase and endonuclease enzymes regulated by inducible promoters, that induces the re-excision and linearization of the p-element targeting construct. Linearization of this construct induces the cell's DNA double-strand break repair pathway to integrate this construct into the endogenous locus of interest at a low frequency (~4%). This method allows for the introduction of very specific mutations into the loci of genes while maintaining endogenous gene regulation and expression patterns.

Targeted mutagenesis by homologous recombination circumvents problems with studying ion channel gene function in other expression systems. Introducing mutations within these genes that specifically disrupt editing at distinct sites generates a system that is useful in assessing RNA editing function. Since dADAR expression as well as editing of other gene targets remains intact, this system is ideal for investigating the phenotypic consequences of *Shaker* and *eag* editing in *Drosophila*.

Methods

Generating *Shaker* and *eag* targeting vectors for homologous recombination.

Unique features of the targeting vector, P[W25], are illustrated in Figure 5.1 and include a *miniWhite*$^{+}$ selectable marker gene to identify transgenic flies by eye color. This marker is flanked by LoxP sites to facilitate removal of the marker following targeting by the expression of Cre-recombinase. Furthermore, two pairs of restriction sites flank the *miniWhite*$^{+}$ gene that is used to integrate homology arms into the targeting vector (AscI/BsiWI and NotI/Acc65I). The entire region consisting of the homology arms and marker are flanked by FRT sites (Flp Recognition Targets) that mobilizes this region from the site of initial integration in the presence of FLP recombinase. Mobilized DNA is then by digested by the I-SceI restriction endonuclease, which recognizes two, 18-base recognition sequences contained on either side of the FRT site that linearize the DNA and initiate homologous recombination. An overview of the targeting events is illustrated in Figure 5.2.

The first step in generating targeting constructs for homologous recombination involves the design and generation of homology arms (~2.5 kB per arm) by PCR amplification. Primers were designed to amplify regions in the *Shaker* and *eag* locus that encompass both the editing sites and the putative ECS elements (Figure 5.3). Additionally, the design needs to account for the presence of the marker gene during targeting so the intervening sequence space between the two arms should be placed within an intronic region of the gene. In the case of *eag* constructs, the ECS elements were separated into two arms to facilitate mutagenesis. Furthermore, primers contain

terminal sequences, which introduce restriction sites into the flanking ends of the PCR products.

PCR amplification to generate homology arms was carried out using a high-fidelity Taq polymerase (Invitrogen Platinum Taq), and the manufacturer's recommended 50 μL reaction conditions were followed (2μL template, 2μM primers, 10X buffer, 2.5mM dNTP, 0.5μL Platinum Taq). Standard wild type Canton S. lab stocks were the source of genomic DNA used as templates in these reactions. Genomic DNA was prepared from 4 whole flies using the Maxwell 16 Tissue DNA Purification kit (Promega AS1030) and run on a Maxwell 16 automated system for nucleic acid isolation (Promega). PCR products were run on and excised from 0.8% agarose gel and PCR products were purified using the Wizard SV Gel and PCR Clean-up System (Promega A9282). PCR products were then cloned into PCR cloning vectors (Invitrogen TOPO-TA PCR Cloning Kit) and transformed into standard XL-blue competent cells. Individual clones for each arm (~10) were selected and plasmids were purified (Promega Pure-Yield Plasmid Miniprep System A1222). These clones were sequenced using Big Dye Terminator v.3.1 (Applied Biosystems) and cleaned with Agencourt Clean Seq magnetic beads on a magnetic plate (Agencourt Bioscience Co. SPRIPlate 96 well). Sequence samples were washed twice with freshly-prepared 80% ethanol, then dried and eluted in 40 μL of nuclease-free water and submitted for processing (University of Madison Biotech Center, Madison, WI). Sequences were analyzed for any mutations introduced during PCR and to check the integrity of the introduced restriction sites. Clones that contain mutations were discarded. Wild type homology arms free of mutations were cloned into P[W25] directly to generate wild type targeting constructs

and were also stored in the TOPO vector (@ -20°C) for use as templates in mutagenesis (see below).

PCR-based mutagenesis (Stratagene Quick Change II Site-Directed Mutagenesis Kit) was carried out using wild type homology arms in TOPO vectors as a template. Primers were designed with the desired mutation centered within the primer and flanked by 20-23 bases on either side. In the case of deletions, primers were designed that flank the region to be deleted and contained PacI restriction sites to amplify the vector excluding the region and re-ligate the vector following digestion with PacI. Reaction conditions and cycling parameters were based on manufacturer's recommendations (Stratagene). Following PCR cycling, the template plasmid was digested with methylation-specific DpnI restriction enzyme (provided in the Quick Change II kit) to selectively digest the template DNA. The newly synthesized plasmid was transformed into XL-Gold Ultracompetent Cells (Stratagene) per manufacturer's transformation guidelines. Again, these plasmids were sequenced with Big Dye Terminator v3.1 sequencing methods similar to wild-type homology arms. Plasmids containing the desired mutations and lacking any unintentional mutations were cloned into P[W25] to generate mutant targeting constructs (see below).

In order to generate finished targeting constructs, both wild type and mutant homology arms were digested with either NotI/Acc65I or AscI/BsiWI restriction enzymes (New England Biolabs) in a 30 μL reaction with 3 μL plasmid DNA and 1 μL of each enzyme. These reactions also contained the appropriate buffers (supplied by New England Biolabs) and recommended incubation temperatures were observed. Digests were incubated for 1 hour to liberate the homology arm from the TOPO vector. Digests

were separated on 0.8% agarose gel and the ~2.5 kB homology arm insert was purified (Promega SV Gel and PCR Clean-Up System). Similarly, the P[W25] vector was also digested with either NotI/Acc65I or AscI/BsiWI, in a similar 30 μL reaction. Furthermore, the vector digest reaction was treated with CIP (Calf Intestinal Alkaline Phosphatase, New England Biolabs) for one hour at 37°C following restriction digestion to inhibit re-ligation of the vector. The digested P[W25] vector was gel purified in a similar manner to homology arm preparation.

Ligation of the first homology arm was accomplished using T4 DNA Ligase (New England Biolabs) and supplied 10X buffer in a 30 μL reaction containing 1μL of CIP-treated linear P[W25] purified vector and 4 μL of purified homology arm DNA. Samples were incubated at 15°C overnight and transformed into standard XL-Blue competent cells. Plasmids were purified using Promega Pure-Yield Plasmid Miniprep System and were digested with the appropriate restriction nucleases to verify homology arm integration into P[W25].

P[W25] constructs containing the first homology arm were digested again with the second set of restriction enzymes and the second homology arm to be integrated was digested and purified as well. The above ligation reaction was repeated to integrate the second arm into the targeting vector, and again restriction digestion verified homology arm integration.

Once both homology arms were integrated into P[W25], sequencing was performed using primers internal to the homology arm that will sequence across the junctions between the homology arms and targeting vector to verify proper integration of the arms into P[W25]. Furthermore, these sequences also allow for the verification that

other important features of the targeting vector (FRT, I-SceI, and LoxP sites) are intact and free of mutations prior to using these plasmids for germline transformation and subsequent targeting.

The finished targeting construct was grown in a large-scale (40 mL) overnight culture inoculated with a single colony. Multiple minipreps were performed from this single culture. The resulting purified plasmid DNA was pooled and restriction digests were performed to verify construct integrity and to determine the quality and concentration of the DNA. Plasmids were sent to an outside vendor (Genetic Services Inc., Cambridge, MA) for embryo injection.

Targeting *Shaker* and *eag* in Transgenic Flies

Once transgenic flies were received from the outside vendor, these lines were stocked as homozygotes and targeting was initiated. Figure 5.4 illustrates the crossing scheme used to initiate homologous recombination. Homozygous male transgenic flies were crossed to virgin females (4 to 5 flies of each gender with a total of 20 independent crosses) carrying a FLP recombinase and I-SceI transgene under the control of a heat-shock inducible promoter (y w;FLP-I-SceI/noc^{Sco}, CyO). Flies were allowed to mate for 48 hours, at which time the parents were transferred to new vials. The initial vials containing embryos were then heat-shocked in a 37-39°C water bath for one hour each day for two days. Parents were again transferred to new vials and the second set of vials was heat-shocked in a similar manner. A total of three sets of vials per individual cross were heat-shocked to induce expression of FLP recombinase and I-SceI endonuclease in these embryos.

When heat-shocked progeny eclosed, white-eye or mosaic (indicative of transgene mobilization) virgin females were collected and 1-2 females were mated to male flies containing a FLP recombinase transgene under the expression of the *eyeless* promoter (y w; ey-FLP). Approximately 100 individual crosses were set-up for each transgene targeted. Crossing to *ey*-FLP males will rule out many false positive (solid red eye) progeny from the previous cross by supplying an additional source of FLP recombinase. Solid eye color in the next generation could be the result of the transgene failing to mobilize during heat-shock treatments and is thus "false positive". These failed mobilization events will still have two available FRT sites, while mobilization and targeting during heat shock eliminates these sites. By crossing mosaic or white-eye virgins to *ey*-FLP, stable red-eye females (*ey*-FLP is not expressed in males) in the next generation have likely undergone targeting events while loss of stable eye-color will rule out negative events.

Virgin females from the above cross with solid-eye color represent potential targeting events. These virgins were single-pair mated to balancer stock males, in this case Fm7a since both *eag* and *Sh* are located on the X-chromosome. Once crosses were established and progeny were visible, these females were sacrificed and their genomic DNA isolated (Maxwell 16 Tissue DNA kit). PCR validation for integration was performed on these females to see if the endogenous locus was targeted (Figure 5.5). This is accomplished by amplifying both homology arm regions using primers specific to the targeting vector in P[W25] and primers specific to the *eag* or *Shaker* locus outside the targeting region. PCR products produced in these reactions are confirmed targeting

events, while no PCR product(s) are considered false-positives and the crosses are discarded.

In female flies that validated for the integration of both homology arms, the PCR product that corresponded to the desired mutation of interest was purified and sequenced to confirm integration of the mutation. This is required due to the migration ability of Holliday junction intermediates during recombination. Depending on where the crossover event takes place in the homology arm, mutations can be either included or excluded in independent targeting events. Additional independent wild-type alleles can be generated in this manner.

Once mutant and wild type targeted flies were validated and stocked over Fm7a balancers, crosses were established to remove the *miniWhite*$^{+}$ marker from the targeted allele by Cre recombinase recognition of LoxP sites flanking the marker gene. In the case of targeting certain genes, the introduction of the *miniWhite*$^{+}$ gene, which is approximately 5 kB in length can result in lethality likely due to the disruption of gene expression. This was not the case for targeting events in either *Shaker* or *eag*, which was not surprising since mutant animals null for these genes are typically viable. A crossing scheme to remove the *miniWhite*$^{+}$ marker from these loci is illustrated in Figure 5.6. Removal of the marker gene requires PCR validation to identify and follow the targeted allele both during Cre-removal of *miniWhite*$^{+}$, as well as during subsequent backcrossing to introduce the targeted allele into a standard genetic background. This is performed by PCR and restriction digest analysis. Following Cre-removal of the marker, a single LoxP site flanked by Acc65I and AscI restriction sites is left behind in the gene region between the two homology arms. Validation involves the PCR amplification and subsequent

digestion with either of these two enzymes to confirm the targeted allele. Since pre-Cre *Shaker*- and *eag*-targeted flies are viable and X-linked, this process becomes simplified. Starting with homozygous targeted virgin females, crossing them to males expressing Cre-recombinase linked to CyO on the second chromosome (y w; noc^{Sco}/CyO, Cre) will yield hemizygous curly-winged (white eye) or straight-winged males (red eye). The white-eye curly-winged males can be crossed directly to virgin females of the desired genetic background, in this case w^1 flies. Only in the second generation of backcrosses where single male progeny are crossed to virgin w^1 stocks, do parental males need to be validated for the mutant allele. Setting up a minimum of 10-15 single pair crosses at this point is typically sufficient to find males that validate for the target allele. For behavioral analysis in mutant flies a minimum of three-generations of backcrossing is required, and five generations is preferable.

Once mutant flies were backcrossed into the w^1 background, cDNA sequence analysis was performed to determine editing perturbations in *Sh* and *eag* transcripts for both mutant and wild type alleles. This is achieved by methods similarly outlined in Chapter 2.

Developmental analysis of *eag* editing was achieved in a similar manner to methods outlined in Chapter 3. RNA was isolated from Canton S. synchronized cultures held at 25°C. The time points when RNA was extracted after two, one-hour egg laying sessions are as follows: embryo (18 hours), L1 (36 hours), L2 (60 hours), L3 (96 hours), early pupae (144 hours) and late pupae (192 hours). Three-day old adults were also used in this study (head RNA only). RNA was only extracted from cultures generated during the second hour egg lay session to ensure synchronicity. RNA samples were subject to

RT-PCR using gene-specific primers and further amplified by PCR and Big Dye Terminator sequencing of bulk cDNA products. Quantification of editing levels was achieved by averaging the ratio of areas under mixed peaks in sequencing chromatograms for three independent RT-PCR reactions.

Drosophila activity monitor studies involved the use of the *Drosophila* Activity Monitor System (TriKinetics Inc. Waltham, MA). Flies were reared in 25°C incubators in a 12-hour light: dark cycle. 3-5 day old male flies were then housed individually within glass tubes containing food at one end and a cotton plug at the other. These units were then placed in the DAM system where a laser beam is focused at the midpoint of the vials. Fly movement results in beam breaks that were then tallied by the activity monitor software. Flies are placed in these chambers for five days under the same temperature and light: dark cycles as the incubator conditions in which they were grown. The first two days are not recorded to allow flies time to adjust to the new environment. Beam breaks are then counted for 72 hours and different time points are averaged between the three days.

Results

Mutations Within Conserved Intronic Elements in *eag* Disrupt RNA Editing

To disrupt RNA editing in *eag* transcripts, mutations were introduced into the putative ECS elements thought to direct editing of two sites: the Y/C and N/D sites located in the intracellular C-terminal domain of the protein (see Chapter 4). Figure 5.7 illustrates the specific mutations introduced into these regions to disrupt the local secondary structure surrounding the editing sites. Additionally, the most distal ECS

element (E1) to the edited exon was deleted ("E1Pac") in case the more modest changes were insufficient to disrupt editing. These mutations were analyzed by the Sfold nucleic acid folding web server to further verify predicted disruptions to the duplex structures prior to introducing them into the *eag* locus (see Figures 5.18-20). Structural predictions for the E1 deletion mutants demonstrated a destabilization of both duplexes approximately 80% of the time, while E2 was still predicted to base pair around its corresponding editing site with 20% probability (Figure 5.18). Mutations in E2 were predicted to form two major classes of structures (90% probability) where the duplex formed between E2 and site B were disrupted, while E1 was still predicted to form a duplex around site C (Figure 5.19). A minor class (10% probability) with this mutation was predicted to destabilize both duplex structures. Mutations in E1 yielded two structural classes, both of which disrupted the structure around site C while the E2/site B structure was left intact (Figure 5.20).

Sequence analysis of *eag* transcripts from these mutant flies demonstrate that indeed the conserved intronic sequences are the ECS elements directing editing at these sites. While editing of a particular site was specifically disrupted with mutations in the corresponding ECS element, editing could also be affected in the alternate site as well (Figures 5.8 and 5.9). Mutations within E2 eliminated editing of site B (Y/C) as predicted, but editing of site C (N/D) was slightly reduced as well (~14%). Furthermore, mutations in E1 also eliminated editing at its predicted target, site C, but also reduced editing levels at site B by nearly 30%. When E1 is deleted from the locus, editing at both sites is eliminated (with ~5% editing detected for site B) (Figure 5.10).

Additional temporal analysis of editing events was performed for *eag*, in which editing of all four sites was compared across development (Figure 5.12). The two K/R editing sites (sites A and D), located in separate exons, recode amino acids located in the outer region of the pore and in the intracellular C-terminal domain. These sites exhibit different editing profiles across development. The pore site is edited at high levels (>80%) throughout development and then decreases to 50% in adults, while the other site in the C-terminus is edited at relatively low levels during larval development and increases as metamorphosis and adult stages are reached, with highest levels of editing (>70%) occurring in adult flies. The two sites disrupted using homologous recombination (sites B and C), however, were tightly linked having similar levels of editing at every stage throughout development. Sequencing of single cDNAs from two different developmental time points indeed confirmed the tight linkage observed in the developmental profile (Figure 5.13).

Preliminary phenotypic examination of these mutant flies has begun and includes assessing overall activity levels using a *Drosophila* Activity Monitor System that can record fly activity over the course of multiple days. Figure 5.14 shows overall activity levels for wild type targeted as well as E2 mutants and E1 deletion (E1Pac) flies for three days. Activity levels were not appreciably different between wild type and mutant flies and peaks of activity normally exhibited in morning and evening was unaffected. Examination of excitability at the larval neuromuscular junction in these mutants is being conducted by an outside collaborator (Dr. Leslie Griffith, Brandeis University). Figure 5.15 is an example of preliminary data illustrating excitatory junction potentials recorded from larval muscles. Mutations that disrupt site B specifically or both sites B and C (E1

Pac) were shown to have increased frequencies of excitatory potentials. Loss of editing at both sites resulted in a higher frequency of these spontaneous potentials than loss of one site alone.

Mutations within *Shaker* Eliminate Editing and Provide a Human Disease Model in Flies

Studies utilizing homologous recombination to investigate the functional consequences of *Shaker* RNA editing were limited to the I/M site located proximal to the S4 voltage sensor (site C). This site is edited at relatively high levels throughout development (>60%) and is heavily utilized in tissues enriched for sensory neurons (see Chapter 3). The edited adenosine is located within the 3rd position of the reading frame where an ATA codon that codes isoleucine is recoded to ATG (methionine) through RNA editing. The generation of editing deficient flies for this site simply involves substituting the edited adenosine so that either the edited form or the genomic form of the channel is produced. In this case, the ATA codon normally found in the genome was changed to either ATC to abolish editing or to ATG to mimic constitutive editing.

In addition to perturbing RNA editing at the I/M site in *Shaker*, homologous recombination was also employed to introduce a known human disease allele into the *Shaker* locus in an attempt to generate a human disease model in *Drosophila*. A missense mutation (L305F) in the S4 voltage sensor of the human *Shaker* homolog, *KCNA1*, was identified through pedigree analysis and subsequent sequencing in a family exhibiting chronic neuromyotonia (see Chapter 1, Poujois, Antoine et al. 2006). Although this is just one of many missense mutations identified within this gene that results in either neuromyotonia or other forms of episodic ataxias and generalized epilepsies, we found

that this leucine residue is conserved between human and *Drosophila* (L375) and is also located within one of the homology arms previously used in targeting. This same disease mutation (L375F) was introduced into the *Shaker* locus by homologous recombination. These mutant flies have increased levels of overall activity compared to wild type controls in activity monitor studies (Figure 5.16). This increase in activity is apparent both at night and during midday "siesta" periods were wild type flies normally have decreased activity levels. These disease mutant flies do exhibit peak activity during early morning and late evening, similar to control flies. This data set was further analyzed to see if the increase levels in activity are the result of sleep defects, since *Shaker* has been implicated in the regulation of sleep maintenance (see Chapter 1). Indeed, these mutants do exhibit defects in sleep where mutant flies sleep less during the day compared to wild-type targeted controls and also have marked reduction in sleep amounts during early morning hours (Figure 5.17). Additionally, these flies exhibit seizure activity: flies fall on their backs and have difficulty righting themselves. During these events, periods of complete immobilization and/or high frequency wing beating are observed. These processes appear to be age dependent, as flies less than one week of age do not exhibit such behaviors, and the frequency and intensity of these events become more prominent in flies older than two weeks of age. Unexpectedly, male flies bearing the neuromyotonia mutation have also been observed to exhibit increased aggression and male-male courtship behavior.

Discussion

Mutations in *eag* disrupt editing of sites B and C and site linkage.

Although editing deficient mutants that specifically knockout editing of sites B and C were generated as predicted, the effects of the E1 deletion (loss of both sites) were not anticipated. These results demonstrate a requirement for E1 in editing of these two sites. It is possible that the binding of E1 is an initial requirement for the formation of both duplex structures, thus bringing E2 in closer proximity to its target sequences. However, if this were the case I would not have expected such a drastic reduction in site B editing since structural predictions still had E2 base pair with site B approximately 20% of the time in the absence of E1 (Figure 5.18). Furthermore, E2 is the more proximal element to the edited exon (~450 bases upstream) and should still be able to find its target sequence albeit at a lower frequency. Alternatively, the binding of both ECS elements may be required to form a higher-ordered tertiary structure that attracts dADAR to the substrate. While wild-type targeted flies did not show any significant changes in editing of these two sites (Figure 5.11), mutations and/or deletions in either ECS element generated flies deficient for one or both editing sites but no single site could be affected without affecting the other. The formation of a tertiary structure between both duplexes could explain these results. A model structure is depicted in Figure 5.21 that may explain how this structure could direct and position dADAR on the substrate in a manner that would be consistent with the observed effects in editing in mutant flies. Since the dADAR enzyme requires the formation of a dimer for catalytic activity, it is possible that each enzyme binds both duplex structures through its two double-stranded RNA binding domains in opposing configurations. Once binding of two ADARs is

achieved, the catalytic domains of each unit can be positioned over each site, allowing for deamination of site B and C. This structure can be further examined in the future by introducing mutations that disrupt binding of ADAR in the periphery of the duplex to see if editing in the opposite duplex is affected while leaving the local structure surrounding each editing site intact. Furthermore, the possibility of supplying a duplex in *trans,* such as an E1/site C duplex in an E1 deletion background to see if editing of site B can be rescued. These experiments could help to further support this model of a tertiary structure.

The linkage observed between sites B and C throughout development helps to further validate the tight regulation observed between these two sites in targeted mutant flies and again argues in favor of a tertiary structure regulating and linking editing of these two sites. Interestingly, mutations in either ECS element that specifically disrupt editing at the predicted site essentially uncouples these two editing sites and perturbs the tight regulation that exists for these editing sites *in vivo*. Although in-depth behavioral analysis still needs to be examined in detail, it is possible that these mutants may exhibit behavioral defects that are unique from flies in which both sites are abolished.

The preliminary analysis of excitability at the larval neuromuscular junction in these mutant flies demonstrate effects that appear to be cell body specific since they are lost when axons are severed from the brain and ventral nerve cord during larval preparation. This demonstrates that this phenotype is not the result of defects within the axon, and indicates that editing of these channels may play a larger role in regulating neuronal activity than simply affecting excitability at the synapse. Additional studies have begun to investigate the expression levels and distribution of the mutant channels

using immunohistochemistry methods. Additional behavioral analysis including mating song characterization as well as courtship behavior and conditioning remain to be examined in further detail for these mutants.

Shaker Editing and Neuromyotonia Mutant Flies

Multiple independent targeted lines have been generated for both types of *Shaker* site C editing mutants (constitutive and deficient) and are currently in the process of being backcrossed into a w^1 background in preparation for behavioral studies. It will be interesting to see what types of effects these single nucleotide mutations will have on fly behavior and physiology. Considering the heavy utilization of this site in sensory tissue, loss of editing at this site may perturb various sensory modalities such as vision, gustation, and olfaction. Defects in these senses by loss of editing may result in the fly's inability to generate correct behavioral outputs to different environmental stimuli.

The chronic neuromyotonia disease model mutants revealed an array of striking phenotypes when introduced into the fly. Although these behaviors still need to be characterized under controlled experimental conditions, the aggression and courtship defects are very obvious and are not displayed by wild type targeted control flies. These behaviors need to be quantitated in timed assays between male: male and male: female pairings to further understand the extent of these phenotypes. Furthermore, genetic interactions can be studied to further investigate these behaviors in detail through crossing these mutants to other mutant lines with known aggression and courtship behavioral defects. The seizure activity of these mutants needs to be examined as well, particularly with respect to the age of onset for seizure activity. Flies at various ages

from various aged flies need to have seizure activity measured at regular time points in the adult lifespan. Furthermore, overall lifespans appear to be shorter than control flies and thus need to be measured as well. These flies do exhibit an increase in overall daily activity levels as well as sleep defects. These sleep defects are apparent in midday levels of total sleep being less than wild-type flies and are even more striking in the early morning hours (from 2 am to 8 am) where total sleep is nearly half of the amount compared to control flies. It is not yet known whether circadian rhythms are disrupted in these animals and would require additional activity monitor studies in total dark conditions over multiple days to determine any defects. This disease model recapitulates some of the human disease features with respect to seizure activity, and uncovers a previously unidentified involvement of *Shaker* in the regulation of aggression and male-male courtship behaviors in *Drosophila*.

Literature Cited

Bhalla, T., J. J. Rosenthal, et al. (2004). "Control of human potassium channel inactivation by editing of a small mRNA hairpin." Nat Struct Mol Biol 11(10): 950-6.

Jepson, J. E. and R. A. Reenan (2007). "Genetic approaches to studying adenosine-to-inosine RNA editing." Methods Enzymol 424: 265-87.

Poujois, A., J. C. Antoine, et al. (2006). "Chronic neuromyotonia as a phenotypic variation associated with a new mutation in the KCNA1 gene." J Neurol 253(7): 957-9.

Reenan, R. A. (2005). "Molecular determinants and guided evolution of species-specific RNA editing." Nature 434(7031): 409-13.

Rong, Y. S. and K. G. Golic (2000). "Gene targeting by homologous recombination in Drosophila." Science 288(5473): 2013-8.

Rong, Y. S., S. W. Titen, et al. (2002). "Targeted mutagenesis by homologous recombination in D. melanogaster." Genes Dev 16(12): 1568-81.

Spradling, A. C. and G. M. Rubin (1982). "Transposition of cloned P elements into Drosophila germ line chromosomes." Science 218(4570): 341-7.

Staber, C. J., Gell, S., Jepson, J.E. and Reenan, R.A. (2010). "Perturbing A-to-I RNA Editing Using Genetics and Homologous Recombination." Methods in Molecular Biology in press.

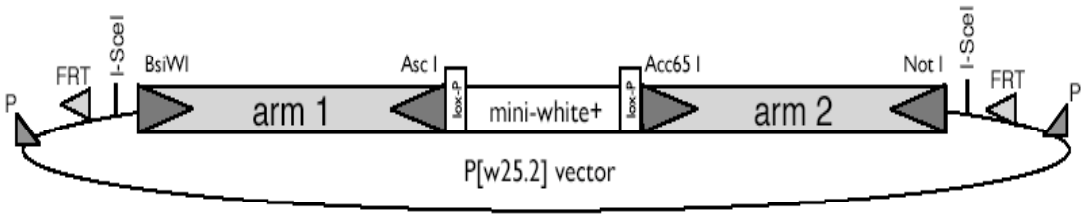

Figure 5.1: P[W25.2] Targeting Vector Map.
P[W25.2] vector map for use in homologous recombination in *Drosophila* (Staber et al. 2010). The vector is approximately 9 kB in length (including the ~5kB *mini-white*$^{+}$ marker). When both homology arms are integrated, the total size of the complete targeting vector is 14 kB (if 2.5 kB arms are used). Features of this vector include FRT sites to mobilize the intervening sequence in the presence of FLP recombinase following p-element (P) mediated transformation. I-SceI restriction sites within the mobilized DNA will be cut to linearize this DNA. The marker gene is flanked by LoxP sites to facilitate removal following targeting. Homology arms are integrated into the vector via two sets of restriction sites (NotI/Acc65I and AscI/BsiWI) which flank the *mini-white*$^{+}$ marker.

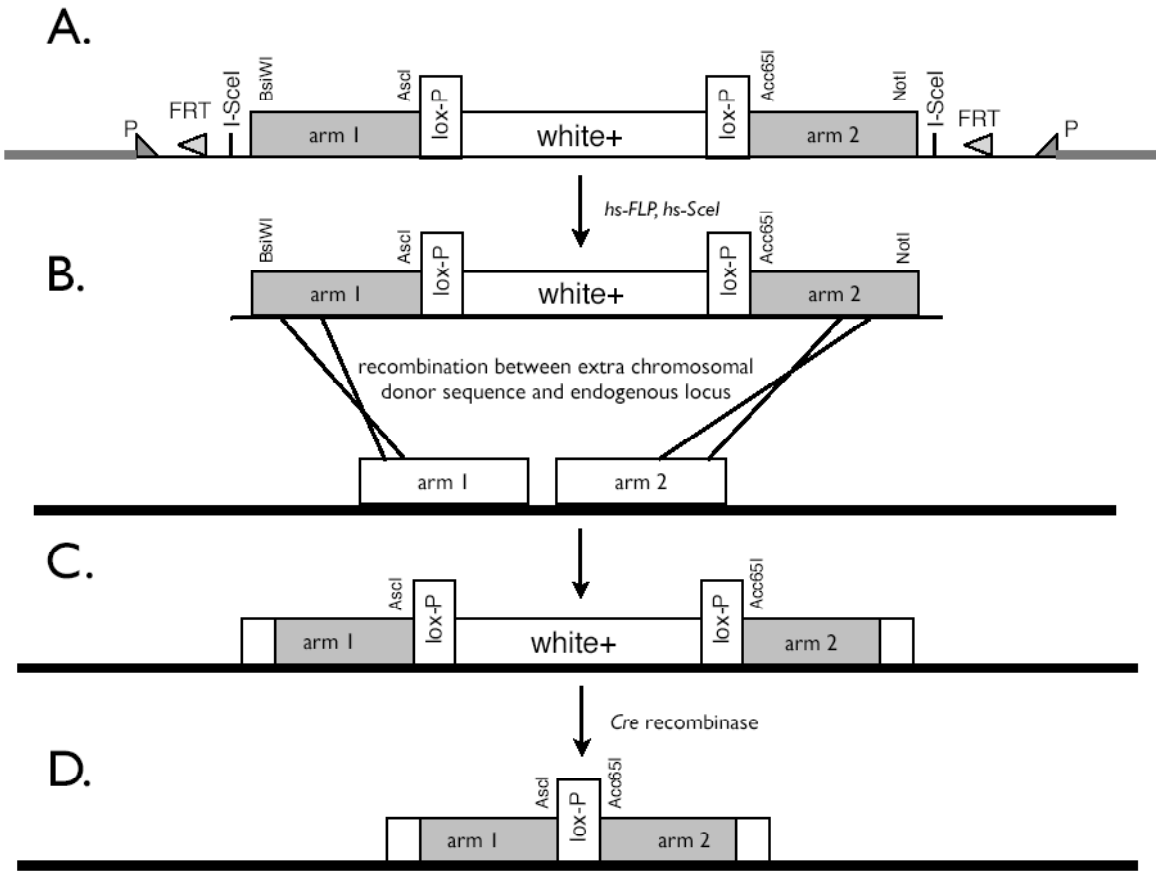

Figure 5.2: Overview of Targeting Events.
Part A depicts the targeting vector randomly integrated into the *Drosophila* genome following p-element mediated transformation. (B) Homologous recombination is initiated by the expression of FLP recombinase and I-SceI enzymes that remobilize and linearize the donor DNA. (C) Following targeting, the donor DNA has been integrated into the genomic locus along with the marker gene flanked by LoxP sites. (D) Expression of Cre recombinase removes this marker gene from the locus, leaving behind a single Lox P site in the targeted region (Staber et al. 2010).

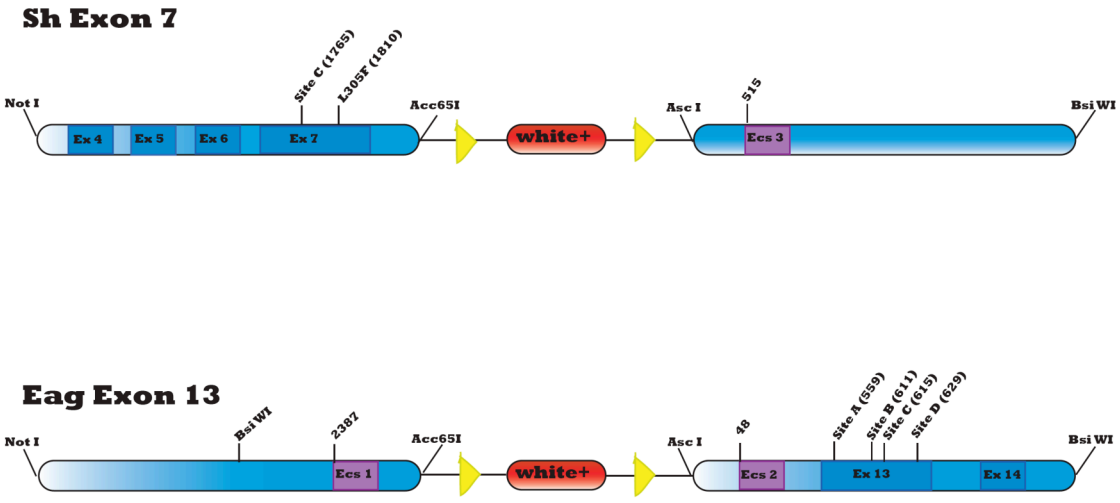

Figure 5.3: Targeting Constructs for *Shaker* and *eag*.
Top diagram details the targeting construct used to introduce mutations into exon 7 of the *Shaker* locus. Four exons are contained within the first homology arm, while the ECS element is located on the second arm. Mutations were introduced to disrupt editing at site C and to introduce a human disease allele (L305F) in this exon. Lower diagram details the targeting vector used to introduce mutations into the *eag* locus. The ECS elements were separated onto two arms. Editing sites in exon 13 are labeled. Editing is disrupted by introducing mutations into ECS1 and ECS2, as well as the deletion of ECS1. In this diagram, site A and site C produce the amino acid substitutions, Y/C and N/D respectively. Sites B and D are in third-positions in the reading frame and do not result in any substitutions.

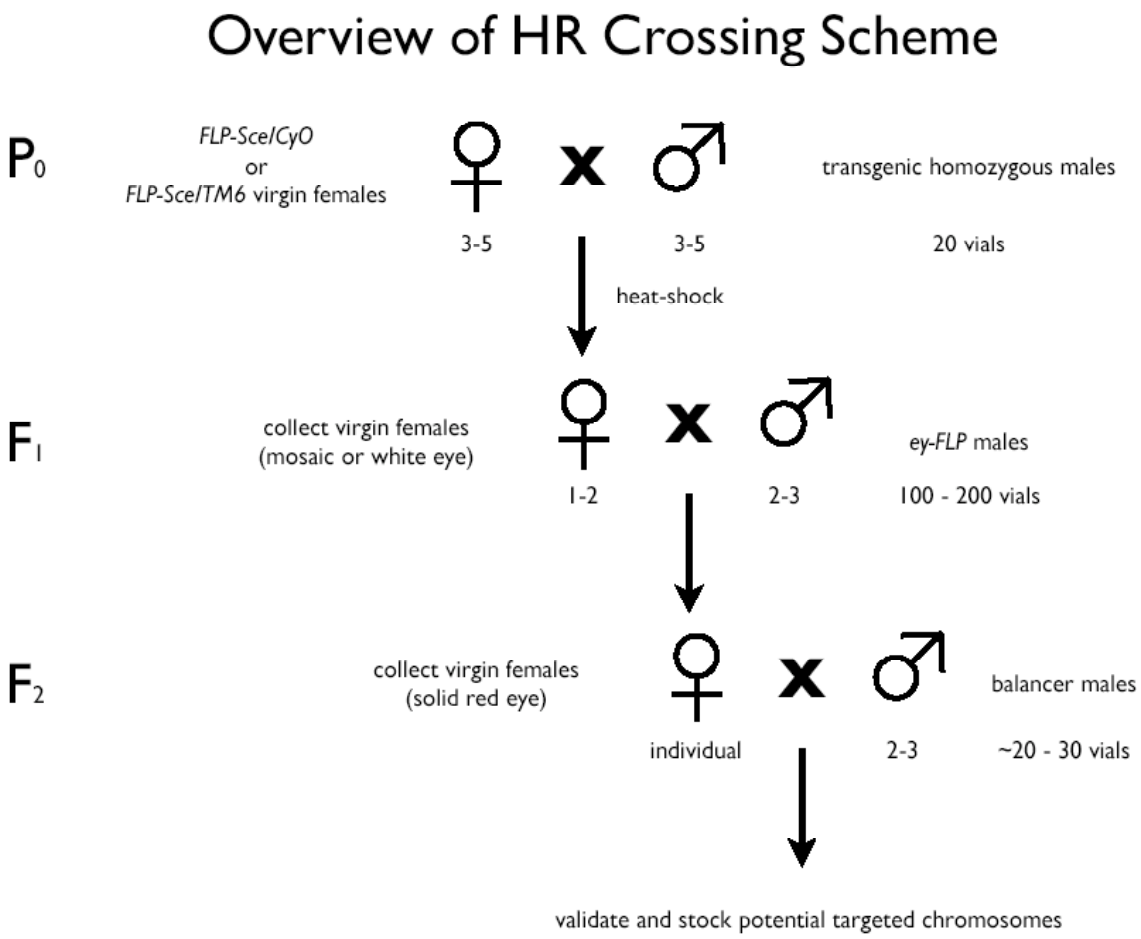

Figure 5.4: Crossing Scheme to Initiate Homologous Recombination.
Homologous recombination is initiated by crossing transgenic males (containing the targeting construct) to females bearing a FLP, I-SceI transgene regulated by a heat-shock promoter. Embryos from this cross are heat-shocked to induce the expression of FLP recombinase and I-SceI endonuclease. Heat-shocked virgin females (white eye or mosaic) are then crossed to ey-FLP males to provide an additional source of FLP recombinase in female progeny. This is used to reduce false positive events in the following generation. Females from this cross with solid red eye color are single-mated to balancer males (Fm7a) and later validated for potential targeting events (Staber et al. 2010).

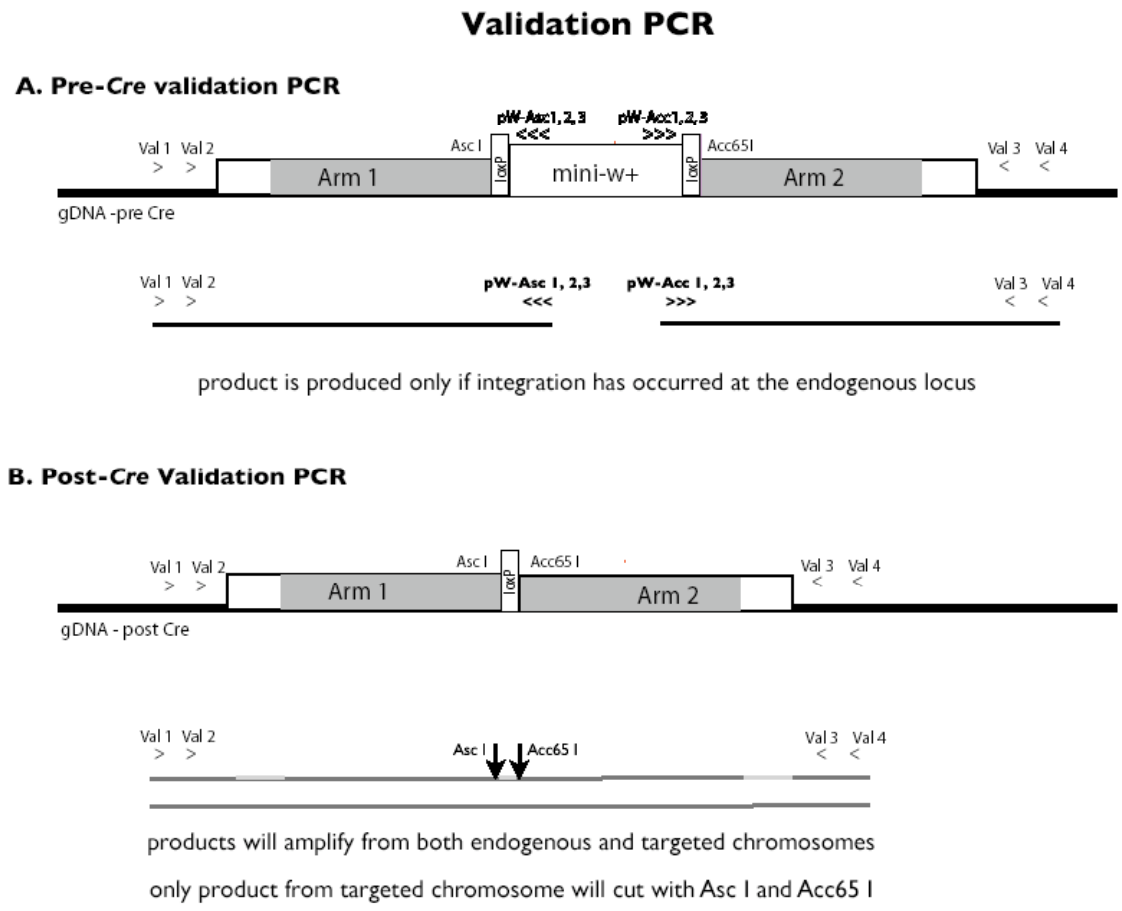

Figure 5.5: Overview of PCR Validation of Targeting Events.
The top panel (A) depicts the validation of targeting events by PCR. Primer pairs for PCR consist of a primer located in the targeting vector (pW-Asc or pW-Acc) and a primer located outside the targeting region (Val). Amplification of the regions encompassing both arms is performed. The generation of PCR products for both reactions is confirmation of a targeting event. The bottom panel (B) outlines PCR validation to follow the targeted allele following Cre-removal of the *mini-white*$^{+}$ marker. The restriction sites AscI/Acc65I remain in the targeted region following removal of the marker. PCR amplification of this region followed by subsequent digestion with either of these enzymes confirms the presence of the targeted allele (Staber et al. 2010).

Cre-Removal of *mini-white*$^{+}$ From Targeted Allele (X-Chromosome)

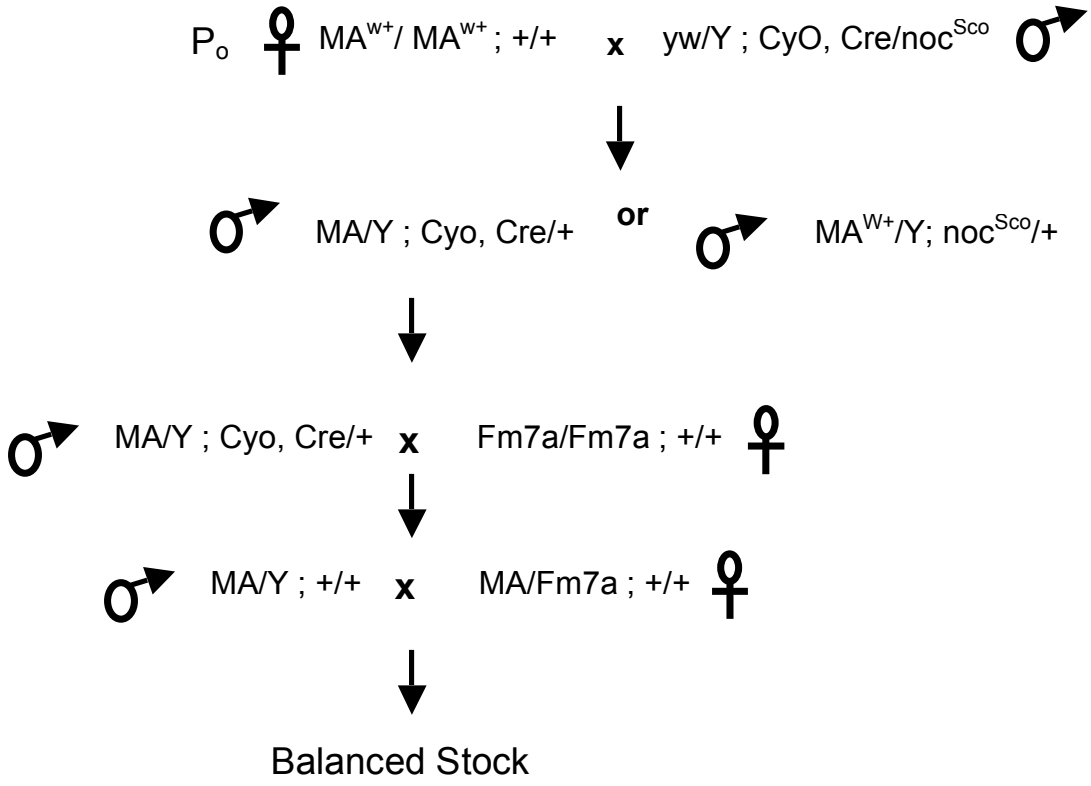

Figure 5.6: Crossing Scheme for Cre-Removal of Marker Gene on the X.
To remove the *mini-white*$^{+}$ marker following targeting, females homozygous for the targeted/mutant allele (MA) are crossed to males expressing Cre recombinase from a transgene on the 2nd chromosome (linked with CyO). Curly wing males (white eye) in the next generation are crossed to a balancer stock (Fm7a). In the following generation mutant males are crossed to balanced mutant females to generate a balanced stock or to homozygose the targeted allele.

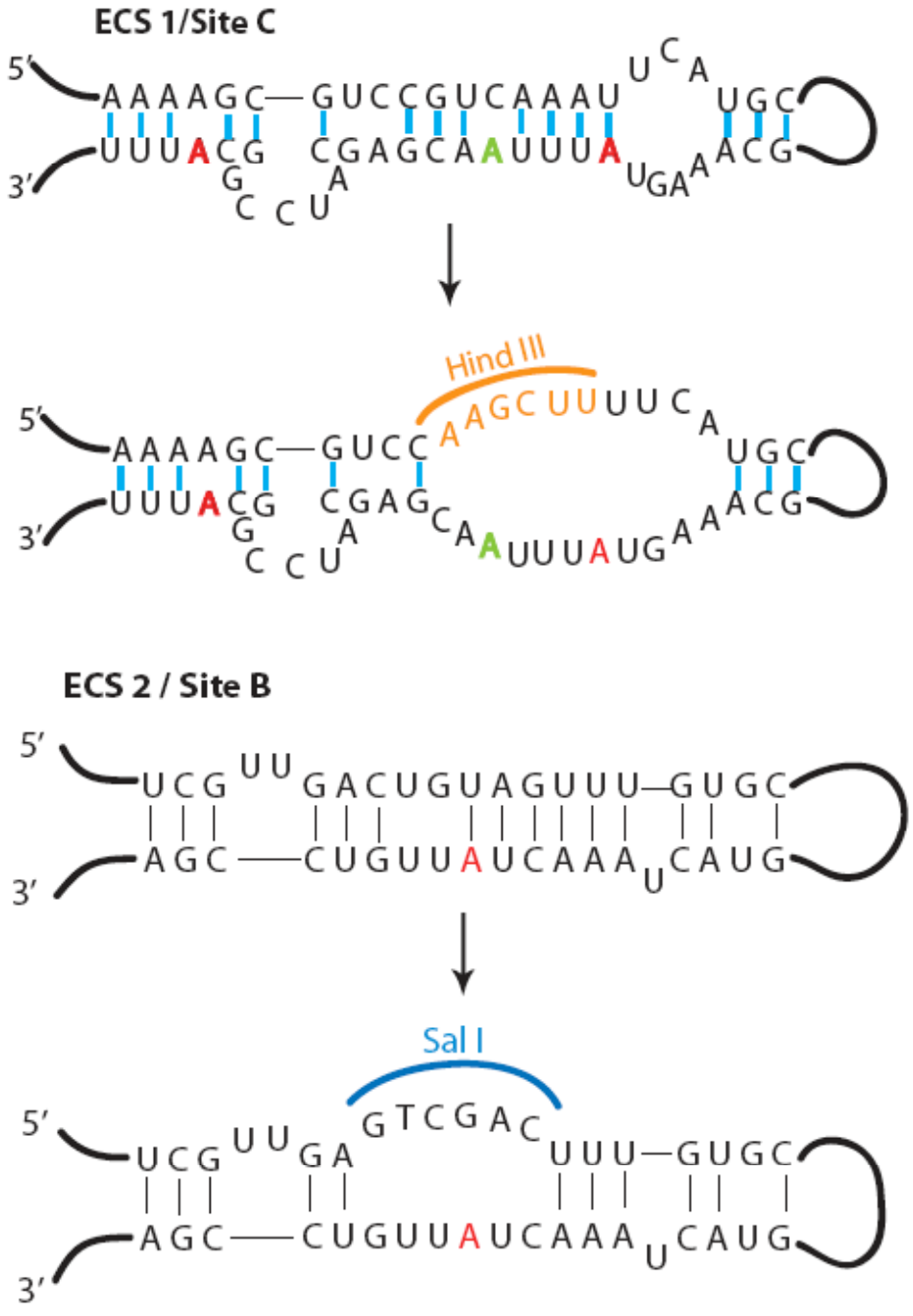

Figure 5.7: Mutations in *eag* ECS Elements Introduced Into the Genome by Homologous Recombination. Hairpin drawings illustrating the local structural environment surrounding editing sites B and C. Edited adenosine is colored red, silent edit sites are shown in green. Engineered mutations in the ECS element, and the predicted effects to the duplex structure, were used to disrupt editing of these sites.

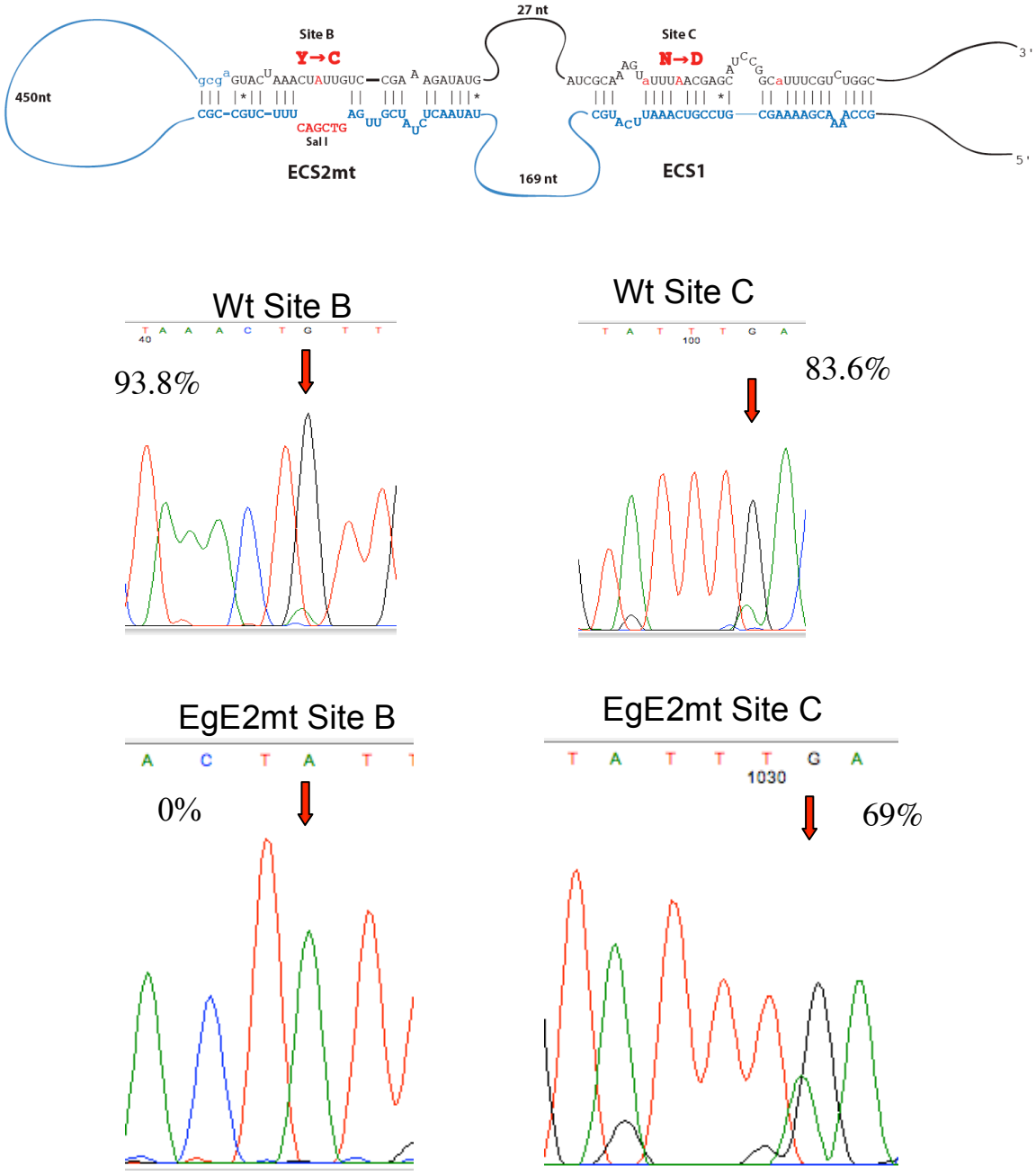

Figure 5.8: Mutations Within E2 Disrupt Editing of *eag* Site B.
Top: Diagram depicting the structure of *eag* exon 13, base-paired with both ECS elements. Mutations in E2, and the predicted disruption to the structure is shown. Bottom panels are chromatogram traces for *eag* cDNA for sites B and C in both wild-type targeted and E2 mutant targeted flies. Editing site are indicated by a red arrow. Editing levels are the average of 3 independent RT-PCRs, measured by the mass-ratio differences of areas under the peak, expressed as a percent.

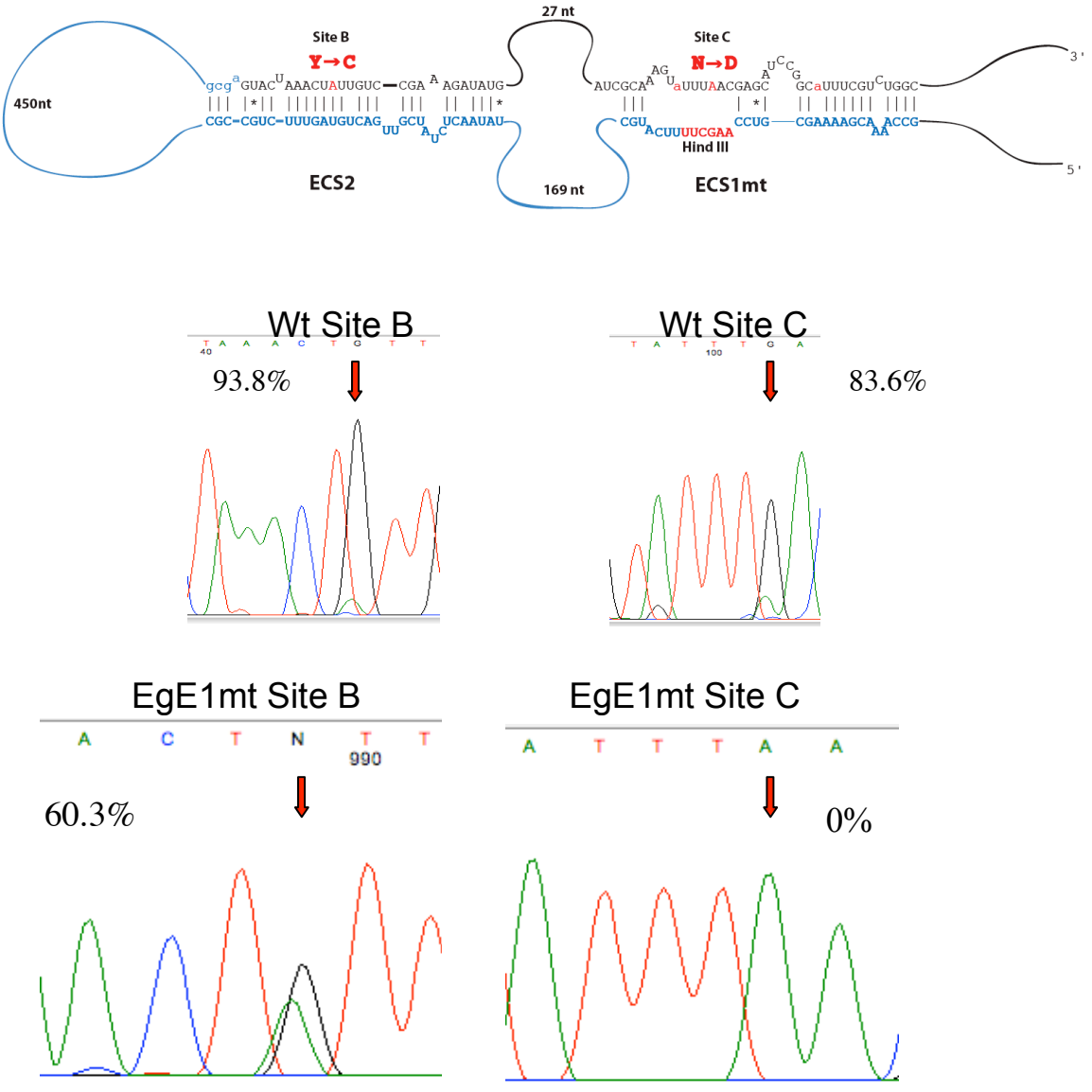

Figure 5.9: Mutations Introduced in *eag* E1 Disrupt Editing of Site C.
Diagram depicting structure of eag RNA in targeted flies. Mutations in E1, and the changes to structural environment around site C, are shown. Sequence chromatograms of *eag* cDNA from wild-type and E1 mutant targeted flies. Editing sites are depicted by a red arrow. Quantification of editing levels were performed similar to site B in figure 5.8.

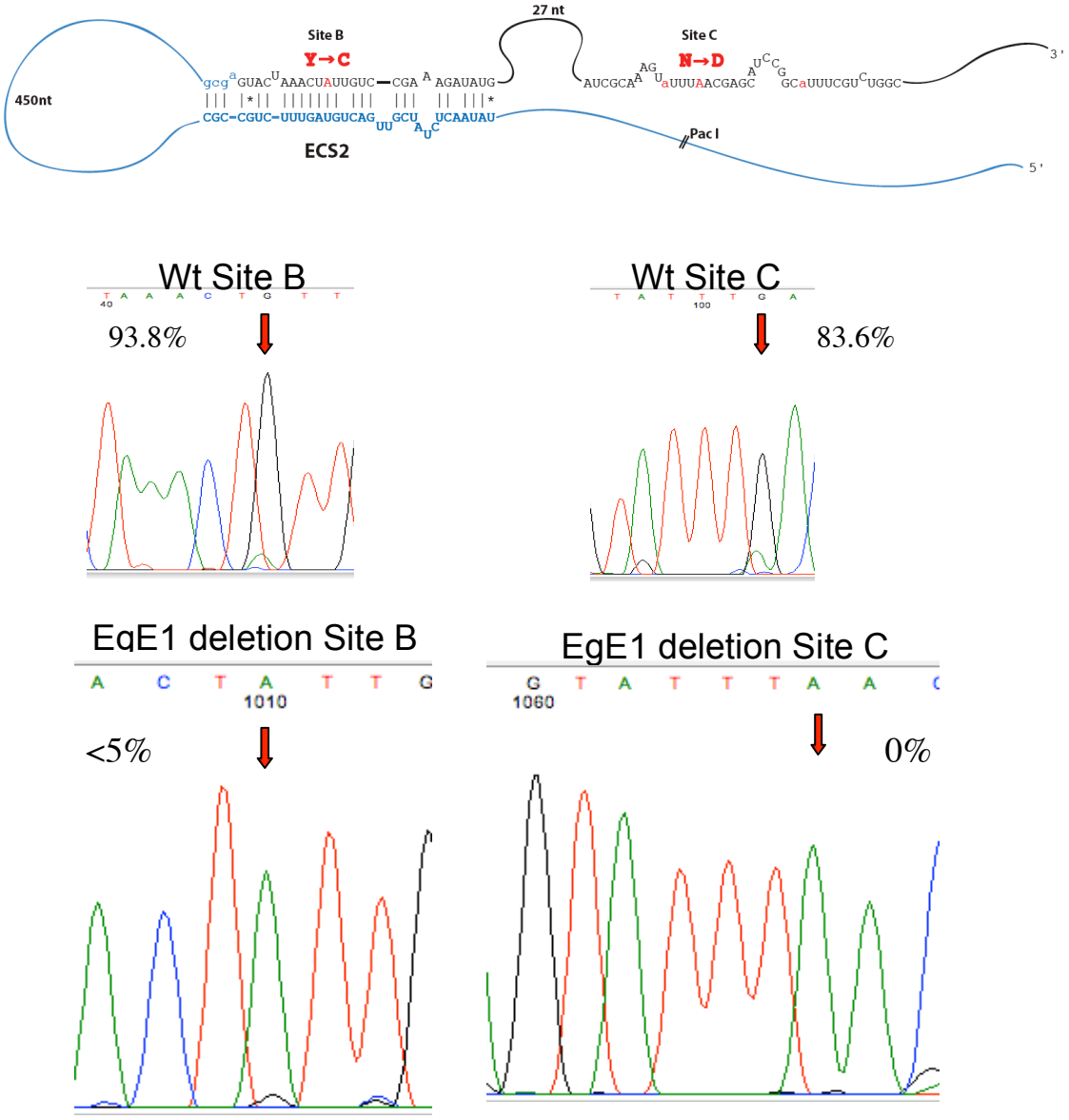

Figure 5.10: Deletion of E1 in *eag* Disrupts Editing of Both Sites B and C.
Deletion of E1 from the *eag* locus results in loss of editing at both sites in targeted flies. Sequence chromatograms of cDNAs generated from E1 deletion mutants demonstrate loss of editing. Site B may have some editing still present (bottom left trace) where a small G-signal (black) is still detectable. Arrows indicate the editing site.

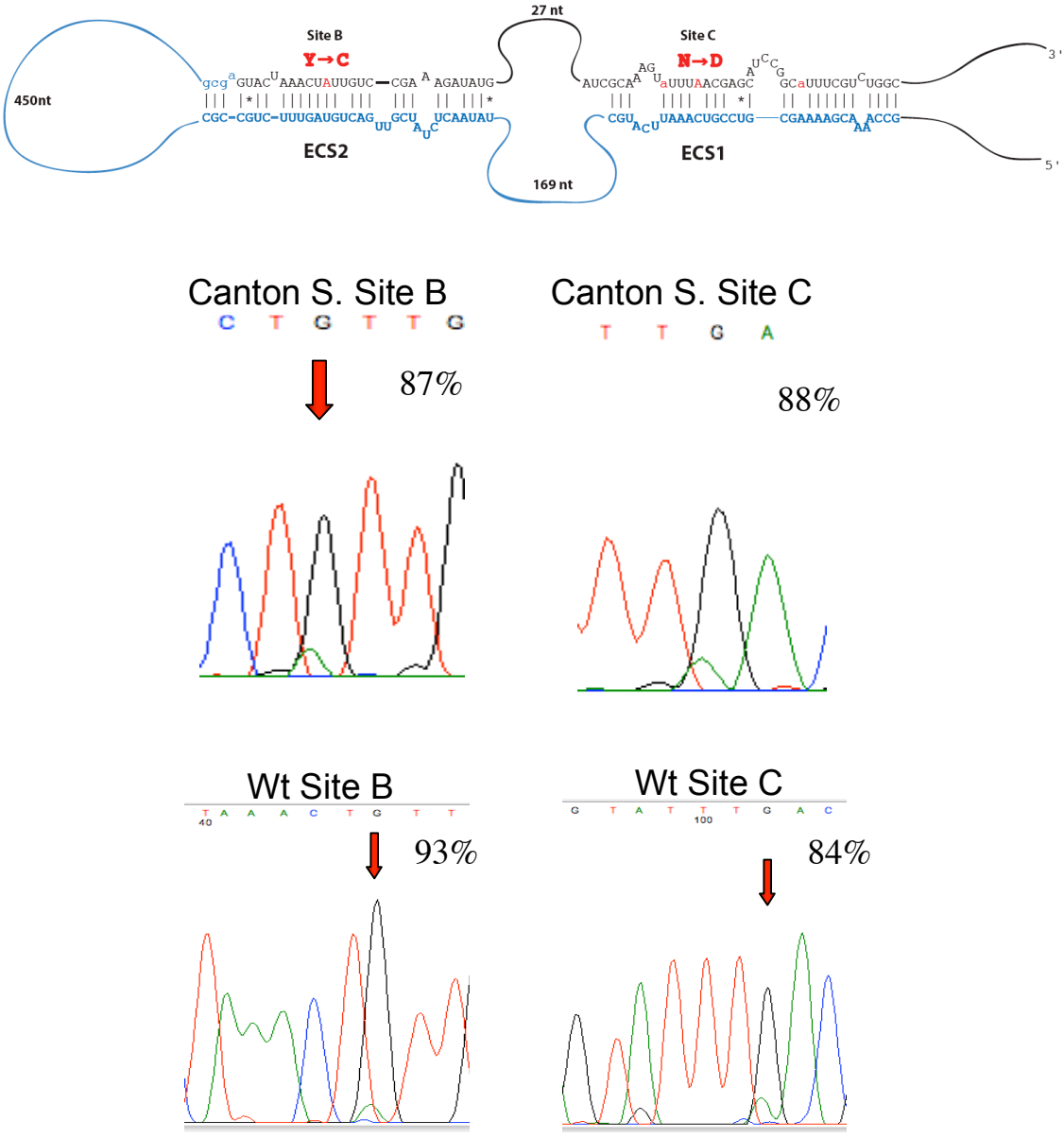

Figure 5.11: Wild-type *eag* Targeted Flies Do Not Have Defects in Editing. Top panel illustrates the structure of the mRNA duplex in wild-type targeted *eag* flies. Sequence chromatograms from cDNAs generated from Canton S., untargeted control flies and wild-type *eag* targeted flies. Editing levels were measured similar to manner described in figure 5.8.

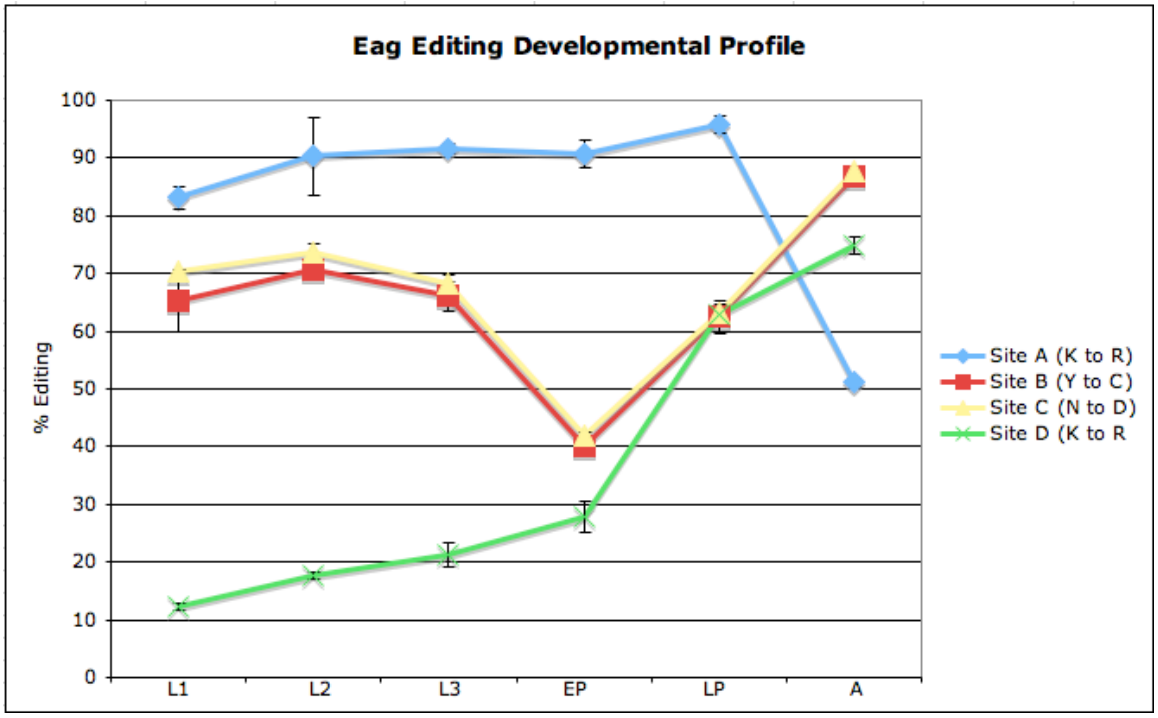

Figure 5.12: Developmental Profile of *eag* RNA Editing.
Editing of four sites in *eag* were measured for different developmental time points in Canton S. flies. Quantification of editing levels is described in Methods. Editing sites and the resulting amino acid substitutions are listed to the right of the graph. Error bars represent the standard error mean of editing levels at each time point.

@ EP: Site B, 40% Site C, 42%

	Expected Frequency	Observed Frequency	$(O-E)^2 / E$
AA	17.05	33	14.92
AG	12.34	0	12.34
GA	11.37	1	9.46
GG	8.23	15	5.57
	49		$\chi^2 = 42.29$

@ L3: Site B, 66% Site C, 68%

	Expected Frequency	Observed Frequency	$(O-E)^2 / E$
AA	4.90	17	29.88
AG	10.40	1	8.50
GA	9.50	3	4.45
GG	20.20	24	0.715
	45		$\chi^2 = 43.55$

Figure 5.13: Linkage Analysis of *eag* Sites B and C.
Individual cDNAs of *eag* transcripts were cloned and sequenced for two developmental time points. Chi-square analysis of editing between sites B and C was performed at both time points. 3rd instar larvae and early pupae were chosen due to the high levels of editing at both sites during other stages of development. In both time points, the two major classes of transcripts were either fully unedited or edited at both sites.

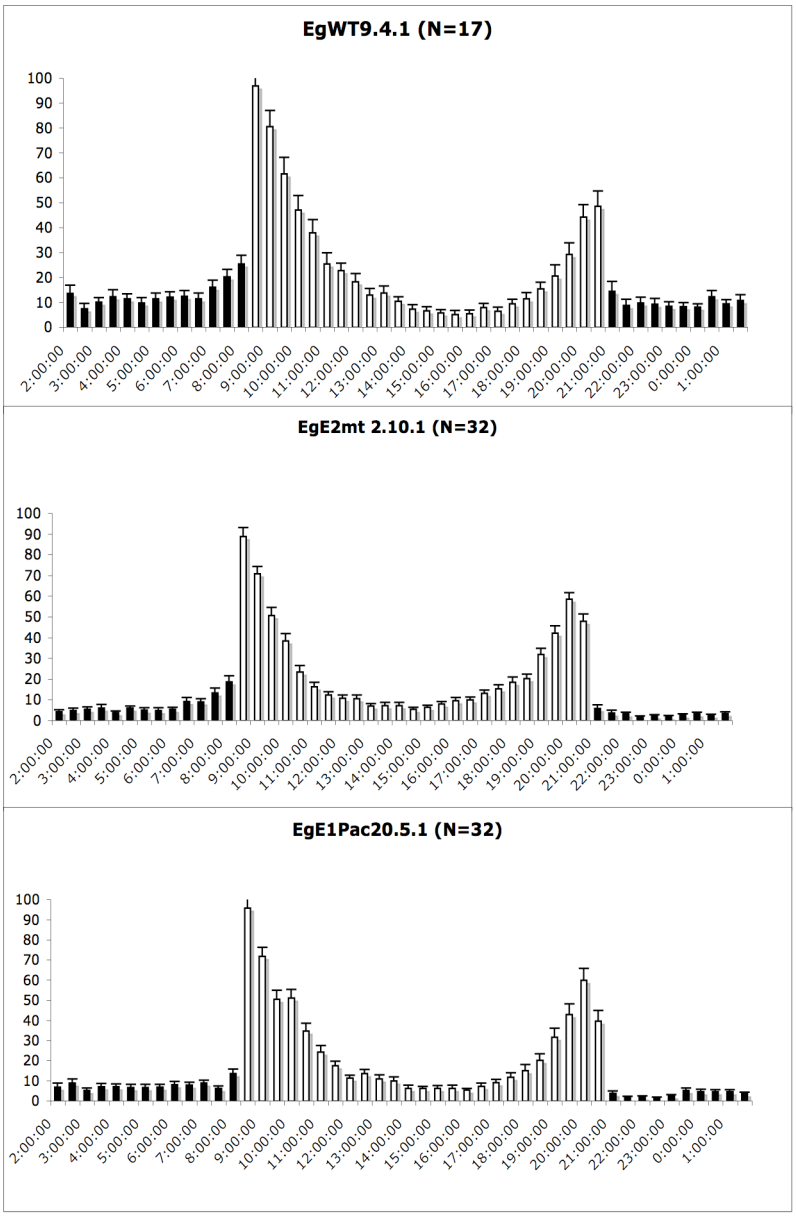

Figure 5.14: *Drosophila* Activity Monitor Studies for *eag* Targeted Flies.
Wild-type targeted, as well as E2 mutant and E1 deletion mutant flies were assayed for overall activity levels using a *Drosophila* Activity Monitor System (DAM) (see Methods). The x-axis denotes time points over a 24-hour period. The y-axis represents the average number of beam breaks. Bars represent the average beam breaks during that time point averaged over three days. Error bars represent the standard error for these averages. White bars illustrate time points when the lights in the incubator are on, while dark bars denote dark conditions.

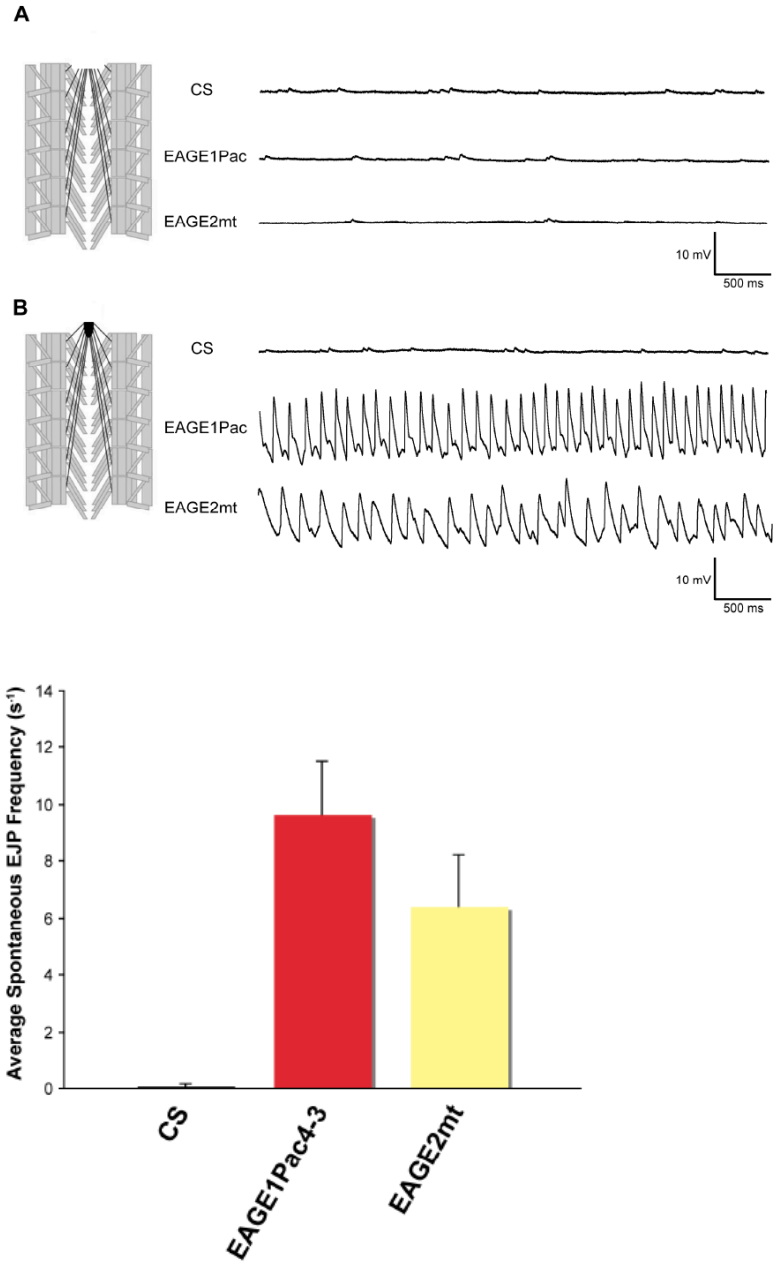

Figure 5.15: Excitability Properties of Larval NMJ in *eag* Mutants.
Diagram of larval muscle preparations either with the brain and ventral ganglion removed (top left) or left intact (bottom left). Current traces from larval muscle recordings in these different preparations are shown to the right of the diagrams. Bottom panel is a graph of the average frequency of spontaneous excitatory junction potentials in larval preparations (with brain and vent. ganglion intact). Error bars represent standard error mean. These experiments were performed by P. Bronk, Brandeis University, Waltham, MA.

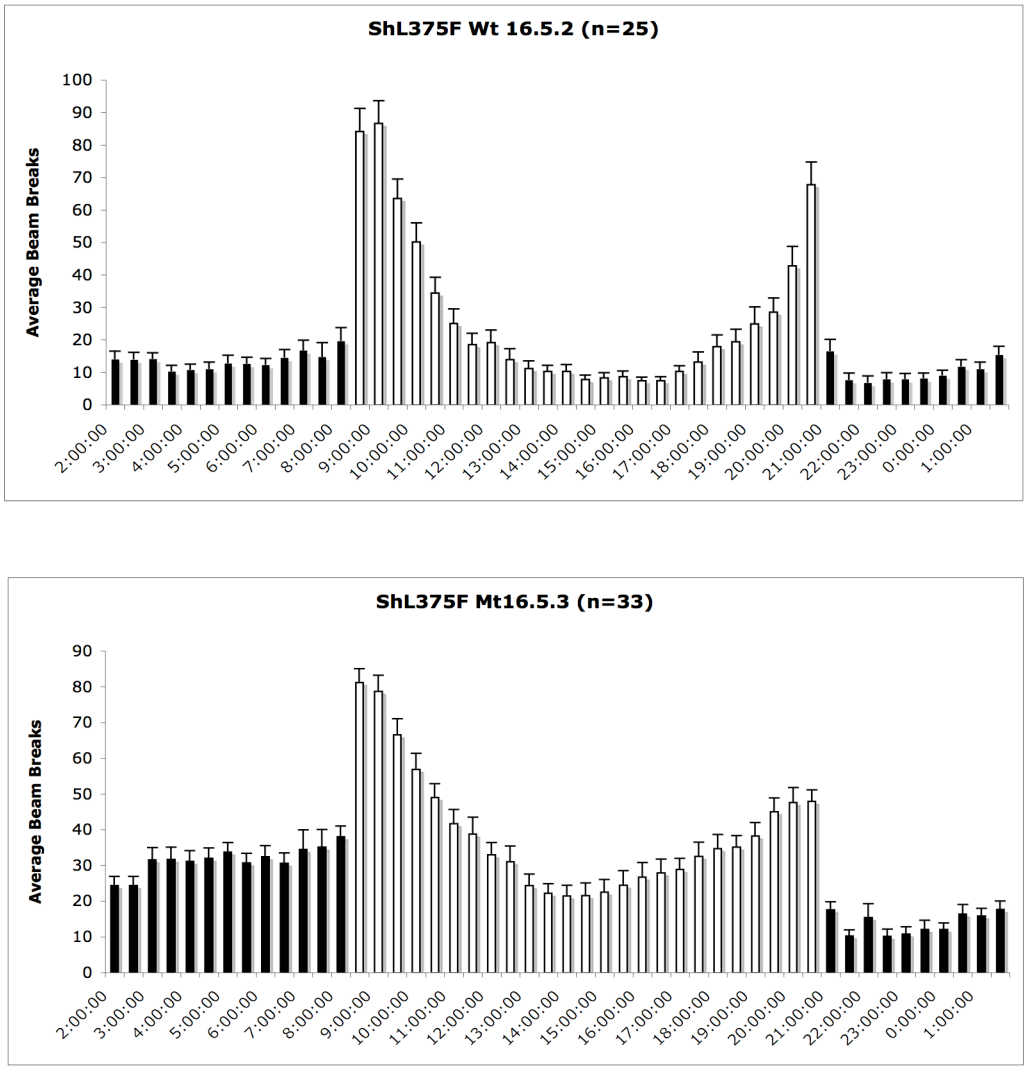

Figure 5.16: *Drosophila* Activity Monitor Studies for Neuromyotonia Mutant Flies. Neuromyotonia mutant flies (ShL375F) and targeted wild-type controls were placed in the *Drosophila* Activity Monitor to assess overall activity levels. White bars denote light conditions, while black bars denote dark conditions. Each bar represents the average beam breaks over three days for that time point. Error bars represent the standard error mean.

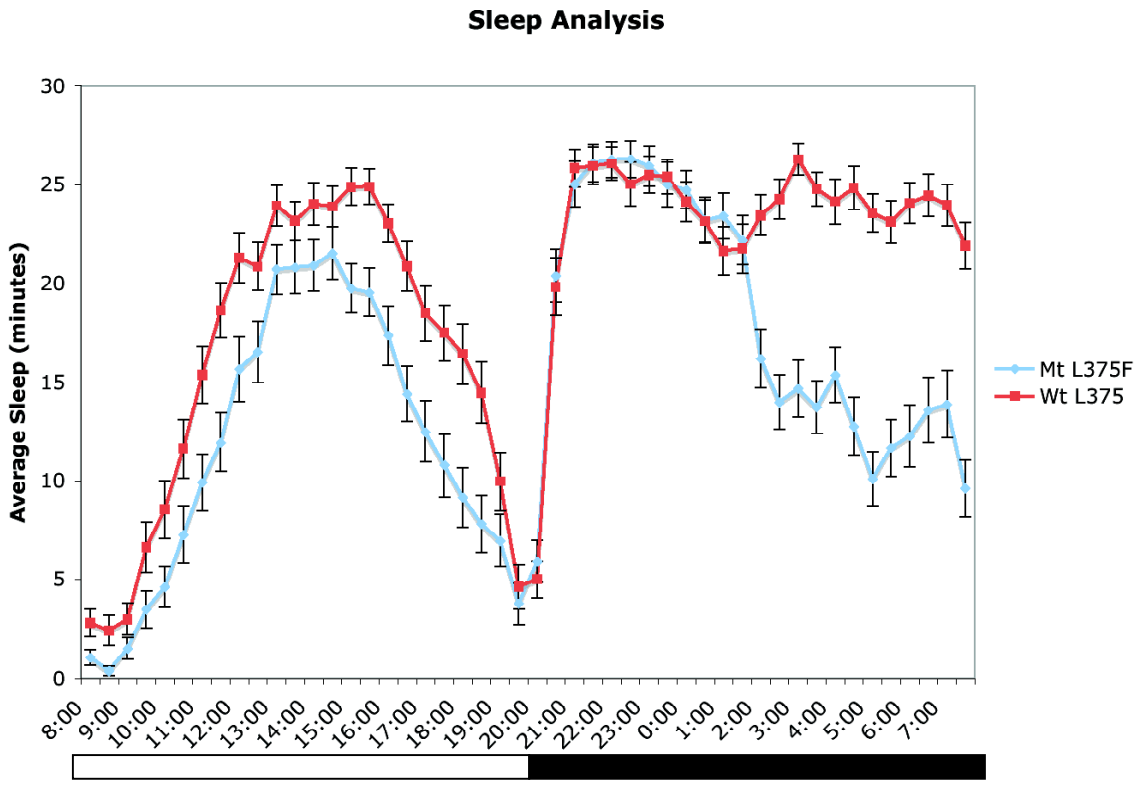

Figure 5.17: Sleep Analysis for Neuromyotonia Mutant Flies.
Neuromyotonia mutant flies (Sh L375F) and wild-type targeted control flies were analyzed for total sleep using the *Drosophila* Activity Monitor System. Time points represent average sleep amounts (in minutes) for each half-hour for a total of 24 hours where each time point represents the average sleep amount for three days. Sleep is defined by inactivity for a minimum of five minutes. Mutants (n=55) and wild-type (n=60). White bar and black bar denote light and dark conditions within the activity monitor incubator.

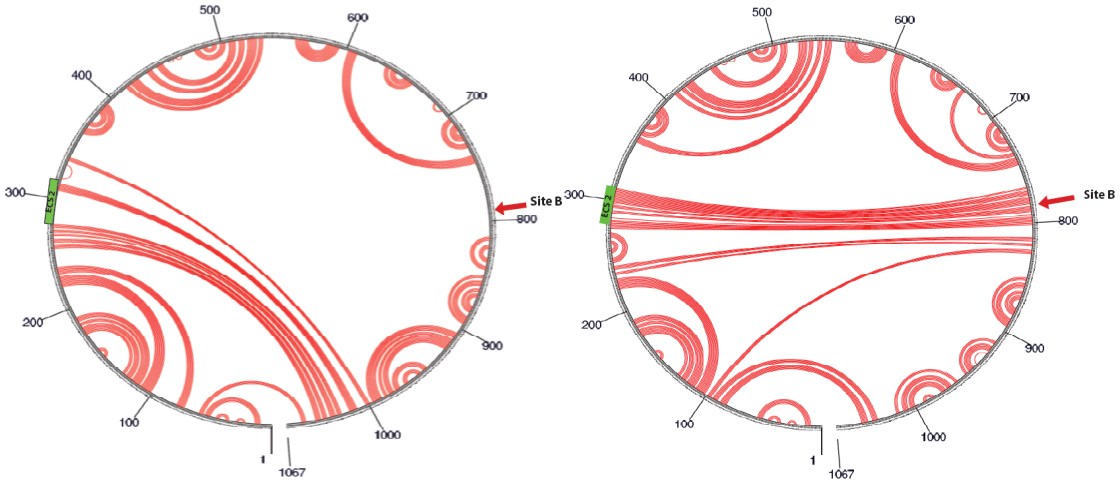

Figure 5.18: Structural Predictions for *eag* E1 Deletion Mutant Region.
The genomic region within *eag* spanning the conserved ECS elements, with ECS 1 deleted, through exon 13 was folded using the Sfold web server (http://sfold.wadsworth.org). ECS 2 is indicated by a green box while the corresponding editing site (B) is indicated by a red arrow. Base-pair interactions are displayed as red lines. Two structural classes are predicted, where the class on the left has a probability mass of 0.797 while the second class, which pairs ECS2 to site B, has a probability mass of 0.203.

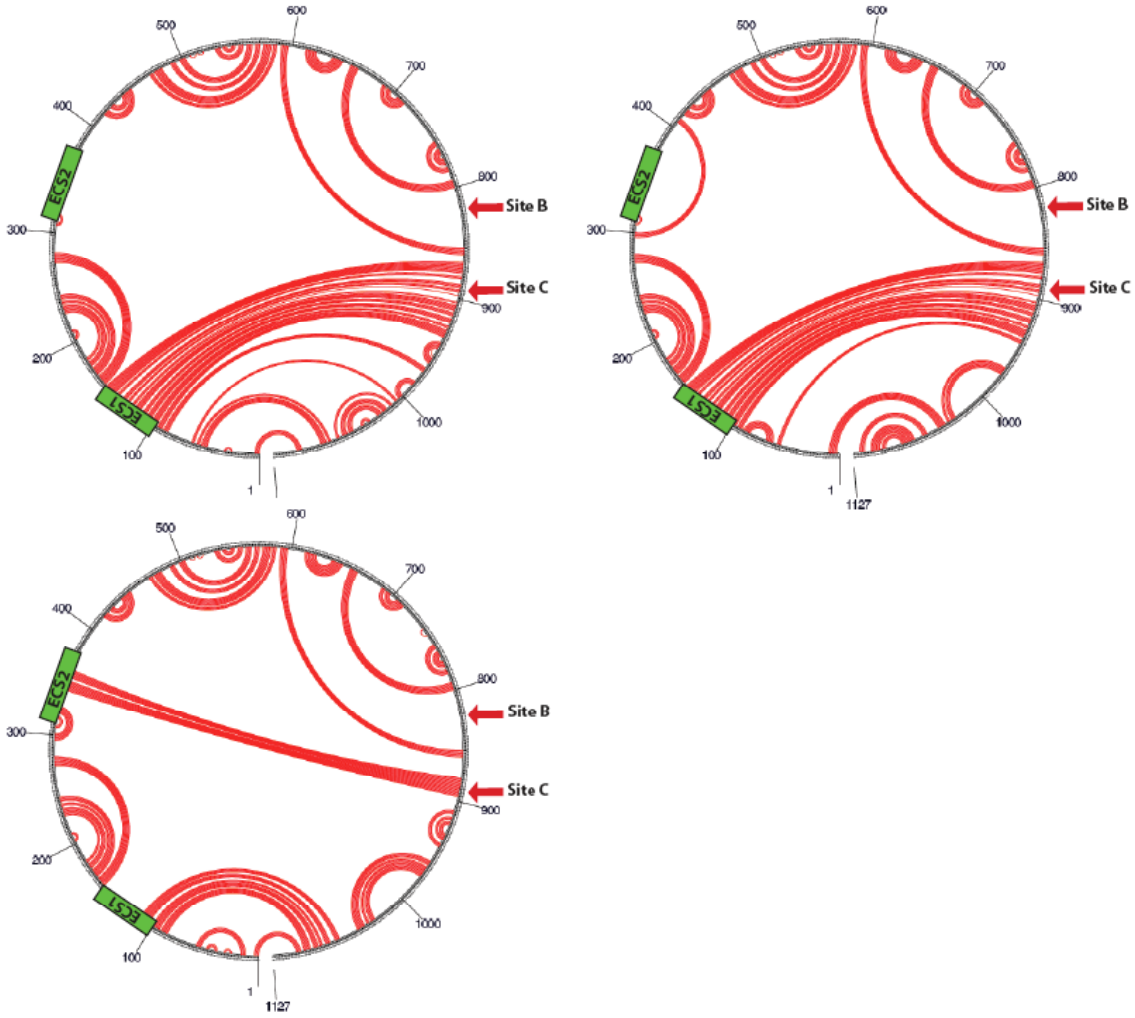

Figure 5.19: Structural Predictions for *eag* ECS2 Mutations.
Structural predictions for eag region containing ECS1, ECS2 with the Sal I restriction site mutation (as depicted in figure 5.7) and exon 13. Regions containing the ECS elements are shown with green boxes and editing sites B and C are indicated by red arrows. Base-pair interactions are shown as red lines. Predictions were generated using the Sfold web server (http://sfold.wadsworth.org). Three classes of structures are predicted for this sequence. Class 1 (upper left) has a probability mass of 0.636, class 2 (upper right) has a probability mass of 0.249 while class 3 (bottom left) has a probability mass of 0.115.

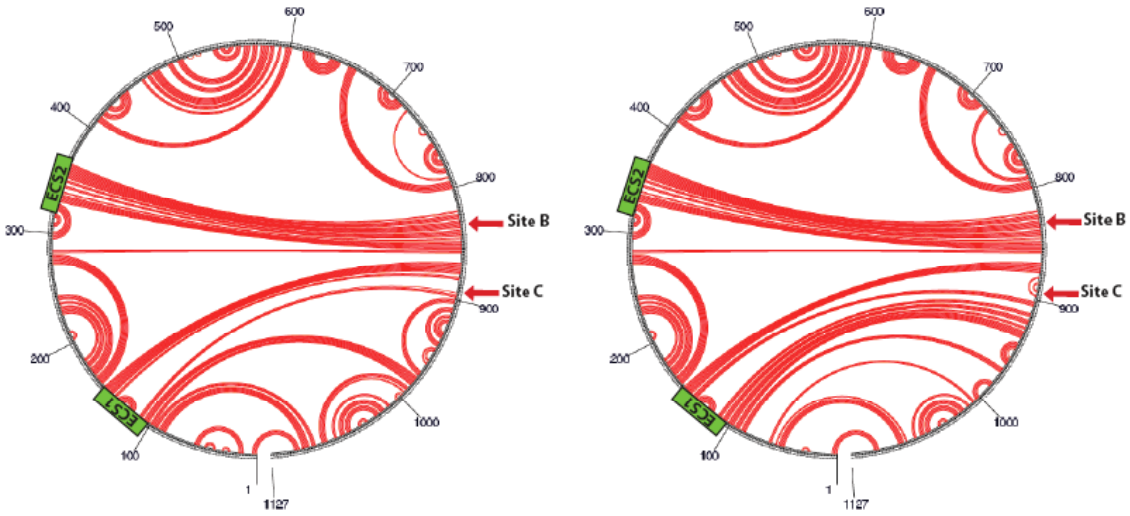

Figure 5.20: Structural Predictions for *eag* ECS1 mutation.
Structural predictions for the *eag* region containing ECS1 with the Hind III restriction site mutation (depicted in figure 5.7), ECS2 and exon 13. Predictions were generated using the Sfold web server (http://sfold.wadsworth.org). Locations of the ECS elements are displayed with green boxes, while editing sites are indicated with red arrows. Base-pair interactions are shown as red lines. Two classes of structures are predicted. The first class of structures (left), have a probability mass of 0.904 and the second class (right) has a probability mass of 0.096.

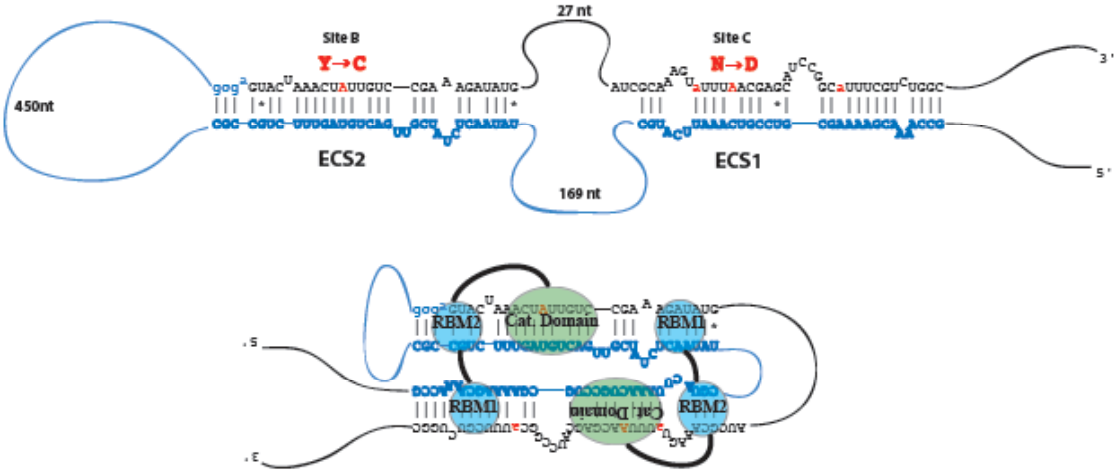

Figure 5.21: Tertiary Structure Formation Model for *eag* Editing Regulation and Linkage. Top figure represents the two duplex structures generated between ECS elements 1 and 2 with editing sites B and C in *eag* transcripts. The tight linkage observed between these two sites in both wild-type and *eag* mutant flies could be explained by the formation of a tertiary structure (bottom figure) where the two duplex structures form a higher-ordered complex which ADAR binds. Activity of ADARs is dependent on enzyme dimerization. This particular substrate would allow for each ADAR unit to bind both duplexes when dimerizing prior to deamination of sites B and C. In this model, perturbations to either structure could affect editing efficiency at both sites, or in the case of E1 deletion mutants, abolish editing of both sites by preventing the formation of this higher-ordered structure.

Chapter 6: Discussion

RNA Editing of K_V Channels in *Drosophila* is Highly Conserved and Tightly Regulated.

A descriptive analysis of RNA editing in K_V channel genes in *Drosophila* was required at the beginning of this study in order to better understand the nature of this form of gene regulation in flies. Prior to this study, we only knew that editing occurs within *Shaker*, *Shab*, and *eag* transcripts at specific sites (Hoopengardner, Bhalla et al. 2003). Through cDNA analysis of *Shaker* editing from multiple *Drosophila* species, we determined that editing of this gene is highly conserved. Not only are these sites largely conserved but so are the levels of editing observed for each site. This indicates that editing in *Shaker* has evolved and is retained by natural selection because it is fundamentally important for nervous system function in closely related species. The lack of conservation of *Shaker* editing in other insect species could indicate that these animals modulate nervous system function by adapting an alternative strategy. The presence of species-specific sites in other known gene targets of RNA editing suggests that conservation of editing sites occurs in a gene-specific manner. Therefore, the conservation of *Shab* and *eag* editing sites could be different between species than that of *Shaker*.

Conservation of editing allowed us to identify the ECS elements directing editing of *Shaker* through a comparative genomics approach (Figure 4.4). Although the conservation of editing in *eag* is still unknown, comparative genomics were also useful in identifying two ECS elements directing editing of site B and C (Figure 4.6). The fact that

this approach worked for *eag*, and the identification of highly conserved ECS elements in fly genome databases, does suggest that editing at these two sites is likely conserved as well. Thus, the conservation of editing in *Shaker* supports the idea that editing underlies fundamental processes shared by all species of flies needed for normal nervous system function, while species-specific editing in other genes is likely important for the generation of species-specific behaviors.

In addition to conservation of editing in K_V channels, multiple levels of editing regulation also exist in both a temporal and spatial manner. Also, evidence of linkage between editing sites can be observed. Temporal control of RNA editing is observed for editing sites in both *Shaker* and *eag* as well as a single editing site in *Shab* (Figures 2.1, 3.1, and 5.12). When measuring the editing levels during different developmental time points, three patterns of regulation can be observed between these three genes. First, editing levels can be constitutive throughout development. The levels of editing from one site to another may vary greatly, but the level of editing for any given site does not vary greatly from first-instar larvae through adult. This is the case for most sites in *Shab* and for the I/M site (site C) in *Shaker*. A second pattern of regulation exhibits low levels of editing early in development (L1 to L3) and begins to rise during early pupae and usually peaks near or at adult stages. This can be observed for the last 3 editing sites in *Shaker* as well as the K/R site in the C-terminus of *eag*. It is thought that some sites are regulated in this manner due to a possible function in metamorphosis or adult nervous system function such as generating adult-specific behaviors. Lastly, the opposite pattern of editing can be observed for the T/A editing site in *Shab* and the K/R pore editing site in *eag*. Here, editing levels are constitutively high during early development and then

decrease as flies approach the adult stage. This suggests that editing of these sites is important for larval nervous system function and possibly metamorphosis as well. These three patterns of temporal regulation suggest that editing of different sites, even within the same gene, is utilized differentially to modify excitability in the nervous system at different stages of development. Certainly the pupal stage is a time where most profiles seem to shift in coordination with the nervous system remodeling events that occur at this time as well as increases in the expression of dADAR enzyme isoforms (Palladino, Keegan et al. 2000). The ability of the fly to modify excitability through RNA editing of K_V channels is a versatile mechanism to meet the changing demands that two different nervous system types require in the course of fly development.

Spatial distribution of *Shaker* editing was examined in multiple tissue types in *Drosophila*. The four editing sites (C through F) spanning the S4 voltage-sensor to the C-terminus could potentially yield 16 possible different editing isoforms. However, not all isoforms are present in the fly. In fact, editing isoforms are generated in a tissue-specific manner (Figure 3.2). For example, in the fly head only three or four isoforms of editing are in abundance. In this case, it appears that within the central nervous system, editing of the last two sites is preferentially utilized. In contrast, the peripheral nervous system (thorax), fully unedited isoforms are most abundant. When enriching for sensory tissues such eye, antennae, and wing the dominant isoform includes editing of site C only. This demonstrates that not all possible isoforms of *Shaker* editing occur *in vivo*, and furthermore, specific tissues utilize editing differently to accomplish their unique functions. Since the ECS elements directing editing of these sites is present in all nascent

mRNA transcripts in every tissue, the observed spatial regulation is likely accomplished through cell-type specific factors which either assist in, or inhibit editing of, these sites.

Lastly, linkage between editing sites have been observed for both *Shaker* and *eag* (Figures 3.2, 5.12, and 5.13). In both cases, the linked sites are contained within the same exon, but not necessarily predicted to be in the same duplex structure. In the case of *Shaker* editing sites E and F, which are separated by 7 nucleotides, editing at site F is dependent upon editing at site E. This can be observed in the spatial distribution of edited isoforms where few or no isoforms that contain site F edited without first being editing at site E. These sites are contained within the same duplex structure where editing at site E likely changes the local structural environment in a manner that facilitates editing at site F. In *eag*, two editing sites (B and C) located in the same exon,but over 50 nucleotides apart, also show linkage in both developmental and mutant analyses. Suprisingly, these sites are predicted to be located in separate duplex structural domains. In this case, the requirement for the ECS that forms a duplex around site C appears necessary for editing at both sites B and C. Indeed, sequencing of individual cDNAs demonstrate that either both are edited or neither. Additionally, mutant flies show decreases in editing of one site when the local structure around the other site is perturbed. This could possibly be the result of some higher-ordered structure that forms only when both duplexes form, and this tertiary structure is needed for proper editing (Figure 5.21). Further mutational analysis in these ECS elements will be required in order to determine the mechanisms for linkage in both *Shaker* and *eag*. These include mutations that can disrupt the duplex regions where ADAR binding domains interact with the substrate to see if effects in one structure can affect editing in the other structure in a

specific manner. This would help to indicate whether a high-ordered structure is serving to regulate and link these sites *in vivo*.

The spatial and temporal control of RNA editing in K_V channels, and the linkage observed between certain sites, suggest that the functional diversity generated through RNA editing must be tightly regulated in the fly nervous system for normal function. Furthermore, this regulation allows for dynamic changes in excitability required either during development or in a manner specific to the functioning of discrete cell types.

RNA Editing of K_V Channels Alters Channel Function

The effects of RNA editing on channel function have been demonstrated in this study for both Shab and Shaker channels. In both cases, the amino acid substitutions generated through editing can affect gating kinetics. In the Shab channel, these effects were studied in the context of loss of editing at specific sites due to the constitutive and somewhat high levels of editing that exist in these channels *in vivo* (Chapter 2). Loss of editing in some sites resulted in decreases in rates of deactivation. Loss of editing at two sites shifts the voltage-dependent activation of the channel to more positive potentials. Taken together, it appears that editing of these sites in Shab act to decrease voltage-sensitivity and also to decrease the rates of gating kinetics. Additionally, one site (Y/C) in the outer vestibule of the pore was shown to confer resistance to a channel blocker, TEA. In Shaker channels, the picture was much less clear. In this case, and array of effects could be observed in rates of deactivation kinetics and recovery from inactivation (Chapter 3). These effects on channel function were entirely context dependent and no

single site could be predicted to consistently alter function in a specific manner. These epistatic effects help reveal that in Shaker these editing sites can interact to produce unique channel properties. Considering the spatial distribution of *Shaker* editing isoforms, it would be interesting to understand how specific channel types generated facilitate cell-specific functions. Overall, RNA editing in these channels appear to generate an array of different functional channels with unique gating characteristics to suit the needs of various cell populations within the nervous system. Additionally, editing also appears effect a channel's sensitivity to both intrinsic and extrinsic forms of inactivation or block as is the case for both Shab and h K_V1.1 (see Chapter 1).

Generation of Editing Mutants in *Drosophila* by Homologous Recombination

Studying ion channel function in the fly can prove to be difficult with standard methods using transgene expression systems, particularly if behavioral phenotypes are to be studied. This is because ectopic transgene expression systems do not allow for the fine level of control of ion channel expression observed *in vivo*. Perturbations in the expression levels and patterns of K_V channels will likely result in phenotypes unrelated to the process or mutation under investigation. In order to investigate the function of RNA editing in K_V channel genes, a method must be employed that allows for endogenous regulation of the channel to remain intact. This was accomplished by using homologous recombination to introduce mutations into the genomic locus that specifically perturb RNA editing of each site individually. Identification of the ECS elements directing editing in both *Shaker* and *eag* provided regions where mutations can be introduced to specifically disrupt editing by changing the local structural environment surrounding an

editing site in duplex RNA. Furthermore, editing can also be disrupted by the introduction of point mutations within the edited codon to remove the available editing site, as in the case of *Shaker* mutants for the I/M editing site. The introduction of these mutations into the *eag* and *Shaker* loci produce a system to study the *in vivo* consequences of RNA editing in these genes that is far superior to other methods of gene analysis. Not only is endogenous regulation of these genes left intact, but the activity of the dADAR enzyme along with editing of all other endogenous sites is also preserved. This allows for the investigation of specific contributions that *Shaker* and *eag* editing make to nervous system function and behavior.

Mutants that specifically disrupt editing for the I/M site in *Shaker*, and also for the N/D and Y/C editing sites in *eag* have been generated. While much of the behavioral analysis remains to be performed on these mutants, some interesting preliminary data in the *eag* mutants suggest that behavioral phenotypes will likely result from disrupting editing in these sites. Although overall activity levels appear to be normal in these flies, studies from collaborators investigating neuromuscular junction excitability found increased frequencies in spontaneous excitatory potentials (Figure 5.15). This effect was only observed when the axon remained in communication with the cell body. Severed axons did not produce this effect, therefore, the phenotype observed is not the result of hyperexcitability in the axon and a higher order of control is likely being affected. This is very promising considering the two editing sites disrupted in these mutants recode residues within the C-terminal domain where interactions with intracellular signaling molecules occur. Many experiments still need to be performed to assess behavioral defects, however, most studies will likely involve defects in learning and/or memory

since previous mutant alleles of *eag* were demonstrated to affect these processes and are mediated through interactions in the region of the channel containing these editing sites.

Analysis of RNA editing in these *eag* mutants did provide insights into the regulation of editing these sites. The two editing sites in these mutants are tightly linked and mutations in either ECS element resulted in effects in both sites in these flies. Additionally, single ECS mutations effectively disrupted editing of the predicted site, uncoupling these sites from each other in both combinations. It will be interesting to see if any novel effects are generated in these mutants that may reveal the functional significance for tightly regulating these two sites.

Phenotypic analysis has not yet started for the mutant flies lacking editing at the I/M site in *Shaker*. Although editing at this site occurs at constitutively high levels throughout development, these mutants are viable and do not appear to have any gross abnormal defects. The spatial regulation of editing indicates that this site is highly utilized by tissues enriched for various populations of sensory neurons. Therefore, phenotype analysis focused on assessing various modes of sensory perception such as gustation, olfaction, vision, and mechanosensation may reveal effects in this mutant background.

Generation of these mutant lines provides an excellent foundation to study the specific involvement of RNA editing of K_V channels in nervous system function and behavior. In the future, these mutants can also be used to investigate the genetic interactions of editing in multiple genes to reveal the networks of gene regulation required for the generation of complex behaviors.

Mimicking a Human Disease Allele in *Shaker* Generates Unique Phenotypes

Targeting of the *Shaker* locus by homologous recombination presented an opportunity to investigate the use of gene targeting for the generation of human disease models in the fly. Such a model would allow for experiments aimed at understanding mechanisms of pathogenesis that would be technically difficult in higher organisms. For example, disease models in flies may serve as a starting point for mutant screens by providing a sensitized genetic background that can aid in the identification of new genes involved in either suppression or enhancement of the disease phenotype. Additionally, disease models can be used to test various pharmacological agents that may affect disease processes.

A previously identified disease allele for chronic neuromyotonia was introduced into the homologous residue in *Shaker*. This mutation contains a missense mutation of a highly conserved leucine residue located within the S4 voltage sensor. This disease largely results in hyperexcitability at the neuromuscular junction. People afflicted with this condition can suffer from episodes of ataxia (uncoordinated movement), muscle fasciculation (rippling), as well as severe muscle cramping and stiffness. Cold temperatures, physical exertion and emotional stress exacerbate these symptoms. This allele was introduced in the fly to see if any of these disease features would be maintained. Initial examination of these mutants did indicate that they are hyperexcitable (Figure 5.16), have decreased amounts of total sleep (Figure 5.17), exhibit leg shaking under ether anesthesia, and display age-dependent seizure activity. Unexpectedly, increased levels of aggression were observed in these mutants in addition to increased incidence of male-male courtship behavior. These phenotypes were completely

unanticipated, and implicate Shaker-mediated excitability in neuronal circuits governing these behaviors. In order to determine the role of Shaker activity in the generation of these behavioral phenotypes, the effects of this mutation will need to be studied both the level of channel physiology as well as behavioral assays to determine any defects in a specific sensory modality. Previous studies have implicated pheromone perception as well as defects within sexually dimorphic neural circuits in the brain in generating simultaneous effects in both aggression as well as courtship behavior defects (Broughton, Kitamoto et al. 2004; Vrontou, Nilsen et al. 2006; Certel, Savella et al. 2007; Chan and Kravitz 2007; Wang and Anderson 2010). It is possible that this mutation in *Shaker* results in defects in pheromone perception and/or excitability changes in the same neural circuits that govern these behaviors. Behavioral experiments as well as genetic studies with other mutants affecting these regulatory pathways may assist in identifying the mechanism of Shaker activity in generating these phenotypes. These mutants provide a model in which studies looking at excitability in the regulation of aggressive behaviors and courtship display can be examined in further detail, and additionally provide a system in which the disease features of neuromyotonia can be further studied as well.

Concluding Remarks

The experiments performed in this study have helped to elucidate the nature, regulation, and functional consequences resulting from A-to-I RNA editing in K_V channel genes. The amino acid substitutions generated by RNA editing suggest that editing is required to generate the necessary diversity in protein function in order to satisfy the demands of specific cell types in the functioning nervous system and to generate

appropriate behaviors. However, little is known about the significance of this form of post-transcriptional regulation for the specific genes subjected to editing. Mutations in K_V channel genes in *Drosophila* have been previously demonstrated to generate various behavioral defects. Investigating editing in these channels have identified sites that are coordinately regulated as well as spatial and temporal specific patterns of editing in the fly. The *cis*-regulatory (ECS) elements directing editing of these sites have been identified by comparative genomics approaches and used in the generation of editing deficient mutant flies. This work provides a starting point to investigate the behavioral processes regulated by RNA editing in K_V channel genes. Furthermore, the identification of possible cell-specific factors may further elucidate the regulatory mechanisms that govern this form of post-transcriptional modification and generate the specific spatial and temporal patterns of editing identified here.

Literature Cited

Broughton, S. J., T. Kitamoto, et al. (2004). "Excitatory and inhibitory switches for courtship in the brain of Drosophila melanogaster." Curr Biol **14**(7): 538-47.

Certel, S. J., M. G. Savella, et al. (2007). "Modulation of Drosophila male behavioral choice." Proc Natl Acad Sci U S A **104**(11): 4706-11.

Chan, Y. B. and E. A. Kravitz (2007). "Specific subgroups of FruM neurons control sexually dimorphic patterns of aggression in Drosophila melanogaster." Proc Natl Acad Sci U S A **104**(49): 19577-82.

Hoopengardner, B., T. Bhalla, et al. (2003). "Nervous system targets of RNA editing identified by comparative genomics." Science **301**(5634): 832-6.

Palladino, M.J., L.P. Keegan, et al. (2000). "dADAR, a Drosophila double-stranded RNA-specific adenosine deaminase is highly developmentally regulated and is itself a target for RNA editing." RNA **6**(7): 1004-18.

Vrontou, E., S. P. Nilsen, et al. (2006). "fruitless regulates aggression and dominance in Drosophila." Nat Neurosci **9**(12): 1469-71.

Wang, L. and D. J. Anderson (2010). "Identification of an aggression-promoting pheromone and its receptor neurons in Drosophila." Nature **463**(7278): 227-31.